

university  
of south africa



---

**UNISA**

**METHODS DEVELOPMENT FOR DETERMINATION OF  
NEONICOTINOID PESTICIDES FROM SELECTED VEGETABLE  
OILS USING HPLC-DAD**

by

**Sengane Musiwa Victoria (13402951)**

submitted in accordance with the requirements for  
the degree of

**Master of science**

in Chemistry

at the

UNIVERSITY OF SOUTH AFRICA

SUPERVISOR: Prof N Mketo

CO-SUPERVISOR: Prof PN Nomngongo

**February 2024**

## DECLARATION

---

Name: Sengane Musiiwa Victoria  
Student number: 13402951  
Degree: Master of Science in Chemistry

Exact wording of the title of the dissertation as appearing on the electronic copy submitted for examination:

Methods development for determination of neonicotinoid pesticides from selected vegetable oils using HPLC-DAD.

---

---

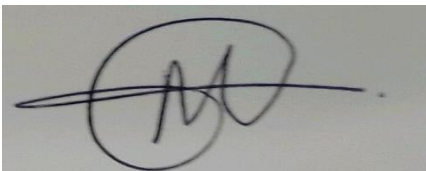
---

I declare that the above dissertation is my own work and that all the sources that I have used or quoted have been indicated and acknowledged by means of complete references.

I further declare that I submitted the dissertation to originality checking software and that it falls within the accepted requirements for originality.

I further declare that I have not previously submitted this work, or part of it, for examination at Unisa for another qualification or at any other higher education institution.

*(The dissertation will not be examined unless this statement has been submitted.)*



---

SIGNATURE

DATE: 29/02/2024

## UNIVERSITY OF SOUTH AFRICA

### **KEY TERMS DESCRIBING THE TOPIC OF A DISSERTATION/THESIS**

The Executive Committee of Senate decided that in order to assist the Library with retrieval of information, master's and doctoral students must list approximately ten key terms which describe the topic of the dissertation/thesis at the end of the summary of the dissertation/thesis.

If the dissertation/thesis is not written in English, the key terms in English must be listed at the end of the English summary.

The following is an example of key terms used for a thesis/dissertation:

#### **Title of thesis/dissertation:**

Methods development for determination of neonicotinoid pesticides from selected vegetable oils using HPLC-DAD.

#### **KEY TERMS:**

Magnetic solid phase microextraction, neonicotinoid pesticides, deep eutectic solvent, dispersive liquid-liquid microextraction, magnetic nanocomposite, characterisation, AGREE.

## **DEDICATION**

---

This work is dedicated to my late father (Mr M.D Sengane) and my mother (Mrs S.R Sengane).

## ACKNOWLEDGEMENTS

---

I would like to extend my gratitude to my supervisor, Prof N Mketo and my co-supervisor, Prof P.N Nomngongo for their continuous support and guidance during the MSc studies.

Special thanks go to my colleagues (Ms T Kgoedi, Mr N Mdluli and Mr BK Munjanja) and UNISA, Food and Environmental Analytical Chemistry research group for being there for me when I needed them the most.

I would also like to acknowledge UNISA, Chemistry Department for supplying me with analytical instruments, laboratory space and chemicals that I need for my research project.

I also extended my gratitude to Dr S Mpelane (UJ), Mrs O Sebabi (UJ), Dr L Mathevula (UNISA, Physics Department) and Dr M Sihlahla for assisting me with TEM, P-RXD, SEM-EDX and proofreading, respectively.

I would like to also acknowledge UNISA-Women-In-Research funding and UNISA-CSET bursary for their financial support.

Exceptional gratitude goes to my wonderful mother (Mrs S.R Sengane), my brother (Mr M Sengane) and my sister (Ms E.J Sengane) for their continuous support throughout this journey.

## MANUSCRIPTS AND BOOK CHAPTERS

---

1. M.V Sengane<sup>a</sup>, N Mket<sup>a</sup>. *Chitosan - an abundant biopolymer used for water treatment* **(SUBMITTED)**.
2. M.V Sengane<sup>a</sup>, P.N Nomngongo<sup>b</sup>, N Mket<sup>a</sup>. *Development of the magnetic solid phase microextraction method for the determination of neonicotinoid pesticides from vegetable oils* **(IN PREPARATION)**.
3. M.V Sengane<sup>a</sup>, P.N Nomngongo<sup>b</sup>, N Mket<sup>a</sup>. *Development of a greener dispersive liquid-liquid microextraction method for determination of selected neonicotinoid pesticides in vegetable oils* **(IN PREPARATION)**.

## CONFERENCE(S)

---

1. M.V Sengane, P.N Nomngongo, **N. Mketto**, *Development of a rapid and efficient preconcentration method for determination of neonicotinoid pesticides in vegetable oils using  $Fe_3O_4@Al_2O_3/AC$  and HPLC-DAD*", (**Oral**), ACC2023 conference, Thessaloniki, Greece, November 2023.

## ABSTRACT

---

The neonicotinoid pesticides (NEOs) have been used over the years for plant protection. The use of these NEOs on crops and oil seed plants has led to vegetable oil and crop produce contamination. The four selected NEOs for this study are acetamiprid, imidacloprid, thiacloprid and thiamethoxam. Their accumulation in oil crops is through absorption via roots and plant leaves. The presence of NEOs in the vegetable oils results in human health problems, hence there is a need for monitoring and control of their concentration levels present in agricultural products. Different organisations like World Health Organization (WHO), Codex Alimentarius Commission (CAC) and European Union (EU) have maximum residue limits set for NEOs in countries like Japan, China and US at less than  $0.5 \text{ mg.kg}^{-1}$ . Different chromatographic techniques have been used for determination of NEOs in various sample matrices. The high-performance liquid chromatography with diode-array detection (HPLC-DAD) was among the most reported chromatographic techniques for detection of NEOs. However, due to the complexity of vegetable oils and the trace concentration levels of NEOs, sample preparation step is required prior to chromatographic detection. The solid phase extraction (SPE) and liquid-liquid extraction (LLE) methods are popular for extraction of various targeted analytes. However, these two extraction methods suffer from different limitations like use of large amount of organic solvents, tediousness, costly adsorbents and production of hazardous waste.

Therefore, the aim of the study was to develop rapid, greener, and efficient extraction methods followed by HPLC-DAD analysis for determination NEOs in selected vegetable oils. The magnetic solid phase microextraction (MSPME) was the first extraction method to be investigated. A novel magnetic adsorbent ( $\text{Fe}_3\text{O}_4@\text{Al}_2\text{O}_3/\text{AC}$ ) was synthesized using maize waste material and characterized using various techniques such Fourier transform infrared spectrometry (FTIR), Powdered X-ray diffraction (PXRD), Scanning electron microscope coupled to energy dispersive X-ray spectroscopy (SEM-EDS), Thermogravimetric analysis (TGA), Transmission electron microscopy (TEM), and Ultraviolet visible spectroscopy (UV-Vis) to confirm the formation of the adsorbent material. The proposed MSPME method achieved high accuracy (80-119.21 %) and precision ( $\leq 10$  %) for all the investigated NEOs. Furthermore, the obtained limit of detection (LOD) ranged from  $0.5\text{-}1.76 \text{ ng.}\mu\text{L}^{-1}$ , limit of quantification (LOQ) ranged from  $1.87\text{-}6.62 \text{ ng.}\mu\text{L}^{-1}$ , with satisfactory high



preconcentration factors (73.02-407) were comparable with literature reported studies. The Analytical GREENess calculator (AGREE) analysis confirmed the 0.54 greenness scale, suggesting that the MSPME was environmentally friendly.

Deep eutectic solvent- dispersive liquid-liquid microextraction (DES-DLLME) was the second examined extraction method prior to chromatographic determination of NEOs in vegetable oils. The GREENess of the proposed DES-DLLME was attributed using “greener” more environmentally friendly solvent known as deep eutectic solvents. The method achieved good limit of detection (LOD) ranging from 0.4 to 4.95 ng.  $\mu\text{L}^{-1}$  and limit of quantification (LOQ) ranging from 1.43 to 9.7 ng. $\mu\text{L}^{-1}$ . The method also showed good accuracy (79-119.6 %) and precision (0.1 to 0.9 %). Method greenness was studied using the Analytical GREENess calculator (AGREE) in full tool and the greenness was 0.67 scale.

The DLLME method has proved to be greener compared to the AGREE calculator as reported above. The method detection limits for MSPME were lower compared to that for DES-DLLME. The MSPME also shows the high preconcentration factors than the DES-DLLME. The accuracy for the DES-DLLME was good and higher compared to that for MSPME. Both the methods were conducted under room temperature. The precision for DES-DLLME was lower compared to that of MSPME which shows that DES-DLLME is more sensitive than the MSPME.

## Table of Content

DECLARATION .....	2
DEDICATION .....	4
ACKNOWLEDGEMENTS .....	5
MANUSCRIPTS AND BOOK CHAPTERS .....	6
CONFERENCE(S) .....	7
ABSTRACT .....	8
LIST OF FIGURES.....	14
LIST OF TABLES .....	16
LIST OF EQUATIONS.....	17
LIST OF ABBREVIATIONS AND ACRONYMS .....	18
CHAPTER I (INTRODUCTION).....	22
PREAMBLE .....	22
<b>1.1. Background</b> .....	22
<b>1.2. Problem statement</b> .....	27
<b>1.3. Aim and objectives.</b> .....	28
<b>1.3.1 Aim</b> .....	28
<b>1.3.2 Specific objectives</b> .....	29
<b>1.4. Justification of the study</b> .....	30
<b>1.5. Hypothesis</b> .....	31
<b>1.6. Research questions</b> .....	31
<b>1.7. Dissertation outline</b> .....	33
References .....	34
CHAPTER II (LITERATURE REVIEW).....	39
PREAMBLE .....	39
<b>2.1 Background</b> .....	39
<b>2.1.1 Neonicotinoid pesticides</b> .....	39
<b>2.1.2 Pesticides contamination on plants</b> .....	43
<b>2.1.3. Effects of neonicotinoid pesticides in humans and insects</b> .....	45
<b>2.2 Determination of NEOs in food samples</b> .....	47
<b>2.2.1 Liquid-liquid extraction</b> .....	49
<b>2.2.2 Solid phase extraction</b> .....	57
<b>2.2.3 Optimization of the influential parameters of sample preparation methods</b> .....	69
<b>2.2.3.1. Univariate optimization</b> .....	70
<b>2.2.3.2. Multivariate optimization</b> .....	70
<b>2.2.3.2.1. Screening (1<sup>st</sup> order)</b> .....	70

2.2.3.2.2.	<i>Further optimization (2<sup>nd</sup> order)</i> .....	70
2.2.3.2.3.	Overview summary of sample preparation methods.....	71
2.2.3.1	<i>Univariate vs multivariate</i> .....	72
2.2.3.2	<i>Chromatographic determination of NEOs over the 10 years</i> .....	72
2.3	Conclusion.....	75
	References.....	77
CHAPTER III.....		93
Development of the magnetic solid phase microextraction method for the determination of neonicotinoid pesticides from vegetable oils.....		93
Abstract.....		93
3.1	Background .....	94
3.2	Experimental procedure.....	96
3.2.1.	<i>Reagents, materials, and samples</i> .....	96
3.2.2.	<i>High performance liquid chromatography coupled with diode array detector (HPLC-DAD) instrumentation</i> .....	97
3.2.3.	<i>Preparation calibration standards</i> .....	97
3.2.4.	<i>Cleaning of glassware</i> .....	97
3.3	Synthesis of magnetic nanocomposite ( $Fe_3O_4$ , $Fe_3O_4@Al_2O_3$ , $Fe_3O_4@Al_2O_3/AC$ , AC) .....	98
3.3.1.	<i>Magnetite (<math>Fe_3O_4</math>)</i> .....	98
3.3.2.	<i><math>Fe_3O_4@Al_2O_3</math> nanocomposite</i> .....	99
3.3.3.	<i><math>Fe_3O_4@Al_2O_3/AC</math> nanocomposites</i> .....	99
3.4	Characterisation of the magnetic nanocomposites.....	100
3.4.1.	<i>Fourier transform infrared spectrometry (FTIR)</i> .....	100
3.4.2.	<i>Powdered X-ray diffraction (PXRD)</i> .....	100
3.4.3.	<i>Ultraviolet visible spectroscopy (UV-Vis)</i> .....	100
3.4.4.	<i>Transmission electron microscopy (TEM)</i> .....	101
3.4.5.	<i>Scanning electron microscope coupled to energy dispersive X-ray spectroscopy (SEM-EDS)</i> .....	101
3.4.6.	<i>Thermogravimetric analysis (TGA)</i> .....	101
3.5	Optimization .....	101
3.5.1.	<i>Univariate optimization</i> .....	101
3.5.2.	<i>Multivariate optimization</i> .....	103
3.5.2.1.	<i>Full factorial design (FFD)</i> .....	103
3.5.2.2.	<i>Response surface methodology (RSM)</i> .....	103
3.6	Magnetic solid phase microextraction (MSPME) procedure .....	104
3.7	Method validation.....	105

3.7.1.	<i>Equations for figure of merits</i> .....	106
3.8	Application of MSPME in real commercial vegetable oil samples.....	107
3.9	Reusability and regeneration studies.....	107
3.10	Results and discussion.....	107
3.10.1.	<i>Characterisation of the magnetic nanocomposites</i> .....	107
3.11.	Optimization.....	115
3.12.	Method validation.....	120
3.13.	Comparison of method performance other reported methods.....	121
3.14.	Matrix effect.....	125
3.15.	Enrichment factor.....	126
3.16.	Method greenness assessment.....	127
3.17.	Application of MSPME method in real samples.....	128
3.18.	Reusability and regeneration.....	131
3.19.	Conclusion.....	132
	References.....	134
	CHAPTER IV (MANUSCRIPT 2).....	145
	Abstract.....	145
4.1.	Background.....	146
4.2.	Experimental procedure.....	148
4.2.1.	<i>Reagents, materials, and samples</i> .....	148
4.2.2.	<i>High performance liquid chromatography coupled with diode array detector (HPLC-DAD) instrumentation</i> .....	149
4.2.3.	<i>Preparation calibration standards</i> .....	149
4.2.4.	<i>Cleaning of glassware</i> .....	149
4.2.5.	<i>Synthesis of deep eutectic solvents (DESs)</i> .....	150
4.3.	Characterization of deep eutectic solvents.....	151
4.3.1.	<i>Fourier transform infrared spectrometer (FTIR)</i> .....	151
4.3.2.	<i>Nuclear magnetic resonance spectrometer (NMR)</i> .....	152
4.4.	Preparation of vegetable oil samples.....	153
4.5.	Dispersive liquid-liquid microextraction method.....	153
4.6.	Optimization.....	154
4.6.1.	<i>Univariate optimization</i> .....	154
4.6.2.	<i>Multivariate optimization</i> .....	155
4.6.3.	<i>Full factorial design (FFD)</i> .....	155
4.6.4.	<i>Response surface methodology</i> .....	156
4.7.	Results and discussion.....	158

4.7.1. <b>Characterization</b> .....	158
4.8. <b>Univariate optimization: DES type, sample volume and eluting solvent selection</b> .....	169
4.9. <b>Response surface methodology (RSM)</b> .....	172
4.10. <b>Method validation</b> .....	175
4.11. <b>Comparison of this method with other reported methods</b> .....	176
4.12. <b>Matrix effect</b> .....	179
4.13. <b>Assessment of method greenness</b> .....	180
4.14. <b>Application of DES-DLLME in real vegetable oils</b> .....	181
4.15. <b>Conclusion</b> .....	185
<b>References</b> .....	186
CHAPTER V (Overall conclusion & future recommendations).....	198
5.1 <b>Overall conclusion</b> .....	198
5.2 <b>Future recommendations</b> .....	199
APPENDIX.....	201

## LIST OF FIGURES

---

<b>FIGURE 1. 1:</b> GENERAL OVERVIEW OF CHEMICAL COMPOSITION AND CONTAMINANTS OF VEGETABLE OILS.....	23
<b>FIGURE 1. 2:</b> ILLUSTRATION OF DAMAGE CAUSED BY PESTS ON CROPS. ....	24
<b>FIGURE 1. 3:</b> APPLICATION OF PESTICIDES.....	24
<b>FIGURE 1. 4:</b> THREE SUBGROUPS OF NEONICOTINOID PESTICIDES.....	27
<b>FIGURE 2. 1:</b> REPRESENTATION OF FOUR PHARMACOPHORES OF THE NEONICOTINOID PESTICIDES STRUCTURE.....	41
<b>FIGURE 2. 2:</b> GENERAL PESTICIDES CYCLE BETWEEN THE ENVIRONMENT AND CROPS. ....	44
<b>FIGURE 2. 3:</b> SOME OF THE FACTORS AND MECHANISMS HAVING IMPACT ON PESTICIDES ACCUMULATION IN DIFFERENT SAMPLES AND THEIR PROPERTIES.....	45
<b>FIGURE 2. 4:</b> NEONICOTINOID ACETYLCHOLINE RECEPTORS ACTION IN THE PRESENCE OF ACETYLCHOLINE AND A NEONICOTINOID SUBSTANCE. ....	46
<b>FIGURE 2. 5:</b> OVERVIEW OF SAMPLE PREPARATION METHODS AND THEIR MINIATURIZED METHODS.....	48
<b>FIGURE 2. 6:</b> PRINCIPLES OF DESIGN OF EXPERIMENT. ....	69
<b>FIGURE 2. 7:</b> STUDIES REPORTED ON SAMPLE PREPARATION METHODS FROM 2013 TILL PRESENT. ....	72
<b>FIGURE 2. 8:</b> REPORTED DETECTION TECHNIQUES FROM 2013 UNTIL PRESENT.....	74
<b>FIGURE 2. 9:</b> DIFFERENT DETECTORS PREFERRED OVER THE YEARS (2013 TILL PRESENT) 75	
<b>FIGURE 3. 1:</b> SCHEMATIC DIAGRAM OF MAGNETIC SOLID PHASE MICROEXTRACTION PROCEDURE.....	105
<b>FIGURE 3. 2:</b> FTIR SPECTRA FOR (A) AC, (B) $Fe_3O_4$ , (C) $Fe_3O_4@Al_2O_3$ AND (D) $Fe_3O_4@Al_2O_3/AC$ .....	109
<b>FIGURE 3. 3:</b> PXRD SPECTRA FOR THE SYNTHESISED NANOCOMPOSITE (A) $Fe_3O_4@Al_2O_3$ , (B) $Fe_3O_4@Al_2O_3/AC$ , (C) $Fe_3O_4$ AND (D) AC.....	110
<b>FIGURE 3. 4:</b> REPRESENTATION OF THE UV RESULTS (A) AC, (B) $Fe_3O_4$ , (C) $Fe_3O_4@Al_2O_3$ , AND (D) $Fe_3O_4@Al_2O_3/AC$ . ....	111
<b>FIGURE 3. 5:</b> TEM RESULTS FOR (A) $Fe_3O_4$ NANOPARTICLES, (B) $Fe_3O_4@Al_2O_3$ , (C) $Fe_3O_4@Al_2O_3/AC$ AND (D) AC.....	113
<b>FIGURE 3. 6:</b> SEM-EDS SPECTRUM FOR (A) $Fe_3O_4$ NANOPARTICLES, (B) $Fe_3O_4@Al_2O_3$ , (C) $Fe_3O_4@Al_2O_3/AC$ AND (D) AC. ....	114
<b>FIGURE 3. 7:</b> TGA RESULTS FOR (A) $Fe_3O_4$ NANOPARTICLES, (B) $Fe_3O_4@Al_2O_3$ , (C) $Fe_3O_4@Al_2O_3/AC$ AND (D) AC.....	115
<b>FIGURE 3. 8:</b> EFFECT OF SOLVENT TYPE (MEOH, ACN) AND SAMPLE VOLUME ON PRECONCENTRATION FACTOR.....	116
<b>FIGURE 3. 9:</b> EFFECT OF ADSORBENT TYPE ON EXTRACTION RECOVERIES .....	117
<b>FIGURE 3. 10:</b> PARETO CHARTS RESULTS FOR FFD.....	118
<b>FIGURE 3. 11:</b> RESPONSE SURFACE 3D PLOTS .....	119
<b>FIGURE 3. 12:</b> MATRIX EFFECTS STUDIED FOR DIFFERENT ANALYTES FROM SELECTED VEGETABLE OILS. ....	126
<b>FIGURE 3. 13:</b> ENRICHMENT FACTOR EFFECT ON SELECTED VEGETABLE OILS. ....	126
<b>FIGURE 3. 14:</b> DEVELOPED MSPME METHOD AGREE PICTOGRAM.....	127

<b>FIGURE 3. 15:</b> CHROMATOGRAMS OF REAL COMMERCIAL VEGETABLE OILS AND SPIKED VEGETABLE OILS <b>(A)</b> REAL SAMPLE, <b>(B)</b> ANALYTES STANDARD, <b>(C)</b> SPIKED REAL SAMPLE 40 NG.L <sup>-1</sup> AND <b>(D)</b> SPIKED REAL SAMPLE 80 NG.L <sup>-1</sup> . .....	130
<b>FIGURE 3. 16:</b> REUSABILITY CYCLES FOR Fe <sub>3</sub> O <sub>4</sub> @Al <sub>2</sub> O <sub>3</sub> /AC NANOCOMPOSITE.....	132
<b>FIGURE 4. 1:</b> FOURIER TRANSFORM INFRARED SPECTROMETER INSTRUMENT .....	152
<b>FIGURE 4. 2:</b> NUCLEAR MAGNETIC RESONANCE SPECTROSCOPY INSTRUMENT. ....	153
<b>FIGURE 4. 3:</b> GENERAL REPRESENTATION OF DES-DLLME METHOD.....	154
<b>FIGURE 4. 4:</b> SPECTRUM FOR DES 1 AND ITS REAGENTS. (A) ETHYLENE GLYCOL (EG), (B) CHOLINE CHLORIDE (CCL) AND (C) DES 1.....	160
<b>FIGURE 4. 5:</b> SPECTRUM FOR DES 2 AND ITS REAGENTS; (A) CHOLINE CHLORIDE (CCL), (B) ETHYLENE GLYCOL (EG) AND (C) DES 2 .....	161
<b>FIGURE 4. 6:</b> SPECTRUM FOR DES 3 AND ITS REAGENTS; (A) DES 3, (B) CHOLINE CHLORIDE (CCL) AND (C) UREA.....	163
<b>FIGURE 4. 7:</b> <b>DES 1</b> <sup>13</sup> C NMR SPECTRUM.....	164
<b>FIGURE 4. 8:</b> PROTON NMR FOR <b>DES 1</b> .....	165
<b>FIGURE 4. 9:</b> <b>DES 2</b> <sup>13</sup> C NMR SPECTRUM.....	166
<b>FIGURE 4. 10:</b> PROTON NMR FOR <b>DES 2</b> .....	167
<b>FIGURE 4. 11:</b> <b>DES 3</b> <sup>13</sup> C NMR SPECTRUM.....	168
<b>FIGURE 4. 12:</b> PROTON NMR FOR <b>DES 3</b> .....	169
<b>FIGURE 4. 13:</b> EFFECT OF DES TYPE VERSUS SAMPLE VOLUME.....	170
<b>FIGURE 4. 14:</b> EFFECT OF ELUTING SOLVENT TYPE. ....	171
<b>FIGURE 4. 15:</b> PARETO CHARTS FOR <b>(A)</b> ACT, <b>(B)</b> IMI, <b>(C)</b> TCL AND <b>(D)</b> TMX. ....	172
<b>FIGURE 4. 16:</b> SURFACE PLOTS FOR ELUENT VOLUME VERSUS ELUTING TIME <b>(A)</b> ACT, <b>(B)</b> IMI, <b>(C)</b> TCL AND <b>(D)</b> TMX. ....	174
<b>FIGURE 4. 17:</b> EFFECT OF MATRIX EFFECT IN SELECTED VEGETABLE OIL.....	180
<b>FIGURE 4. 18:</b> AGREE PICTOGRAM FOR DLLME.....	181
<b>FIGURE 4. 19:</b> CHROMATOGRAMS OF REAL COMMERCIAL VEGETABLE OILS AND SPIKED VEGETABLE OILS <b>(A)</b> REAL SAMPLE, <b>(B)</b> ANALYTES STANDARD, <b>(C)</b> SPIKED REAL SAMPLE 50 NG.L <sup>-1</sup> AND SPIKED REAL SAMPLE 300 NG.L <sup>-1</sup> . ....	184

## LIST OF TABLES

---

<b>TABLE 2. 1:</b> PHYSICAL AND CHEMICAL PROPERTIES OF SOME OF THE MOST COMMON COMMERCIAL NEONICOTINOID PESTICIDES REPORTED.....	42
<b>TABLE 2. 2:</b> OVERVIEW OF LLE AND THEIR MINIATURIZED METHODS REPORTED BETWEEN 2013-2023. ....	53
<b>TABLE 2. 3:</b> AN OVERVIEW OF SOLID PHASE EXTRACTION AND THEIR MINIATURIZED METHODS REPORTED FOR EXTRACTION OF NEOs FROM 2013 TO 2023. QUECHERS A TYPE OF DISPERSIVE SOLID PHASE EXTRACTION METHOD REPORTED USED FOR EXTRACTION OF THE NEONICOTINOID PESTICIDES IN FOOD SAMPLES. ....	61
<b>TABLE 3. 1:</b> FFD PARAMETERS .....	103
<b>TABLE 3. 2:</b> RSM PARAMETERS .....	104
<b>TABLE 3. 3:</b> ANALYTES LINEARITY .....	121
<b>TABLE 3. 4:</b> COMPARISON OF MSPME WITH OTHER REPORTED METHODS IN EDIBLE VEGETABLE OILS. ....	123
<b>TABLE 3. 5:</b> APPLICATION OF THE DEVELOPED MSPME IN SELECTED VEGETABLE OILS ..	128
<b>TABLE 3. 6:</b> DIFFERENT CONCENTRATIONS STUDIED .....	129
<b>TABLE 4. 1:</b> FFD SCREENING PARAMETERS.....	156
<b>TABLE 4. 2:</b> RESPONSE SURFACE METHODOLOGY PARAMETERS.....	158
<b>TABLE 4. 3:</b> REPRESENTATION OF THE CALIBRATION EQUATIONS AND CORRELATION COEFFICIENTS OF EACH ANALYTE.....	175
<b>TABLE 4. 4:</b> COMPARISON OF THE DEVELOPED METHOD WITH OTHER REPORTED METHODS .....	177
<b>TABLE 4. 5:</b> CONCENTRATION LEVELS OF THE NEOs IN SELECTED VEGETABLE OIL SAMPLES. ....	182
<b>TABLE 4. 6:</b> DIFFERENT CONCENTRATIONS STUDIED IN FOUR VEGETABLE OILS.....	183



## LIST OF EQUATIONS

---

EQUATION 3. 1 .....	106
EQUATION 3. 2 .....	106
EQUATION 3. 3 .....	106
EQUATION 3. 4 .....	106
EQUATION 3. 5 .....	106
EQUATION 3. 6 .....	106
EQUATION 3. 7 .....	106
EQUATION 3. 8 .....	107
EQUATION 3. 9 .....	120
EQUATION 3. 10 .....	121
EQUATION 3. 11 .....	121
EQUATION 3. 12 .....	121
EQUATION 4. 1 .....	157
EQUATION 4. 2 .....	157
EQUATION 4. 3 .....	157
EQUATION 4. 4 .....	157
EQUATION 4. 5 .....	157
EQUATION 4. 6 .....	158
EQUATION 4. 7 .....	158
EQUATION 4. 8 .....	173
EQUATION 4. 9 .....	173
EQUATION 4. 10 .....	173
EQUATION 4. 11 .....	173

## LIST OF ABBREVIATIONS AND ACRONYMS

---

AC – Activated carbon  
ACN - Acetonitrile  
ACT – Acetamiprid  
AGREE - Analytical GREEness  
ANOVA - Analysis of variance  
BET – Brunauer-Emmett-Teller  
IMI – Imidacloprid  
CAC - Codex Alimentarius Commission  
CCD – Central composite design  
CCPR - Codex Committee on Pesticides Residues  
CCI – Choline chloride  
CHC – Hexachlorocyclohexane  
CHCl<sub>3</sub> – Chloroform  
CLO – Clothianidin  
COF - Covalent organic framework  
CMC - Critical micelle concentration  
CPE - Cloud point extraction  
CPT - Cloud point temperature  
CRM – Certified Reference Material  
DAD – Diode array detector  
DCM – Dichloromethane  
DDT – Dichlorodiphenyltrichloroethane  
DES – Deep eutectic solvent  
DIN – Dinotefuran  
DLLME – Dispersive liquid-liquid microextraction  
DMSO - Dimethyl sulfoxide-d<sub>6</sub>  
DoE – Design of experiment  
d-SPE – Dispersive solid phase extraction  
EG – Ethylene glycol  
EDS - Energy-dispersive X-ray spectroscopy  
EF – Enrichment factor

EPA – Emergency protection agency  
ESI – Electrospray ionization  
EtOH – Ethanol  
EU – European union  
FA - Formic acid  
FAO – Food and agriculture organization  
FFD – Full factorial design  
FLD – Fluorescence detector  
FTIR – Fourier-transform infrared spectroscopy  
GAC - green analytical chemistry  
TCL – Thiacloprid  
TMX – Thiamethoxam  
NEOs – Neonicotinoid pesticides  
GC-MS – Gas chromatography mass spectrometry  
GO - Graphene oxide  
HBA – Hydrogen bond acceptor  
HBD – Hydrogen bond donor  
HCl – Hydrochloric acid  
HF-MMLLE - Hollow-fibre microporous  
HF-LPME - Hollow-fiber liquid-phase microextraction  
HPLC – High performance liquid spectrometry  
H<sub>2</sub>SO<sub>4</sub> – Sulfuric acid  
IR – Infrared  
IUPAC - International Union of Pure and Applied Chemistry  
K<sub>oc</sub> - Organic carbon partition coefficient  
K<sub>ow</sub> - Octanol water partition coefficient  
LA – Levulinic acid  
LLE – Liquid-liquid extraction  
LOD – Limit of detection  
LOQ – Limit of quantification  
LPME - Liquid phase microextraction  
MAE – Microwave-assisted extraction  
ME – Matrix effect  
MEKC - Micellar electrokinetic chromatography

MeOH – Methanol  
MLLE - Micro-liquid-liquid extraction  
MNP - Magnetic nanoparticles  
MOF - Metal-organic framework  
MRLs – Maximum residue limits  
MS – Mass spectrometry  
MS/MS - Triple quadrupole tandem mass spectrometry  
MSPD - Matrix solid-phase dispersion  
NA – Not applicable  
nAChRs - Nicotinic acetylcholine receptors  
NaOH – Sodium hydroxide  
NEOs – Neonicotinoids  
NIT – Nitenpyram  
NMR – Nuclear magnetic resonance  
NP – Nanoparticles  
NR – Not reported  
pK<sub>a</sub> - Dissociation constant  
PFE – Pressurised fluid extraction  
ppb - Parts per billion  
ppm - Parts per million  
ppt - Parts per trillion  
PSA - Primary Secondary Amine  
PXRD – Powder X-Ray diffraction  
QqQ - triple quadrupole  
QuEChERS - Quick, easy, cheap, effective, rugged, and safe  
R – Recovery  
RF - Radio frequency  
RSD – Relative standard deviation  
RSM – Response surface methodology  
RTIL – Room temperature ionic liquid  
SD – Standard deviation  
SED - Secondary electron detector  
SEM – Scanning electron microscopy  
SPE – Solid phase extraction

SPME - Solid-phase micro-extraction  
SULLE - Salting-out assisted liquid-liquid extraction  
S/N – Signal to noise ratio  
TEM – Transmission electron microscopy  
TGA – Thermogravimetric analysis  
UA-LLME - Ultrasound assisted liquid-liquid microextraction  
UHPLC - Ultrahigh performance liquid  
UPLC - Ultra-high performance liquid chromatography  
US – United states  
VA-LLME - Vortex assisted liquid-liquid microextraction  
UV-Vis – Ultraviolet visible spectroscopy  
WHO – World health organisation

## CHAPTER I (INTRODUCTION)

---

### PREAMBLE

This chapter entails more information about the background of vegetable oils, including their origin, the pesticides, and an extensive study on them. The toxicological effect of the pesticides, which is the backbone of the study of these vegetable oils, have been outlined in this chapter. This chapter also focuses on the study's problem statement, aims and objectives, research questions to be addressed by this study, justification, hypothesis, and thesis outline. Furthermore, a brief outline of the whole thesis is discussed in this chapter.

### 1.1. Background

Various vegetable oils have been regarded as an important part of the human daily diet since they provide energy and essential fatty acids, both of which are necessary for the effective development of the human body [1]. The most known vegetable oils include olives, avocado, sunflower, rapeseed, and corn. These vegetable oils contain saturated and unsaturated fatty acids, triglycerides, antioxidants, and other fat-soluble vitamins as indicated in **Figure 1.1** below. Moreover, these oils have been used widely in the cooking and food processing industries because of their high nutritional value [2]. These oils are also used in pharmaceutical and cosmetic/personal products. Vegetable oils are industrially processed to optimise consumer acceptance by removing components that can negatively affect appearance, taste, nutritional value and shelf life stability [3]. The production and consumption of these vegetable oils have increased over the years globally [4]. The quality of these vegetable oils is more critical to both oil producers and consumers [5]. Approximately 98 % of these vegetable oils are triacylglycerols, varying in complexity, substitution order, and the degree of saturation of fatty acid chains. Other compounds like sugars, sterols, carotenes, phospholipids, esters, and lipid-soluble vitamins constitute the remaining 2 % [6].

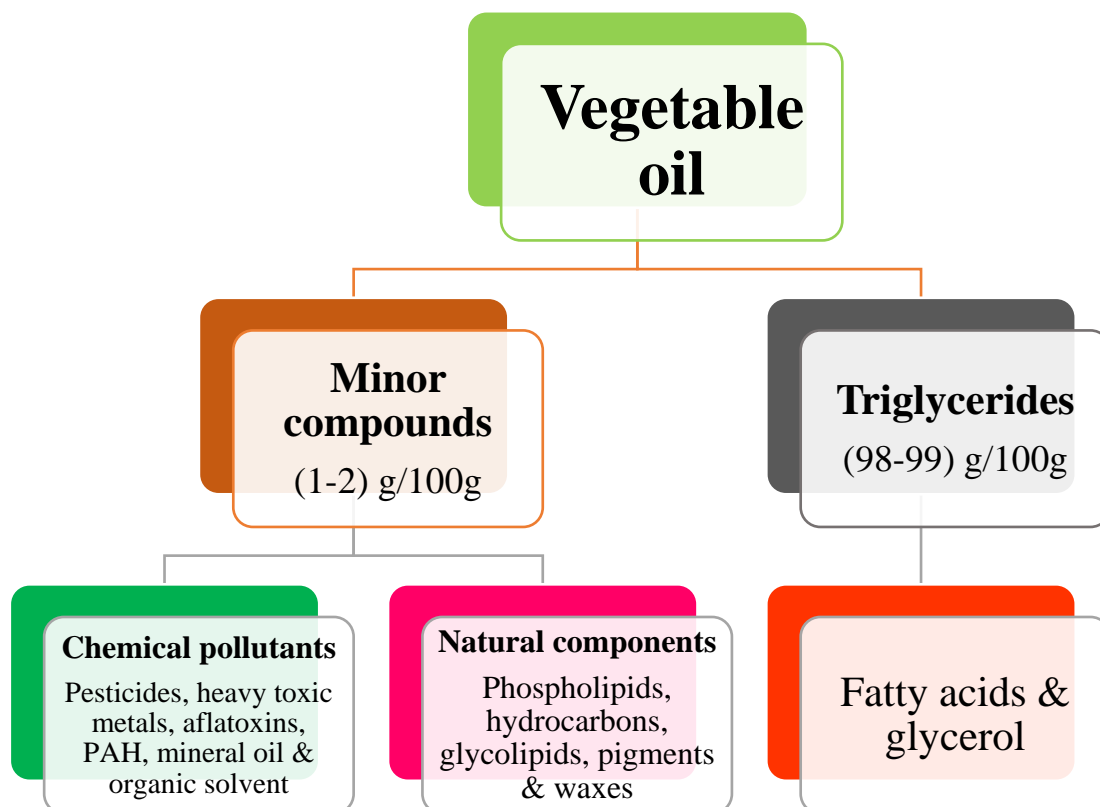


**Figure 1. 1:** General overview of chemical composition and contaminants of vegetable oils [2].

Additionally, contributing to the components of the compounds found in vegetable oils, some toxic contaminants that are detrimental to human health have been reported. This study focuses on the presence neonicotinoid pesticides (NEOs) as organic pollutants in these edible vegetable oils. To better control production and good yield of vegetable seeds used for making the vegetable oils, the whole plantation process needs to be well monitored. Furthermore, good agricultural practices and measures should be taken to control the development of crops to ensure their safety [7]. Pesticides have been used for the longest time by farmers to help control the development of their crops and good yield production. These pesticides have been used for controlling weeds, insect infestation and diseases, as shown in **Figure 1.2** below [8] [9]. The use of pesticides has been increasing in the agri-food sector with the vision of increasing the production quality of vegetable oils. The most common reported type of pesticides are the neonicotinoid pesticides. These pesticides can easily accumulate in the environment matrices, plants and animals because of their high-fat solubility, chemical stability and long-distance migration, especially in animals and plant adipose tissues [10]. Many studies have shown that these NEOs are associated with many common chronic diseases, including cancer, chronic respiratory

diseases, neurodegenerative diseases, cardiovascular diseases, endocrine disorders and diabetes.



**Figure 1. 2:** Illustration of damage caused by pests on crops [11] [12] [13].

Due to pest infestation and the damage caused by them, there is a need to employ pesticides to mitigate/reduce pest infestations, monitor crop growth and production. **Figure 1.3** shows the application process of pesticides for pest control. Moreover, neonicotinoids are soluble in water and can be systemically absorbed by plants via the xylem. Additionally, when employed as seed treatments, they are durable in the environment and transfer to residues in the pollen and nectar of treated plants. These insecticides are extremely hazardous to aquatic species and pollute waterways/ waterbodies [14].



**Figure 1. 3:** Application of pesticides [15].

Due to the toxicity effects of these pesticides on human health and the environment, different organisations globally have set the tolerable maximum residue



limits (MRLs) of these NEOs to monitor human health while regulating higher yields [16]. This was implemented to monitor the daily acceptable intake of these vegetable oils consisting of the trace amount of these contaminants. Countries like Japan, China and the US have their MRLs for oil producing crops at  $0.04 \text{ mg.kg}^{-1}$ ,  $0.05\text{-}0.5 \text{ mg.kg}^{-1}$  and  $0.05\text{-}3.5 \text{ mg.kg}^{-1}$ , respectively. Due to health risks caused by these NEOs, some countries have restricted their usage [17].

Moreover, implementing the MRLs was due to the risks they pose to public health and contamination by unwanted and harmful substances, which causes financial losses and lowers the revenues of products made from vegetable oil in international trade. The bodies that establish these MRLs are government and international organisations like World Health Organization (WHO) and Food and Agriculture Organization (FAO), as it has been reported for the pesticides [18]. Moreover, it is worth noting that the NEOs mostly accumulate in crops via plant absorption of NEOs used for crop protection from insects/pests, fungi infection or any microbial infection, and weeds at different stages of cultivation that can affect the high-yield production of these crops. For instance, the MRL for dichlorodiphenyltrichloroethane (DDT) and hexachlorocyclohexane (HCH) in soybeans is set at  $0.05 \text{ mg/kg}$  [18]. The NEOs, which have been regarded as food-borne contaminants, are most common in these vegetable oils. The occurrence of these food contaminants in different food products is not only a health concern but also results in economic losses and image damage [4]. These compounds can also be found in other foods derivatives such as bread, bakery items, margarine, similar foods, and meat, among others [19].

Since the discovery of NEOs in the late 80s, their large-scale application for crop protection has been through a wide range of various crops, which includes vegetables and fruits, veterinary products, and biocides, to invertebrate pest control in fish farming among others. It was reported that their usage has greatly increased globally, contributing to about 25 % of the market in 2014. This is good news for the production industry of agrochemicals (pesticides, herbicides and fungicides) and increased crop protection from insect infestation, while increasing crop production [20]. Since the whole process concerns growing the economy and eliminating or reducing unemployment, such production is economically friendly. These pesticides are persistent in the environment [21]. Moreover, NEOs have a low acute toxicity in

vertebrates but a substantial acute toxicity in insects due to variations in these receptors [22]. The insects' neural systems are fully disrupted by compounds' ongoing action, leading to sublethal effects such as rejection, lowered or cessation of feeding, decreased or cessation of reproductive activity, reduced mobility, and even death [23]. These NEOs have been reported to exist in different groups based on the different parental compound groups. There is a total of thirteen of these NEOs, however, only seven have been reported to be more abundant. Out of the seven most abundant pesticides, we have them divided into three subgroups based on the difference in parent groups, and they have been outlined in **Figure 1.4** [24]. The "First generation group" is distinguished by the chloropyridine group, the "Second generation group" is indicated by the chlorothiazole group and the "Third generation group" is characterised by the 3-tetra-hydrofuran ring [24].

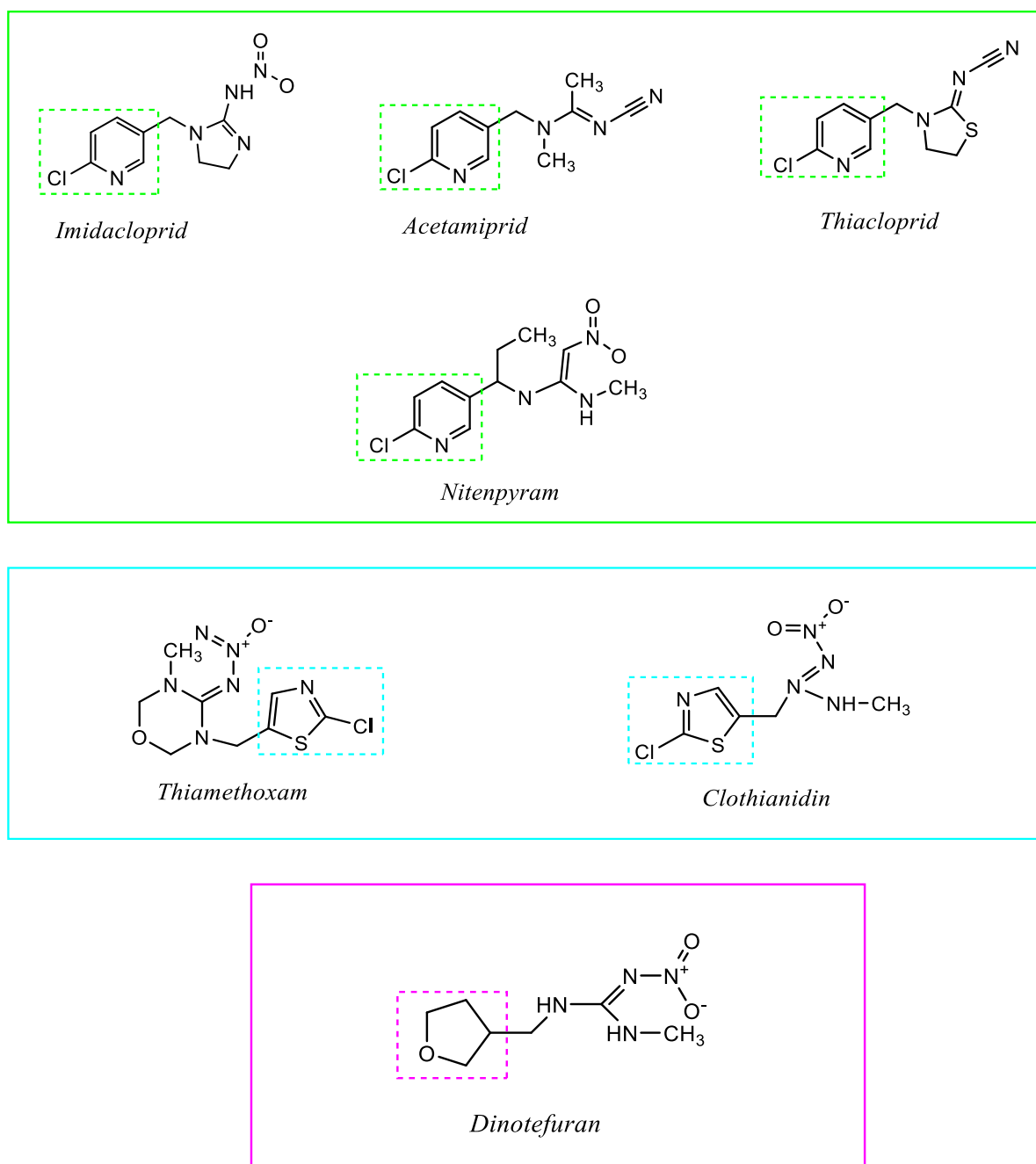


**Figure 1. 4:** Three subgroups of neonicotinoid pesticides [24].

## 1.2. Problem statement

The current study focuses on developing sample analytical preparation methods which involve “greener” extraction procedures followed by chromatographic techniques for determining NEOs in various vegetable oils of interest. This study's motive is due to the toxic effects of these pesticides on human and animal health, and adverse environmental effects. It is also worth indicating that these pesticides are found in our daily food products that form our diet, such as margarine, meat, processed

dairy products, vegetable oils, among others. However, these compounds are toxic and if consumed in certain amounts that surpasses the threshold limits the pose serious health effects in both humans and animals; therefore, there is a need to monitor daily dose exposure, and precautionary measures should be taken into consideration when consuming food containing these pollutants [25].

Furthermore, different sample preparation methods have been developed and reported for the determination of these contaminants. The reported conventional methods have several disadvantages such as being cost-effective, using large amounts of organic solvents, laboriousness, not environmentally friendly and require additional or coupled sample pre-treatment methods for sample clean-up. Since the pesticides are poorly volatile with high polarity, gas chromatography with mass spectrometry (GC-MS) has been utilised as a sensitive and conventional technique, thus requirement of an additional sample preparation step known as the derivatisation step before sample quantification, which involved additional use of organic solvents [26] [27]. The derivatisation method is typically performed to change the properties of the sample and analyte for compatibility with detection instrument and achieve better separation and improve method sensitivity [28]. Other chromatographic detection techniques such as liquid chromatography mass spectrometry (LC-MS), use expensive instrumentation and high operating costs [29]. These techniques are not ideal for on-site detection of high-throughput screening of samples, and drawback with the techniques is overcoming matrix interference while retaining sensitivity since majority of samples cannot be directly analysed [30].

### **1.3. Aim and objectives.**

#### **1.3.1 Aim**

This proposed research project aimed to develop simple, greener, and sensitive extraction methods (Deep eutectic solvent-dispersive liquid-liquid micro-extraction and magnetic solid phase microextraction) followed by high-performance liquid chromatography-diode array detector (HPLC-DAD) analysis for determination of the selected NEOs (thiamethoxam, imidacloprid, thiacloprid and acetamiprid) in various vegetable oils.

### 1.3.2 Specific objectives

The specific objectives of the proposed research project were to;

**(i) Develop Magnetic solid-phase microextraction (MSPME) method for preconcentration and extraction of thiamethoxam, imidacloprid, thiacloprid and acetamiprid in vegetable oil samples followed by chromatographic determination.**

- Synthesize and characterize Magnetic nanocomposite adsorbent ( $\text{Fe}_3\text{O}_4@\text{Al}_2\text{O}_3/\text{AC}$ ), using various analytical techniques such as Fourier transform infrared spectrometry (FTIR), Powdered X-ray diffraction (PXRD), Scanning electron microscope coupled to energy dispersive X-ray spectroscopy (SEM-EDS), Thermogravimetric analysis (TGA), Transmission electron microscopy (TEM), Brunauer-Emmett-Teller analysis (BET) and Ultraviolet visible spectroscopy (UV-Vis) among others.
- Apply the synthesised magnetic nanocomposite for development of MSPME method for preconcentration and extraction of thiamethoxam, imidacloprid, thiacloprid and acetamiprid.
- Optimize the proposed MSPME parameters (adsorbent mass, sample pH and volume, extraction time, eluent concentration and volume, solvent type and solvent volume) using chemometrics tools.
- Apply the MSPME procedure at optimum conditions to preconcentrate and quantify the concentrations of thiamethoxam, imidacloprid, thiacloprid and acetamiprid in real vegetable oil samples.
- Quantification using MSPME will be the basis for comparison with literature-reported method studies.

**(ii) Use the developed Deep eutectic solvent-dispersive liquid-liquid micro-extraction for preconcentration and extraction of thiamethoxam, imidacloprid, thiacloprid and acetamiprid in vegetable oil samples followed by chromatographic determination**

- Use various deep eutectic solvents to evaluate the Deep eutectic solvent-dispersive liquid-liquid micro-extraction (DES-DLLME) of thiamethoxam, imidacloprid, thiacloprid and acetamiprid in different vegetable oils.

- Synthesize and characterise the deep-eutectic solvents (DES) using nuclear magnetic resonance (NMR) and Fourier transform infrared spectrometry (FTIR).
- Apply DES-DLLME method for preconcentration and extraction of thiamethoxam, imidacloprid, thiacloprid and acetamiprid.
- Optimize several extraction parameters such as pH of the sample solution, type of DES, DES volume, vortex time, eluting time and eluting solvent using multivariate approach to obtain maximum extraction efficiency of the proposed DES-DLLME method.
- Apply the DES-DLLME procedure to preconcentrate and extract thiamethoxam, imidacloprid, thiacloprid and acetamiprid in vegetable oil samples before chromatographic determination.
- Compare the DLLME method performance with other literature reported preconcentration extraction methods in terms of analytical figure of merits.

#### **1.4. Justification of the study**

Many researchers have adopted different sample preparation methods to determine these neonicotinoid pesticides. The preparation methods adopted suffered from several challenges that led to their lack of application/ elimination or replacement by simpler and greener methods with minimum drawbacks and offer several advantages over conventional methods. Majority of the studies reported in literature were tedious, required large amounts of organic solvents and used reagents that were not environmentally friendly. This research project is driven by the aim of developing “greener” environmentally friendly methods for sample preparation, which only require small volumes “microliter” reagents, utilising waste materials to synthesize adsorbent materials to minimise the toxicity that the waste pose on the environment. The adopted sample preparation methods for this research project were designed to be cost-effective and simple. The adopted sample preparation methods for this research project were cost-effective and simple.

The magnetic solid phase microextraction (MSPME) technique was employed for its several benefits: simple, efficient, cost-effective, and improved selectivity. The MSPME procedure is favoured because the separation of analytes is very simple since the sorbent with analytes of interest is achieved using an external magnetic field, thus

making the extraction quicker and easier [31]. The DES-DLLME has the advantages of being simple, inexpensive, eco-friendly extraction technique, and offers high enrichment factors [32]. The extraction of analytes of interest from the sample matrix was enhanced by adding chlorinated ionic liquids [33].

Most of the procedures outlined in some literature reports such as conventional pressurised-fluid extraction (PFE), microwave-assisted extraction (MAE), SPE (solid phase extraction), LLE (Liquid-liquid extraction etc.) are environmentally unfriendly, have high running costs, arduous due to the analytical matrix's complexity and typically require homogenising samples containing a significant amount of organic and inorganic solvents [34]. The HPLC-DAD employed in this study is a good quantification technique for the selected pesticides, and the LC-MS; an efficient validation detection technique because it is more compatible with green chemistry, more sensitivity with better detection limits. The technique provides several advantages which include robustness, reduced operation costs, higher speed, and gain in sensitivity. The instrument requires small sample volumes for analysis (micro and nano) in a routine analytical lab. Adopting these sample preparation methods (MSPME and DES-DLLME) that are aligned with principles of green chemistry for determining NEOs in vegetable oil samples to assist with establishing daily intake control measures by monitoring presence and quantification of NEOs, development of NEOs legislations and ensuring safe agricultural produce.

## **1.5. Hypothesis**

The developed pre-concentration and extraction methods (MSPME and DES-DLLME) have high tendencies to comply with the principles of green chemistry like being rapid and selective for determining the selected NEOs in vegetable oils.

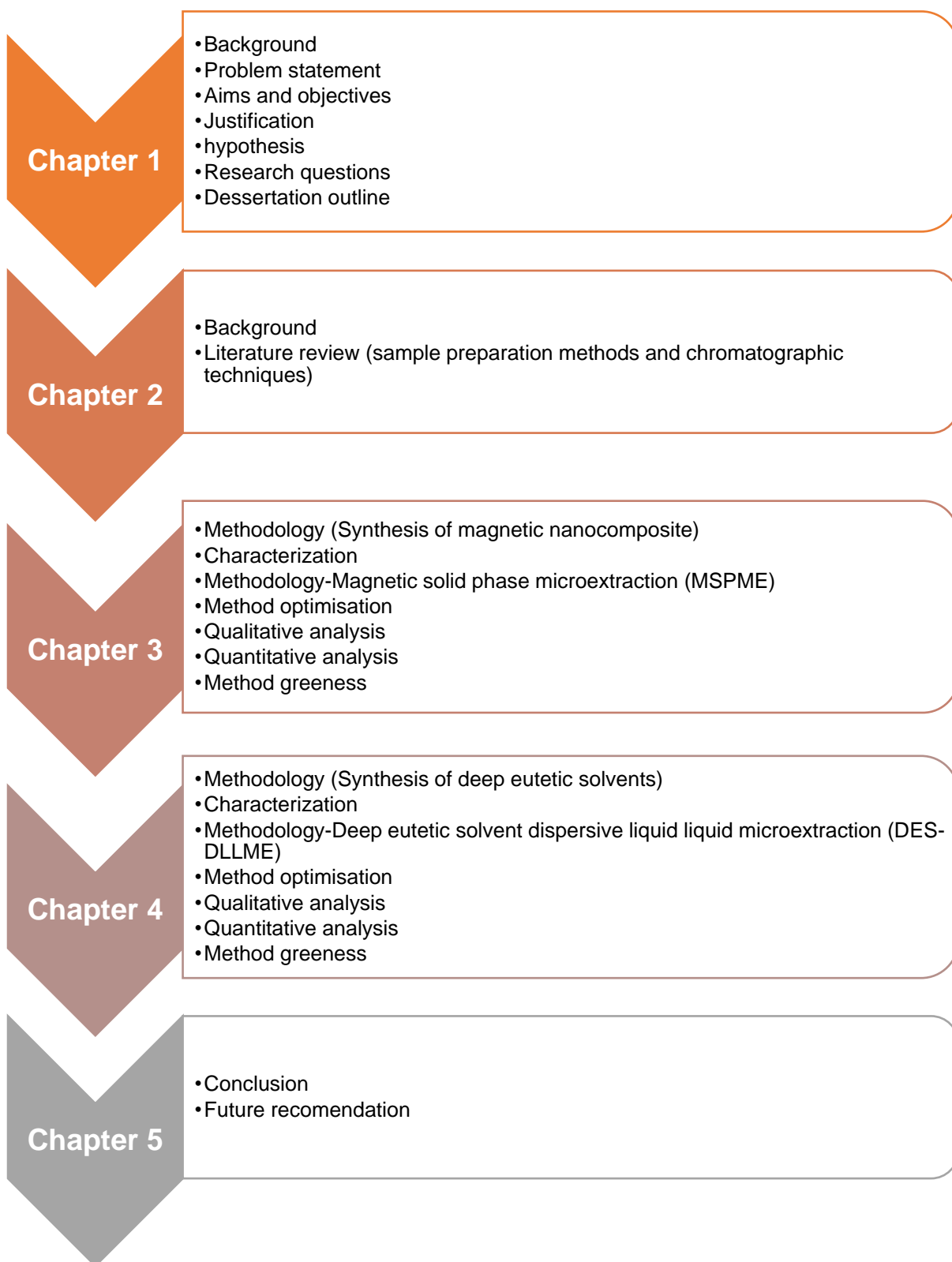
## **1.6. Research questions.**

- I. Will the magnetic nanocomposite be able to preconcentrate the NEOs?
- II. How many times can the magnetic nanocomposite be re-used?
- III. What are the factors that affect the extraction of analytes when using MSPME and DES-DLLME?
- IV. Between MSPME and DES-DLLME, which sample preparation method will have more merits for the extraction of the NEOs from vegetable oils?

V. Which sample preparation method will be greener when assessed by AGREE tool?



## 1.7. Dissertation outline



## REFERENCES

- [1] R. Jamwal, S. Kumari, S. Sharma, S. Kelly, A. Cannavan, and D. Kumar, "Vibrational Spectroscopy Recent trends in the use of FTIR spectroscopy integrated with chemometrics for the detection of edible oil adulteration," *Vib. Spectrosc.*, vol. 113, no. January, p. 103222, 2021, doi: 10.1016/j.vibspec.2021.103222.
- [2] X. Mao, A. Yan, Y. Wan, D. Luo, and H. Yang, "Dispersive solid-phase extraction using microporous sorbent UiO-66 coupled to gas chromatography-tandem mass spectrometry: A QuEChERS-Type method for the determination of organophosphorus pesticide residues in edible vegetable oils without matrix interfer," *J. Agric. Food Chem.*, vol. 67, no. 6, pp. 1760–1770, 2019, doi: 10.1021/acs.jafc.8b04980.
- [3] S. Macmahon, T. H. Begley, and G. W. Diachenko, "Analysis of processing contaminants in edible oils. Part 2. Liquid chromatography-tandem mass spectrometry method for the direct detection of 3-monochloropropanediol and 2-monochloropropanediol diesters," *J. Agric. Food Chem.*, vol. 61, no. 20, pp. 4748–4757, 2013, doi: 10.1021/jf400581g.
- [4] R. Jędrkiewicz, M. Kupska, A. Głowacz, J. Gromadzka, and J. Namieśnik, "3-MCPD: A Worldwide Problem of Food Chemistry," *Crit. Rev. Food Sci. Nutr.*, vol. 56, no. 14, pp. 2268–2277, Oct. 2016, doi: 10.1080/10408398.2013.829414.
- [5] K. Kamikata *et al.*, "Occurrence of 3-MCPD , 2-MCPD and glycidyl esters in extra virgin olive oils , olive oils and oil blends and correlation with identity and quality parameters," *Food Control*, vol. 95, no. June 2018, pp. 135–141, 2019, doi: 10.1016/j.foodcont.2018.07.051.
- [6] M. Azizi-lalabadi, M. Mousavi, Z. Piravi-vanak, and S. Azadmard-damirchi, "MCPD fatty acid esters in vegetable oils : formation , analysis and toxicology," *Journal of Food and Bioprocess Engineering* vol. 1, no. 1, pp. 71–80, 2018.
- [7] E. Sagri *et al.*, "The molecular biology of the olive fly comes of age," *BMC Genomics* vol. 15, no. Suppl 2, 2014.

- [8] H. E. Ramírez-Guerra *et al.*, “Protective Effect of an Edible Tomato Plant Extract / Chitosan Coating on the Quality and Shelf Life of Sierra Fish Fillets,” *Hindawi Journal of Chemistry* vol. 2018, 2018.
- [9] J. Chen, L. Zhang, Q. Li, M. Wang, Y. Dong, and X. Yu, “Comparative study on the evolution of polar compound composition of four common vegetable oils during different oxidation processes,” *Lwt*, vol. 129, no. April, 2020, doi: 10.1016/j.lwt.2020.109538.
- [10] E. Hakme, A. Lozano, C. Ferrer, and A. R. Fern, “Analysis of pesticide residues in olive oil and other vegetable oils,” *Trends in Analytical Chemistry* vol. 100, 2018, doi: 10.1016/j.trac.2017.12.016.
- [11] “Pests Destroy up to 40% of Global Crops and Cost \$220 Billion - Seed World Canada.” <https://germination.ca/pests-destroy-up-to-40-of-global-crops-and-cost-220-billion/> (accessed Jan. 29, 2024).
- [12] “Insect pests of vegetables | Agriculture and Food.” <https://www.agric.wa.gov.au/pest-insects/insect-pests-vegetables> (accessed Jan. 29, 2024).
- [13] “Symptoms and Prevention of Verticillium Wilt Fungus.” <https://www.thespruce.com/verticillium-wilt-fungus-4845966> (accessed Jan. 29, 2024).
- [14] M. A. Farajzadeh, R. Afshar, and A. Akbar, “Determination of neonicotinoid insecticide residues in edible oils by water-induced performance liquid chromatography-diode array,” *RSC Advances* pp. 77501–77507, 2015, doi: 10.1039/c5ra13059j.
- [15] “Pin on Knitted washcloths.” <https://za.pinterest.com/pin/621637554800257954/> (accessed Jan. 29, 2024).
- [16] G. Smaghe, “Neonicotinoids in bees : a review on concentrations , side-effects and risk assessment,” *Ecotoxicology* pp. 973–992, 2012, doi: 10.1007/s10646-012-0863-x.
- [17] L. Chen *et al.*, “Determination of thiamethoxam and its metabolite clothianidin residue and dissipation in cowpea by QuEChERS combining with ultrahigh-

- performance liquid chromatography–tandem mass spectrometry,” *Environ. Sci. Pollut. Res.*, vol. 28, no. 7, pp. 8844–8852, 2021, doi: 10.1007/s11356-020-11164-6.
- [18] D. Zheng *et al.*, “Flowerlike Ni – NiO composite as magnetic solid-phase extraction sorbent for analysis of carbendazim and thiabendazole in edible vegetable oils by liquid chromatography-mass spectrometry,” *Food Chem.*, vol. 374, no. October 2021, p. 131761, 2022, doi: 10.1016/j.foodchem.2021.131761.
- [19] X. Cui *et al.*, “Dietary exposure of general Chinese population to fatty acid esters of 3-monochloropropane-1, 2-diol (3-MCPD) from edible oils and oil-containing foods,” *Food Addit. Contam. - Part A Chem. Anal. Control. Expo. Risk Assess.*, vol. 38, no. 1, pp. 60–69, 2021, doi: 10.1080/19440049.2020.1834151.
- [20] E. Food and S. Authority, “Evaluation of the data on clothianidin , imidacloprid and thiamethoxam for the updated risk assessment to bees for seed treatments and granules in the EU,” no. February, pp. 1–31, 2018, doi: 10.2903/sp.efsa.2018.EN-1378.
- [21] T. Tuzimski and T. Rejczak, “Application of HPLC-DAD after SPE/QuEChERS with ZrO<sub>2</sub>-based sorbent in d-SPE clean-up step for pesticide analysis in edible oils,” *Food Chem.*, vol. 190, pp. 71–79, 2016, doi: 10.1016/j.foodchem.2015.05.072.
- [22] J. Li, D. Liu, T. Wu, W. Zhao, Z. Zhou, and P. Wang, “A simplified procedure for the determination of organochlorine pesticides and polychlorobiphenyls in edible vegetable oils,” *Food Chem.*, vol. 151, pp. 47–52, 2014, doi: 10.1016/j.foodchem.2013.11.047.
- [23] L. Zhao, T. Szakas, M. Churley, and D. Lucas, “Multi-class multi-residue analysis of pesticides in edible oils by gas chromatography-tandem mass spectrometry using liquid-liquid extraction and enhanced matrix removal lipid cartridge cleanup,” *J. Chromatogr. A*, vol. 1584, pp. 1–12, 2019, doi: 10.1016/j.chroma.2018.11.022.
- [24] J. Jiménez-López, E. J. Llorent-Martínez, P. Ortega-Barrales, and A. Ruiz-

- Medina, "Analysis of neonicotinoid pesticides in the agri-food sector: a critical assessment of the state of the art," *Applied Spectroscopy Reviews*, vol. 55, no. 8. Taylor and Francis Inc., pp. 613–646, Sep. 13, 2020. doi: 10.1080/05704928.2019.1608111.
- [25] P. Wang *et al.*, "Multi-residue method for determination of seven neonicotinoid insecticides in grains using dispersive solid-phase extraction and dispersive liquid-liquid micro-extraction by high performance liquid chromatography," *Food Chem.*, vol. 134, no. 3, pp. 1691–1698, 2012, doi: 10.1016/j.foodchem.2012.03.103.
- [26] S. Yang and K. Kwon, "Improvement of a GC – MS analytical method for the simultaneous detection of 3-MCPD and 1, 3-DCP in food," *Food Sci. Biotechnol.*, vol. 27, no. 3, pp. 869–876, 2018, doi: 10.1007/s10068-018-0312-6.
- [27] H. Tsai, J. Hsu, C. Fang, and N. Su, "Determination of glycidyl esters and 3-MCPD esters in edible oils by sample pretreatment with the combination of lipase hydrolysis and modified QuEChERS for GC-MS analysis," 2021.
- [28] W. Kim *et al.*, "Analysis of 3-MCPD and 1, 3-DCP in Various Foodstuffs Using GC-MS," *Journal of Korean Society of Toxicology* vol. 31, no. 3, pp. 313–319, 2015.
- [29] J. Renata, A. Or, J. Namie, and M. Tobiszewski, "Green analytical chemistry introduction to chloropropanols determination at no economic and analytical performance costs?," *Talanta* vol. 147, pp. 282–288, 2016, doi: 10.1016/j.talanta.2015.10.001.
- [30] J. Werner, "Novel deep eutectic solvent-based ultrasounds-assisted dispersive liquid- liquid microextraction with solidification of the aqueous phase for HPLC-UV determination of aromatic amines in environmental samples .," *Microchem. J.*, vol. 153, no. November 2019, p. 104405, 2020, doi: 10.1016/j.microc.2019.104405.
- [31] H. Rezaei, M. Moazzen, N. Shariatifar, and G. J. Khaniki, "Measurement of phthalate acid esters in non-alcoholic malt beverages by MSPE-GC / MS method in Tehran city : *chemometrics*," 2021.

- [32] M. Rezaee, Y. Assadi, and M. M. Hosseini, "Determination of organic compounds in water using dispersive liquid – liquid microextraction," *Journal of Chromatography A* vol. 1116, pp. 1–9, 2006, doi: 10.1016/j.chroma.2006.03.007.
- [33] M. Sajid, "Magnetic ionic liquids in analytical sample preparation: A literature review," *TrAC - Trends Anal. Chem.*, vol. 113, pp. 210–223, 2019, doi: 10.1016/j.trac.2019.02.007.
- [34] I. S. Ibarra, J. A. Rodriguez, C. A. Galán-vidal, A. Cepeda, and J. M. Miranda, "Magnetic Solid Phase Extraction Applied to Food Analysis," *Hindawi Journal of Chemistry* vol. 2015, 2015.

## CHAPTER II (LITERATURE REVIEW)

---

### PREAMBLE

This chapter discusses the qualitative and quantitative techniques reported by researchers in the literature. The neonicotinoid pesticides (NEOs) have been said to be poorly volatile with high polarity. Various methods have been reported for investigation of these types of pesticides wherein the general principle of the methods that have been reported. Sample preparation methods and quantification techniques developed during the investigation of these pesticides are also reported in this chapter. The knowledge and understanding of how these pollutants are introduced in food samples and which methods are the best for sample preparation and quantification of these analytes of interest are discussed at the end of this chapter. The merits and possible limitations of these sample preparation methods are also addressed. Additionally, the analytical performances of the various published sample preparation methods are evaluated in terms of accuracy, detection limit, precision, etc. Moreover, this chapter highlights the gaps in pretreatment and preconcentration methods, chromatographic determination of neonicotinoid pesticides, and possible future developments.

### 2.1 Background

#### 2.1.1 *Neonicotinoid pesticides*

Pesticides used in agricultural practices for pest control, weed control and plant growth regulation were introduced long time ago. The positive effect of these pesticides has been reported. However, during their application, they tend to accumulate in the food via absorption through the roots and leaves. Human consumption of food consisting of these organic pollutants poses some adverse health effects [1]. The neonicotinoids, also known as the NEOs or Neonics were discovered in the late 1980s and their usage has increased worldwide at large scale [2]. The use of these neonicotinoid pesticides results in various environmental problems such as polluting the water streams, affecting soil quality, and being absorbed by the plants. Moreover, the pests are responsible for inhibiting the development and normal growth of the crops, while the weeds are responsible for competing with the crops/ plants in sharing water, sunlight and manure. Additionally, they tend to grow faster than the planted crops whereas diseases infestation tend to destroy a whole crop development

and if left untreated the crops end up dying [3]. Different types of neonicotinoids compounds exist, and they have also been subdivided into three groups based on the differences on main functional groups. In comparison with pesticides in other classes, they have the advantages of being very poisonous to insects, having a wide variety of application options, and being less hazardous to vertebrates.

However, the conventional commercial NEOs, including thiacloprid (TCL), imidacloprid (IMI) , dinotefuran (DIN), nitenpyram (NIT), thiamethoxam (TMX), acetamiprid (ACT) and clothianidin (CLO) are widely used due to their outstanding effectiveness against insects and relatively low toxicity towards humans and other mammals [4]. Neonicotinoids are an inconsistent/ reactive group of chemicals, as seen by their tendency to disintegrate into derivative components in the soil, how they are metabolised in the bodies of insects, and how they negatively affect the bee's metabolism. Four components are shared by the chemical structures of neonicotinoids developed in the recent decades: (1) Hydro-heterocyclic, or guanidine/amidine groups, (2) elastic bonds, (3) aromatic heterocyclic groups, and (4) electron withdrawing groups as shown in **Figure 2.1** [5]. It is also feasible to divide these subclasses further into nitroguanidine and cyanoamidine. Due to their chemical structures, clothianidin have been counted the most toxic substances to honeybees [6]. Nitroguanidine-type neonicotinoids are substantially more polar and reactive due to the presence of oxygen atom-containing N-nitro groups within their structure [7]. Imidacloprid, thiamethoxam, and clothianidin are among the members of this group. Neonicotinoids of the cyanoamidine type are less polar and less reactive due to their cyanoamidine groups which do not include oxygen atoms instead of nitro groups in their particles. Such substances include acetamiprid and thiacloprid. Neonicotinoids of the nitroguanidine group, are toxic to bees [7]. Neonicotinoids of the cyanoamidine group, non-toxic to bees. The most prevalent insecticide currently being used worldwide is imidacloprid. Additionally, from the three classes (organochlorine, organophosphate and carbamate) of insecticides, imidacloprid have been viewed as safer alternatives to more toxic insecticides [8]. In 2016 the Scopus database reported the neonicotinoids constituting about 3.76% among other pesticides population [9]. Products labelled for use on agricultural crops include acetamiprid and dinotefuran; however, their applications are more common in the greenhouse and nursery use. The acetamiprid and dinotefuran are not used for seed treatment [10]. **Table 2.1**



summarises the physical and chemical properties of some neonicotinoid pesticides. The physical and chemical characteristics of thiamethoxam, imidacloprid, and clothianidin are also comparable. The physicochemical properties of the clothianidin, thiamethoxam and imidacloprid have shown low octanol-water partition ( $K_{ow}$ ) coefficients, low vapour pressures, low Henry's Law constants, and they are readily soluble in water [11]. These kinds of compounds are not likely to volatilize, are mobile in topwater and groundwater, and are easily soluble in water [12]. Furthermore, their organic carbon partition coefficient ( $K_{oc}$ ) values align with compounds that exhibit strong leachability. Their physicochemical properties, which are primarily evaluated in terms of their dissociation constant ( $pK_a$ ) and octanol water partition coefficient ( $K_{ow}$ ), allow them to enter plant tissues and spread across the entire plant [11].

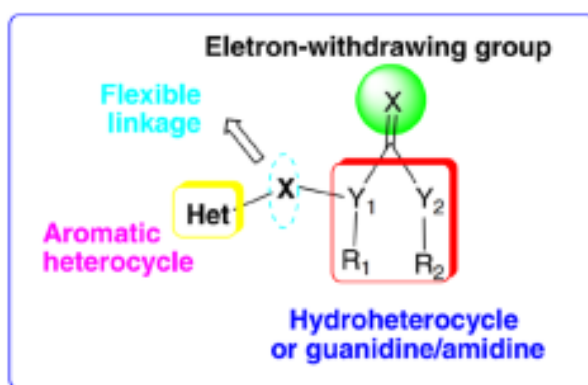


**Figure 2. 1:** Representation of four pharmacophores of the neonicotinoid pesticides structure [13].

**Table 2. 1:** Physical and chemical properties of some of the most common commercial neonicotinoid pesticides reported.

Name of neonicotinoid pesticide	Water Solubility (mg.L <sup>-1</sup> ) at 20 °C	Octanol water partition coefficient (Log K <sub>ow</sub> )	Organic carbon partition coefficient (mL.g <sup>-1</sup> ) (K <sub>ow</sub> )	pK <sub>a</sub> Value	Molecular formula	Molecular weight (g.mol <sup>-1</sup> )	Ref
Acetamiprid	4250	0.8	169.05	0.7	C <sub>10</sub> H <sub>11</sub> CIN <sub>4</sub>	222.68	[14]
Clothianidin	327	0.7	215	7.472	C <sub>6</sub> H <sub>8</sub> CIN <sub>5</sub> O <sub>2</sub> S	249.68	[15]
Dinotefuran	39830	-0.55	NA	12.6	C <sub>7</sub> H <sub>14</sub> N <sub>4</sub> O <sub>3</sub>	202.2	
Imidacloprid	610	0.57	260	pKa <sub>1</sub> = 1.56 & pKa <sub>2</sub> = 11.12	C <sub>9</sub> H <sub>10</sub> CIN <sub>5</sub> O <sub>2</sub>	255.7	[16]
Nitenpyram	590000	-0.66	NA	3.1	C <sub>11</sub> H <sub>15</sub> CIN <sub>4</sub> O <sub>2</sub>	270.7	[17]
Thiacloprid	184	1.26	615	NA	C <sub>10</sub> H <sub>9</sub> CIN <sub>4</sub> S	252.72	[18]
Thiamethoxam	4100	-0.13	70	NA	C <sub>8</sub> H <sub>10</sub> CIN <sub>5</sub> O <sub>3</sub> S	291.71	[19]

**NA-** Not Applicable (has no basic or acidic properties in aqueous solutions)

### **2.1.2 Pesticides contamination on plants**

The neonicotinoid pesticides (NEOs) have been reported to be persistent in the environment and translocate to residues in pollen and nectar of treated plants when utilized as seed treatments. The NEOs can be applied directly to the soil by runoff, seed dressing, and spray drift, among other methods [20]. NEOs go through several transit and transformation mechanisms once they are in the soil-water ecosystem. NEOs are mostly transported by leaching, surface runoff, and plant absorption in soil settings [21]. NEOs fate and routes of transportation in soil settings are influenced by the chemical qualities of the insecticide (their capacity of leaching, solubility, volatility, and period for its radioactive isotope to decay), the natural composition of the soil, and techniques used for administration [22]. NEOs are small compounds having low volatility and high solubility in water that ranges from 184 and 590 mg.L<sup>-1</sup>. This escalates concerns about the possibility that NEOs could contaminate surface and groundwater through leaching or surface run-offs [23]. NEOs are among the most significant categories of insecticides due to their potency, ability to kill a wide variety of insects as well as some grubs, and decreased toxicity towards mammals [24]. Furthermore, NEOs are extremely versatile in plants and environmental matrices and have been found in surface water from surrounding agricultural areas throughout the world, their usage has recently become a source of concern due to their possibility of being environmental contaminants [25]. These insecticides are reported to be extremely hazardous to aquatic species.

Since NEOs pesticides are readily absorbed by plant roots or leaves and transported throughout plant tissues [26]. They can be transported systemically through plants via the xylem and the process is well represented in **Figure 2.2** [9]. Several factors like soil texture, temperature and organic carbon content (OC) influences adsorption of the NEOs [27].

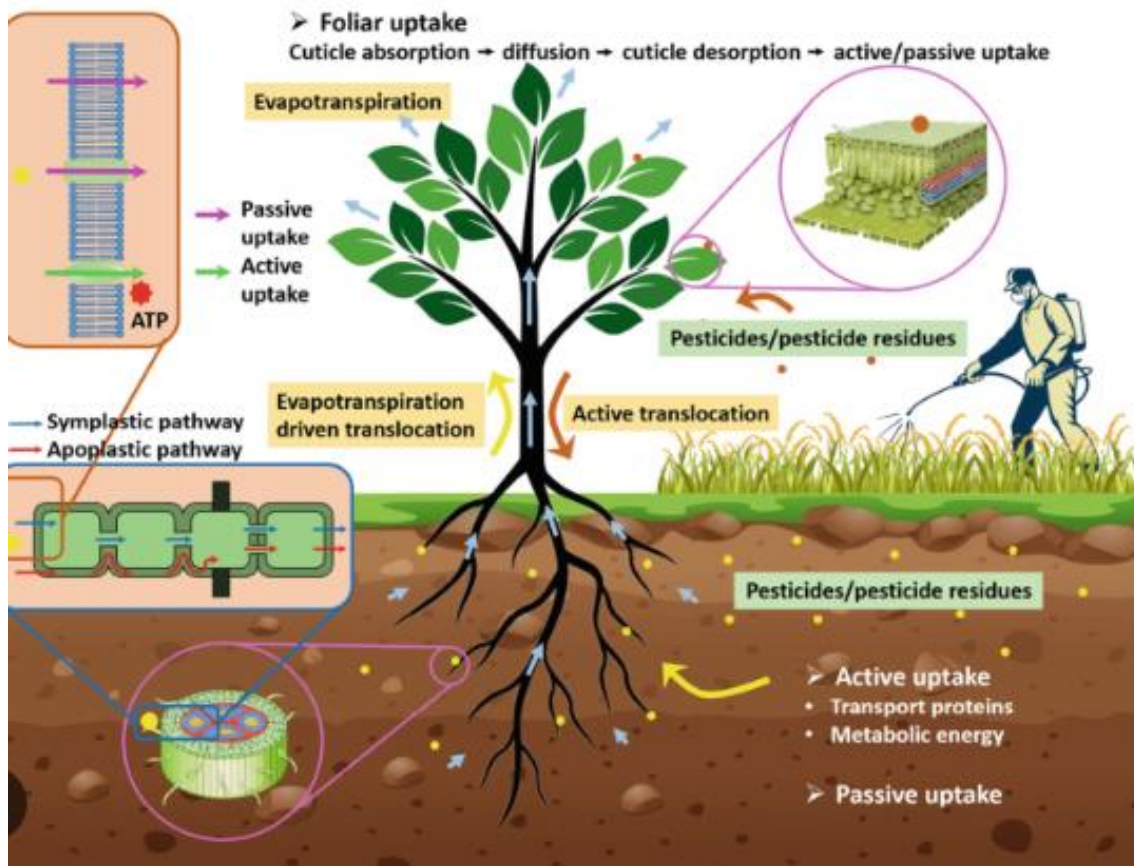


**Figure 2. 2:** General pesticides cycle between the environment and crops [9].

Additionally, **Figure 2.3** gives other factors influencing accumulation of the pesticides in crops [11]. Various factors have been reported to have an influence in the accumulation of these pesticides from different systems. The physicochemical characteristics of the pesticides, the environmental factors, and the plant physiology all influence the accumulation mechanisms [28]. All these factors contribute to the persistence of these pesticides within the environment. All these factors assist researchers with generating knowledge and understanding of the life cycle and the behaviour of these contaminants and how they elicit the toxicity on different samples [29]. The knowledge from all these will assist on how to handle and control NEOs accumulation and control their further damage on humans and environment. The NEOs go through a number of transportation and transformation steps once they are in the soil-water ecosystem [30]. When NEOs remain in the soil-water ecosystem, they degrade both biologically and chemically [31].

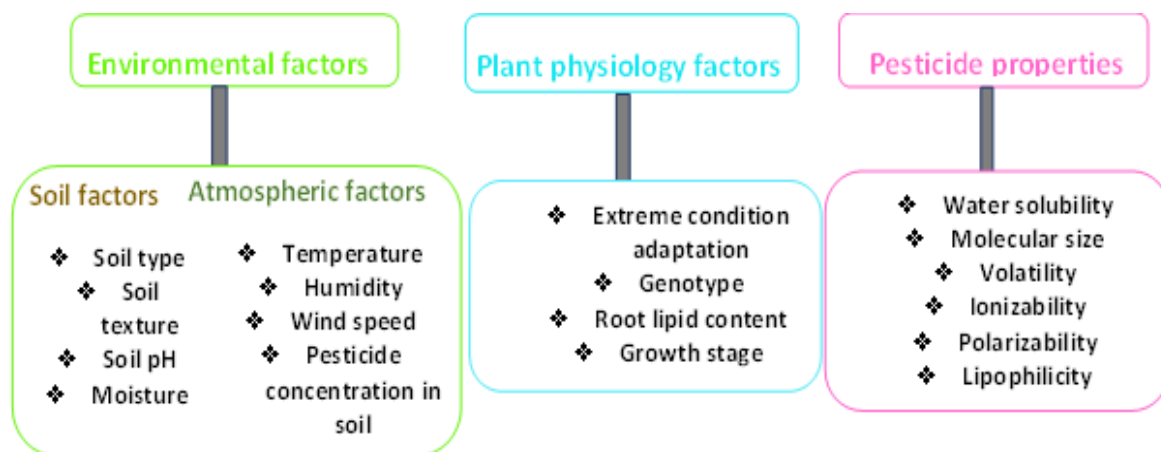


**Figure 2. 3:** Some of the factors and mechanisms having impact on pesticides accumulation in different samples and their properties [11] [32].

### 2.1.3. Effects of neonicotinoid pesticides in humans and insects

Consumption of vegetable oils contaminated with NEOs at trace levels fosters significant health issues such as headaches, abdominal pains, dizziness, vomiting, nausea, and eye problems among others. The NEOs toxicity affects the nervous system and they are also carcinogenic in nature. The long term health effects associated with exposure to NEOs include memory disorders, cancer, respiratory problems, dermatologic conditions neurologic deficits, depression, miscarriages and birth defects [33]. The NEOs bonds strongly to nicotinic acetylcholine receptors in the central nervous system. They function similarly to the neurotransmitter and bind strongly to the nicotinic acetylcholine receptors (nAChRs) in insects' central nervous systems, thereby stimulating the nervous system at low doses and causing receptor blockage, paralysis, and death at greater concentrations. **Figure 2.4** shows an illustration of the mechanism on neonicotinoid pesticides in the central nervous system [13]. They bind more strongly to receptors in insects than to those of vertebrates, so they are selectively more toxic to insects. Moreover, due to the toxicity caused by these pesticides in human and animal health, certain countries have established the maximum residual limits (MRLs) [34]. The primary objective of the Codex Committee on Pesticides Residues (CCPR), a supporting body of the Codex Alimentarius Commission (CAC), is to offer guidelines on pesticide residues in food [10]. For instance, the MRLs for thiamethoxam and imidacloprid in nations that are a part of the European Union (EU) are 20 mg.kg<sup>-1</sup> and 0.05 mg.kg<sup>-1</sup>, respectively. Conversely, the MRLs for imidacloprid and thiamethoxam in Japan are 10 and 15 mg.kg<sup>-1</sup>, respectively,

whereas in China, imidacloprid is set at 0.5 mg.kg<sup>-1</sup>. Vegetable oils are industrially processed to optimize consumer safety and acceptance by removal of components that can pose negative effect on appearance, taste, and shelf stability [35]. Additionally, other effects of pesticides accumulation on the environment involves biodiversity decreases in soil and poor water retention [5].

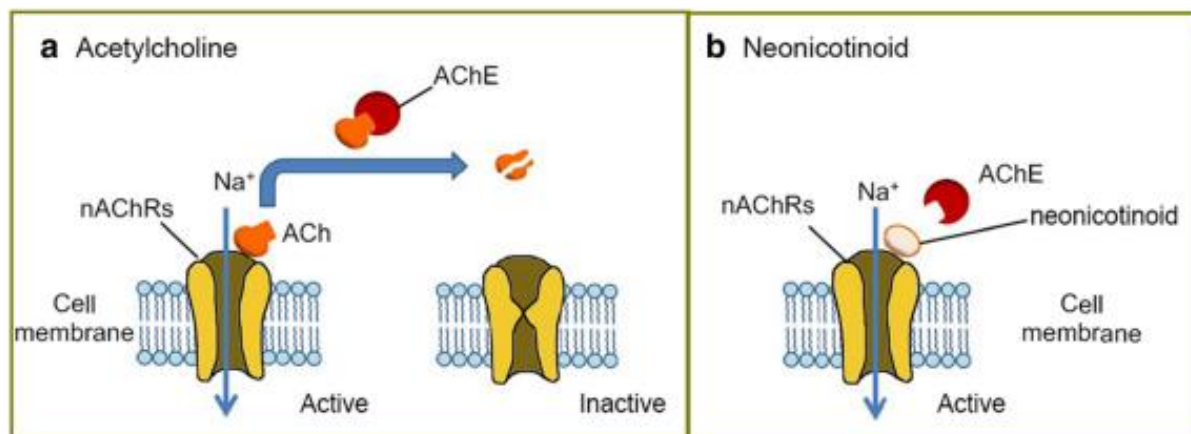


**Figure 2. 4:** Neonicotinoid acetylcholine receptors action in the presence of acetylcholine and a neonicotinoid substance [13].

Due to these pesticides' toxicity in humans, there is a need for their monitoring in vegetable oils and other various environmental matrices to preserve humans' health. Researchers have been developing different methods for determination, monitoring, and control/ mitigation of these contaminants in different food samples as they are present in trace levels concentrations. Considering the growing research interest about NEOs analysis, the contents of this study have consistent number of studies for trace NEOs measurement in a variety of matrices that have been reported from 2010 till 2024 have been reviewed in this chapter. The aim of this chapter is:

- (i) To provide an overview of the various sample preparation procedures for NEOs in samples of different origin and composition, food, and biological matrices, before instrumental quantification.
- (ii) To present the key features of each reported study in table format for an easy comparison of different research studies based on the selected analytes, sample preparation technique matrix, instrumental quantification, recovery, and sensitivity.

- (iii) To gather and briefly describe, as a function of the type of matrix, the various pretreatment procedures, that are summarized highlighting their key aspects and commented in terms of extraction efficiency, precision, and sensitivity.

## 2.1 Determination of NEOs in food samples

As a way of controlling and monitoring purposes, researchers have developed chromatographic methods for determination of NEOs in various food samples [36]. However, since food matrices are complex, there was a crucial need to develop sample preparation methods prior to chromatographic determination of NEOs [37]. The most common reported sample preparation methods were liquid-liquid extraction (LLE) and solid phase extraction (SPE) [25].

Sample preparation step is the most crucial step for determination of these NEOs in different samples, since majority of the samples cannot be directly analysed due to them not being compatible to the instrument. This has led to development of different sample preparation methods. During the sample preparation method, the target analyte(s) are extracted together with other components in samples and these co-extracted components are removed from the matrix [38]. In pretreatment stage objective targets include removing interfering species, extracting analytes, and preconcentrating the target analyte(s) to increase analyte final detection signal [39]. Analytes are preconcentrated when the target analyte is extracted from comparatively high sample volumes and placed in a small number of microliters of eluent. In bringing the analyte concentration into the dynamic range of the particular analytical apparatus, this procedure increases the precision and accuracy of the results [40]. **Figure 2.5** shows a general overview of some of the preconcentration, sample preparation and clean up methods that have been studied and reported along with their derivatives [41].

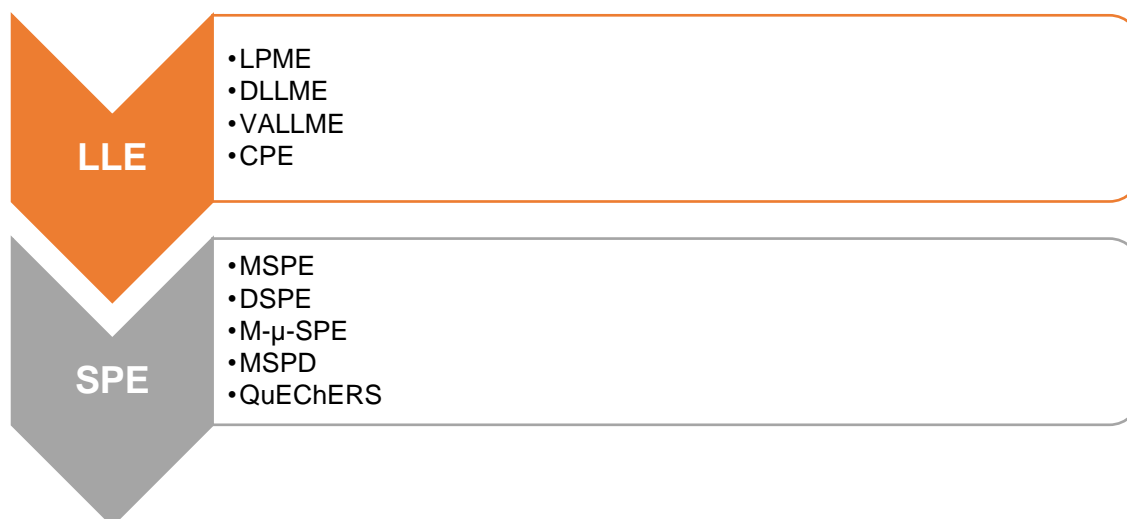


**Figure 2. 5:** Overview of sample preparation methods and their miniaturized methods.

The problem related with food safety raised interest in scientific research field to try and provide the best extraction and analytical methods for analysis of pesticide residues in different food samples. The NEOs have been identified on a wide scale in the environment, with concentrations ranges of parts per billion (ppb) – parts per million (ppm) in soil, parts per trillion (ppt)–ppb in water, and ppb–ppm in plants [9]. As a result of the complexity of oil matrices, the study is quite arduous. Significant effort has to be put in during extraction of pesticides from sample matrices and clean-up of lipids prior to analysis. An efficient clean-up method of the oil extract is necessary to improve instrument column lifetime and reduce the instrument downtime due to maintenance [42]. Inefficient sample clean-up could lead to matrix co-extractives to accumulate on the instrument flow channel, limiting the sensitivity of the analyte by lowering the inertness of the flow channel. The physicochemical characteristics of pesticides (polarity, pH sensitivity, thermal stability, etc.), interference in the sample matrix (water, fat, lipids, non-volatile material, compounds containing acidic or basic groups, etc.), instrument components, such as active sites in the gas chromatography (GC) system (the injector line or the column), and the analyte concentration are all factors that relate to matrix effects (MEs) [43] [44]. Factors to consider when selecting a sample preparation method to avoid undesirable matrix effects during chromatographic analysis [45]:

- ❖ Recovery as close to 100% as possible
- ❖ Good precision and accuracy of analytical values



- ❖ Low cost (reduced usage of organic solvents, reagents, SPE cartridges, etc.)
- ❖ Quick and easy operation
- ❖ Safety

However, the traditional SPE and LLE sample preparation methods require large amount of harmful organic solvents that pose danger to human health and the environment, formation of emulsion, and low enrichment factor (EF). However, regardless of these disadvantages that these methods have, some researchers still use them.

### **2.1.1 Liquid-liquid extraction**

Liquid-liquid extraction (LLE) is one of traditional sample preparation method involving the partition between the aqueous phase and the organic phase. LLE gained more application due to its advantages such as easiness, effectiveness, and wide acceptance in many standard methods [46]. Nonetheless, the main disadvantages of LLE are that it is tedious, has low enrichment factors, and uses a lot of hazardous organic solvents [47]. Therefore, to overcome these drawbacks, miniaturized liquid phase extraction methods have been developed and some of them are discussed below [48]. **Table 2.2** below gives an overview of some of the LLE and their miniaturized methods that have been reported under the determination of these pesticides in food samples.

#### **2.1.1.1 Liquid phase microextraction**

The liquid phase microextraction (LPME) approach has garnered increased interest as an alternative for LLE in sample preparation and analyte enrichment [49]. In LPME, the extraction procedure typically occurs in small volumes of microliter aliquots of the acceptor phase, sometimes referred to as the extractant, a water-impermeable solvent [50]. A drop of extractant is captured at the tip of a micro syringe needle in the simplest type of LPME, known as "headspace extraction," the extractant is then either suspended above the sample's surface or immersed directly into it [51].

#### **2.1.1.2 Dispersive liquid-liquid extraction**

The dispersive liquid-liquid extraction (DLLME) is based on a ternary component solvent system, and the cloudy microdroplets are formed upon injection of

a mixture of an extractant (typically non-miscible organic solvent) and dispersants (miscible organic solvents) into an aqueous sample [52]. The main advantages of DLLME include easy operation, larger area between sample and extraction phase, greenness, rapidity, low cost, easy handling, low consumption of organic solvents, high factor enrichment (EF), high extraction recoveries (ERs) and satisfactory compatibility with the chromatographic techniques [8]. However, it is worth noting that not all DLLME methods are green, their GREENess depends on the type of solvents used. To enhance the extraction efficiency of analytes, dispersive solvents, which are used in DLLME, need to be miscible with aqueous samples as well as extracting solvents such as methanol, ethanol, acetone, and acetonitrile among others which are commonly used. Additionally, these solvents efficiently distribute the extracting solvent in water [53]. Most of these dispersants are slightly hazardous, highly volatile, and flammable. Deep eutectic solvents are receiving a lot of interest these days. Deep eutectic solvent (DES) is a novel class of extraction solvent that Abbot et al. (2023) recently studied [54]. The latter consist of a variety of inexpensive, environmentally friendly, safe, renewable and organic molecules that can yield compounds with a melting point that is far lower than that of any individual component through hydrogen bonds formation. Unique qualities of deep eutectic solvents that stand out are their great purity and environmental friendliness [45]. Certain characteristics, such as a high affinity for the analytes being extracted, low solubility in aqueous solution, and ease of dispersion into water, are required of an extraction solvent known as a deep eutectic solvent. Another solvent that has been reported for DLLME is ionic liquids (IL). The usage of IL is restricted by its relatively high cost, difficult synthesis method, and possible toxicity [45]. Deep eutectic solvents show similar physicochemical properties to ionic liquids, but they are much cheaper and safer for their use as solvents as compared to ionic liquids in synthetic transformations [42]. As compared to room temperature ionic liquids (RTILs), DESs have, however, notable advantages such as (i) their convenient synthesis (100 % atom economy), (ii) their very low price since most of DESs can be prepared from readily accessible chemicals and (iii) their low toxicity especially DESs derived from choline chloride (CCI) and renewable chemicals. Choline chloride is a commonly used organic salt for DESs, since it is biocompatible and most of the HBDs are cheap and environmentally benign such as urea, glycerol, or carboxylic acids. Additionally, DESs do not produce toxic metabolites and are biodegradable [45]. Moreover, a range of modified DLLME techniques, including air,

effervescence-assisted liquid-liquid microextraction (LLME), vortex assisted, ultrasound, and vortex, have been developed to remove dispersive solvents.

### **2.1.1.3 Cloud point extraction**

Since cloud point extraction (CPE) employs smaller amounts of non-toxic organic surfactants than harmful organic solvents, it adheres to the "green chemistry" principles. Furthermore, in contrast to the organic solvents used, it is less dangerous, simple to use, affordable, quick, and incredibly effective. A surfactant solution is added to the sample at concentrations greater than the critical micelle concentration (CMC), allowing the production of micelles, in order to carry out cloud point extraction [45]. Two immiscible isotropic phases form as the analytes dissolve and partition into the micelles. The extracted analytes are found in the first phase, which is surfactant rich. The surfactant-rich phase and most of the aqueous phase are in balance. Phase separation in CPE is induced by temperature over the cloud point temperature (CPT) [55]. The temperature at which non-ionic surfactant aqueous solutions get turbid is known as the cloud point. More precisely, above the cloud point, the solution splits into two phases: a rich phase that is closer to the critical micelle concentration and has a high surfactant concentration in a limited volume, and a poor phase that is closer to the critical micelle concentration [56]. Extraction on NEOs analytes using non-CPE is regarded as non-hazardous due to its use of organic solvents. It can focus on the analyte that has a high rate of recovery. In addition, it is less expensive and safer because just a tiny quantity of the comparatively non-flammable and non-volatile surfactant is needed. When it comes to CPE for analyte extraction, ionic surfactant is superior to hazardous organic solvent. It can focus on the analyte with the highest recoveries reported [57]. Moreover, in 2018 Kachangoon et al. reported about the determination of neonicotinoids pesticides in water samples following the CPE method. The developed method showed EFs in the range of 20 to 333 that were acceptable. The ranges of the LODs and LOQs were 0.0003 to 0.002  $\mu\text{g. mL}^{-1}$  and 0.001 to 0.0067  $\mu\text{g. mL}^{-1}$ , respectively. Additionally, good linearity, reproducibility, repeatability, and recoveries were attained. In addition, it is less expensive and safer.

#### **2.1.1.4      *Hollow fibre liquid-phase microextraction***

Hollow fibre liquid-phase microextraction (HF-LPME), salting-out assisted liquid-liquid extraction, and a very tiny amount of the comparatively non-flammable and non-volatile surfactant are needed [58].

**Table 2. 2:** Overview of LLE and their miniaturized methods reported between 2013-2023.

<b>Matrix</b>	<b>LLE method</b>	<b>Analytes</b>	<b>Detection technique</b>	<b>LOD (<math>\mu\text{g.mL}^{-1}</math>)</b>	<b>Extraction time (min)</b>	<b>Recoveries (%)</b>	<b>RSD (%)</b>	<b>Ref</b>
Rapeseed, Rapeseed Oil & Rapeseed Meal	LLE	ACT, IMI, TCL, TMX	LC-MS/MS	NR	6	70-118	NR	[59]
Cucumber	DLLME	ACT, IMI, TCL, IMD	MEKC	0.0008-0.0012	16	79.7-98	3.8-7.1	[60]
Sunflower seeds	LLE	ACT, IMI, CLO, TCL, TMX, DIN, NIT	LC-MS/MS	0.0003-0.0012	10	70-120	2.4-9.6	[61]
Surface water & Fruits juice	VLLME-SFO	ACT, CLO, NIT, IMI, TMX	HPLC-DAD	1-5	11	85-105	1.10-3.45	[62]

Tea infusion	LLE	NIT, TMX, IMI, TCL	LC-MS/ -MS	0.03	140	57.7-98	< 11	[63]
Milk	DLLME	IMI	HPLC-MSMS	0.09-0.27	17	81.94	< 9	[64]
Fruits	DES-LPME	ACT, IMI	HPLC-DAD	0.04-0.31	3.30	64-89	≤7.2	[65]
Cucumber & tomato	DLLME	IMI, ACT	HPLC MS/MS	3.4-10.4	19.30	86-104	< 12	[66]
Milk	LLE	ACT, CLO, IMI, TCL, TMX	UHPLC-MS/MS	NR	14	77-125	2-16	[67]
Grenadine & black current juice	SE-VA- DLLME	ACT, IMI	HPLC-DAD	0.45-0.83	20	61.6-99.63	2.6-6.7	[68]
Honey	HLLME- CIME	ACT, CLO, IMI, TCL	HPLC-MS	0.01	10.30	86-100	2.68-5.38	[69]
Green onion	MLLE	TCL	LC-MSMS	NR	16	97.2-101.5	9.7-13.8	[70]

Sugarcane	LLE	ACT, CLO, IMI, TCL, TMX	LC-ESI-MS/MS	0.0007- 0.002	40	62.06- 129.93	2.52-14.57	[71]
Orange juice	HF-MMLLE	ACT, IMI	LC-ES-MSMS	0.018-0.16	42	70-118	5.9-13.8	[72]
Honey	SULLE	ACT, IMI, TCL	HPLC-DAD	21-27	NR	91.49-97.73	< 5	[73]
Tomato, pepper, lemon, orange, grape.	DLLME	ACT, CLO, IMI, TCL, TMX	LC-MS	0.025-0.5	73	84.1-119	3.3-15	[74]
Milk	DLLME	NIT, ACT, IMI, TCL	HPLC-DAD	0.13-0.21	12	73-85	< 5.9	[75]
Green onion	PLE	ACT, IMI, CLO, TCL, TMX, DIN, NIT	LC-MS	NR	14	94.7-99.5	0.4-3.7	[76]
Cucumber, honey, orange	CPE	ACT, IMI, CLO, TCL	HPLC-PDA	0.0003- 0.001	18	70-119	< 10	[77]

Honey	CPE	NIT, IMI, TCL, TMX	UHPLC-MS/MS QQQ	0.13-0.18	43	85.3-104.5	2.0-11.5	[78]
-------	-----	-----------------------	--------------------	-----------	----	------------	----------	------

---

**LLE**- Liquid-liquid extraction, **DLLME**-Dispersive liquid-liquid extraction, **PLE**- Pressurized liquid extraction, **HPLC-DAD**- High performance liquid chromatography diode array detector, **LC-MSMS**- Liquid chromatography tandem mass spectrometry, **CPE**- Cloud point extraction, **UHPLC-MS/MS-QQQ**- Ultra high-performance liquid chromatography coupled with triple quadrupole tandem mass spectrometry, **LC-MS**- Liquid Chromatography Mass Spectrometry, **HPLC-PDA**- High performance liquid chromatography photo diode array, **SULLE**- Salting-out assisted liquid-liquid extraction, **HF-MMLE**- Hollow-fibre microporous membrane liquid-liquid extraction, **MLLE**- Micro-liquid-liquid extraction, **HLLME-CIME**- Homogeneous liquid-liquid microextraction-cold induced aggregation microextraction, **SE-VA-DLLME**- Surfactant-emulsified vortex-assisted dispersive liquid-liquid microextraction, **DES-LPME**- Deep eutectic solvent liquid phase microextraction, **VSLLME-SFO**- Vortex-assisted surfactant-enhanced-emulsification liquid-liquid microextraction, **MEKC**- Micellar electrokinetic chromatography, **LC-ESI-MS/MS**- Liquid Chromatography Electrospray Ionization Tandem Mass Spectrometric, **LC-ES-MSMS**- Liquid chromatography-electrospray tandem mass spectrometry



### 2.1.2 Solid phase extraction

Solid phase extraction (SPE) is a straightforward, dependable, and efficient pretreatment technique that is used to achieve selective extraction and preconcentration of different analytes. Partitioning target analyte(s) between a liquid phase (sample solution) and a solid phase (adsorbent) is the fundamental principle behind this approach [79]. The sample loading, cleaning, elution, and sorbent activation are the crucial steps in this procedure. SPE has numerous advantages over LLE, including exceptional selectivity, considerable flexibility, reduced solvent usage, improved purification effect, and major automation possibilities [80]. Additional benefits include high enrichment factors, variable sorbent selection, speed, ease of usage, and convenience of use [81]. Neonicotinoid insecticides have been extensively extracted from a variety of substrates via solid phase extraction [82]. Nevertheless, depending on the sorbent type utilised, this approach may have certain disadvantages. In the extraction step, SPE often necessitates numerous manual operating procedures, takes a considerable amount of time, and presents the issue of cartridge obstruction when utilising a traditional immobilised column [83].

Several studies have been conducted and reported in literature where SPE was applied in determination of NEOs, in 2021, Moustafa et al reported about the determination of imidacloprid pesticides in water using the AgNPs@chitosan adsorbent for SPE method in water samples and the removal efficiency of the pseudo-second-order kinetic model was at a satisfying linearity of 0.9938 [84]. The extraction apparatus's miniaturisation, the pretreatment process's decrease in steps and duration, and the enhancement of selectively reducing the matrix effect are examples of advantages that new developments in sample preparation provide [85]. Solid-phase microextraction (SPME) and liquid-phase microextraction (LPME) are two more microextraction techniques that were developed to address drawback of conventional LLE and SPE techniques. Sampling, extraction, concentration, and sample introduction are all combined into one solvent-free step using SPME. Nevertheless, there are certain drawbacks with the fibre that is utilised, namely its high cost, carry-over impact, fragility, and short lifespan [86]. Approaches based on liquid phase microextraction are far more economical and versatile, allowing for the employment of CPE (cloud point extraction) among other techniques. Additionally, **Table 2.3** below

shows some of the reported SPE methods, and their miniaturized derivative methods for determination of the neonicotinoid pesticides.

### **2.1.2.1 *Dispersive solid phase extraction***

The dispersive solid phase extraction (dSPE) method, after mixing and stirring the extracted solution and the distributed adsorbent, the two are separated by high-speed centrifugation [87]. The solid phase extraction of dispersants (dSPE) is not the same as the SPE of sorbent packed onto a column. The extraction sorbents huge specific surface area allows for a significant reduction in the equilibrium period between the sorbents and sample solution, even a small amount of adsorbent may fulfil the criteria for enrichment [88]. The parameters of the extraction process are critical to enrichment effectiveness. The pH of the aqueous solution influences the molecular form of the analytes as well as the charge species and density on the adsorbent surface [89]. The viscosity of an aqueous solution and the analytes' ion-exchange interaction with the adsorption materials are both influenced by the medium's ion strength [90]. The type of extraction sorbent, elution solvent, and working time all guarantee a sufficient extraction and elution of target analytes. The primary disadvantage of dSPE is that the technique requires high-speed centrifugation [46].

### **2.1.2.2 *Magnetic solid phase extraction***

By using an external magnetic field to separate the sorbent from the sample solution, magnetic solid phase extraction (MSPE) utilises magnetic nanoparticles as extraction adsorbents. The use of magnetic nanoparticles (MNPs) in the extraction, separation, and cleanup of a variety of environmental toxins has been the subject of research interest recently [91]. Additionally, there are a few elements in nature that have magnetic properties, including iron, cobalt, and nickel, so their nanoparticles and their derivative compounds are magnetized, respectively [92].

There are different methods of synthesis and preparation methods of these magnetic nanosized powder NPs preparation which include co-precipitation, microwave assisted, sol-gel, hydrolysis, hydrothermal, and thermal decomposition [93]. Among the various kinds of MNPs that have been studied,  $\text{Fe}_2\text{O}_4$  is the most common because of these advantages; excellent paramagnetic properties, stability, large surface area, tiny particle size, and water dispersity, less toxicity and its ease of synthesis and functionalization. MNPs have been extensively employed in many

matrices investigations and are crucial in the removal of metal ions, organic pollutants, and pesticide residues [94]. However, these MNPs have their own limitations which include their agglomeration, low extraction efficiency, MNPs oxidize easily, and instability in an acidic environment [95]. To overcome these restrictions, MNPs have been improved, modified, and functionalized using a variety of organic and inorganic materials, such as silica, polymers, imprinted molecules, hemi-micelles, micelles, ionic liquids, alkoxides, membranes, proteins, and enzymes that are appropriate for the required matrices compatibility [96]. In batch mode, functionalized MNPs have been used as MSPE sorbents to extract metal ions, chemical molecules, and biological materials [97]. Modified MSPE sorbents have demonstrated increased selectivity, reusability, compatibility in a variety of matrices, and good stability [98]. For the target analytes, the prepared magnetic sorbent's adsorption capacity is typically either higher or equal to that of the nonmagnetic sorbent's original value [99]. As a result, MSPE can address the shortcomings of the rapid centrifugation required by dSPE in addition to having all the benefits of dSPE [100]. Graphene oxide (GO), metal–organic frameworks (MOFs), covalent organic frameworks (COFs), nanocellulose, porous porphyrin organic polymer, and porous carbon have all been modified using magnetic particles as magnetic extraction sorbents [98]. The added advantage of this method is the reusability of the adsorbent [101].

Some advantages of magnetic nanoparticles are their high capacity for adsorption, ease of separation from the reaction medium, and simplicity in surface modification through the addition of functional groups. These benefits make magnetic nanoparticles attractive options for the quick, efficient, and targeted extraction and preconcentration of neonicotinoid pesticides. Recently, MOFs have gained more recognition by researchers due to their notable and considerable properties, which include variable pore volume and size, high surface area, and straightforward functionalization [102].

### **2.1.2.3 Solid phase microextraction**

A solvent-free sample preparation method called solid phase microextraction (SPME) usually integrates sampling, extraction, and concentration into a single fibre arrangement. Its benefits include miniaturisation, automated operation linked with chromatographic instruments. It also avoids labour-intensive manual operations and

enormous solvent usage [103]. One of the main characteristics of this method is its large-volume thin-film sorbent or membrane extraction phase, which has a high surface area-to-volume ratio and offers higher extraction efficiency and recovery than conventional fibre SPME methods [104].

#### **2.1.2.4 QuEChERS**

The method was introduced early in 2003, the QuEChERS method is a fast, simple, affordable, reliable, secure, and robust approach to sample preparation that has been effectively evaluated for the removal and cleanup of pesticide residues, particularly in food samples [105]. Among other methods, QuEChERS offers several advantages over most conventional techniques, such as simple operations, no need for auxiliary equipment, lower organic solvent consumption, and high extraction recoveries [106]. The method has been highly recommended because of its low selectivity for multiresidue extraction. Nonetheless, the technique has been adjusted to maximise efficacy based on the target substances and the matrices that need to be examined [107]. This method's basic idea is to partition or extract liquid from liquid or solid samples, or to perform a salting-out aided liquid-liquid extraction (SULLE), usually with acetonitrile (ACN) as the extraction solvent, and then clean up the sample [108]. To achieve adequate results in terms of sensitivity and selectivity, its employment prior to separation techniques like LC or GC paired with MS detection is required due to its lack of selectivity and lack of a preconcentration phase [109]. A more extensive study about this method have been reported on **Table 2.3**.

**Table 2. 3:** An overview of solid phase extraction and their miniaturized methods reported for extraction of NEOs from 2013 to 2023. QuEChERS a type of dispersive solid phase extraction method reported used for extraction of the neonicotinoid pesticides in food samples.

Matrix	Pesticide	Method	Adsorbent	Detection technique	LOD (ng. mL <sup>-1</sup> )	%RSD	Recoveries (%)	EF	Extraction time (min)	Ref
Water & honey	ACT, TMX, IMI, TCL	SPE	TAPA-BPDA-COFs	HPLC-DAD	0.08-0.12 & 2.6-3.3	< 7.6	80.0-121.9	67-427	NR	[110]
Sunflower seed	ACT, TMX, IMI, TCL	SPE	CH <sub>3</sub> NH-G	UPLC-MSMS	< 6	1.7-2.9	74.3-119.1	NR	5	[111]
Tea infusions & water	IMI	SPE	MIL-101(Cr)@DES	HPLC-DAD	NR	NR	90-98	NR	8	[112]
Green pepper & tomato	ACT, IMI, CLO, TCL,	SPE	ENVI-Carb II/PSA cartridge	LC-MS/MS	NR	≤ 7.5	71.7-122.3	NR	30	[113]



Environmental water	ACT, TMX, IMI, TCL, CLO	MSPE	Fe <sub>3</sub> O <sub>4</sub> /ZIF-67/GO	HPLC-MSMS	0.06-1.0	1.8-16.5	83.5-117	NR	50	[118]
Pear & Tomato	ACT, TMX, IMI, TCL	MSPE	Fe <sub>3</sub> O <sub>4</sub> @SiO <sub>2</sub> -G	HPLC-DAD	0.08-0.15	2.1-6.3	93.1-107.4	177 - 195	20	[119]
Environmental water & peanut milk	ACT, TMX, IMI, TCL	MSPE	MOPC-ZSM-5	HPLC-UV	0.1-0.2 & 1.0-2.0	4.8-7.4	96.74 - 112.40	NR	20	[120]
Surface water	ACT, CLO, IMI, TCL	M-μ-SPE	MP-POP	HPLC-DAD	0.013-0.032	< 5	91 - 99.3	94-110	15	[121]
Rice	IMI	MSPD	MIP & C18	LC-MS/MS	2.4	4.5-5.9 & 4.8-7.1	83.8-92.5	NR	8	[122]
Water	ACT, IMI, TCL,	DSPE	MOF-Uio66	HPLC-MS	0.02-0.4	8.5-13.1	73.7-119.	NR	5	[123]

	CLO, TMX										
Tea infusion	IMI, ACT, TMX, IMI	DSPE	GO		UPLCMS/MS	0.46-1.4	1.5-4.7	72.2-95	NR	10	[124]
Rapeseed Peanut Soybean Sesame seeds	ACT, TCL	QuEChERS	NR		LC-MS/MS	0.5-7.5	< 13	70.5-100	NR	NR	[125]
Cucumber Cabbage Orange Apple	ACT	QuEChERS	NR		GC-MS/MS	0.0001 - 0.0026	14.3	75.3-113.6	NR	12	[126]
Olive oil Olives Avocado	ACT, TMX, TCL	QuEChERS	Z-Sep <sup>+</sup> or Z-Sep		UHPLC-MS/MS	NR	< 10	NR	NR	11.30	[127]



Chicken muscle	ACT, TMX	QuEChERS	C18	UHPLC-QToF-MS	0.85 & 0.19	1.91–5.17	84.92-101.34		8.10	[128]
Kiwi fruit	ACT, CLO, IMI, TMX	QuEChERS	NR	LC-MS/MS	0.0003 - 0.0014	0.95-4.17	70-120	NR	12.30	[129]
Eggs	ACT, IMI, TMX	QuEChERS	NR	UHPLC-MS/MS	0.1-1.0	15.3	74.4-115.2	NR	11	[130]
Canned and fresh peach	TMX	QuEChERS	NR	GC-MS	NR	< 20	69-125	NR	28.20	[131]
Avocado & Almond	ACT, IMI, TCL, TMX	QuEChERS	PSA-C18, silica, Z-Sep and Z-Sep+	LC-MS/MS	NR	1-2	70-120	NR	48.30	[132]
Olives & Olive Oil	IMI, TCL	QuEChERS	NR	LC/DAD/E SI/MS	0.005 & 0.08	NR	85-110	NR	22	[133]
Virgin olive oil	ACT, IMI, TCL, TMX	QuEChERS dSPE	NR	Nanoflow	NR	< 19	75-119	NR	19	[134]

					LC/ESI Q- Orbitrap- MS							
Olive oil	ACT, IMI, d-SPE, SPE TCL, & TMX QuEChERS	NR			UHPLC- MS/MS	NR	< 20	70-120	NR	18		[135]
Olives	ACT, IMI, MSPD & TCL, QuEChERS TMX	C18			LC-MS/MS	<10	NR	70-120	NR	3.30		[136]
Pistachio	ACT, IMI QuEChERS- DES-DLLME	NR			HPLC-UV	1.5 & 3.0	< 7	95.6-99.4	NR	138.30		[137]
Spinach, cucumber, apple, pomelo	ACT, IMI, QuEChERS CLO, TCL, TMX, IMD	NR			LC-MS/MS	0.2- 0.85	≤ 14.0	73.7-103.8	NR	40.30		[138]
Cabbage	ACT, IMI, QuEChERS CLO, TCL,	NR			UPLCMS/ MS	0.2-0.5	< 5.1	79-108.4	NR	23		[139]

	TMX, DIN, NIT										
Cucumber, egg plant, spinach	ACT, IMI, CLO, TCL, TMX, DIN, NIT	SPE- QuEChERS	NR	HPLC- DAD	0.001- 0.012	< 10	83-100	NR	37	[140]	
Honey	ACT, IMI, CLO, TCL, TMX, DIN, NIT	QuEChERS	C18	UHPLC- MS/MS	< 0.6	≤ 20	80-109	NR	12	[141]	
Tea	ACT, IMI, CLO, TCL, TMX, DIN, NIT	QuEChERS	NR	LC-HR-MS	NR	1.6-9.8	85.2-116	NR	18.30	[142]	

---

**SPE-** Solid phase extraction, **MSPE-** Magnetic solid phase extraction, **DSPE-** Dispersive solid phase extraction, **MSPD-** Matrix solid-phase dispersion, **M-μ-SPE-** Magmatic μ-solid phase extraction, **MP-POP-** Magnetic porphyrin-based porous organic polymer, **Rut-MOP-** Magnetic porous organic polymer, **MGO/MIL-** Magnetic nanocomposite composed of graphene oxide metal-organic framework, **TAPA-BPDA-COFs-** tris(4-

aminophenyl)amine (TAPA) and 4,4'-biphenyldicarboxaldehyde (BPDA) covalent organic framework, **C18**- SPE cartridges, **Fe<sub>3</sub>O<sub>4</sub>@COF-(NO<sub>2</sub>)<sub>2</sub>**- Iron oxide functionalized with covalent organic framework containing the nitro group, **CH<sub>3</sub>NH-G**- Methylamine modified graphene, **Co-MNPC**- Cobalt functionalized magnetic nanoporous carbon, **Fe<sub>3</sub>O<sub>4</sub>/ZIF-67/GO**- Iron oxide zeolitic imidazolate framework 67/graphene oxide, **Fe<sub>3</sub>O<sub>4</sub>@SiO<sub>2</sub>-G**- Graphene grafted silica-coated Fe<sub>3</sub>O<sub>4</sub>, **MIP**- Molecular imprinted polymer, **MOF-UiO66**- Metal-organic framework UiO-66, **MOPC-ZSM-5**- Magnetic ordered porous carbon synthesized using zeolite ZSM-5, **MIL-101(Cr)@DES-GO**- MIL-101(Cr) metal-organic frameworks based on deep eutectic solvent, **HPLC-UV**- High-performance liquid chromatography ultra-violet spectroscopy, **HPLC-DAD**- High performance liquid chromatography diode array detector, **LC-MSMS**- Liquid chromatography tandem mass spectrometry, **HPLC-MS**- High performance liquid chromatography mass spectrometry, **HPLC-MSMS**- High performance liquid chromatography tandem mass spectrometry, **UPLC-MSMS**- Ultra Performance Liquid Chromatography-Tandem Mass Spectrometry, **QuEChERS**- Quick, Easy, Cheap, Effective, Rugged and Safe, **dSPE**- Dispersive solid phase extraction, **DES**- Deep eutectic solvent, **DLLME**- Dispersive liquid-liquid microextraction, **UHPLC-MS/MS**- Ultra high-performance liquid chromatography tandem mass spectrometry, **LC-HR-MS**- Liquid chromatography high resolution mass spectrometry, **GC-MS**- Gas chromatography mass spectrometry, **LC/DAD/ESI/MS**- Liquid chromatography diode array detector electrospray ionization mass spectrometry, **Nanoflow LC/ESI Q-Orbitrap-MS**- Liquid chromatography quadrupole-Orbitrap mass spectrometry, **UHPLC-QToF-MS**- Ultra high-performance liquid chromatography quadrupole time-of-flight mass spectrometry

### 2.1.3 Optimization of the influential parameters of sample preparation methods

Method optimization is one of the most crucial steps for sample preparation. These must be investigated to monitor how the certain parameters suite the sample matrix and the analytes studied. Different parameters like pH, concentration, temperature, extraction time, sample mass/volume, eluting solvent, extracting solvent and its volume, among others have been investigated either by univariate or multivariate approach. The design of experiment (DoE) utilised for screening and optimization using the mathematical tools. The two optimization routes have been utilised and reported by different researchers over the years. The general overview of experimental design is shown on **Figure 2.6** [143].

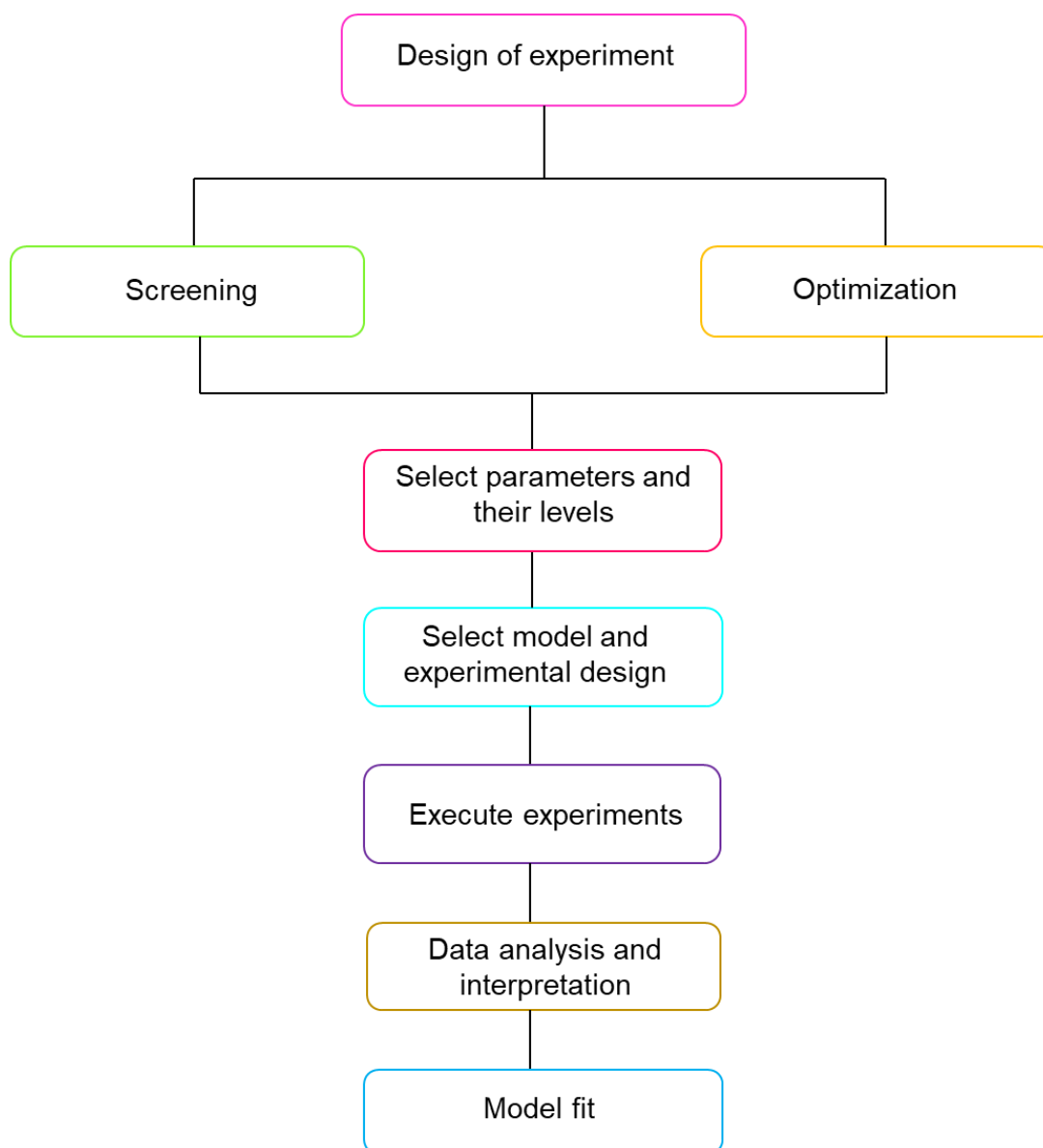


**Figure 2. 6:** Principles of design of experiment.

### **2.2.3.1. Univariate optimization**

The univariate optimization follows a route of studying one parameter at a time. The univariate approach, which necessitates a large number of tests and, as a result, increases waste production and running costs [144]. By repeatedly assessing various values of the variable, this approach aims to maximise or minimise an objective function until an optimal value is attained. The advantages associated with this approach are computational efficiency, simple and ease of interpretation [87]. However, the approach suffers limitations like having a limited scope, wherein it overlooks interactions between many factors that could have a substantial impact on one another's behaviour. These constraint limit its relevance in real-life situations with interdependent variables [145].

### **2.2.3.2. Multivariate optimization**

The multivariate optimization follows a route of studying multiple parameters at a time. The multiple parameters can start from two to five or more. This method provides a number of benefits, including thorough analysis, enhanced efficiency, and accurate model simulations [146]. The limitations associated with the multivariate approach are interpretation challenges and interpretability challenges. The results of multivariable optimisations may be difficult to comprehend owing to the complex interactions between the several parameters [147]. Different mathematical models like JMP, MATLAB, MINITAB, Statistica, and Stat graphics, Stat-Ease Design-Expert, MODDE, Design-Expert, Fusion Pro are used for design of experiments (DoE) for both univariate and multivariate optimization [52].

#### **2.2.3.2.1. Screening (1<sup>st</sup> order)**

To determine which factors and interactions have a substantial impact on the outcomes, the screening process entails examining all pertinent experimental factors that could affect the response or responses. Full factorial, Plackett-Burman, fractional factorial, and D-optimal screening designs are the most reported [148].

#### **2.2.3.2.2. Further optimization (2<sup>nd</sup> order)**

To determine the factor settings that produce the best values for optimized parameters, the most significant factors found throughout the screening process are optimized. Additionally, an examination is conducted into the type of connection that

exists between the factors and the measured responses [149]. Different designs of response surface methodology (RSM) are followed which include Box-Behnken, Central composite design (CCD), D-optimal design, face-centered composite design (CCF), circumscribed central composite (CCC) and Doehlert designs [150]. During technique validation, robustness testing is done to demonstrate lack of substantial effect.

#### **2.2.3.2.3. Overview summary of sample preparation methods**

A wide range of miniaturized methods of LLE and SPE have been developed, applied and reported. Their performance has shown to have improved and promising. Their precision, accuracy, sensitivity and efficiency has improved.

#### **2.2.4.1. LLE vs SPE and their miniaturized methods over 10-year period.**

From **Figure 2.7** shown gives a brief overview on the reported sample preparation methods that have been adopted for determination of these NEOs in a wide variety of sample matrices. The most reported methods here were LLE and SPE. There has been an exponential increase in studies conducted over the years range of 2010 till 2024. For SPE, different adsorbents have been developed and functionalized for them to be compatible to the type of analytes studied and the matrices of interest. In 2020, it has shown that LLE have been favoured more over SPE, and this can be attributed to researchers moving towards the use of environmentally friendly DES that have also been “greener solvents”. A wide range of these DES have been synthesised and applied in different matrices. A recent review by Feng et al. (2024) has a detailed extensive study about these DES studies that have been conducted over the years [151]. However, alternatively, with SPE the MSPE have played a significant role in keeping the SPE on the poll of being utilised due to its simplicity with separation by using the magnetic field. Additionally, the use of mesoporous adsorbents and other wide range of novel adsorbents has gained the SPE a recognition and continuous utilisation. In overall, the other methods have not gained much of the interest over the years due to their undeveloped and unfriendliness of the methods that requires large organic solvents, the cost effectiveness of the method and their requirement of trained personnel for operation. However, their limitation includes the high temperatures and longer hours involved during their synthesis.

This review was compiled with the studies that have been done from 2013 until 2024. The data below will be showing the statistics for the sample preparation, preconcentration and clean up methods that have been adopted for the determination of these pesticides in different food samples over the years.

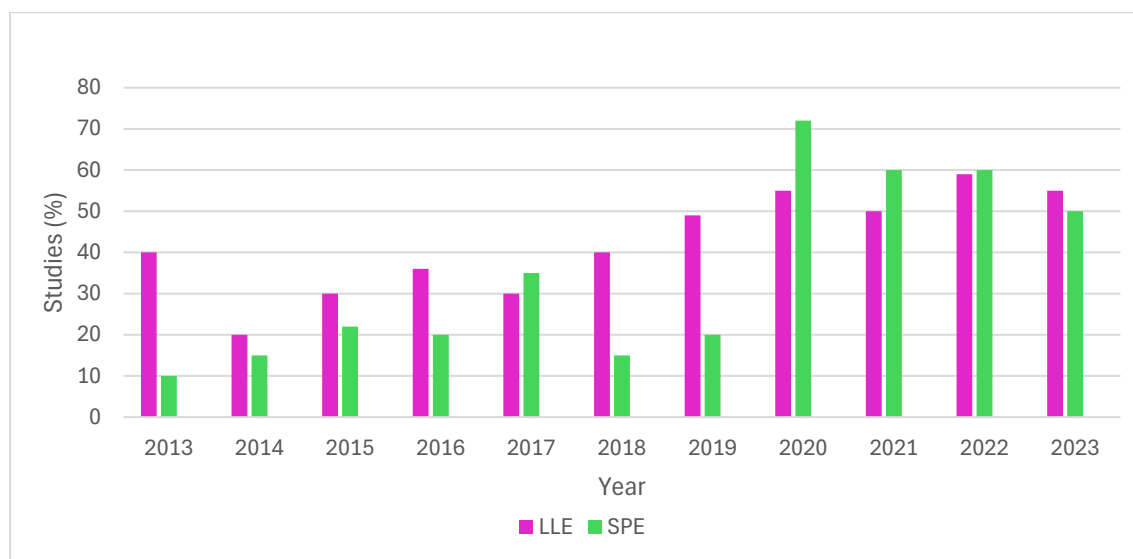


**Figure 2. 7:** Studies reported on sample preparation methods from 2013 till 2024.

### **2.2.3.1 Univariate vs multivariate**

The univariate and multivariate optimization have been utilised for over the years by researchers for different sample preparation methods. Due to the limitations of univariate optimization, the multivariate optimization has been favoured over the years. However, it is worth to note that some researchers still utilise the univariate approach for investigation of the sample volume, sample mass, type of eluting solvent, type of extractant solvent, type of dispersive solvent. Alternatively, the two approaches are being used simultaneously while the multivariate is utilised for design of experiment. The multivariate optimization preference by many reports was due to its additional advantages of investigation of the different parameters at the same time adding to time efficiency and cost effectiveness of this approach.

### **2.2.3.2 Chromatographic determination of NEOs over the 10 years**

A sample preparation method is the initial step which prepares and preconcentrate the analytes before their quantification. Several chromatographic detection techniques have been reported for analysis of pesticides. These include



the HPLC, LC-MS and GC-MS among others. Different detectors have been coupled with these instruments to suit the analytes nature and for better detection [152]. Since neonicotinoid pesticides are poorly volatile with high polarity and thermolability, the HPLC have been a preferred technique for analysis of NEOs [24]. Furthermore, the use of HPLC coupled with different detectors such as fluorescence (FLD), diode array detector (DAD), triple quadrupole tandem mass spectrometry (MS/MS), ultraviolet (UV) and mass spectrometry (MS) have been reported in many studies [31]. However, the DAD and MS/MS have been among the most applied and reported detection techniques [153]. These two most preferred detectors have several advantages; DAD provides low cost and high availability wherein the advantages of MS/MS is the identification and confirmation of the target analyte(s) [154]. Few studies have used gas chromatography (GC) to detect neonicotinoid insecticides because of their high polarity and poor volatility, which prevents them from being directly recognised [102]. High-performance liquid chromatography (HPLC) is typically used to determine these compounds using a variety of detection techniques, such as ultraviolet, diode array detection, thermal lens spectrometry, mass spectrometry, and fluorescence [155]. Some alternative techniques, including LC-MS and LCMS/MS, which are used to determine these analytes, are not widely accessible in typical analytical laboratories and are expensive [102]. However, due to the extremely low concentration of NEOs in the complex matrices, direct instrumental analysis of neonicotinoids is typically not achievable, indicating the need for a sample preparation step [156].

This literature review was compiled on the studies that have been done from 2010 until 2024. The data below will be showing the statistics for both the chromatographic methods and their detectors that have been adopted for the determination of these pesticides in different food samples over the years. The extensive studies have been reported on **Table 2.2** and **2.3**. **Figure 2.8** have shown that the HPLC chromatographic method have been more preferred over the others coupled with a DAD since the statistics in **Figure 2.9** also reports that the DAD detector has been preferred over the other detectors, wherein these is due to the instrument's compatibility to these NEO pesticides. The NEOs physical and chemical properties has enabled them to be compatible with other chromatographic methods, especially with the LC. NEOs poor volatility, high polarity and thermolability have

greatly influenced their incompatibility to be analysed using the GC instrument, respectively. The LC chromatographic method have been the second most preferred method. This instrument is not easily available in most laboratory due to its cost effectiveness and an extensive operation by trained personnel hence it is not found in most common laboratories. In most cases it is coupled with MS or MS/MS detectors hence **Figure 2.9** have presented a higher percentage of the use of those detectors over the others over the years.

However, all the influential parameters affecting the reported sample preparation methods were optimised to get the optimum efficiency.

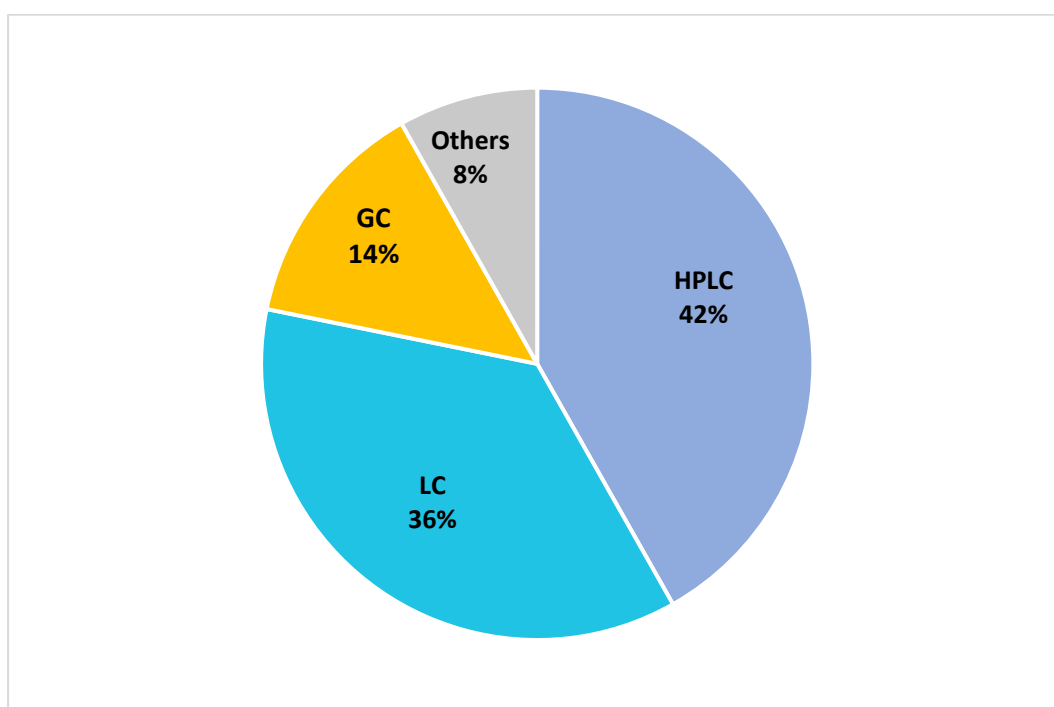


**Figure 2. 8:** Reported detection techniques from 2013 until 2024.

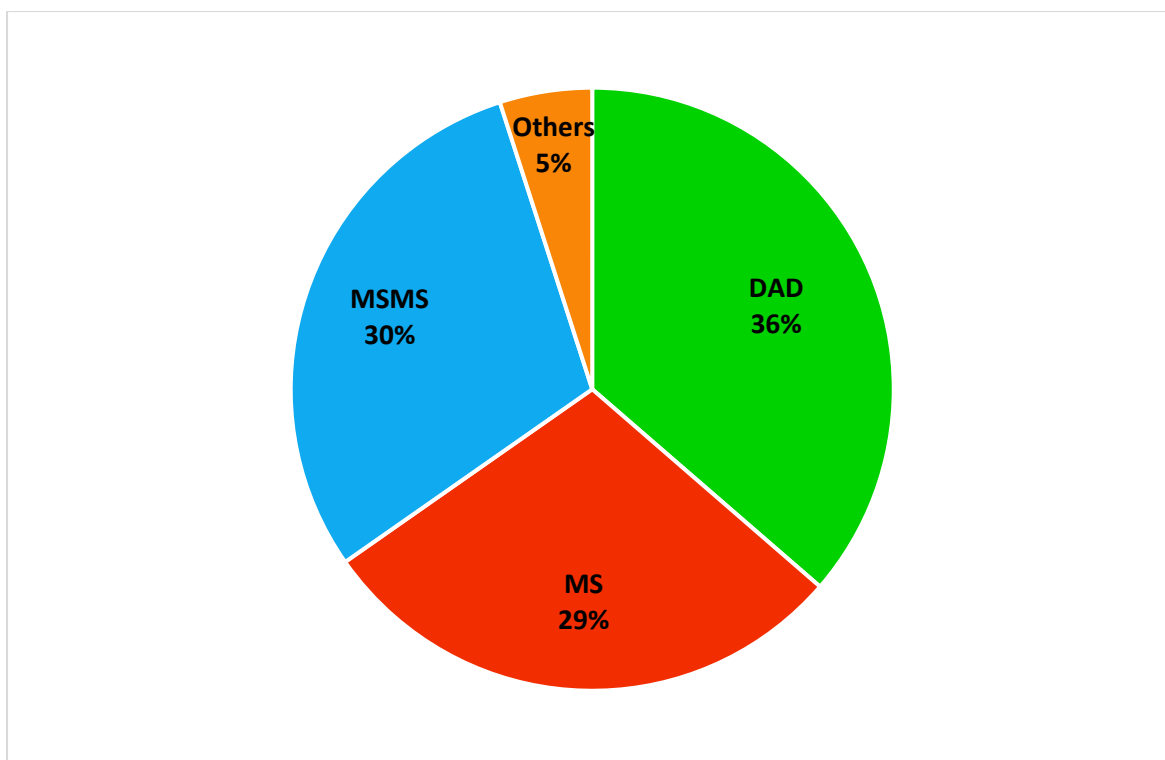


**Figure 2. 9:** Different detectors preferred over the years (2013 - 2024)

### 2.3 Conclusion

From the reported studies in literature and to the best of our knowledge the most used quantification technique for determination of the neonicotinoid pesticides was found to be the HPLC. Since these neonicotinoids are poorly volatile with high polarity, the use of the HPLC instrument is more relevant because it allows determination of low-volatile and thermolabile compounds. A variety of packings and bonded phases as well as eluents and their combinations make this technique very useful in analysis of food contaminants. The HPLC also perform in an increased speed compared to other chromatography methods improving its efficiency for routine sample analysis. However, the performance of the HPLC is also influenced by the type of detector it is coupled with. The review was compiled using the reported data from 2013 to 2024. The most reported neonicotinoid pesticides that are most found in different samples were found to be Acetamiprid, Imidacloprid, Thiamethoxam and Thiocloprid. These pesticides make about 88% of the neonicotinoid pesticides found in different samples according to the reports on different articles. Common reported sample preparation methods for determination of neonicotinoid pesticides ranking them from the most method reported to less QuEChERS, LPME and SPME.

QuEChERS, which is a sample preparation method towards multiple pesticide residue analysis, for extraction and clean purposes. QuEChERS has been preferred over the other sample preparation methods based on the following advantages: minimum the usage of chemical solvents (environmentally friendly), non-labour-intensive process (only a few simple steps), produce high recovery rate, have high precision and accuracy and no chlorinated solvents included covering a wide range of pesticides. QuEChERS has proved to give high recovery rate, and low coefficient of variation in HPLC analysis. Solid phase microextraction (SPME) and liquid phase microextraction (LPME) are the two categories of microextraction techniques that have been developed. LPME originated with the use of a drop of extraction solvent and is based on the use of very small volumes (at the microliter level) of solvent. Sampling, extraction, concentration, and sample introduction are all combined into one solvent-free step using SPME. While eliminating and/or reducing the amount of organic solvents consumed, SPME and LPME are often labour-intensive procedures.

Moreover, it is worth noting that the techniques and methods reported did not address the principle of green chemistry in their studies. For this study, the greener methods were developed that made use of agricultural wastes and making use of greener environmentally friendly solvents that are easy to prepare. The methods that are developed on this study are in microextraction, influencing the micro level volumes used for this study which contributes to the cost effectiveness of the methods. The use of activated carbon as the support material for the magnetic solid phase microextraction preconcentration method was due to its high surface area that will enhance the adsorption process. The magnetic solid phase microextraction (MSPME) method used a magnetic adsorbent that was easy to separate using the magnetic field and the dispersive liquid-liquid extraction (DLLME) made use of the DES that have now gained recognition by many researchers due to their environmental friendliness and simple synthetic process.

## References

- [1] A. M. Cimino, A. L. Boyles, K. A. Thayer, and M. J. Perry, "Effects of neonicotinoid pesticide exposure on human health: A systematic review," *Environ. Health Perspect.*, vol. 125, no. 2, pp. 155–162, 2017, doi: 10.1289/EHP515.
- [2] S. Godecharle, B. Nemery, and K. Dierickx, "Integrity training: Conflicting practices," *Science (80-. )*, vol. 340, no. 6139, p. 1403, 2013, doi: 10.1126/science.340.6139.1403-b.
- [3] G. R. Williams *et al.*, "Neonicotinoid pesticides severely affect honey bee queens," *Sci. Rep.*, vol. 5, pp. 1–8, 2015, doi: 10.1038/srep14621.
- [4] H. A. Craddock, D. Huang, P. C. Turner, L. Quirós-Alcalá, and D. C. Payne-Sturges, "Trends in neonicotinoid pesticide residues in food and water in the United States, 1999-2015," *Environ. Heal. A Glob. Access Sci. Source*, vol. 18, no. 1, pp. 1–16, 2019, doi: 10.1186/s12940-018-0441-7.
- [5] M. Gbylik-Sikorska, T. Sniegocki, and A. Posyniak, "Determination of neonicotinoid insecticides and their metabolites in honey bee and honey by liquid chromatography tandem mass spectrometry," *J. Chromatogr. B Anal. Technol. Biomed. Life Sci.*, vol. 990, pp. 132–140, 2015, doi: 10.1016/j.jchromb.2015.03.016.
- [6] T. BALKAN, "Domates numunelerinde bazı Neonicotinoid Grubu İnektisit Kalıntılarının saptanm," *J. Agric. Fac. Gaziosmanpasa Univ.*, vol. 37, no. 2020–1, pp. 30–37, 2020, doi: 10.13002/jafag4662.
- [7] R. Rasool, B. K. Kang, and K. Mandal, "Estimation of thiamethoxam and its metabolites in wheat using QuEChERS methodology combined with LC-MS/MS," *Int. J. Environ. Anal. Chem.*, vol. 00, no. 00, pp. 1–13, 2022, doi: 10.1080/03067319.2022.2041003.
- [8] V. G. Amelin, D. S. Bol'Shakov, and A. V. Tret'Yakov, "Dispersive liquid-liquid microextraction and solid-phase extraction of polar pesticides from natural water and their determination by micellar electrokinetic chromatography," *J. Anal. Chem.*, vol. 68, no. 5, pp. 386–397, 2013, doi: 10.1134/S1061934813050031.
- [9] S. Sabzevari and J. Hofman, *Currently Used Pesticides' Occurrence in Soils: Recent Results and Advances in Soil-Monitoring and Survey Studies*, vol. 113. 2022. doi: 10.1007/698\_2021\_805.
- [10] C. Adelantado, Á. Ríos, and M. Zougagh, "Magnetic nanocellulose hybrid nanoparticles and ionic liquid for extraction of neonicotinoid insecticides from milk samples prior to determination by liquid chromatography-mass spectrometry," *Food Addit. Contam. - Part A Chem. Anal. Control. Expo. Risk Assess.*, vol. 35, no. 9, pp. 1755–1766, 2018, doi: 10.1080/19440049.2018.1492156.
- [11] J. F. Borsuah, T. L. Messer, D. D. Snow, S. D. Comfort, and A. R. Mittelstet, "Literature review: Global neonicotinoid insecticide occurrence in aquatic environments," *Water (Switzerland)*, vol. 12, no. 12, pp. 1–17, 2020, doi:

10.3390/w12123388.

- [12] G. Ettiene, R. Bauza, M. R. Plata, A. M. Contento, and Á. Ríos, "Determination of neonicotinoid insecticides in environmental samples by micellar electrokinetic chromatography using solid-phase treatments," *Electrophoresis*, vol. 33, no. 19–20, pp. 2969–2977, 2012, doi: 10.1002/elps.201200241.
- [13] B. Buszewski, M. Bukowska, M. Ligor, and I. Staneczko-Baranowska, "A holistic study of neonicotinoids neuroactive insecticides—properties, applications, occurrence, and analysis," *Environ. Sci. Pollut. Res.*, vol. 26, no. 34, pp. 34723–34740, 2019, doi: 10.1007/s11356-019-06114-w.
- [14] EPA, "Name of Chemical : Acetamiprid Reason for Issuance : Conditional Registration," *Pestic. Fact Sheet*, pp. 1–14, 2002.
- [15] A. Report, "concerning the making available on the market and use of biocidal products Clothianidin ( Insecticides , Acaricides and Products to control other Arthropods )," vol. 18, no. 528, 2014.
- [16] E. Watanabe, "Review of sample preparation methods for chromatographic analysis of neonicotinoids in agricultural and environmental matrices: From classical to state-of-the-art methods," *J. Chromatogr. A*, vol. 1643, p. 462042, 2021, doi: 10.1016/j.chroma.2021.462042.
- [17] S. Senger *et al.*, "Neonicotinoid pesticides in Wisconsin groundwater and surface water," *AGRICULTURAL CHEMICAL MANAGEMENT BUREAU* p. 49, 2019.
- [18] D. Sonderberg, J. Doherty, and R. Travaglini, "Opp Official Record Health Effects Division Scientific Data Reviews Epa Series 316." p. 55, 2003.
- [19] I. R. Faria, A. J. Palumbo, T. L. Fojut, and R. S. Tjeerdema, "Water Quality Criteria Report for Malathion Phase III : Application of the pesticide water quality criteria methodology," no. March, 2010.
- [20] J. Hou *et al.*, "Simultaneous determination of ten neonicotinoid insecticides and two metabolites in honey and Royal-jelly by solid–phase extraction and liquid chromatography–tandem mass spectrometry," *Food Chem.*, vol. 270, no. January 2018, pp. 204–213, 2019, doi: 10.1016/j.foodchem.2018.07.068.
- [21] W. Jiao *et al.*, "Optimized combination of dilution and refined QuEChERS to overcome matrix effects of six types of tea for determination eight neonicotinoid insecticides by ultra performance liquid chromatography-electrospray tandem mass spectrometry," *Food Chem.*, vol. 210, pp. 26–34, 2016, doi: 10.1016/j.foodchem.2016.04.097.
- [22] A. Kamel, "Refined methodology for the determination of neonicotinoid pesticides and their metabolites in honey bees and bee products by liquid chromatography-tandem mass spectrometry (LC-MS/MS)," *J. Agric. Food Chem.*, vol. 58, no. 10, pp. 5926–5931, 2010, doi: 10.1021/jf904120n.
- [23] K. Moyakao, Y. Santaladchaiyakit, S. Srijaranai, and J. Vichapong, "Preconcentration of trace neonicotinoid insecticide residues using vortex-assisted dispersive micro solid-phase extraction with montmorillonite as an efficient sorbent," *Molecules*, vol. 23, no. 4, pp. 1–15, 2018, doi:

10.3390/molecules23040883.

- [24] E. Watanabe, Y. Kobara, K. Baba, and H. Eun, "Determination of Seven Neonicotinoid Insecticides in Cucumber and Eggplant by Water-Based Extraction and High-Performance Liquid Chromatography," *Anal. Lett.*, vol. 48, no. 2, pp. 213–220, 2015, doi: 10.1080/00032719.2014.938346.
- [25] S. Valverde, A. M. Ares, M. Arribas, J. L. Bernal, M. J. Nozal, and J. Bernal, "Development and validation of UHPLC–MS/MS methods for determination of neonicotinoid insecticides in royal jelly-based products," *J. Food Compos. Anal.*, vol. 70, no. April, pp. 105–113, 2018, doi: 10.1016/j.jfca.2018.05.002.
- [26] J. Li, Y. Jiang, and D. Li, "Determination of imidacloprid and its relevant metabolites in tomato using modified QuEChERS combined with ultrahigh-pressure liquid chromatography/Orbitrap tandem mass spectrometry," *J. Sci. Food Agric.*, vol. 99, no. 11, pp. 5211–5218, 2019, doi: 10.1002/jsfa.9769.
- [27] S. Li, D. Chen, B. Lv, J. Li, Y. Zhao, and Y. Wu, "Enhanced Sensitivity and Effective Cleanup Strategy for Analysis of Neonicotinoids in Complex Dietary Samples and the Application in the Total Diet Study," *J. Agric. Food Chem.*, vol. 67, no. 9, pp. 2732–2740, 2019, doi: 10.1021/acs.jafc.9b00113.
- [28] X. Li *et al.*, "Simultaneous determination of neonicotinoids and fipronil and its metabolites in environmental water from coastal bay using disk-based solid-phase extraction and high-performance liquid chromatography–tandem mass spectrometry," *Chemosphere*, vol. 234, pp. 224–231, 2019, doi: 10.1016/j.chemosphere.2019.05.243.
- [29] Q. Zhang *et al.*, "Simultaneous determination of nine neonicotinoids in human urine using isotope-dilution ultra-performance liquid chromatography–tandem mass spectrometry," *Environ. Pollut.*, vol. 240, pp. 647–652, 2018, doi: 10.1016/j.envpol.2018.04.144.
- [30] K. Nakamura, T. Otake, and N. Hanari, "Evaluation of supercritical fluid extraction for the determination of neonicotinoid pesticides in green onion," *J. Environ. Sci. Heal. - Part B Pestic. Food Contam. Agric. Wastes*, vol. 55, no. 7, pp. 604–612, 2020, doi: 10.1080/03601234.2020.1747905.
- [31] S. Liu *et al.*, "Simultaneous determination of seven neonicotinoid pesticide residues in food by ultraperformance liquid chromatography tandem mass spectrometry," *J. Agric. Food Chem.*, vol. 58, no. 6, pp. 3271–3278, 2010, doi: 10.1021/jf904045j.
- [32] T. Rodríguez-Cabo, J. Casado, I. Rodríguez, M. Ramil, and R. Cela, "Selective extraction and determination of neonicotinoid insecticides in wine by liquid chromatography–tandem mass spectrometry," *J. Chromatogr. A*, vol. 1460, pp. 9–15, 2016, doi: 10.1016/j.chroma.2016.07.004.
- [33] R. Jędrkiewicz, M. Kupska, A. Głowacz, J. Gromadzka, and J. Namieśnik, "3-MCPD: A Worldwide Problem of Food Chemistry," *Crit. Rev. Food Sci. Nutr.*, vol. 56, no. 14, pp. 2268–2277, Oct. 2016, doi: 10.1080/10408398.2013.829414.
- [34] M. A. Farajzadeh, M. R. Afshar Mogaddam, and A. A. Alizadeh, "Determination of neonicotinoid insecticide residues in edible oils by water-induced

- homogeneous liquid-liquid extraction and dispersive liquid-liquid extraction followed by high performance liquid chromatography-diode array detection," *RSC Adv.*, vol. 5, no. 95, pp. 77501–77507, 2015, doi: 10.1039/c5ra13059j.
- [35] S. Macmahon, T. H. Begley, and G. W. Diachenko, "Analysis of processing contaminants in edible oils. Part 2. Liquid chromatography-tandem mass spectrometry method for the direct detection of 3-monochloropropanediol and 2-monochloropropanediol diesters," *J. Agric. Food Chem.*, vol. 61, no. 20, pp. 4748–4757, 2013, doi: 10.1021/jf400581g.
- [36] S. Song, Y. He, B. Zhang, M. Gui, J. Ouyang, and T. Zhang, "A novel extraction method for simultaneous determination of neonicotinoid insecticides and their metabolites in human urine," *Anal. Methods*, vol. 11, no. 19, pp. 2571–2578, 2019, doi: 10.1039/c9ay00288j.
- [37] J. M. Bonmatin *et al.*, "Environmental fate and exposure; neonicotinoids and fipronil," *Environ. Sci. Pollut. Res.*, vol. 22, no. 1, pp. 35–67, 2015, doi: 10.1007/s11356-014-3332-7.
- [38] G. Tanner and C. Czerwenka, "LC-MS/MS analysis of neonicotinoid insecticides in honey: Methodology and residue findings in Austrian honeys," *J. Agric. Food Chem.*, vol. 59, no. 23, pp. 12271–12277, 2011, doi: 10.1021/jf202775m.
- [39] M. Mrzlikar, D. Heath, E. Heath, J. Markelj, A. Kandolf Borovšak, and H. Prosen, "Investigation of neonicotinoid pesticides in Slovenian honey by LC-MS/MS," *Lwt*, vol. 104, no. November 2018, pp. 45–52, 2019, doi: 10.1016/j.lwt.2019.01.017.
- [40] S. Seccia, P. Fidente, D. Montesano, and P. Morrica, "Determination of neonicotinoid insecticides residues in bovine milk samples by solid-phase extraction clean-up and liquid chromatography with diode-array detection," *J. Chromatogr. A*, vol. 1214, no. 1–2, pp. 115–120, 2008, doi: 10.1016/j.chroma.2008.10.088.
- [41] S. Song *et al.*, "Simultaneous determination of neonicotinoid insecticides and insect growth regulators residues in honey using LC–MS/MS with anion exchanger-disposable pipette extraction," *J. Chromatogr. A*, vol. 1557, pp. 51–61, 2018, doi: 10.1016/j.chroma.2018.05.003.
- [42] Z. Ju, J. Fan, Z. Meng, R. Lu, H. Gao, and W. Zhou, "A high-throughput semi-automated dispersive liquid–liquid microextraction based on deep eutectic solvent for the determination of neonicotinoid pesticides in edible oils," *Microchem. J.*, vol. 185, no. November 2022, p. 108193, 2023, doi: 10.1016/j.microc.2022.108193.
- [43] S. Stehle *et al.*, "Neonicotinoid insecticides in global agricultural surface waters – Exposure, risks and regulatory challenges," *Sci. Total Environ.*, vol. 867, no. January, 2023, doi: 10.1016/j.scitotenv.2022.161383.
- [44] E. Rutkowska and P. Kaczy, "Three approaches to minimize matrix effects in residue analysis of multiclass pesticides in dried complex matrices using gas chromatography tandem mass spectrometry," vol. 279, no. July 2018, pp. 20–29, 2019, doi: 10.1016/j.foodchem.2018.11.130.



- [45] R. Kachangoon, J. Vichapong, Y. Santaladchaiyakit, and S. Srijaranai, "Cloud-point extraction coupled to in-situ metathesis reaction of deep eutectic solvents for preconcentration and liquid chromatographic analysis of neonicotinoid insecticide residues in water, soil and urine samples," *Microchem. J.*, vol. 152, no. July 2019, p. 104377, 2020, doi: 10.1016/j.microc.2019.104377.
- [46] Y. Wang *et al.*, "A comprehensive review on the pretreatment and detection methods of neonicotinoid insecticides in food and environmental samples," *Food Chem. X*, vol. 15, no. April, p. 100375, 2022, doi: 10.1016/j.fochx.2022.100375.
- [47] F. Baroudi *et al.*, "Liquid-liquid extraction procedure for nonvolatile pesticides determination in acacia honey as environmental biomonitor," *Euro-Mediterranean J. Environ. Integr.*, vol. 6, no. 3, pp. 1-8, 2021, doi: 10.1007/s41207-021-00282-3.
- [48] C. Hao, D. Morse, X. Zhao, and L. Sui, "Liquid chromatography/tandem mass spectrometry analysis of neonicotinoids in environmental water," *Rapid Commun. Mass Spectrom.*, vol. 29, no. 23, pp. 2225-2232, 2015, doi: 10.1002/rcm.7381.
- [49] J. Vichapong, K. Moyakao, R. Kachangoon, R. Burakham, Y. Santaladchaiyakit, and S. Srijaranai, "B-Cyclodextrin assisted liquid-liquid microextraction based on solidification of the floating organic droplets method for determination of neonicotinoid residues," *Molecules*, vol. 24, no. 21, 2019, doi: 10.3390/molecules24213954.
- [50] K. P. Yáñez, J. L. Bernal, M. J. Nozal, M. T. Martín, and J. Bernal, "Determination of seven neonicotinoid insecticides in beeswax by liquid chromatography coupled to electrospray-mass spectrometry using a fused-core column," *J. Chromatogr. A*, vol. 1285, pp. 110-117, 2013, doi: 10.1016/j.chroma.2013.02.032.
- [51] A. C. Martel and C. Lair, "Validation of a highly sensitive method for the determination of neonicotinoid insecticides residues in honeybees by liquid chromatography with electrospray tandem mass spectrometry," *Int. J. Environ. Anal. Chem.*, vol. 91, no. 10, pp. 978-988, 2011, doi: 10.1080/03067310903524822.
- [52] P. Jovanov *et al.*, "Multi-residue method for determination of selected neonicotinoid insecticides in honey using optimized dispersive liquid-liquid microextraction combined with liquid chromatography-tandem mass spectrometry," *Talanta*, vol. 111, pp. 125-133, 2013, doi: 10.1016/j.talanta.2013.02.059.
- [53] L. Ma, Y. Wang, H. Li, F. Peng, B. Qiu, and Z. Yang, "Development of QuEChERS-DLLME method for determination of neonicotinoid pesticide residues in grains by liquid chromatography-tandem mass spectrometry," *Food Chem.*, vol. 331, no. October 2019, p. 127190, 2020, doi: 10.1016/j.foodchem.2020.127190.
- [54] E. L. Smith, A. P. Abbott, and K. S. Ryder, "Deep Eutectic Solvents (DESs) and Their Applications," *Chem. Rev.*, vol. 114, no. 21, pp. 11060-11082, 2014, doi: 10.1021/cr300162p.

- [55] R. Kachangoon, J. Vichapong, R. Burakham, Y. Santaladchaiyakit, and S. Srijaranai, "Ultrasonically modified amended-cloud point extraction for simultaneous pre-concentration of neonicotinoid insecticide residues," *Molecules*, vol. 23, no. 5, 2018, doi: 10.3390/molecules23051165.
- [56] R. Halko, I. Hagarová, and V. Andruch, "Innovative approaches in cloud-point extraction," *J. Chromatogr. A*, vol. 1701, p. 464053, 2023, doi: 10.1016/j.chroma.2023.464053.
- [57] D. Snigur, E. A. Azooz, O. Zhukovetska, O. Guzenko, and W. Mortada, "Recent innovations in cloud point extraction towards a more efficient and environmentally friendly procedure," *TrAC - Trends Anal. Chem.*, vol. 164, p. 117113, 2023, doi: 10.1016/j.trac.2023.117113.
- [58] Z. Liu *et al.*, "Determination of carbendazim and thiabendazole in apple juice by hollow fibre-based liquid phase microextraction-high performance liquid chromatography with fluorescence detection," *Int. J. Environ. Anal. Chem.*, vol. 92, no. 5, pp. 582–591, 2012, doi: 10.1080/03067311003628646.
- [59] Y. Jiang, Y. Li, Y. Jiang, J. Li, and C. Pan, "Determination of multiresidues in rapeseed, rapeseed oil, and rapeseed meal by acetonitrile extraction, low-temperature cleanup, and detection by liquid chromatography with tandem mass spectrometry," *J. Agric. Food Chem.*, vol. 60, no. 20, pp. 5089–5098, 2012, doi: 10.1021/jf3004064.
- [60] S. Zhang, X. Yang, X. Yin, C. Wang, and Z. Wang, "Dispersive liquid-liquid microextraction combined with sweeping micellar electrokinetic chromatography for the determination of some neonicotinoid insecticides in cucumber samples," *Food Chem.*, vol. 133, no. 2, pp. 544–550, 2012, doi: 10.1016/j.foodchem.2012.01.028.
- [61] L. Sánchez-Hernández, M. Higes, M. T. Martín, M. J. Nozal, and J. L. Bernal, "Simultaneous determination of neonicotinoid insecticides in sunflower-treated seeds (hull and kernel) by LC-MS/MS," *Food Addit. Contam. - Part A Chem. Anal. Control. Expo. Risk Assess.*, vol. 33, no. 3, pp. 442–451, 2016, doi: 10.1080/19440049.2015.1128565.
- [62] J. Vichapong, R. Burakham, and S. Srijaranai, "Vortex-assisted surfactant-enhanced-emulsification liquid-liquid microextraction with solidification of floating organic droplet combined with HPLC for the determination of neonicotinoid pesticides," *Talanta*, vol. 117, pp. 221–228, 2013, doi: 10.1016/j.talanta.2013.08.034.
- [63] H. Zhao *et al.*, "Phenolic-based non-ionic deep eutectic solvent for rapid determination of water soluble neonicotinoid insecticides in tea infusion," *Food Chem.*, vol. 416, no. 5, p. 135737, 2023, doi: 10.1016/j.foodchem.2023.135737.
- [64] J. Hou *et al.*, "Simultaneous Determination of Neonicotinoid Insecticides and Metabolites Residues in Milk and Infant Formula Milk Powder by EMR-Liquid Chromatography-Tandem Mass Spectrometry," *Food Anal. Methods*, vol. 16, no. 7, pp. 1215–1226, 2023, doi: 10.1007/s12161-023-02484-7.
- [65] D. Li *et al.*, "Neonicotinoid insecticide and their metabolite residues in fruit

- juices: Implications for dietary intake in China,” *Chemosphere*, vol. 261, p. 127682, 2020, doi: 10.1016/j.chemosphere.2020.127682.
- [66] Z. Dashtbozorgi, M. K. Ramezani, and S. Waqif-Husain, “Optimization and validation of a new pesticide residue method for cucumber and tomato using acetonitrile-based extraction-dispersive liquid-liquid microextraction followed by liquid chromatography-tandem mass spectrometry,” *Anal. Methods*, vol. 5, no. 5, pp. 1192–1198, 2013, doi: 10.1039/c2ay26287h.
- [67] L. Lachat and G. Glauser, “Development and Validation of an Ultra-Sensitive UHPLC-MS/MS Method for Neonicotinoid Analysis in Milk,” *J. Agric. Food Chem.*, vol. 66, no. 32, pp. 8639–8646, 2018, doi: 10.1021/acs.jafc.8b03005.
- [68] J. Tursen, T. Yang, L. Bai, D. Li, and R. Tan, “Determination of imidacloprid and acetamiprid in bottled juice by a new DLLME-HPLC,” *Environ. Sci. Pollut. Res.*, vol. 28, no. 36, pp. 50867–50877, 2021, doi: 10.1007/s11356-021-13540-2.
- [69] J. Vichapong, R. Burakham, Y. Santaladchaiyakit, and S. Srijaranai, “A preconcentration method for analysis of neonicotinoids in honey samples by ionic liquid-based cold-induced aggregation microextraction,” *Talanta*, vol. 155, pp. 216–221, 2016, doi: 10.1016/j.talanta.2016.04.045.
- [70] O. I. Abdallah and F. M. Malhat, “Thiacloprid Residues in Green Onion (*Allium cepa*) Using Micro Liquid–Liquid Extraction and Liquid Chromatography–Tandem Mass Spectrometry,” *Agric. Res.*, vol. 9, no. 3, pp. 340–348, 2020, doi: 10.1007/s40003-019-00440-8.
- [71] A. Suganthi, K. Bhuvaneswari, and M. Ramya, “Determination of neonicotinoid insecticide residues in sugarcane juice using LCMSMS,” *Food Chem.*, vol. 241, no. December 2016, pp. 275–280, 2018, doi: 10.1016/j.foodchem.2017.08.098.
- [72] G. C. Bedendo, I. C. S. F. Jardim, and E. Carasek, “Multiresidue determination of pesticides in industrial and fresh orange juice by hollow fiber microporous membrane liquid-liquid extraction and detection by liquid chromatography-electrospray-tandem mass spectrometry,” *Talanta*, vol. 88, pp. 573–580, 2012, doi: 10.1016/j.talanta.2011.11.037.
- [73] W. Chen *et al.*, “Matrix-Induced Sugaring-Out: A Simple and Rapid Sample Preparation Method for the Determination of Neonicotinoid Pesticides in Honey”, *Molecules*. vol 24(15), pp. 2761. 2019.
- [74] M. Pastor-Belda *et al.*, “Determination of spirocyclic tetronic/tetramic acid derivatives and neonicotinoid insecticides in fruits and vegetables by liquid chromatography and mass spectrometry after dispersive liquid-liquid microextraction,” *Food Chem.*, vol. 202, pp. 389–395, 2016, doi: 10.1016/j.foodchem.2016.01.143.
- [75] S. Anvar Nojedeh Sadat, R. Atazadeh, and M. R. Afshar Mogaddam, “Application of in-situ formed polymer-based dispersive solid phase extraction in combination with solidification of floating organic droplet-based dispersive liquid–liquid microextraction for the extraction of neonicotinoid pesticides from milk samples,” *J. Sep. Sci.*, vol. 46, no. 13, 2023, doi:

10.1002/jssc.202200889.

- [76] K. Nakamura, T. Otake, and N. Hanari, "Evaluation of pressurized liquid extraction for th[1] K. Nakamura, T. Otake, and N. Hanari, 'Evaluation of pressurized liquid extraction for the determination of neonicotinoid pesticides in green onion,' *J. Environ. Sci. Heal. - Part B Pestic. Food Contam.*" *J. Environ. Sci. Heal. - Part B Pestic. Food Contam. Agric. Wastes*, vol. 54, no. 8, pp. 640–646, 2019, doi: 10.1080/03601234.2019.1621633.
- [77] J. Vichapong, R. Kachangoon, R. Burakham, Y. Santaladchaiyakit, and S. Srijaranai, "Ringer Tablet-Based Micelle-Mediated Extraction-Solvent Back Extraction Coupled with High-Performance Liquid Chromatography for Preconcentration and Determination of Neonicotinoid Pesticides," *Food Anal. Methods*, vol. 15, no. 4, pp. 970–980, 2022, doi: 10.1007/s12161-021-02067-4.
- [78] A. Q. Abdulhusein, A. K. Mohd Jamil, and N. K. Abu Bakar, "Cloud point extraction (CPE) coupled with QuEChERS for extraction and clean up of neonicotinoid pesticide residues in honey," *Int. J. Environ. Anal. Chem.*, vol. 00, no. 00, pp. 1–16, 2022, doi: 10.1080/03067319.2022.2038146.
- [79] X. Tu and W. Chen, "Overview of Analytical Methods for the Determination of Neonicotinoid Pesticides in Honeybee Products and Honeybee," *Crit. Rev. Anal. Chem.*, vol. 51, no. 4, pp. 329–338, 2021, doi: 10.1080/10408347.2020.1728516.
- [80] R. C. Duca, G. Salquebre, E. Hardy, and B. M. R. Appenzeller, "Comparison of solid phase- and liquid/liquid-extraction for the purification of hair extract prior to multi-class pesticides analysis," *J. Chromatogr. B Anal. Technol. Biomed. Life Sci.*, vol. 955–956, no. 1, pp. 98–107, 2014, doi: 10.1016/j.jchromb.2014.02.035.
- [81] R. Raina-Fulton, "Determination of neonicotinoid insecticides and strobilurin fungicides in particle phase atmospheric samples by liquid chromatography-tandem mass spectrometry," *J. Agric. Food Chem.*, vol. 63, no. 21, pp. 5152–5162, 2015, doi: 10.1021/acs.jafc.5b01347.
- [82] R. Y. Hou, W. T. Jiao, X. S. Qian, X. H. Wang, Y. Xiao, and X. C. Wan, "Effective extraction method for determination of neonicotinoid residues in tea," *J. Agric. Food Chem.*, vol. 61, no. 51, pp. 12565–12571, 2013, doi: 10.1021/jf404100x.
- [83] E. Watanabe and S. Miyake, "Quantitative Determination of Neonicotinoid Insecticide Thiamethoxam in Agricultural Samples: A Comparative Verification Between High-Performance Liquid Chromatography and Monoclonal Antibody-Based Immunoassay," *Food Anal. Methods*, vol. 6, no. 2, pp. 658–666, 2013, doi: 10.1007/s12161-012-9461-z.
- [84] M. Moustafa *et al.*, "Chitosan functionalized AgNPs for efficient removal of Imidacloprid pesticide through a pressure-free design," *Int. J. Biol. Macromol.*, vol. 168, pp. 116–123, 2021, doi: 10.1016/j.ijbiomac.2020.12.055.
- [85] M. A. Farajzadeh, M. Bamorowat, and M. R. A. Mogaddam, "Ringer tablet-based ionic liquid phase microextraction: Application in extraction and preconcentration of neonicotinoid insecticides from fruit juice and vegetable

- samples," *Talanta*, vol. 160, pp. 211–216, 2016, doi: 10.1016/j.talanta.2016.03.097.
- [86] S. Li *et al.*, "Synthesis of nitrogen-rich magnetic hypercrosslinked polymer as robust adsorbent for the detection of neonicotinoids in honey , tomatoes , lettuce and Chinese cabbage," *J. Chromatogr. A*, vol. 1677, p. 463326, 2022, doi: 10.1016/j.chroma.2022.463326.
- [87] S. Zheng, H. Wu, Z. Li, J. Wang, H. Zhang, and M. Qian, "Ultrasound/microwave-assisted solid-liquid-solid dispersive extraction with high-performance liquid chromatography coupled to tandem mass spectrometry for the determination of neonicotinoid insecticides in *Dendrobium officinale*," *J. Sep. Sci.*, vol. 38, no. 1, pp. 121–127, 2015, doi: 10.1002/jssc.201400872.
- [88] Y. Qin *et al.*, "Multi-residue method for determination of selected neonicotinoid insecticides in traditional chinese medicine using modified dispersive solid-phase extraction combined with ultraperformance liquid chromatography tandem mass spectrometry," *Anal. Sci.*, vol. 31, no. 8, pp. 823–830, 2015, doi: 10.2116/analsci.31.823.
- [89] M. Chen, E. M. Collins, L. Tao, and C. Lu, "Simultaneous determination of residues in pollen and high-fructose corn syrup from eight neonicotinoid insecticides by liquid chromatography-tandem mass spectrometry," *Anal. Bioanal. Chem.*, vol. 405, no. 28, pp. 9251–9264, 2013, doi: 10.1007/s00216-013-7338-7.
- [90] C. Jabot, M. Fieu, B. Giroud, A. Buleté, H. Casabianca, and E. Vulliet, "Trace-level determination of pyrethroid, neonicotinoid and carboxamide pesticides in beeswax using dispersive solid-phase extraction followed by ultra-high-performance liquid chromatography-tandem mass spectrometry," *Int. J. Environ. Anal. Chem.*, vol. 95, no. 3, pp. 240–257, 2015, doi: 10.1080/03067319.2015.1016011.
- [91] S. Ahn, S. Son, B. Kim, and K. Choi, "Development of an isotope dilution liquid chromatography/tandem mass spectrometry method for the accurate determination of neonicotinoid pesticides, imidacloprid, clothianidin, and thiamethoxam in kimchi cabbage reference materials," *J. Anal. Sci. Technol.*, vol. 13, no. 1, 2022, doi: 10.1186/s40543-022-00319-4.
- [92] H. Ding *et al.*, "A spherical metal-organic coordination polymer for the microextraction of neonicotinoid insecticides prior to their determination by HPLC," *Microchim. Acta*, vol. 186, no. 2, 2019, doi: 10.1007/s00604-018-3210-y.
- [93] W. A. Wan Ibrahim, H. R. Nodeh, H. Y. Aboul-Enein, and M. M. Sanagi, "Magnetic Solid-Phase Extraction Based on Modified Ferum Oxides for Enrichment, Preconcentration, and Isolation of Pesticides and Selected Pollutants," *Crit. Rev. Anal. Chem.*, vol. 45, no. 3, pp. 270–287, 2015, doi: 10.1080/10408347.2014.938148.
- [94] L. Z. Liu, R. Zhou, Y. L. Li, Y. H. Pang, X. F. Shen, and J. Liu, "Covalent organic framework-sodium alginate-Ca<sup>2+</sup>-polyacrylic acid composite beads for convenient dispersive solid-phase extraction of neonicotinoid insecticides in

- fruit and vegetables," *Food Chem.*, vol. 441, no. November 2023, p. 138357, 2024, doi: 10.1016/j.foodchem.2024.138357.
- [95] S. Valverde, A. M. Ares, J. L. Bernal, M. J. Nozal, and J. Bernal, "Fast determination of neonicotinoid insecticides in beeswax by ultra-high performance liquid chromatography-tandem mass spectrometry using an enhanced matrix removal-lipid sorbent for clean-up," *Microchem. J.*, vol. 142, no. June, pp. 70–77, 2018, doi: 10.1016/j.microc.2018.06.020.
- [96] L. Guo *et al.*, "Design of hydroxyl-functionalized nanoporous organic polymer with tunable hydrophilic-hydrophobic surface for solid phase extraction of neonicotinoid insecticides," *Talanta*, vol. 258, no. January, p. 124441, 2023, doi: 10.1016/j.talanta.2023.124441.
- [97] R. Alizadeh, B. mashalavi, A. Yeganeh Faal, and S. Seidi, "Development of ultrasound assisted dispersive micro solid phase extraction based on CuO nanoplate-polyaniline composite as a new sorbent for insecticides analysis in wheat samples," *Microchem. J.*, vol. 168, no. May, p. 106422, 2021, doi: 10.1016/j.microc.2021.106422.
- [98] W. Si *et al.*, "Zeolite H-Beta as a Dispersive Solid-Phase Extraction Sorbent for the Determination of Eight Neonicotinoid Insecticides Using Ultra-High-Performance Liquid Chromatography—Tandem Mass Spectrometry," *Appl. Sci.*, vol. 12, no. 9, 2022, doi: 10.3390/app12094316.
- [99] C. Mohan, Y. Kumar, J. Madan, and N. Saxena, "Multiresidue analysis of neonicotinoids by solid-phase extraction technique using high-performance liquid chromatography," *Environ. Monit. Assess.*, vol. 165, no. 1–4, pp. 573–576, 2010, doi: 10.1007/s10661-009-0968-8.
- [100] L. Carbonell-Rozas, F. J. Lara, M. del Olmo Iruela, and A. M. García-Campaña, "Micellar electrokinetic chromatography as efficient alternative for the multiresidue determination of seven neonicotinoids and 6-chloronicotinic acid in environmental samples," *Anal. Bioanal. Chem.*, vol. 412, no. 24, pp. 6231–6240, 2020, doi: 10.1007/s00216-019-02233-y.
- [101] L. Carbonell-Rozas, F. J. Lara, and A. M. García-Campaña, "Analytical Methods Based on Liquid Chromatography and Capillary Electrophoresis to Determine Neonicotinoid Residues in Complex Matrices. A Comprehensive Review," *Crit. Rev. Anal. Chem.*, vol. 0, no. 0, pp. 1–29, 2023, doi: 10.1080/10408347.2023.2186700.
- [102] A. Ghiasi, A. Malekpour, and S. Mahpishanian, "Metal-organic framework MIL101 (Cr)-NH<sub>2</sub> functionalized magnetic graphene oxide for ultrasonic-assisted magnetic solid phase extraction of neonicotinoid insecticides from fruit and water samples," *Talanta*, vol. 217, no. January, p. 121120, 2020, doi: 10.1016/j.talanta.2020.121120.
- [103] Z. Xiao, Y. Yang, Y. Li, X. Fan, and S. Ding, "Determination of neonicotinoid insecticides residues in eels using subcritical water extraction and ultra-performance liquid chromatography-tandem mass spectrometry," *Anal. Chim. Acta*, vol. 777, pp. 32–40, 2013, doi: 10.1016/j.aca.2013.03.026.
- [104] R. Kachangoon, J. Vichapong, Y. Santaladchaiyakit, R. Burakham, and S.

- Srijaranai, "Sample Preparation Approach by In Situ Formation of Supramolecular Solvent Microextraction for Enrichment of Neonicotinoid Insecticide Residues," *Food Anal. Methods*, vol. 16, no. 2, pp. 330–339, 2023, doi: 10.1007/s12161-022-02417-w.
- [105] O. I. Abdallah, R. M. Abd El-Hamid, N. S. Ahmed, S. S. Alhewairini, and S. B. Abdel Ghani, "Development of Green and Facile Sample Preparation Method for Determination of Seven Neonicotinoids in Fresh Vegetables, and Dissipation and Risk Assessment of Imidacloprid and Dinotefuran," *Foods*, vol. 13, no. 7, 2024, doi: 10.3390/foods13071106.
- [106] F. Leyton-Soto, Z. D. Schultz, R. Ormazábal-Toledo, D. Ruiz-León, A. Giordano, and M. Isaacs, "Suitability study of Ag nanosheet SERS substrates as a screening method for imidacloprid after QuEChERS extraction†," *New J. Chem.*, vol. 48, no. 9, pp. 3924–3932, 2024, doi: 10.1039/d3nj05956a.
- [107] I. Hrynko, G. Ilyasova, M. Jankowska, E. Rutkowska, P. Kaczyński, and B. Łozowicka, "Behavior of Thiamethoxam and Clothianidin in Young Oilseed Rape Plants before Flowering, Monitored by QuEChERS/LC–MS/MS Protocol," *Agric.*, vol. 14, no. 5, 2024, doi: 10.3390/agriculture14050759.
- [108] M. H. Kabir, S. Yasmin, S. Islam, M. A. A. Shaikh, and M. Moniruzzaman, "Residue determination of thiamethoxam and its metabolite clothianidin in okra using the modified QuEChERS method with d-SPE clean-up coupled with LC-MS/MS," *Food Chem. Adv.*, vol. 5, no. May, p. 100754, 2024, doi: 10.1016/j.focha.2024.100754.
- [109] B. Yang *et al.*, "Neonicotinoid insecticides in plant-derived Foodstuffs: A review of separation and determination methods based on liquid chromatography," *Food Chem.*, vol. 444, no. 18, p. 138695, 2024, doi: 10.1016/j.foodchem.2024.138695.
- [110] W. Liu *et al.*, "Facile synthesis of uniform spherical covalent organic frameworks for determination of neonicotinoid insecticides," *Food Chem.*, vol. 367, no. July 2021, p. 130653, 2022, doi: 10.1016/j.foodchem.2021.130653.
- [111] Z. Shi, S. Zhang, Q. Huai, D. Xu, and H. Zhang, "Methylamine-modified graphene-based solid phase extraction combined with UPLC-MS/MS for the analysis of neonicotinoid insecticides in sunflower seeds," *Talanta*, vol. 162, no. June 2016, pp. 300–308, 2017, doi: 10.1016/j.talanta.2016.10.042.
- [112] O. Ozalp, Z. P. Gumus, and M. Soylak, "MIL-101(Cr) metal–organic frameworks based on deep eutectic solvent (ChCl: Urea) for solid phase extraction of imidacloprid in tea infusions and water samples," *J. Mol. Liq.*, vol. 378, p. 121589, 2023, doi: 10.1016/j.molliq.2023.121589.
- [113] T. Iwafune, T. Ogino, and E. Watanabe, "Water-based extraction and liquid chromatography-tandem mass spectrometry analysis of neonicotinoid insecticides and their metabolites in green pepper/tomato samples," *J. Agric. Food Chem.*, vol. 62, no. 13, pp. 2790–2796, 2014, doi: 10.1021/jf405311y.
- [114] S. Jiang *et al.*, "Green synthesis of novel magnetic porous organic polymer for magnetic solid phase extraction of neonicotinoids in lemon juice and honey samples," *Food Chem.*, vol. 383, no. March, p. 132599, 2022, doi:

- 10.1016/j.foodchem.2022.132599.
- [115] L. Liu, T. Feng, C. Wang, Q. Wu, and Z. Wang, "Enrichment of neonicotinoid insecticides from lemon juice sample with magnetic three-dimensional graphene as the adsorbent followed by determination with high-performance liquid chromatography," *J. Sep. Sci.*, vol. 37, no. 11, pp. 1276–1282, 2014, doi: 10.1002/jssc.201301382.
- [116] J. Lu *et al.*, "A functionalized magnetic covalent organic framework for sensitive determination of trace neonicotinoid residues in vegetable samples," *J. Chromatogr. A*, vol. 1618, p. 460898, 2020, doi: 10.1016/j.chroma.2020.460898.
- [117] L. Hao, C. Wang, Q. Wu, Z. Li, X. Zang, and Z. Wang, "Metal-organic framework derived magnetic nanoporous carbon: Novel adsorbent for magnetic solid-phase extraction," *Anal. Chem.*, vol. 86, no. 24, pp. 12199–12205, 2014, doi: 10.1021/ac5031896.
- [118] X. Cao *et al.*, "One-pot synthesis of magnetic zeolitic imidazolate framework/grapheme oxide composites for the extraction of neonicotinoid insecticides from environmental water samples," *J. Sep. Sci.*, vol. 40, no. 24, pp. 4747–4756, 2017, doi: 10.1002/jssc.201700674.
- [119] X. Ma *et al.*, "Magnetic solid-phase extraction of neonicotinoid pesticides from pear and tomato samples using graphene grafted silica-coated Fe<sub>3</sub>O<sub>4</sub> as the magnetic adsorbent," *Anal. Methods*, vol. 5, no. 11, pp. 2809–2815, 2013, doi: 10.1039/c3ay40207j.
- [120] L. Liu, Y. Hao, X. Zhou, C. Wang, Q. Wu, and Z. Wang, "Magnetic porous carbon based solid-phase extraction coupled with high performance liquid chromatography for the determination of neonicotinoid insecticides in environmental water and peanut milk samples," *Anal. Methods*, vol. 7, no. 6, pp. 2762–2769, 2015, doi: 10.1039/c4ay02990a.
- [121] S. K. Selahle, N. J. Waleng, A. Mpupa, and P. N. Nomngongo, "Magnetic Solid Phase Extraction Based on Nanostructured Magnetic Porous Porphyrin Organic Polymer for Simultaneous Extraction and Preconcentration of Neonicotinoid Insecticides From Surface Water," *Front. Chem.*, vol. 8, no. September, pp. 1–15, 2020, doi: 10.3389/fchem.2020.555847.
- [122] L. Chen and B. Li, "Determination of imidacloprid in rice by molecularly imprinted-matrix solid-phase dispersion with liquid chromatography tandem mass spectrometry," *J. Chromatogr. B Anal. Technol. Biomed. Life Sci.*, vol. 897, pp. 32–36, 2012, doi: 10.1016/j.jchromb.2012.04.004.
- [123] X. Cao *et al.*, "Metal-organic framework UiO-66 for rapid dispersive solid phase extraction of neonicotinoid insecticides in water samples," *J. Chromatogr. B Anal. Technol. Biomed. Life Sci.*, vol. 1077–1078, no. October 2017, pp. 92–97, 2018, doi: 10.1016/j.jchromb.2017.11.034.
- [124] M. Zhang, H. Chen, L. Zhu, C. Wang, G. Ma, and X. Liu, "Solid-phase purification and extraction for the determination of trace neonicotinoid pesticides in tea infusion," *J. Sep. Sci.*, vol. 39, no. 5, pp. 910–917, 2016, doi: 10.1002/jssc.201501129.



- [125] W. Guan *et al.*, "Amine modified graphene as reversed-dispersive solid phase extraction materials combined with liquid chromatography-tandem mass spectrometry for pesticide multi-residue analysis in oil crops," *J. Chromatogr. A*, vol. 1286, pp. 1–8, 2013, doi: 10.1016/j.chroma.2013.02.043.
- [126] S. Wang *et al.*, "A functionalized carbon nanotube nanohybrids-based QuEChERS method for detection of pesticide residues in vegetables and fruits," *J. Chromatogr. A*, vol. 1631, 2020, doi: 10.1016/j.chroma.2020.461526.
- [127] R. López-Blanco *et al.*, "Evaluation of different cleanup sorbents for multiresidue pesticide analysis in fatty vegetable matrices by liquid chromatography tandem mass spectrometry," *J. Chromatogr. A*, vol. 1456, pp. 89–104, 2016, doi: 10.1016/j.chroma.2016.06.019.
- [128] R. Weng *et al.*, "Multi-residue analysis of 126 pesticides in chicken muscle by ultra-high-performance liquid chromatography coupled to quadrupole time-of-flight mass spectrometry," *Food Chem.*, vol. 309, no. April 2019, p. 125503, 2020, doi: 10.1016/j.foodchem.2019.125503.
- [129] Y. A. Kim *et al.*, "Method development, matrix effect, and risk assessment of 49 multiclass pesticides in kiwifruit using liquid chromatography coupled to tandem mass spectrometry," *J. Chromatogr. B Anal. Technol. Biomed. Life Sci.*, vol. 1076, no. January, pp. 130–138, 2018, doi: 10.1016/j.jchromb.2018.01.015.
- [130] X. Zhang *et al.*, "Simultaneous determination of 58 pesticides and relevant metabolites in eggs with a multi-functional filter by ultra-high performance liquid chromatography-tandem mass spectrometry," *J. Chromatogr. A*, vol. 1593, pp. 81–90, 2019, doi: 10.1016/j.chroma.2019.01.074.
- [131] F. P. Costa, S. S. Caldas, and E. G. Primel, "Comparison of QuEChERS sample preparation methods for the analysis of pesticide residues in canned and fresh peach," *Food Chem.*, vol. 165, pp. 587–593, 2014, doi: 10.1016/j.foodchem.2014.05.099.
- [132] Ł. Rajski, A. Lozano, A. Uclés, C. Ferrer, and A. R. Fernández-Alba, "Determination of pesticide residues in high oil vegetal commodities by using various multi-residue methods and clean-ups followed by liquid chromatography tandem mass spectrometry," *J. Chromatogr. A*, vol. 1304, pp. 109–120, 2013, doi: 10.1016/j.chroma.2013.06.070.
- [133] A. Angioni, L. Porcu, and F. Pirisi, "LC/DAD/ESI/MS method for the determination of imidacloprid, thiacloprid, and spinosad in olives and olive oil after field treatment," *J. Agric. Food Chem.*, vol. 59, no. 20, pp. 11359–11366, 2011, doi: 10.1021/jf2028363.
- [134] D. Moreno-González, J. Alcántara-Durán, S. M. Addona, and M. Beneito-Cambra, "Multi-residue pesticide analysis in virgin olive oil by nanoflow liquid chromatography high resolution mass spectrometry," *J. Chromatogr. A*, vol. 1562, pp. 27–35, 2018, doi: 10.1016/j.chroma.2018.05.053.
- [135] J. V. Dias, V. Cutillas, A. Lozano, I. R. Pizzutti, and A. R. Fernández-Alba, "Determination of pesticides in edible oils by liquid chromatography-tandem mass spectrometry employing new generation materials for dispersive solid

- phase extraction clean-up," *J. Chromatogr. A*, vol. 1462, pp. 8–18, 2016, doi: 10.1016/j.chroma.2016.07.072.
- [136] B. Gilbert-López, J. F. García-Reyes, A. Lozano, A. R. Fernández-Alba, and A. Molina-Díaz, "Large-scale pesticide testing in olives by liquid chromatography-electrospray tandem mass spectrometry using two sample preparation methods based on matrix solid-phase dispersion and QuEChERS," *J. Chromatogr. A*, vol. 1217, no. 39, pp. 6022–6035, 2010, doi: 10.1016/j.chroma.2010.07.062.
- [137] H. Khanehzar, M. Faraji, A. Nezhadali, and Y. Yamini, "Combining of modified QuEChERS and dispersive liquid-liquid microextraction as an efficient sample preparation method for extraction of acetamiprid and imidacloprid from pistachio samples," *J. Iran. Chem. Soc.*, vol. 18, no. 3, pp. 641–649, 2021, doi: 10.1007/s13738-020-02050-6.
- [138] F. Zhang, Y. Li, C. Yu, and C. Pan, "Determination of six neonicotinoid insecticides residues in spinach, cucumber, apple and pomelo by QuEChERS method and LC-MS/MS," *Bull. Environ. Contam. Toxicol.*, vol. 88, no. 6, pp. 885–890, 2012, doi: 10.1007/s00128-012-0579-x.
- [139] B. Yang *et al.*, "Determination of eight neonicotinoid insecticides in Chinese cabbage using a modified QuEChERS method combined with ultra performance liquid chromatography-tandem mass spectrometry," *Food Chem.*, vol. 387, no. March, p. 132935, 2022, doi: 10.1016/j.foodchem.2022.132935.
- [140] E. Watanabe, T. Iwafune, K. Baba, and Y. Kobara, "Organic Solvent-Saving Sample Preparation for Systematic Residue Analysis of Neonicotinoid Insecticides in Agricultural Products Using Liquid Chromatography-Diode Array Detection," *Food Anal. Methods*, vol. 9, no. 1, pp. 245–254, 2016, doi: 10.1007/s12161-015-0189-4.
- [141] S. Valverde, M. Ibáñez, J. L. Bernal, M. J. Nozal, F. Hernández, and J. Bernal, "Development and validation of ultra high performance-liquid chromatography-tandem mass spectrometry based methods for the determination of neonicotinoid insecticides in honey," *Food Chem.*, vol. 266, no. June, pp. 215–222, 2018, doi: 10.1016/j.foodchem.2018.06.004.
- [142] Y. Zhang, Q. Zhang, S. Li, Y. Zhao, D. Chen, and Y. Wu, "Simultaneous determination of neonicotinoids and fipronils in tea using a modified QuEChERS method and liquid chromatography-high resolution mass spectrometry," *Food Chem.*, vol. 329, no. May, p. 127159, 2020, doi: 10.1016/j.foodchem.2020.127159.
- [143] U. A. Thorsteinsdóttir and M. Thorsteinsdóttir, "Design of experiments for development and optimization of a liquid chromatography coupled to tandem mass spectrometry bioanalytical assay," *J. Mass Spectrom.*, vol. 56, no. 9, pp. 1–19, 2021, doi: 10.1002/jms.4727.
- [144] C. Zhang *et al.*, "Accurate prediction and further dissection of neonicotinoid elimination in the water treatment by CTS@AgBC using multihead attention-based convolutional neural network combined with the time-dependent Cox regression model," *J. Hazard. Mater.*, vol. 423, no. PA, p. 127029, 2022, doi: 10.1016/j.jhazmat.2021.127029.

- [145] A. Schaafsma, V. Limay-Rios, T. Baute, J. Smith, and Y. Xue, "Neonicotinoid insecticide residues in surface water and soil associated with commercial maize (corn) fields in Southwestern Ontario," *PLoS One*, vol. 10, no. 2, pp. 1–21, 2015, doi: 10.1371/journal.pone.0118139.
- [146] M. Aliste, C. M. Martínez, I. Garrido, P. Hellín, P. Flores, and J. Fenoll, "Multivariate effect of inorganic wastewater matrix on the removal of pesticides by solar photo-Fenton," *J. Environ. Manage.*, vol. 345, no. May, p. 118699, 2023, doi: 10.1016/j.jenvman.2023.118699.
- [147] N. S. Mdluli, C. D. Knottenbelt, P. N. Nomngongo, and N. Mketi, "Microwave-assisted hydrogen peroxide digestion followed by ICP-OES for determination of metals in selected fuel oils," *Sci. Rep.*, vol. 14, no. 1, pp. 1–11, 2024, doi: 10.1038/s41598-024-52898-4.
- [148] N. S. Mdluli, "Development of Greener Sample Preparation Methods for Extraction and Spectrometric Determination of Metals in Selected Fuel Samples," *University of South Africa Thesis* no. February, 2022.
- [149] M. Carabajal, C. M. Teglia, S. Cerutti, M. J. Culzoni, and H. C. Goicoechea, "Applications of liquid-phase microextraction procedures to complex samples assisted by response surface methodology for optimization," *Microchem. J.*, vol. 152, no. August 2019, p. 104436, 2020, doi: 10.1016/j.microc.2019.104436.
- [150] N. S. Mdluli, P. N. Nomngongo, and N. Mketi, "Ionic liquid assisted extraction induced by emulsion breaking for extraction of trace metals in diesel, gasoline and kerosene prior to ICP-OES analysis," *Heliyon*, vol. 10, no. 5, p. e26605, 2024, doi: 10.1016/j.heliyon.2024.e26605.
- [151] C. Hu, J. Feng, Y. Cao, L. Chen, and Y. Li, "Deep eutectic solvents in sample preparation and determination methods of pesticides: Recent advances and future prospects," *Talanta*, vol. 266, no. P2, p. 125092, 2024, doi: 10.1016/j.talanta.2023.125092.
- [152] Z. Wang, J. Chen, T. Zhan, X. He, and B. Wang, "Simultaneous determination of eight neonicotinoid insecticides, fipronil and its three transformation products in sediments by continuous solvent extraction coupled with liquid chromatography-tandem mass spectrometry," *Ecotoxicol. Environ. Saf.*, vol. 189, no. December 2019, p. 110002, 2020, doi: 10.1016/j.ecoenv.2019.110002.
- [153] C. Wu, F. Dong, X. Mei, J. Ning, and D. She, "Isotope-labeled internal standards and grouping scheme for determination of neonicotinoid insecticides and their metabolites in fruits, vegetables and cereals – A compensation of matrix effects," *Food Chem.*, vol. 311, no. July 2019, p. 125871, 2020, doi: 10.1016/j.foodchem.2019.125871.
- [154] W. Xie, C. Han, Y. Qian, H. Ding, X. Chen, and J. Xi, "Determination of neonicotinoid pesticides residues in agricultural samples by solid-phase extraction combined with liquid chromatography-tandem mass spectrometry," *J. Chromatogr. A*, vol. 1218, no. 28, pp. 4426–4433, 2011, doi: 10.1016/j.chroma.2011.05.026.

- [155] Y. Ikenaka *et al.*, “Contamination by neonicotinoid insecticides and their metabolites in Sri Lankan black tea leaves and Japanese green tea leaves,” *Toxicol. Reports*, vol. 5, no. June, pp. 744–749, 2018, doi: 10.1016/j.toxrep.2018.06.008.
- [156] J. Jiménez-López, E. J. Llorent-Martínez, P. Ortega-Barrales, and A. Ruiz-Medina, “Analysis of neonicotinoid pesticides in the agri-food sector: a critical assessment of the state of the art,” *Appl. Spectrosc. Rev.*, vol. 55, no. 8, pp. 613–646, 2020, doi: 10.1080/05704928.2019.1608111.

### DEVELOPMENT OF THE MAGNETIC SOLID PHASE MICROEXTRACTION METHOD FOR THE DETERMINATION OF NEONICOTINOID PESTICIDES FROM VEGETABLE OILS

#### ABSTRACT

A greener sample preparation method based on magnetic solid phase microextraction (MSPME) was developed for the preconcentration of neonicotinoid pesticides (acetamiprid, imidacloprid, thiacloprid and thiamethoxam) in vegetable oil samples. The MSPME method used  $\text{Fe}_3\text{O}_4@\text{Al}_2\text{O}_3/\text{AC}$  nanocomposites, obtained via the green synthesis route, as an adsorbent. The dried lemon peel for preparation of lemon peel solution was used as a surfactant during the synthesis of  $\text{Fe}_3\text{O}_4$  nanocomposites, and the dried corn cobs were used to prepare activated carbon (AC) as support material to form  $\text{Fe}_3\text{O}_4@\text{Al}_2\text{O}_3/\text{AC}$  nanocomposite. Different characterisation techniques such as Fourier Transform Infrared Spectroscopy (FTIR), Powder X-ray diffraction analysis (PXRD), Thermogravimetric Analysis (TGA), Transmission electron microscopy (TEM), Ultraviolet-visible spectroscopy (UV-Vis), and scanning electron microscope and energy-dispersive X-ray spectroscopy (SEM-EDS) confirmed the synthesised magnetic nanocomposites. After that, the  $\text{Fe}_3\text{O}_4$ ,  $\text{Fe}_3\text{O}_4@\text{Al}_2\text{O}_3$  and  $\text{Fe}_3\text{O}_4@\text{Al}_2\text{O}_3/\text{AC}$  adsorbents were applied for extraction and preconcentration of NEOs in vegetable oils followed by separation and quantification using high-performance liquid chromatography with diode array detector (HPLC-DAD). The performance of prepared adsorbents ( $\text{Fe}_3\text{O}_4$ ,  $\text{Fe}_3\text{O}_4@\text{Al}_2\text{O}_3$  and  $\text{Fe}_3\text{O}_4@\text{Al}_2\text{O}_3/\text{AC}$ ) was compared for the preconcentration of NEOs. The  $\text{Fe}_3\text{O}_4@\text{Al}_2\text{O}_3/\text{AC}$  nanocomposite produced acceptable extraction efficiencies (56-119%) and was used for further studies. The most influential parameters affecting the MSPME of NEOs were examined using a multivariate optimisation approach. The optimal parameters obtained were extraction time (8 min), pH (13), sorbent mass (9 mg) and eluent volume (0.5 mL). The proposed MSPME method showed high accuracy (80-119.21%) and precision ( $\leq 10\%$ ) for all the investigated NEOs. Furthermore, the obtained limit of detection (LOD) ranged from 0.5-1.76 ng.  $\mu\text{L}^{-1}$ , the limit of quantification (LOQ) ranged from 1.87-6.62 ng.  $\mu\text{L}^{-1}$  and satisfactory high preconcentration factors (73.02-407) were comparable with literature reported studies.

The Analytical GREENess calculator (AGREE) analysis confirmed the 0.54 greenness scale, implying the method is slightly greener. After that, the validated MSPME method was applied to real vegetable oil samples (avocado, canola, olive and sunflower), and fortunately, all the investigated NEOs were below LODs of the proposed MSPME/HPLC-DAD methods.

**Keywords:** Neonicotinoid pesticides; vegetable oils; magnetic solid phase microextraction (MSPME); HPLC-DAD; AGREE; Fe<sub>3</sub>O<sub>4</sub>@Al<sub>2</sub>O<sub>3</sub>/AC; preconcentration.

### 3.1 Background

Food safety and security are concerns for different organisations in different countries. The agricultural sector uses pesticides for pest control, controlling growth, and reproduction enhancement [1]. However, these pesticides end up accumulating in the crops, soil and groundwater. This study is focusing on NEOs are a group of pesticides, specifically the selected four, which are acetamiprid (ACT), imidacloprid (IMI), thiacloprid (TCL) and thiamethoxam (TMX). These pesticides will be assessed in various vegetable oils. Vegetable oils form part of daily diet requirements in many households. It is worth noting that vegetable oils have nutritional value to human lives and economic benefits for farmers in the market [2]. Contamination of oil crops with these NEOs has poses serious health problems. The possible health problems associated with exposure to NEOs through consumption of contaminated vegetable oils are cancer, birth defects and chronic pulmonary disease among others [3]. Due to the toxicity of these NEOs in oil crops, different countries have set the maximum residue limits (MRLs) [4]. The Codex Alimentarius Commission, the European Union, and the World Health Organization have set the MRLs at less than 0.5 mg.kg<sup>-1</sup> in Japan, US and China [5]. Due to the reasons aforementioned, researchers embarked on a journey of detecting and monitoring these organic pollutants in different food and environmental samples to ensure humans, animals and environmental health.

Different chromatographic methods have been used for the detection of these NEOs compounds, and these include liquid chromatography (LC), gas chromatography (GC) and high-performance liquid chromatography (HPLC) [6]. The nature of the NEOs (poorly volatile, high polarity and thermolability) has made them incompatible for detection with GC [7]. The most reported detection techniques are LC's techniques, which are favoured more due to their availability in many laboratories

and ease of operation [8]. These chromatographic techniques are coupled with different detectors, which include mass spectrometry (MS), triple quadrupole tandem mass spectrometry (MS/MS), diode array detector (DAD), fluorescence detector (FLD) and ultraviolet (UV) [9]. Among the detectors, the DAD and MS/MS have been among the most reported detection techniques [10]. The two most preferred detectors have advantages; with DAD, its advantage is its low cost and high availability wherein the advantages of MS/MS are the identification and confirmation of the analytes [11]. Furthermore, the nature of different sample matrices is not compatible for the direct detection of these NEOs on the chromatographic instrument [12]. Since the chromatography instrument cannot analyse raw samples for the detection of these trace analytes, there is a need of a high-efficient sample preparation method is required prior detection and analysis for the preconcentration of the analytes of interest and clean-up steps [13].

Different types of sample preparation methods have been reported in literature like LLE (liquid-liquid extraction), DLLE (dispersive liquid-liquid extraction), cloud-point extraction (CPE), SPE (Solid phase extraction), MSPE (magnetic solid phase extraction), QuEChERS (Quick, Easy, Cheap, Effective, Rugged and Safe), MSPD (matrix solid phase dispersion) [14][15]. The reported methods suffer from different limitations, including using a large amount of organic solvents. Additionally, these tedious steps can lead to cross-contamination, loss of the analytes of interest, and a large amount of waste [16].

This study aimed to develop a magnetic solid phase microextraction (MSPME) sample preparation method using an HPLC-DAD instrument to quantify selected NEOs in vegetable oils. The MSPME preconcentration method was adopted because it uses magnetic adsorbents with high surface area and simple separation of the analytes. The magnetic adsorbent plays a crucial role in influencing the analytical performance of the method. Moreover, this preconcentration method has attracted the attention of many researchers because of its advantages such as robustness, environmental friendliness, simplicity, robustness and high enrichment factors. The structural, surface and morphological properties of the adsorbent material were characterised using various techniques such as powder X-ray diffraction (PXRD), transmission electron microscopy (TEM), Fourier transform infrared spectroscopy (FTIR), scanning electron microscope coupled to energy dispersive X-ray

spectroscopy (SEM-EDS), thermogravimetric analysis (TGA), and ultraviolet-visible spectroscopy (UV-Vis) [17].

A Minitab software tool was used for the experimental design to determine the optimal extraction parameters of NEOs in vegetable oils. This was used for method development and investigation of the method performance. The use of this software tool for the sample preparation method has assisted with optimising different parameters at the same time, unlike the application of univariate methods where one parameter was investigated at a time [18]. Screening was done following the two-level full factorial design [19]. The multivariate DoE is advantageous in that it minimises the number of experiments which leads to methods cost effectiveness, since it provides optimal parameters such as extraction time, sorbent mass, desorption time and eluent volume at a multivariate optimization [20]. In this study, the DoE followed the full factorial design for experimental design, and the results were presented in Pareto charts. In contrast, response surface methodology (RSM) following the central composite design (CCD) had its results shown on 3D surface plots [21]. The CCD was selected from RSM models because it allows each independent variable to be investigated at five levels, that is, at two-level factorial ( $\pm 1$ ), central points (0) and axis points ( $\pm\alpha$ ) [22].

## **3.2 Experimental procedure**

### **3.2.1. *Reagents, materials, and samples***

All the standards, solvents and reagents were purchased from Merck South Africa. Organic standards for neonicotinoid pesticides acetamiprid, imidacloprid, thiacloprid, and thiamethoxam purchased were of analytical grade. Iron(iii)acetylacetonate, dibenzyl ether, 2-propanol, light petroleum ether, sulphuric acid ( $\text{H}_2\text{SO}_4$ ), hydrochloric acid (HCl), sodium hydroxide (NaOH) solution, deionised water, MilliQ water, acetonitrile (ACN) High performance liquid chromatography grade, oleic acid, lemon peel solution, aluminium isopropoxide, ethanol, formic acid, PVDF micro filters.

The corn cobs were collected from Limpopo province in Vuwani village Ha-Mangilasi during the summer season in December. The lemons were purchased from local supermarkets in South Africa, Johannesburg, Florida Park. Different vegetable



oils (avocado, canola, olive, and sunflower oil) were purchased from local supermarkets in Florida Park, Johannesburg, South Africa.

### **3.2.2. High performance liquid chromatography coupled with diode array detector (HPLC-DAD) instrumentation.**

A Hewlett-Packard 1090 II liquid chromatograph equipped with a DAD Agilent 1260 Infinity high-pressure liquid chromatography (HPLC) system procured from Agilent Technologies (Waldbronn, Germany) was used for separation and determination of NEOs analytes of interest. The chromatographic system consisted of a degasser unit, binary pump, autosampler, auto-injector and thermostatic column compartment. The chromatographic column that was kept at 30 °C was Waters Xterra® C18 3.5 µm 4.6 × 150 mm column obtained from Waters Corporation (Milford, MA, United States). The chromatographic separation was achieved under gradient elution. The chromatograms were recorded at 255 nm and 260 nm for acetamiprid, imidacloprid, thiacloprid and thiamethoxam. Two mobile phases were prepared. Mobile phase A comprised 0.1 % formic acid (FA) in ultrapure water. In comparison, mobile phase B was 100 % acetonitrile using a gradient elution system at a flow rate of 1.0 mL.min<sup>-1</sup> and injection volume of 10 µL. Gradient elution setup was at the following time intervals with the amount of solvent in percentage (%): 0 min 65 % A:35 % B, 2 min 75 % A:25 % B, 2:50 min 55 % A:45 %B and lastly at 4:30 min 65 % A:35 % B [23].

### **3.2.3. Preparation calibration standards**

The standard mix solution of all four different NEOs was prepared in acetonitrile on a 10 mL volumetric flask and stored in a refrigerator at 4 °C for future use. Different calibration standards were also prepared at ten concentrations (8-1000 ng.L<sup>-1</sup>). The peak at 2.11 min is thiamethoxam, at 2.3 min is acetamiprid, at 2.43 min is imidacloprid, and at 3.1 min is thiacloprid. Preparation was done with slight modifications to suit the instrument and the type of analytes [24].

### **3.2.4. Cleaning of glassware**

All the glassware (beakers, volumetric flask, conical flask, measuring cylinder, sample vials) were washed with soap and water, rinsed with MilliQ water and dried in the oven at 100 °C for an hour. After each experimental use, the glassware was

washed with water and soap, rinsed with MilliQ water and soaked in acetone bath. After soaking for overnight, they were then dried in the oven at 80 °C for 30 min.

### 3.3 Synthesis of magnetic nanocomposite ( $\text{Fe}_3\text{O}_4$ , $\text{Fe}_3\text{O}_4@ \text{Al}_2\text{O}_3$ , $\text{Fe}_3\text{O}_4@ \text{Al}_2\text{O}_3/\text{AC}$ , AC)

#### 3.3.1. Magnetite ( $\text{Fe}_3\text{O}_4$ )

The lemons used for this step were purchased from a local supermarket, peeled, and sundried for five days. Once dried, the lemon peel was washed off dust and impurities with deionised water at several washes until the water was clear and free of macroscopic impurities. Moreover, the lemon peel was again dried in the oven overnight at 60 °C prior use to prepare the lemon peel solution. Furthermore, about 50 g of dried lemon peel was used to prepare the solution extract by adding 600 mL of distilled water in a 1000 mL beaker. The mixture was allowed to heat up to boil and removed from a heating mantle after 15 min of boiling. After removal from a heating mantle, the solution was allowed to cool to room temperature before filtering under vacuum. A lime yellow colour solution was obtained. The filtered solution was stored in a closed glass bottle and stored in the refrigerator at 4 °C for further use [25] [26].

The  $\text{Fe}_3\text{O}_4$  nanoparticles were synthesised by thermal decomposition at a higher temperature of 250 °C. The prepared lemon peel solution was used in place of some organic solvents. A 5 g of iron(iii)acetylacetonate was weighed and added in a round neck bottomed flask with 50 mL of dibenzyl ether, 10 mL oleic acid and 8 mL of lemon peel solution. The reaction was conducted under inert refluxing with  $\text{N}_2$  gas for an hour under vigorous stirring at 250 °C in silicone bath oil. After an hour, the reaction was allowed to cool to room temperature.

Furthermore, after the reaction had cooled a magnetic field was introduced on the round-bottomed flask to separate the synthesised  $\text{Fe}_3\text{O}_4$  from the rest of the solution and the solution was discarded. The remaining iron oxide was rinsed in triplicate with 2-propanol: light petroleum ether (1:1 v/v) to eliminate any unreacted compounds. After rinsing, the black synthesised  $\text{Fe}_3\text{O}_4$  was allowed to dry in the oven at 80 °C for 3 hrs. After it has dried out the black  $\text{Fe}_3\text{O}_4$  was stored in the sample vial for further use [27].

### **3.3.2. $Fe_3O_4@Al_2O_3$ nanocomposite.**

The previously synthesised  $Fe_3O_4$  was used here. This was achieved by dissolving a 1 g of aluminium isopropoxide into 100 mL of ethanol in 250 mL beaker at room temperature. A 0.8 g of  $Fe_3O_4$  magnetic nanoparticles was mixed with a solution of aluminium isopropoxide and the mixture was ultrasonicated for 1 hr at room temperature. A solution mixture of water and ethanol (1:5 v/v) was added dropwise during ultrasonication. After an hour of ultrasonication the mixture was allowed to sit and settle at room temperature and a magnetic field was introduced to separate the  $Fe_3O_4@Al_2O_3$  from the solution that was discarded. The  $Fe_3O_4@Al_2O_3$  was rinsed off with 50ml of ethanol to eliminate any unreacted compounds in triplicate washes [28]. The obtained brown  $Fe_3O_4@Al_2O_3$  was dried in the oven for overnight at 105 °C and later stored in the sample vial for further use. From this step, the aluminium isopropoxide was used as a precursor of dispersal of the  $Fe_3O_4$  since they suffered from agglomeration.

### **3.3.3. $Fe_3O_4@Al_2O_3/AC$ nanocomposites**

#### **Step 1: Preparation of the AC material**

An amount of 10 g prepared corn cob powder was weighed and added in a beaker. A 60 mL of concentrated sulfuric acid ( $H_2SO_4$ ) was added to activate the corn cob powder. Immediately after adding  $H_2SO_4$  in corn cob powder, it turned black. The activation was allowed to occur for 24 hrs in a fumehood. After 24 hrs the mixture was washed several times with a 2:1 (v/v) water and sodium hydroxide ratio until a neutral pH was reached. Additionally, after the wash the corn cobs were subjected to thermal activation in the furnace at 500 °C with a heat flow of 25 °C per minute for 2 hrs in the presence of air. After 2 hrs of thermal activation, the AC were taken out of the furnace and allowed to cool to room temperature. After cooling to room temperature, the activated carbon (AC) was stored in an airtight sample vial for future use [29]. The  $Fe_3O_4$  suffers from agglomeration, hence AC was used as a support material to assist with further dispersal of the  $Fe_3O_4$  nanoparticles adding to an increase in pore size and surface area for adsorption of the NEO analytes on its surface during preconcentration and extraction.

## ***Step 2: Preparation of the Fe<sub>3</sub>O<sub>4</sub>@Al<sub>2</sub>O<sub>3</sub> material***

The Fe<sub>3</sub>O<sub>4</sub>@Al<sub>2</sub>O<sub>3</sub> complex was further supported with AC. Weighed mass of 0.7 g Fe<sub>3</sub>O<sub>4</sub>@Al<sub>2</sub>O<sub>3</sub> was mixed with 0.6 g AC in a beaker with 10 mL of distilled water and stirred for 1 hr. After an hour of stirring the mixture was ultrasonicated for 30 min at room temperature. The mixture was activated in a furnace at 110 °C for 2 hrs [30]. After 2 hrs the nanocomposite (Fe<sub>3</sub>O<sub>4</sub>@Al<sub>2</sub>O<sub>3</sub>/AC) were allowed to cool at room temperature and stored in a vial for future use [31].

### **3.4 Characterisation of the magnetic nanocomposites.**

Different characterisation techniques were employed to study the chemical composition and morphology of the synthesised magnetic nanocomposites materials (Fe<sub>3</sub>O<sub>4</sub>, Fe<sub>3</sub>O<sub>4</sub>@Al<sub>2</sub>O<sub>3</sub>, Fe<sub>3</sub>O<sub>4</sub>@Al<sub>2</sub>O<sub>3</sub>/AC and AC). These techniques include Fourier transform infrared spectrometry (FTIR), Powdered X-ray diffraction (PXRD), Scanning electron microscope coupled to energy dispersive X-ray spectroscopy (SEM-EDS), Thermogravimetric analysis (TGA), Transmission electron microscopy (TEM), and Ultraviolet visible spectroscopy (UV-Vis). The detailed function of each characterisation technique will be well discussed from each section.

#### ***3.4.1. Fourier transform infrared spectrometry (FTIR)***

The FTIR was used to study the chemical composition of the nanocomposites. Fourier transform infrared (FTIR) spectrometer (Vertex 70 model, Bruker Optic GmbH, Hamburg, Germany). The magnetic nanocomposite along with the AC were analysed at a wavenumber range from 400-4000 cm<sup>-1</sup>.

#### ***3.4.2. Powdered X-ray diffraction (PXRD)***

Studies the nanocomposites' crystallinity, particle sizes and amorphous nature. The PXRD determines the crystalline and amorphous phase of the compound surface. Powdered X-ray diffraction (X'Pert Phillips) with CuK $\alpha$  radiation (0.1540 nm) polychromator beam in the 2 $\theta$  scan range 20-800.

#### ***3.4.3. Ultraviolet visible spectroscopy (UV-Vis)***

Measures the amount of ultraviolet (UV) and visible light that is absorbed by nanocomposites. Perkin Elmer UV-Vis spectrometer. Shimadzu UV1800

spectrophotometer (RF-5301PC, Shimadzu), connected with a light source of 150 W Xenon lamp was used to confirm the UV-spectra of the synthesised nanoparticle.

#### **3.4.4. *Transmission electron microscopy (TEM)***

Studies the internal morphologies and particles sizes of the nanocomposites. Before analysis, a small amount of the sample was prepared in a certain volume of MeOH and they were ultrasonicated for 20 min. additionally they were prepared on copper grid and allowed to dry before analysis. Instrument model used was JEOL JEM-2100F transmission electron microscope instrument (TEM, JOEL Ltd., Tokyo, Japan). The latter was operated at 200 kV and was equipped with LaB6 source and charge coupled device (CCD) digital camera.

#### **3.4.5. *Scanning electron microscope coupled to energy dispersive X-ray spectroscopy (SEM-EDS)***

Explores the external morphological features of the nanocomposites EDS shows the elemental composition of the nanocomposite. SEM image analysis was carried out on a JEOL JSM 7800F field emission scanning electron microscope run at 5 kV using secondary electron detector (SED) and energy dispersive spectroscopy (EDS).

#### **3.4.6. *Thermogravimetric analysis (TGA)***

Measures the thermal stability of the nanocomposites. TGA Q500 thermogravimetric analyser (TA Instruments, New Castle, DE, USA). The conditions were at a temperature from 30-1000 °C with a segment increase of 25 °C in every 10 min. the nitrogen gas purge was 100 mL/min.

### **3.5 Optimization**

Method development is crucial with optimization of some of the influential parameters. This was done to suit the type of analytes, the type of matrix and the type of adsorbent.

#### **3.5.1. *Univariate optimization***

The univariate optimization was done to study the performance of sample volume, solvent type and type of adsorbent. The optimization followed the general procedure in **Figure 3.1**. The univariate approach makes use of the optimization of one parameter at a time and is thus tedious [23].

### **3.5.1.1. Effect of sample volume**

The volume of the sample solution is one of the most crucial parameters influencing both the extraction efficiency and method sensitivity. The sample volume investigated for the vegetable oils were 1 mL, 5 mL, 10 mL and 20 mL. The eluent type was also a key factor for the preconcentration of these analytes. Methanol and acetonitrile were the two eluting solvents investigated on this study. The two parameters, sample volume and eluent type, were investigated before experimental design. This was to help identify the best volume to suit the method and the best eluent type to be used for the desorption of the analytes from the adsorbent. **Figure 3.1** shows that different sample volumes were measured on a 50 mL centrifuge tube. The pH used was neutral with an adsorbent mass of 60 mg, spiking with a known concentration, and then vortexed for 5 min. After, 5 min, a magnetic field was introduced for simple separation of the adsorbent with adsorbed analytes and the supernatant was discarded. The analytes were desorbed by 1 mL of ACN and vortexed again for 2 min. Additionally, the eluent was filtered using PVDF micro filters of 0.45  $\mu\text{m}$  to the amber glass vial and the samples were taken for analysis by HPLC-DAD instrument. The results were collected and reported in **Figure 3.7**. The adsorbent was ultrasonicated with the solution of ethanol and aluminum isopropoxide followed by being supported with activated carbon through ultrasonication with distilled water. The adsorbent was then dried in the oven for overnight and stored in a closed vial for further use. There was no conditioning done prior use for the preconcentration process.

### **3.5.1.2. Effect of solvent type**

A 5 mL sample volume was used with 60 mg adsorbent, pH at neutral, spiked and vortexed for 5 min. After 5 min of extraction, a magnet was introduced for simple separation of the adsorbent and the supernatant was discarded. Elution was done using 1 mL ACN and MeOH then vortexed for 2 min. Lastly, the eluent was filtered using PVDF micro filters of 0.45  $\mu\text{m}$  into an amber glass and taken for analysis in HPLC-DAD. The results were reported in **Figure 3.7**.

### 3.5.1.3. Extraction efficiency of the adsorbent ( $Fe_3O_4$ , $Fe_3O_4@Al_2O_3$ and $Fe_3O_4@Al_2O_3/AC$ )

This was done following the procedure from **Figure 3.1**, where a 60 mg of adsorbent nanocomposite materials were used with 5 mL sample volume, 5 min extraction time, 1 mL of ACN and 2 min desorption time. The results were reported in **Figure 3.8**.

### 3.5.2. Multivariate optimization

The purpose of using a multivariate strategy is to optimize multiple parameters simultaneously while decreasing the number of experiments performed and providing quantitative data for significant and insignificant parameters of the independent variables and their interactions. This helped to avoid having to optimise each parameter at a time while the other parameters were kept constant.

#### 3.5.2.1. Full factorial design (FFD)

The parameters were screened following the chemometric tool for multivariate optimization approach from DoE following the two-level full factorial design (FFD). The FFD generated 16 experiments and the table of design of these experiments is shown on **Appendix TS1**. The parameters investigated were sorbent mass, extraction time, eluent volume and pH. **Figure 3.1** represents the general procedure followed. The significant parameters were reported in Pareto charts shown in **Figure 3.10**. **Table 3.1** shows the parameters used during screening.

**Table 3. 1:** FFD parameters

Parameters	Low (-)	High (+)
Time (min)	2	8
pH	3	11
Sorbent mass (mg)	20	90
Eluent vol (ml)	0.5	1

#### 3.5.2.2. Response surface methodology (RSM)

For further optimization of the most influential parameters (sorbent mass, pH and eluent volume) generated from FFD in the Pareto chart, RSM was used for DoE using central composite design (CCD). A total of 20 experiments were designed and

done in triplicates and design of these experiments is shown on **Appendix TS2**. This method followed a procedure shown in **Figure 3.1**, and the parameters are in **Table 3.2**. The performance of the parameters was reported in 3D surface plots shown in **Figure 3.11**.

**Table 3. 2:** RSM parameters

Parameters	Low (-)	Central point	High (+)
pH	1.2	7	13
Eluent vol (ml)	0.3	0.75	1.17
Sorbent mass (mg)	3.86	55	113.86

### 3.6 Magnetic solid phase microextraction (MSPME) procedure

**Figure 3.1** is a visual representation of the MSPME method followed for this study. A 5 mL of vegetable oil sample was used for these experiments with other parameters like sorbent mass, eluting volume, pH and time. The choice of the eluting volume was entirely dependent on advantages like environmentally friendliness and non-toxicity on humans and the environment. The use of spiking with an organic standard was done due to the absence of the reference certified material for validation study of the method. The advantage of this method is the simple separation that is achieved by the introducing of the magnetic field for separating the magnetic adsorbents with analytes of interest.

A 5ml sample was added in a 50 mL centrifuge tube. After addition of the vegetable oil the pH was adjusted to either basic or acidic using 0.1 M NaOH and 0.1 M HCl. Furthermore, an addition of the spiking analyte was done and vortexed for 8 min. After 8 min of vortex, a magnet was introduced to separate the adsorbents with the analyte and the remaining solution was discarded. An eluting solvent of acetonitrile was added to the separated adsorbent in the centrifuge tube and further vortexed for 2 min to desorb the analytes. Then the eluent was transferred into a syringe capped with a PVDF microfilter, filtered in a vial. After the vial was closed and taken for analysis at the HPLC-DAD [23]. The separated adsorbent was washed several times with ethanol and dried in the oven for 2 hrs and stored in sample vial for reusability.



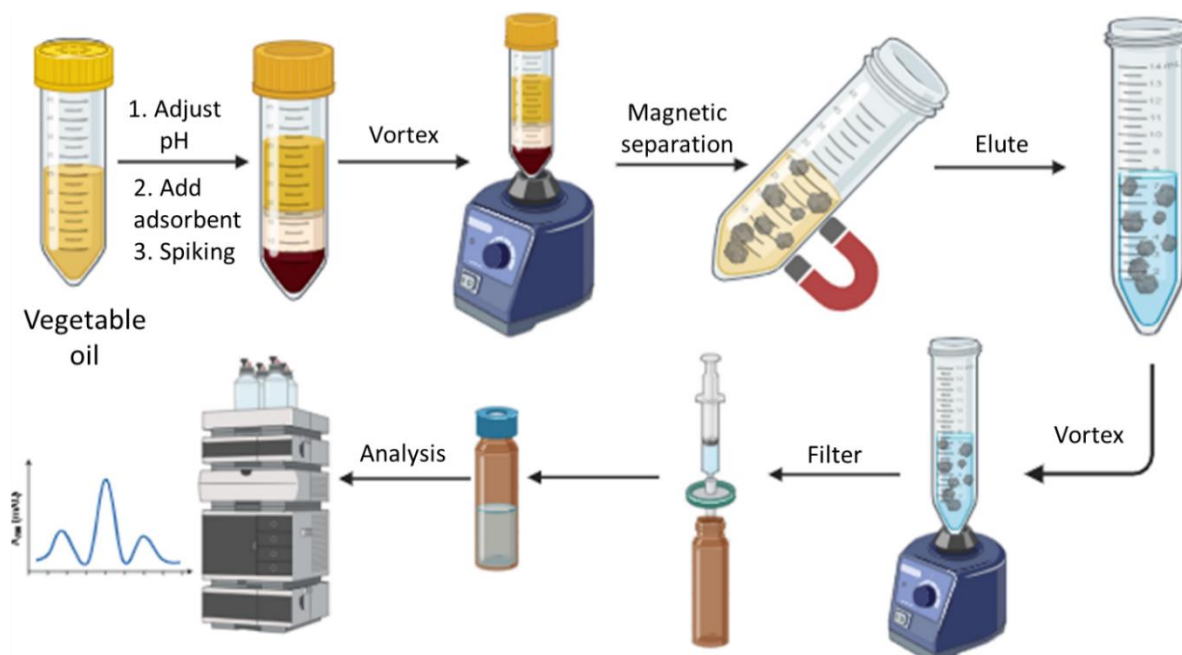


**Figure 3. 1:** Schematic diagram of magnetic solid phase microextraction procedure [23].

### 3.7 Method validation

The MSPME was validated through investigating the analytical figure of merits such as precision (% RSD), accuracy (% R), limit of detection (LOD), limit of quantification (LOQ), matrix effects (ME) and preconcentration factor (PF). Equations (3.1-3.8) were used for calculation of figure of merits. The relative standard deviation (RSD) measures the precision of the average of your results [32]. The accuracy also known as extraction recovery (% R) refers proportion of the known amount of an analyte carried through the sample extraction and processing phases of the procedure that represents the extraction efficiency of an analytical process [33]. Limit of detection (LOD) the lowest concentration that the technique is capable of detecting [34]. Limit of quantification (LOQ) is the lowest concentration at which the analyte may be accurately identified while also meeting certain predetermined standards for bias and imprecision [35]. Matrix effects (ME) the co-eluting compound's promoting or suppressing abilities from the sample analytes [36]. Preconcentration factor (PF) refers to the ratio between final concentration and known concentration [37].

### 3.7.1. Equations for figure of merits

**Limit of detection (LOD)** [38]

$$LOD = \frac{3 \times [Conc]}{S/N} \quad \text{equation 3. 1}$$

**Limit of quantification (LOQ)** [39]

$$LOQ = \frac{10 \times [Conc]}{S/N} \quad \text{equation 3. 2}$$

**Percentage relative standard deviation (%RSD)** [40]

$$\%RSD = \frac{SD}{Mean} \times 100 \quad \text{equation 3. 3}$$

**Standard deviation** [41]

$$\sigma = \sqrt{\frac{\sum_{i=1}^N (x_i - \bar{x})^2}{N-1}} \quad \text{equation 3. 4}$$

**Mean average** [42]

$$\bar{x} = \frac{x_1 + x_2 + \dots + x_n}{n} \quad \text{equation 3. 5}$$

**Extraction recoveries**[43]

$$\%Recovery = \frac{V_f \times c_f}{V_i \times c_i} \times 100 \quad \text{equation 3. 6}$$

**Matrix effects**[44]

$$ME (\%) = \left( \frac{\text{Slope of analytical curve in matrix}}{\text{Slope of analytical curve in acetonitrile}} - 1 \right) \times 100 \quad \text{equation 3. 7}$$

### Preconcentration factor<sup>[45]</sup>

$$PF = \frac{\text{Final concentration}}{\text{Known concentration}} \quad \text{equation 3. 8}$$

### 3.8 Application of MSPME in real commercial vegetable oil samples.

The validated method was applied in real vegetable oil samples for quality control and assessment of NEOs. Thus, is to check the concentration of these NEOs in real vegetable oil samples.

### 3.9 Reusability and regeneration studies

Once the developed method was validated and applied in real samples, the regeneration and reusability studies were conducted to investigate the adsorbent performance on extraction recoveries. This helps to examine the performance of the adsorbent after several runs. After each experiment, the adsorbent was washed with EtOH and dried for 3 hours in an oven at 110 °C before its next use.

### 3.10 Results and discussion

#### 3.10.1. Characterisation of the magnetic nanocomposites

##### 3.10.1.1. Fourier transform infrared spectrometry (FTIR)

Functional group of activated carbon from corn cobs have been shown on the spectrum in **Figure 3.2 (a)**. The stretch at around 3600-3900 cm<sup>-1</sup> region is accounted for by the presence of the -OH group, which facilitates decarboxylation reactions. This functional group is responsible for the chemical decomposition of cellulose during acid treatment. At a 1550 cm<sup>-1</sup> region, we observe a C=C bonding. This is due to the presence of alkenes facilitating the lignin decomposition reaction. At 1010 cm<sup>-1</sup> we observe the C-O stretch accounts for the carboxylic groups found in the corncobs' cellulose and hemicellulose. This leads to the glycosidic bonds' breakage, forming a series of less oxygen-containing compounds. At 553 cm<sup>-1</sup> region we observe a C-H bending through high energy during high-temperature heating during treatment in the furnace, causing complete disruption of the chemical bonds. The C-H bond results from the aromatic group found in the corn cobs [48]. These results showed that the AC was successfully prepared. These results were corroborated with literature reports.

The carbon-carbon and carbon-oxygen functional groups from the lignin, cellulose and hemicellulose from the 1550  $\text{cm}^{-1}$ , 1010  $\text{cm}^{-1}$  and at 553  $\text{cm}^{-1}$  regions has confirmed the successful formation of the AC.

The spectra reveal the functional groups at different wavenumbers, respectively. **Figure 3.2 (b)**  $\text{Fe}_3\text{O}_4$  spectra with a broad stretch at around 3500  $\text{cm}^{-1}$  represent an -OH group from the water used to prepare the lemon peel solution used in synthesis step. At around 1010  $\text{cm}^{-1}$ , a broad peak represents the symmetric and antisymmetric stretching of the C-H bond of the carboxylate group. A strong peak at 510  $\text{cm}^{-1}$  represents Fe-O bond due to magnetite solid-state vibrations [46]. The results were corroborated to results reported in literature.

From the representation of the spectra in **Figure 3.2 (c)**, there is a distinctive observable shift of the spectra as we coat the  $\text{Fe}_3\text{O}_4$  with aluminium isopropoxide to form  $\text{Fe}_3\text{O}_4@\text{Al}_2\text{O}_3$ . A peak at 1495  $\text{cm}^{-1}$  is due to the vibrations of C-C bond from the benzene ring the phytochemicals found in lemon peel extract. At 498  $\text{cm}^{-1}$  is a peak representing a Fe-O group representing the presence of  $\text{Fe}_3\text{O}_4$  nanoparticles, the Al-O stretching vibrations can also be attributed to it. The observable shift in wavelength confirms that  $\text{Al}_2\text{O}_3$  was immobilised on the surface of the  $\text{Fe}_3\text{O}_4$ , respectively [47]. The results were corroborated with the literature reports.

The  $\text{Fe}_3\text{O}_4@\text{Al}_2\text{O}_3/\text{AC}$  magnetic nanocomposite spectrum in **Figure 3.2 (d)** also confirmed the incorporation of the AC into the  $\text{Fe}_3\text{O}_4@\text{Al}_2\text{O}_3$  complex formed. The observable shift with a C-O stretch at 1010  $\text{cm}^{-1}$  accounts for the carboxylic groups found in the corncobs' cellulose and hemicellulose. Furthermore, the intensity of the bands at 600  $\text{cm}^{-1}$  corresponds to the C-H bending substituted by the aromatic rings from the AC. Moreover, the increased absorption band of the  $\text{Fe}_3\text{O}_4@\text{Al}_2\text{O}_3/\text{AC}$  indicated that we managed to immobilise the AC on our  $\text{Fe}_3\text{O}_4@\text{Al}_2\text{O}_3$  magnetic nanocomposite. At 498  $\text{cm}^{-1}$ , a Fe-O group represents a peak due to magnetite solid-state vibrations, representing the presence of  $\text{Fe}_3\text{O}_4$  nanoparticles. These results proved the successful synthesis of the  $\text{Fe}_3\text{O}_4@\text{Al}_2\text{O}_3/\text{AC}$  nanocomposites. The observable shift in wavenumber from the spectrum **(a)**, **(b)** and **(c)** in **Figure 3.2** confirms that the aluminium and AC were successfully immobilised on  $\text{Fe}_3\text{O}_4$  to form our  $\text{Fe}_3\text{O}_4@\text{Al}_2\text{O}_3/\text{AC}$  nanocomposite. These results were corroborated with literature reports, specifically for AC,  $\text{Fe}_3\text{O}_4$  and  $\text{Fe}_3\text{O}_4@\text{Al}_2\text{O}_3$ .

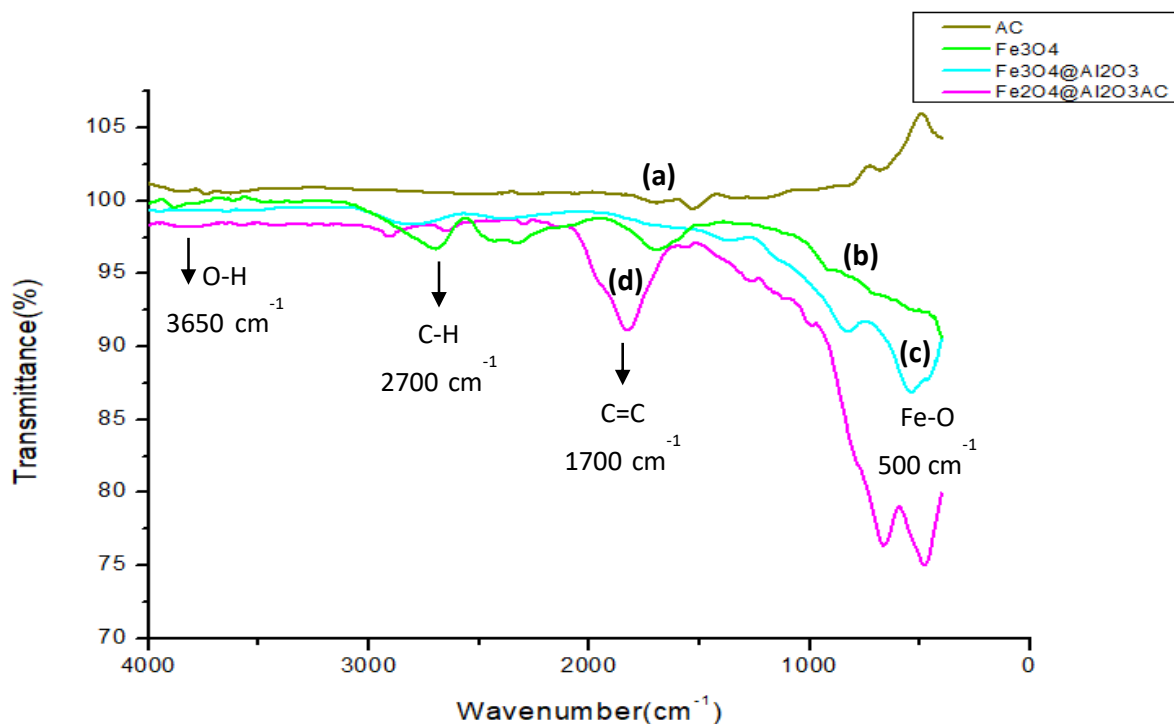


**Figure 3. 2:** FTIR spectra for (a) AC, (b) Fe<sub>3</sub>O<sub>4</sub>, (c) Fe<sub>3</sub>O<sub>4</sub>@Al<sub>2</sub>O<sub>3</sub> and (d) Fe<sub>3</sub>O<sub>4</sub>@Al<sub>2</sub>O<sub>3</sub>/AC

### 3.10.1.2. Powdered X-ray diffraction (PXRD)

**Figure 3.3** shows the AC spectra at  $\sim 26^\circ$  having few hardly observed sharp peaks, representing that the AC's surface is amorphous. The pattern represents a non-crystalline structure at the diffraction peaks of the AC location around the scattering angle ( $2\theta$ ) of  $19^\circ$  and  $21^\circ$ . However, from these results, the AC material has shown its suitability for incorporation with the magnetic adsorbent [49]. The Fe<sub>3</sub>O<sub>4</sub>@Al<sub>2</sub>O<sub>3</sub> diffraction peaks at  $30^\circ$ ,  $32^\circ$ ,  $36^\circ$ ,  $41^\circ$ ,  $43^\circ$ ,  $49^\circ$ ,  $53^\circ$ ,  $55^\circ$  and  $63^\circ$ . In 2023, Samakosh et al, reported the distinctive diffraction peaks at 400 and 440 confirms the immobilization of aluminum isopropoxide on the Fe<sub>3</sub>O<sub>4</sub> nanoparticle. Notably, the scattering angle at  $\sim 26^\circ$  of the AC might be shielded by the strong peaks of the magnetite in Fe<sub>3</sub>O<sub>4</sub>@Al<sub>2</sub>O<sub>3</sub>/AC nanocomposite. The sharp peaks at  $18^\circ$ ,  $21^\circ$ , and  $35^\circ$ , the characteristics of the inverse cubic spinel phase of Fe<sub>3</sub>O<sub>4</sub>, were observed. These suggest forming a crystalline Fe<sub>3</sub>O<sub>4</sub>@Al<sub>2</sub>O<sub>3</sub>/AC structure [50]. The Fe<sub>3</sub>O<sub>4</sub>@Al<sub>2</sub>O<sub>3</sub> have peaks at  $30^\circ$ ,  $35.5^\circ$  and diffraction peaks at  $43^\circ$ ,  $53.75^\circ$ ,  $57^\circ$  and  $63^\circ$  compared to the peaks from the Fe<sub>3</sub>O<sub>4</sub>@Al<sub>2</sub>O<sub>3</sub>/AC confirms the incorporation of the Fe<sub>3</sub>O<sub>4</sub>@Al<sub>2</sub>O<sub>3</sub> with the AC to have successfully formed the magnetic nanocomposite, respectively. These

results were comparable with literature reports, specifically for AC, Fe<sub>3</sub>O<sub>4</sub> and Fe<sub>3</sub>O<sub>4</sub>@Al<sub>2</sub>O<sub>3</sub>. The particle size for the synthesised nano composite and its fragments were calculated using Scherrer equation ( $D = K\lambda/\beta \cdot \cos\theta$ ), wherein K is a constant usually equals to 1,  $\lambda$  is the X-ray wavelength,  $\beta$  is the width and  $\theta$  is the diffraction angle [51]. The calculated particle size for AC was 76.81 nm, for Fe<sub>3</sub>O<sub>4</sub> was 19.95 nm, for Fe<sub>3</sub>O<sub>4</sub>@Al<sub>2</sub>O<sub>3</sub> was 40.73 nm, for Fe<sub>3</sub>O<sub>4</sub>@Al<sub>2</sub>O<sub>3</sub>/AC was 91.48 nm, respectively. Lastly, it is worth noting that there was an increase in particle size after the step of coating with aluminum isopropoxide and supporting with AC which confirms that the two were successfully immobilized on the Fe<sub>3</sub>O<sub>4</sub> nanoparticle [52]. The AC has played the significant role in dispersing the Fe<sub>3</sub>O<sub>4</sub> since it was agglomerated, and it also increased the surface area along with the particle size for subsequent adsorption. The indices confirm the crystallinity of the Fe<sub>3</sub>O<sub>4</sub>, Fe<sub>3</sub>O<sub>4</sub>@Al<sub>2</sub>O<sub>3</sub> and Fe<sub>3</sub>O<sub>4</sub>@Al<sub>2</sub>O<sub>3</sub>/AC nanocomposite. The indices confirms the crystallinity of the Fe from Fe<sub>3</sub>O<sub>4</sub>, the Al from Fe<sub>3</sub>O<sub>4</sub>@Al<sub>2</sub>O<sub>3</sub> and the silica from AC in Fe<sub>3</sub>O<sub>4</sub>@Al<sub>2</sub>O<sub>3</sub>/AC nanocomposite [53]. The PXRD measurement reported in **Figure 3.3** also confirmed the presence of nanocrystalline magnetite phase for the iron (III) acetylacetonate which was used as an iron precursor during the synthesis of Fe<sub>3</sub>O<sub>4</sub> [54]. All these results were corroborated with reports from literature.

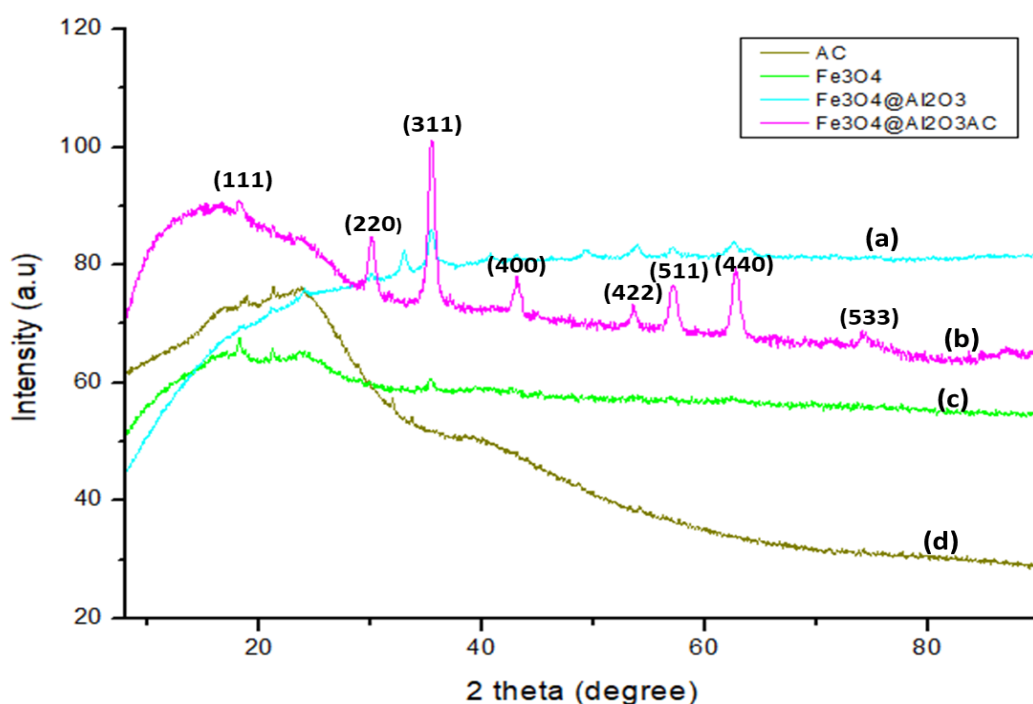


**Figure 3. 3:** PXRD spectra for the synthesised nanocomposite **(a)** Fe<sub>3</sub>O<sub>4</sub>@Al<sub>2</sub>O<sub>3</sub>, **(b)** Fe<sub>3</sub>O<sub>4</sub>@Al<sub>2</sub>O<sub>3</sub>/AC, **(c)** Fe<sub>3</sub>O<sub>4</sub> and **(d)** AC.

### 3.10.1.3. Ultraviolet-visible spectroscopy (UV-Vis)

The absorption range of the UV spectra for the **Figure 3.4 (d)**  $\text{Fe}_3\text{O}_4@/\text{Al}_2\text{O}_3/\text{AC}$  wherein the highest absorption for the magnetic nanoparticles at a range of 270-550 nm, was observed. Supporting with AC on the  $\text{Fe}_3\text{O}_4@/\text{Al}_2\text{O}_3$  has greatly impacted the absorption range. The UV spectrum help with determining the transitions from the ground state to the excited state. The UV absorption spectra of **(a)** AC, **(b)**  $\text{Fe}_3\text{O}_4$ , **(c)**  $\text{Fe}_3\text{O}_4@/\text{Al}_2\text{O}_3$ , and **(d)**  $\text{Fe}_3\text{O}_4@/\text{Al}_2\text{O}_3/\text{AC}$ . The latter displays the AC spectrum which is attributed to by the  $\pi$ - $\pi$  transition attributed to the conjugated C=C band bonds at 270-300 nm. The difference in the absorption intensities was slightly due to the difference in concentrations of the samples [30]. The spectrum shows high band intensities and peaks under visible spectrum. The outer electrons of the materials in their atomic state absorbs the radiant energy and undergoes transition to a higher energy level. The energy band gap equation ( $E_{\text{bg}} = 1240/\lambda$  (eV)) was used to calculate the energy gap at 270-400 nm region, where  $E_{\text{bg}}$  is the energy band gap and  $\lambda$  represents the wavelength (270-400 nm) of the nanoparticles. The energy gap was calculated as 4.593-3.1 eV at 270-400 nm. These results were corroborated with literature reports, specifically for **(a)** AC, **(b)**  $\text{Fe}_3\text{O}_4$  and **(d)**  $\text{Fe}_3\text{O}_4@/\text{Al}_2\text{O}_3$ .

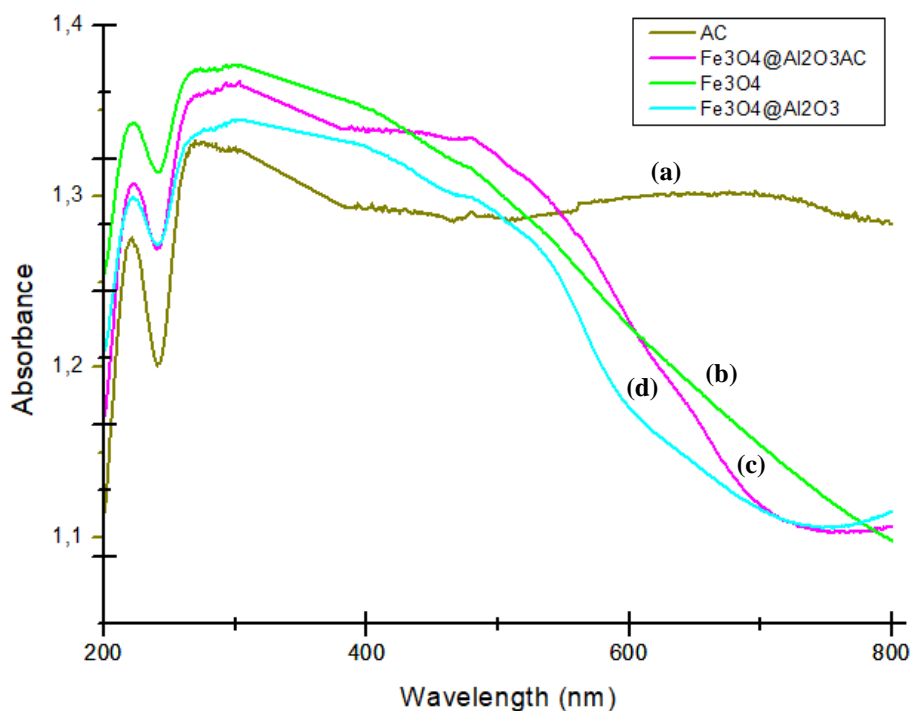


**Figure 3. 4:** Representation of the UV results **(a)** AC, **(b)**  $\text{Fe}_3\text{O}_4$ , **(c)**  $\text{Fe}_3\text{O}_4@/\text{Al}_2\text{O}_3$ , and **(d)**  $\text{Fe}_3\text{O}_4@/\text{Al}_2\text{O}_3/\text{AC}$ .

#### 3.10.1.4. Transmission electron microscopy (TEM)

TEM images of nanoparticles shown in **Figure 3.5. (a)**. They give an overall view on surface morphology of the synthesized nanocomposite materials. The particles showed a high degree of agglomeration due to dipole-dipole interaction. In this **Figure 3.5**, a micrograph, as well as the size distribution of all kinds of nanocomposites, is shown. The lattice fringe patterns were observed in (TEM) images, indicating high crystallinity of the  $\text{Fe}_3\text{O}_4$ . **Figure 3.5. (b)** has shown slight sheets of aluminium isopropoxide immobilised on the  $\text{Fe}_3\text{O}_4$  nanoparticles' surface, which has attributed to the dispersion of the  $\text{Fe}_3\text{O}_4$  nanoparticles with reduced agglomeration. The TEM image has also shown that the  $\text{Fe}_3\text{O}_4@Al_2O_3$  is also crystalline. **Figure 3.5. (c)** represents the surface characteristics of  $\text{Fe}_3\text{O}_4@Al_2O_3/AC$  which has AC deposits successfully immobilised on the  $\text{Fe}_3\text{O}_4@Al_2O_3$ . This is confirmed by a good dispersion of the nanocomposites with a more visible spheric structure of the  $\text{Fe}_3\text{O}_4@Al_2O_3/AC$  nanocomposite. **Figure 3.5. (d)** TEM images for activated corn cob show the distinct microporous nature of the sample material. Moreover, in this figure, the TEM image shows that the  $\text{Fe}_3\text{O}_4@Al_2O_3/AC$  is crystalline. Additionally, the particle size was calculated using the ImageJ software tool.  $\text{Fe}_3\text{O}_4@Al_2O_3$  followed an observable increase in particle size from  $\text{Fe}_3\text{O}_4$  to the final  $\text{Fe}_3\text{O}_4@Al_2O_3/AC$  nanocomposite. This has proved to show that aluminum managed to help reduce agglomeration on  $\text{Fe}_3\text{O}_4$ , and the particle size increased to 40 nm for  $\text{Fe}_3\text{O}_4@Al_2O_3$ . The particle size for  $\text{Fe}_3\text{O}_4$  was at a range of 80 nm. The particle size for  $\text{Fe}_3\text{O}_4@Al_2O_3/AC$  was 112 nm. This leads to the conclusion that AC plays a significant role in dispersing the agglomerated  $\text{Fe}_3\text{O}_4$ . Additionally, it is worth noting that the AC's particle size could not be calculated since it appeared as cloudy sheets without distinctive particles. The crystallinity observed on **Figure 3.5. (c)** was also confirmed by the PXRD on **Figure 3.3 (b)**. Furthermore, the results from **Figure 3.3 (a), (b) and (c)** has also confirmed the evolution from agglomeration observed on **Figure 3.3 (a)**, a little dispersion observed from **Figure 3.3 (b)** wherein some distinctive particles were slightly visible to finally **Figure 3.3 (c)** wherein distinctive particles were observed. The TEM confirms the exponential dispersion of these nanocomposites through each step of synthesis, overcoming the limitation of  $\text{Fe}_3\text{O}_4$  synthesis. The results indicate that the



$\text{Fe}_3\text{O}_4@\text{Al}_2\text{O}_3/\text{AC}$  nanocomposite was successfully synthesised. These results were corroborated with literature reports, specifically for AC,  $\text{Fe}_3\text{O}_4$  and  $\text{Fe}_3\text{O}_4@\text{Al}_2\text{O}_3$ .

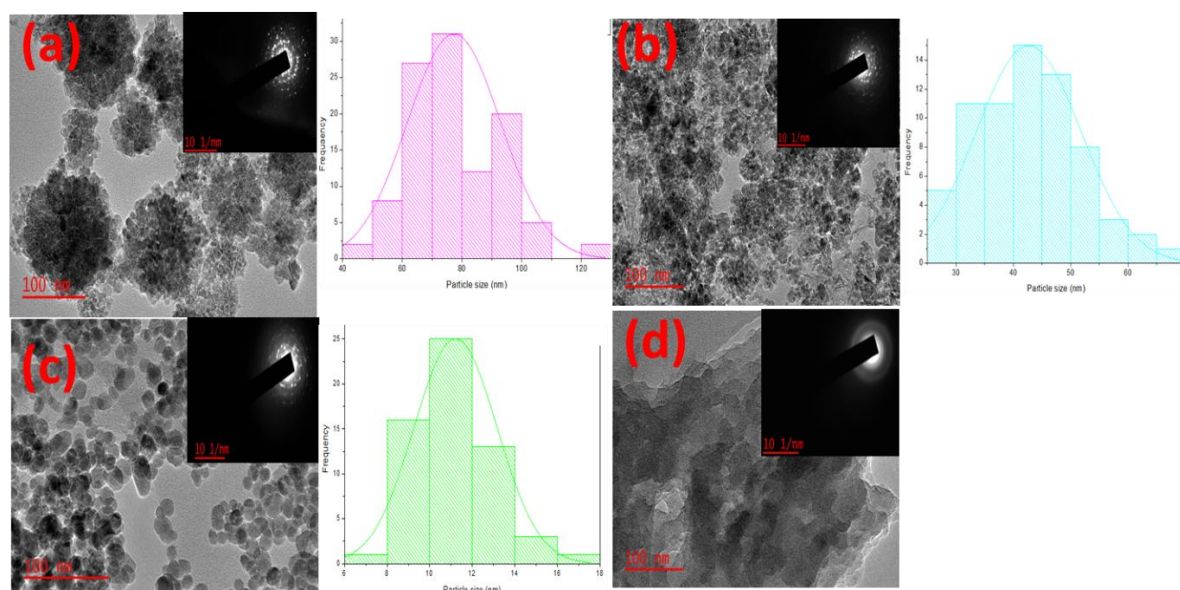


**Figure 3. 5:** TEM results for **(a)**  $\text{Fe}_3\text{O}_4$  nanoparticles, **(b)**  $\text{Fe}_3\text{O}_4@\text{Al}_2\text{O}_3$ , **(c)**  $\text{Fe}_3\text{O}_4@\text{Al}_2\text{O}_3/\text{AC}$  and **(d)** AC.

### 3.10.1.5. Scanning electron microscope coupled to energy dispersive X-ray spectroscopy (SEM-EDS)

**Figure 3.6 (a)** the particles showed a high degree of agglomeration due to dipole-dipole interaction and it also shows that no large particles were produced. From **Figure 3.6 (b)**, incorporating  $\text{Al}_2\text{O}_3$  to  $\text{Fe}_3\text{O}_4$  has caused some dispersion/ reduction in agglomeration of the  $\text{Fe}_3\text{O}_4$  nanocomposite. The EDS elemental composition confirms the successful incorporation of the  $\text{Al}_2\text{O}_3$  on the  $\text{Fe}_3\text{O}_4$ . **Figure 3.6 (c)** shows a good dispersion of the  $\text{Fe}_3\text{O}_4@\text{Al}_2\text{O}_3/\text{AC}$  nanocomposite. The larger masses and aggregation are more visible on this spectrum than on **(b)**, indicating that the AC was successfully immobilised on the surface of  $\text{Fe}_3\text{O}_4@\text{Al}_2\text{O}_3$  nanocomposite. **Figure 3.6 (d)** represents the activated carbon (AC), and it is visible from the spectrum that there is a large pore size subject to a large surface area. The treatment by acid exposed the pores. The presence of the macropores provides an additional surface for adsorption on the analytes of interest. These results were corroborated with literature reports, specifically for AC,  $\text{Fe}_3\text{O}_4$  and  $\text{Fe}_3\text{O}_4@\text{Al}_2\text{O}_3$ .

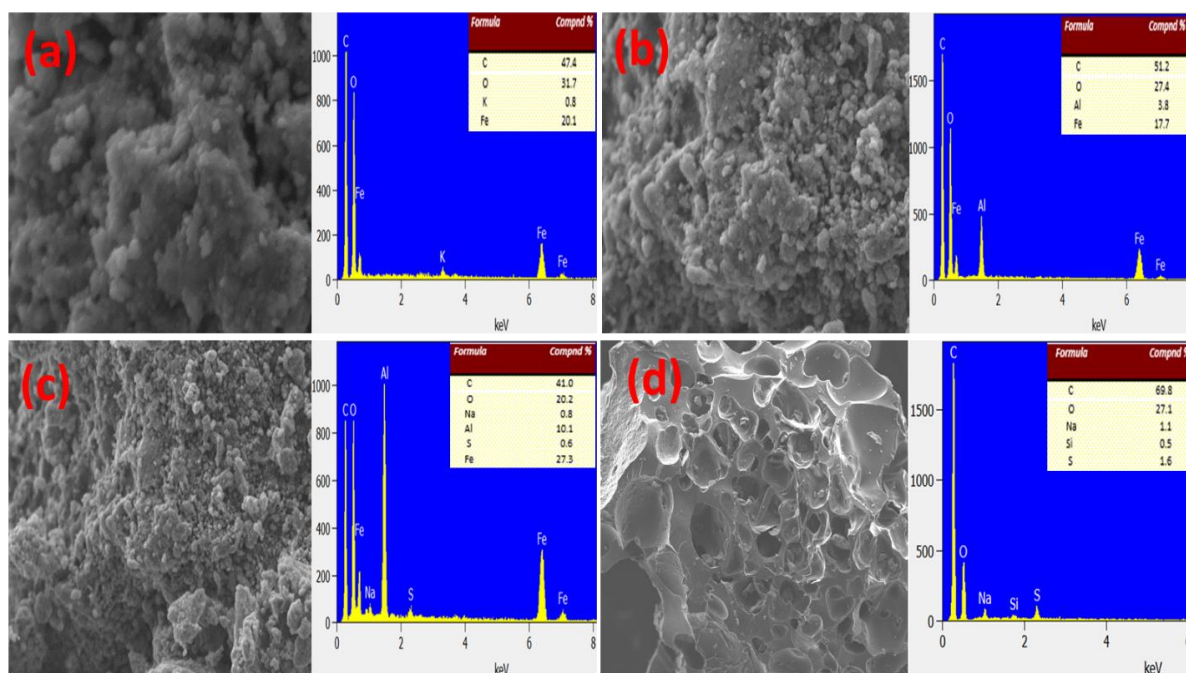


**Figure 3. 6:** SEM-EDS spectrum for **(a)**  $\text{Fe}_3\text{O}_4$  nanoparticles, **(b)**  $\text{Fe}_3\text{O}_4@Al_2O_3$ , **(c)**  $\text{Fe}_3\text{O}_4@Al_2O_3/AC$  and **(d)** AC.

### 3.10.1.6. Thermogravimetric analysis (TGA)

Measures the thermal stability of materials. TGA Q500 thermogravimetric analyser (TA Instruments, New Castle, DE, USA). The degradation occurring at **Figure 3.7 (a)**  $\text{Fe}_3\text{O}_4$  at 150 °C showing the weight loss is due to the removal of water and hydroxyl decomposition of the magnetic  $\text{Fe}_3\text{O}_4$  surface [55]. The  $\text{Fe}_3\text{O}_4$  has shown to be more stable compared to the rest of the fragments used for forming the magnetic nanocomposites. From **Figure 3.7 (b)** we observe two weight loss which is due to the loss of water from the  $\text{Fe}_3\text{O}_4$  at 200-600 °C and  $Al_2O_3$  layer at 150 °C [56]. The  $\text{Fe}_3\text{O}_4@Al_2O_3/AC$  nanocomposite on **Figure 3.7 (c)** has shown two degradations at 150 °C and 250-560 °C which is due to loss of water from the  $\text{Fe}_3\text{O}_4$ ,  $Al_2O_3$  and AC. The degradation at higher temperatures of 250-560 °C is attributed to by the lignin on the surface of the AC. From **Figure 3.7 (d)** initial degradation from 100-200 °C is characteristic of the decomposition of hemicellulose [57]. From the AC it was observed that the maximum rate of mass loss occurred at a temperature range from 290-580 °C [58]. The great thermal stability of the corncob adsorbent is probably due to the presence of lignin, which has a very condensed structure [59]. This can also be characteristic of cellulose degradation, which has greater thermal resistance due to the greater number of inter and intramolecular hydrogen bonds [60]. Another

degradation was visible from 200-360 °C due to the breaking of the C-C bonds of the carboxylate group [61]. The initial degradation at temperature ranges from 100-200 °C was due to the loss of water on all the AC, Fe<sub>3</sub>O<sub>4</sub> and Fe<sub>3</sub>O<sub>4</sub>@Al<sub>2</sub>O<sub>3</sub> and Fe<sub>3</sub>O<sub>4</sub>@Al<sub>2</sub>O<sub>3</sub>/AC. These results were corroborated with literature reports, specifically for AC, Fe<sub>3</sub>O<sub>4</sub> and Fe<sub>3</sub>O<sub>4</sub>@Al<sub>2</sub>O<sub>3</sub>.

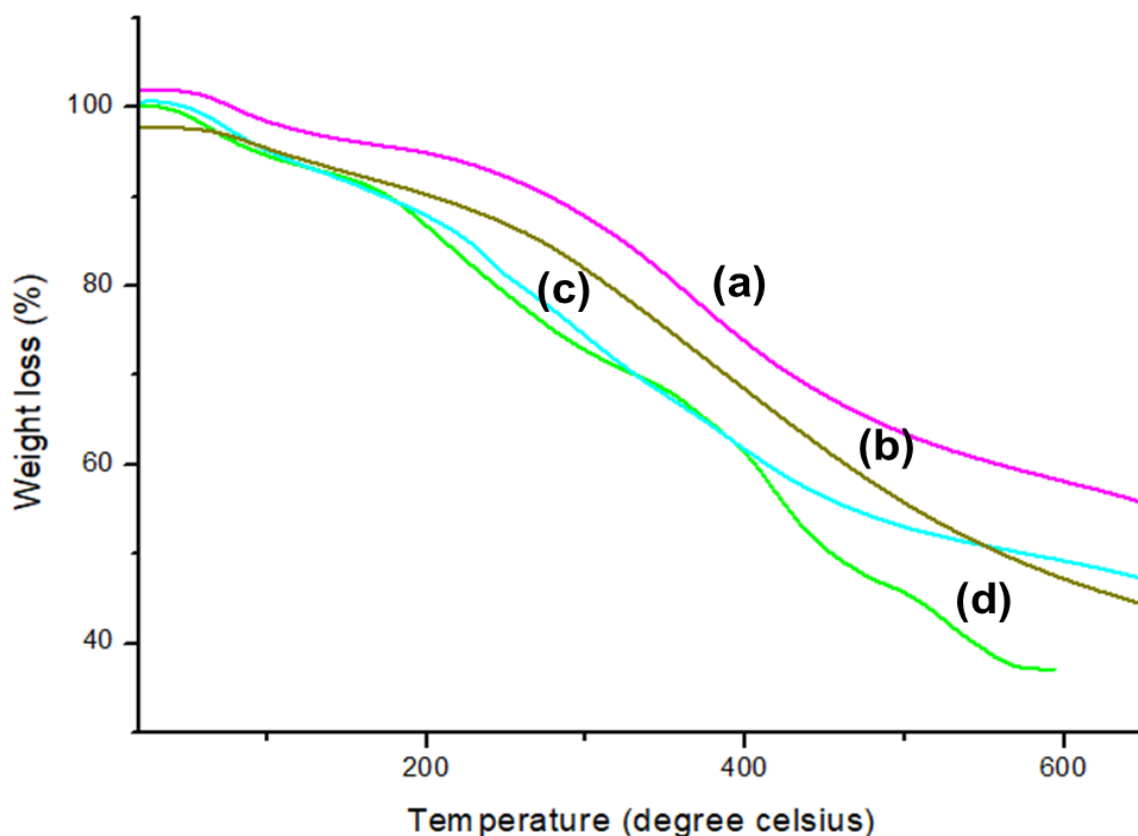


**Figure 3. 7:** TGA results for **(a)** Fe<sub>3</sub>O<sub>4</sub> nanoparticles, **(b)** Fe<sub>3</sub>O<sub>4</sub>@Al<sub>2</sub>O<sub>3</sub>, **(c)** Fe<sub>3</sub>O<sub>4</sub>@Al<sub>2</sub>O<sub>3</sub>/AC and **(d)** AC.

### 3.11. Optimization

#### 3.11.1. Univariate optimization.

##### 3.11.1.1. Effect of solvent type and sample volume

The eluent type investigated were acetonitrile (ACN) and methanol (MeOH) which were HPLC grade. The effect of sample volume was studied in terms of the preconcentration factor. From **Figure 3.8**, four sample volumes were investigated, and 5 mL proved to show the highest preconcentration factor compared to other volumes. Sample volumes 1 and 20 mL were also showing relatively high preconcentration factors. However, a 20 mL sample volume cannot be selected as a good volume due

to considering the cost-effectiveness of the method. A sample volume of 1 mL is acceptable and can be recommended for future studies. A non-optimal ratio between the sample volume and sorbent mass has effect on sample volume. The results in **Figure 3.8** show that ACN had the highest preconcentration factor compared to MeOH. The MeOH could not elute the analytes at 1 mL and 20 mL sample volumes. The results concluded that a sample of 5 mL and ACN solvent would be used for further method development.

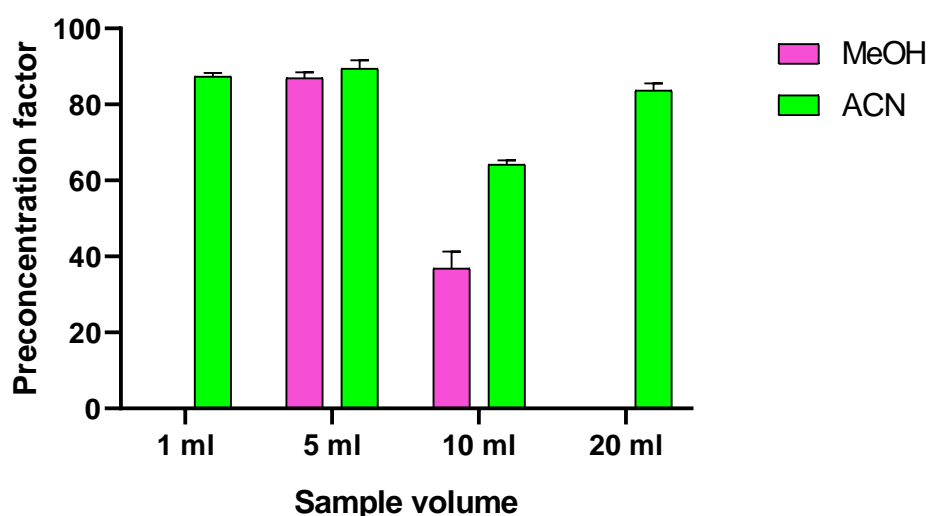


**Figure 3. 8:** Effect of solvent type (MeOH, ACN) and sample volume on preconcentration factor.

#### **3.11.1.2. Effect of adsorbent type on extraction efficiency.**

There was an observable exponential increase in extraction recoveries of the analytes. The extraction recoveries on  $\text{Fe}_3\text{O}_4$  were observed to be lowest for the analytes and highest when using the  $\text{Fe}_3\text{O}_4@ \text{Al}_2\text{O}_3/\text{AC}$  nanocomposites. The highest increase in extraction recovery using the  $\text{Fe}_3\text{O}_4@ \text{Al}_2\text{O}_3/\text{AC}$  adsorbent was observed for IMI, with an equal increase for ACT and TCL. The lowest observed recoveries for TMX have been attributed to its highest molecular formula, which tends to struggle with attaining space on the surface of the magnetic nanocomposite adsorbent. Finally, the results concluded that  $\text{Fe}_3\text{O}_4@ \text{Al}_2\text{O}_3/\text{AC}$  nanocomposite will be used for further method development. These results agree with the characterisation in **Figure 3.4 (c)**, wherein an increase in particle size was observed. The increase in particle size

observed in **Figure 3.4 (c)** has influenced to a certain extent to a higher surface area for absorption of these analytes as observed with  $\text{Fe}_3\text{O}_4@/\text{Al}_2\text{O}_3/\text{AC}$  on **Figure 3.9**.

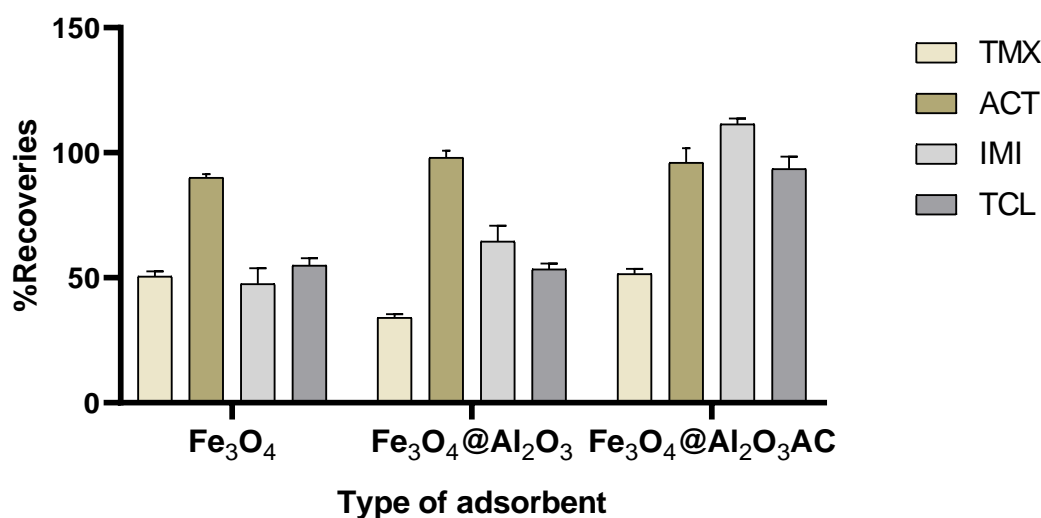


**Figure 3. 9:** Effect of adsorbent type on extraction recoveries

### 3.11.2. *Multivariate optimization*

#### 3.11.2.1. *Full factorial design pareto charts*

From **Figure 3.10** is the Pareto chart results showing the significant and insignificant parameters and their interactions at 95 % confidence interval. The horizontal bar graphs that cross a red dotted line (known as the reference line) show the important parameters. Those horizontal bar graphs below the reference line are said to be insignificant. Columns show the amount of effects, while the vertical line shows statistical significance at  $P = 0.05$ . The significant parameters were investigated for each analyte. From **Figure 3.10 (a)** pH, sorbent mass, and eluent volume were significant. The Pareto chart **(b)** shows that pH and eluent volume are significant. The pareto chart on **(c)** pH, sorbent mass and eluent volume were significant. Lastly, the results on Pareto chart **(d)** also show that pH, sorbent mass, and eluent volume were significant. This have given a conclusive remark that **Figure 3.10 (a), (c) and (d)** have the same parameters (pH, sorbent mass and eluent volume) being significant, while with **Figure 3.10 (b)** only two parameters (pH and eluent volume) were found to be significant. It is worth to note that only extraction time was insignificant. However, the ANOVA results were the guiding tool on selecting which time is best for high extraction

recoveries of these NEOs. Furthermore, this parameter's coefficient value could best assist in making that choice [62]. From the coefficient values, when the reported value is negative, it suggests that further optimization is done using the low extraction time. In contrast, if the coefficient value is positive, it means that high extraction time was used for further optimization, which can lead to high extraction recoveries of the analytes [63]. From this study, a positive coefficient was obtained for time. Hence, a higher extraction time of 8 minutes was selected for further optimization with CCD. For the other significant parameters (pH, sorbent mass and eluent volume), their experimental design was constructed with the RSM, and their interval points are shown in **Table 2.2**.

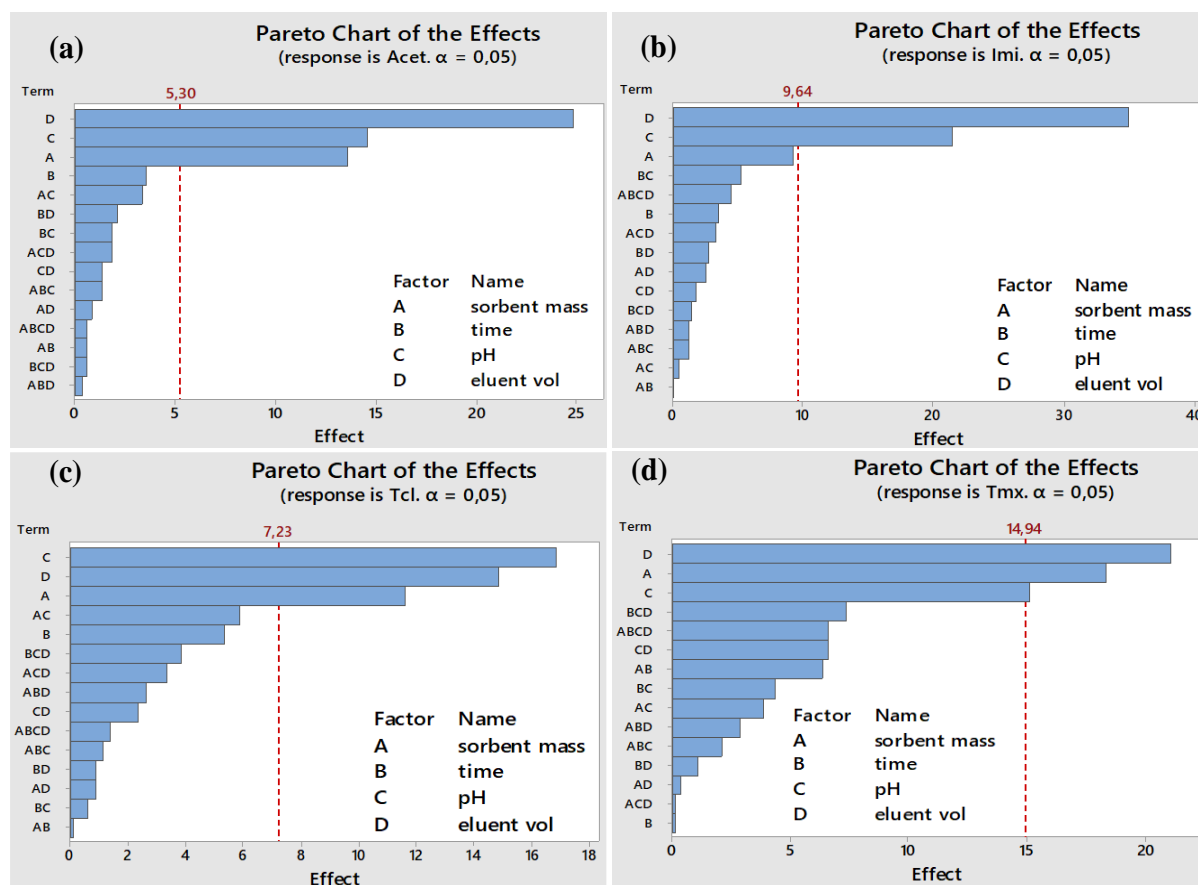


**Figure 3. 10:** Pareto charts result for FFD

### 3.11.2.2. Response surface methodology 3D plots

The results from further optimization are presented on 3D surface plots. The surface plots give the relationship proportionality of the most influential parameters. The results from all the surface plots on **Figure 3.11** from **(a)-(d)** show that when

sorbent mass increases and eluent volume decreases, there is an observable increase in extraction recoveries. These tells us that as we have a larger sorbent mass, the analytes are more adsorbed and have a lower eluting solvent, thus, as desorption occurs, the analytes will be highly concentrated on the eluting solvent. Furthermore, this also have an impact in terms of the less use of the organic solvents which supports the inexpensive microextraction protocols of this study.

Establishing an appropriate pH is crucial to prevent the target analyte from ionising and increase extraction efficiency. The pH of the solution is one of the most significant variables influencing the material's adsorption performance. Solution pH affects the stability and existence form of the target analytes to a certain extent. The surface plots show high extraction recoveries when the sample solution was neutral. This may be because NEOs hydrolyse slowly under acidic and degrade slightly under alkaline conditions. Therefore, for method validation, the pH condition was neutral. The surface plots results showed that as we increased the sorbent mass, the extraction recoveries also increased.

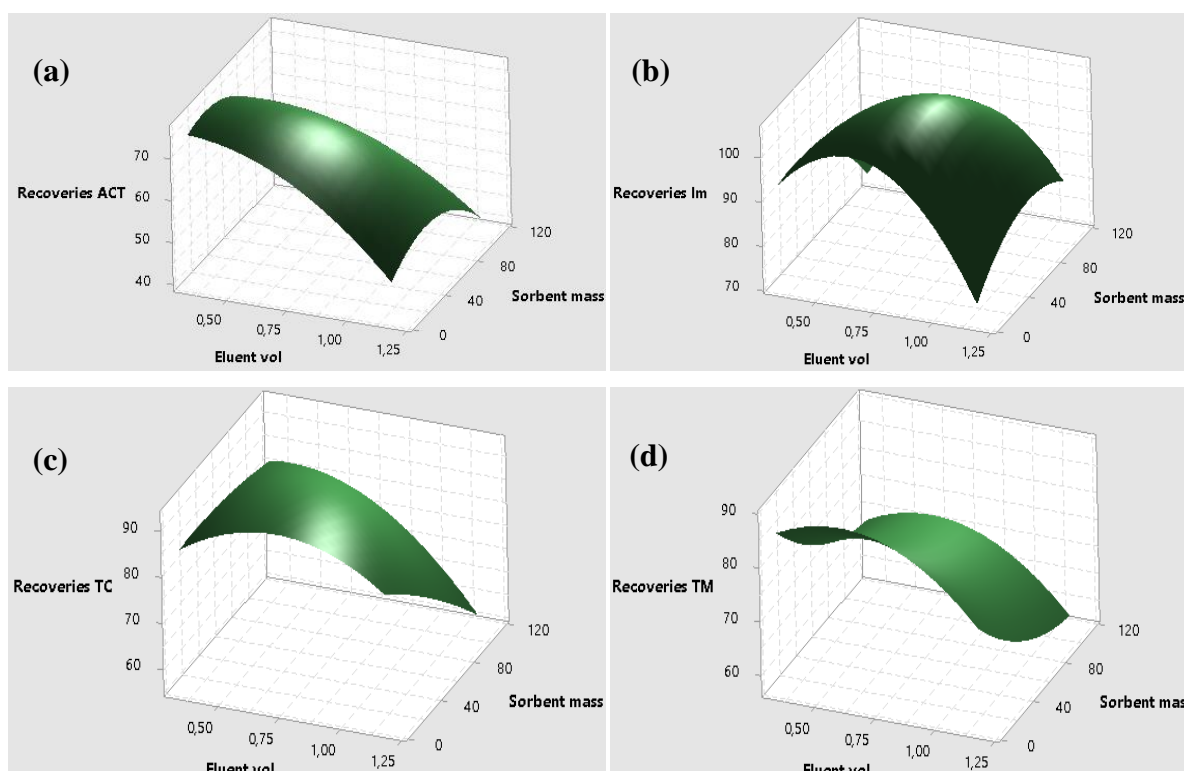


**Figure 3. 11:** Response surface 3D plots

### 3.12. Method validation

Method performance was studied, and the results are shown on equation 3.9-3.12. The developed method was validated in terms of their accuracy (% R), precision (% RSD), limit of detection (LOD), limit of quantification (LOQ), enrichment factor (EF), preconcentration factor (PF) and linearity ( $R^2$ ) shown on **Table 3.3**. The LOQ value of each analyte that correlated with a signal-to-noise ratio (S/N) of 10 was determined to be the lowest point of the calibration curve. In simple terms, the lowest amount of analyte that can be measured accurately enough is known as the limit of quantification, or LOQ, while the analyte concentration that results in a signal-to-noise ratio of three is referred to as LOD. The validation was done following the procedure in **Figure 3.1** with the following parameters: sample volume (5 mL), extraction time (8 min), sorbent mass (90 mg) and eluent volume (0.5 mL).

The equations associated with method validation have been listed below. All the equations used for validation calculations from analytical figures of merits have been listed below. External calibration curves of the analytes of interest were constructed by plotting the peak area of each analyte against the known spiked concentration of the analyte, respectively. This was done by taking the average of the peak areas in triplicate injections from each concentration. Furthermore, from the reported results of this study, the analytes have shown good linearity with values at  $R^2 \geq 0.99$ . Thus, this indicates a linear relationship between different concentrations of the analyte of interest on calibration standards. Comparing the slopes of the regression lines of the analytes in solvent and matrix shows a significant matrix effect when the slopes of the regression lines show a difference of more than 40%, respectively. The linear regression analysis was employed to calculate the target analytes' slopes, intercepts, and determination coefficients. The LODs recorded were 0.56-1.76 ng.  $\mu\text{L}^{-1}$ , LOQs at 1.87-6.62 ng.  $\mu\text{L}^{-1}$ , % RSD < 10 %, % R from 80-119.2%, PF from 73.02-407 and  $R^2$  of 0.9930-0.9982. **Table 3.3** below shows the equations and linearity of each analyte. The analysis of variance (ANOVA) from CCD gave the quadratic equations showing the interaction between the parameters studied. The equations are shown below from equation 3.9-3.12. The factors were A for pH, B for sorbent mass and C for eluent volume.

$$ACT = 47 + 3.8A - 0.87B + 162C + 0.182A^2 + 0.00263B^2 - 124C^2 - 0.0623AB - 0.79AC + 0.36BC \dots \dots \dots \text{equation 3. 9}$$



$$IMI = 43 - 10.7A - 0.39B + 304C + 0.216A^2 + 0.00246B^2 - 233C^2 + 0.0723AB + 7.4AC - 0.81BC \dots \dots \dots \text{equation 3. 10}$$

$$TCL = 13 + 0.23A - 0.654B + 263C + 0.346A^2 + 0.00620B^2 - 1990.0C^2 - 0.0623AB - 0.79AC + 0.245BC \dots \dots \dots \text{equation 3. 11}$$

$$TMX = 29.0 - 5.96A + 0.032B + 250C + 0.335A^2 - 0.00186B^2 - 174.5C^2 + 0.0370AB - 2.45AC - 0.260BC \dots \dots \dots \text{equation 3. 12}$$

Furthermore, it is worth noting that the method has two interaction effects with one degree of freedom and ANOVA effect [64]. The main function of the *P* values is to determine the method's performance as per the analytes studied. The *P* values signifies that if the *P* value from lack of fit is less than 0.05 ( $P < 0.05$ ) it suggests that the analyte does not fit the model [33]. However, if the *P* value is found to be greater than 0.05 ( $P > 0.05$ ), this shows that the analyte does fit the model [5]. From the NEOs of this study, only three analytes, ACT, TCL and TMX, were found not to fit the model. The respective *P* values of these analytes are 0.009 for ACT, 0.020 for TCL and 0.049 for TMX, respectively. On the other hand, only IMI fit the model with a *P* value of 0.324. This gives a conclusive result that the model is not compatible with the analytes since about 99 % of the analytes does not fit the model. However, the model can still be investigated following a different sample preparation method.

**Table 3. 3:** Analytes linearity

Type of analyte	Calibration equation	R <sup>2</sup>
Acetamiprid	Y = 0.0253x + 1.0821	0.9968
Imidacloprid	Y = 0.0166x - 2.2298	0.9930
Thiacloprid	Y = 0.0204x - 2.2778	0.9968
Thiamethoxam	Y = 0.0213x - 1.508	0.9982

### 3.13. Comparison of method performance with other reported methods.

The developed methods performance was compared with other studies reported. The method was compared in terms of extraction time, accuracy, precision,

LOD and EFs and the results are shown in **Table 3.4**. The developed MSPME has been shown to perform best regarding extraction time, accuracy and EFs. It is worth noting that the developed method recorded the lowest extraction time compared to other reported methods. The EFs were at an acceptable range, and many studies reported on **Table 3.4** did not report about the EFs. Lastly, the method gave the highest accuracy at an acceptable range of 70-120 % compared to other reported methods on the same matrix. The MSPME method showed the best performance. Moreover, the method adopted the green chemistry principle by using agricultural waste to synthesise the adsorbent. Furthermore, it is worth noting the novelty of this study, which uses a newly developed adsorbent that has proved to have the best performance in terms of extraction.

**Table 3. 4:** Comparison of MSPME with other reported methods in edible vegetable oils.

Matrix	Pesticide	Method	Adsorbent	Technique	LOD (ng. $\mu\text{L}^{-1}$ )	%RSD	Recoveries (%)	EF	Extraction time (min)	Ref
Olive Oil	ACT	QuEChERS	NR	LC-MS/MS & GC-MS/MS	NR	< 7.2	< 124	NR	NR	[65]
Edible oils	ACT, TMX, IMI, TCL	d-SPE	Z-sep & Z-Sep <sup>+</sup>	UHPLC-QqQ-MS/MS	NR	< 20	70-120	NR	13	[66]
Olive oil & olives	ACT, TMX, IMI, TCL	SPE	PSA	GC-MS/MS & LC-MS/MS	NR	< 25	70-120	NR	720	[67]
Olives & Olive Oil	IMI & TCL	QuEChERS	NR	LC/DAD/ESI/MS	0.04 & 0.14	NR	80-119	NR	NR	[68]
Virgin olive oil	TMX, TCL	QuEChERS - dSPE	NR	nanoflow LC/ESI Q-Orbitrap-MS	NR	< 19	75-119	NR	NR	[69]

Vegetable oils	ACT, TMX, IMI, TCL	MSPME	Fe <sub>3</sub> O <sub>4</sub> @Al <sub>2</sub> O <sub>3</sub> /A C	HPLC-DAD	0.56 - 1.76	≤ 10	80-119.21	52- 14 5	8	This study
----------------	--------------------	-------	--	----------	-------------------	------	-----------	----------------	---	------------

---

**RSD** – Relative standard deviation, **LOD** – Limit of detection, **EF** – Enrichment factor, **NR** – Not reported, **d-SPE** – Dispersive solid phase extraction, **MSPME** – Magnetic solid phase microextraction, **SPE** – Solid phase extraction, **GC-MS/MS** – Gas chromatography coupled with tandem mass spectrometry, **UHPLC-QqQ-MS/MS** - Ultrahigh performance liquid chromatography method coupled with triple quadrupole mass spectrometry, **LC/DAD/ESI/MS** - Liquid chromatography coupled to diode array detection and electrospray ionisation tandem mass spectrometry **HPLC-DAD** – High performance chromatography coupled with diode array detector, **UPLC-MS/MS** – Ultra-high performance liquid chromatography tandem mass spectrometry, **HPLC-MSMS** – High performance liquid chromatography tandem mass spectrometry, **LC-MS/MS** – Liquid chromatography tandem mass spectrometry, **nanoflow LC/ESI Q-Orbitrap-MS** - nanoflow liquid chromatography system coupled to high resolution mass spectrometry, **PSA** - Primary Secondary Amine, **Z-Sep, Z-Sep<sup>+</sup>** - Zirconium dioxide-based sorbent

### 3.14. Matrix effect

The phenomenon matrix effect is associated with the efficiency of the sample preparation method and matrix type. The ionisation and separation processes influence to a certain extent the matrix effects [70]. The matrix effect affects the significant degree the peak area and, therefore, the sensitivity of the analytes. Matrix effect studies were done by spiking the real vegetable oil samples with the known concentrations used to prepare the calibration standards. The **equation 3.7** above was used for the calculation of the matrix effect. The matrix effect was calculated for each analyte in four selected vegetable oils.

The concept of matrix effects can also be studied under specificity. Specificity refers to the method's ability to separate the particular analyte in the presence of other components. If ME is  $\sim 0\%$ , no matrix effect. If  $ME > 0\%$ , ion suppression occurs. If  $ME < 0\%$ , ion enhancement occurs [71]. For further investigation of the matrix effects, any analytes that showed no significant matrix effects, the standard calibration curve could be used to quantify them. However, the results in **Figure 3.12** show that all the analytes suffered from the matrix effects. The analytes were quantified using matrix-matched calibration curves for validation and application in real samples. The results for the matrix effects are shown in **Figure 3.12**. Furthermore, it is worth noting that from **Figure 3.12** the avocado oil, it can be observed that TMX and ACT suffered ion enhancement while IMI and TCL suffered ion suppression. From other types of vegetable oils like canola oil, olive oil, and sunflower oil show that the analytes suffered ion suppression for all the analytes. This shows that the matrix does influence these vegetable oils to a certain extent. Thus, it was also explained that the TMX, ACT and IMI suffered from a low matrix effect from the avocado oil while TCL suffered from a medium matrix effect. Furthermore, on the other hand, canola and olive oil have shown that all the analytes suffer from high matrix effect, respectively. Lastly, with sunflower oil, the results have shown that TMX, ACT and IMI suffer from a medium matrix effect while TCL suffers from a high matrix effect [72].

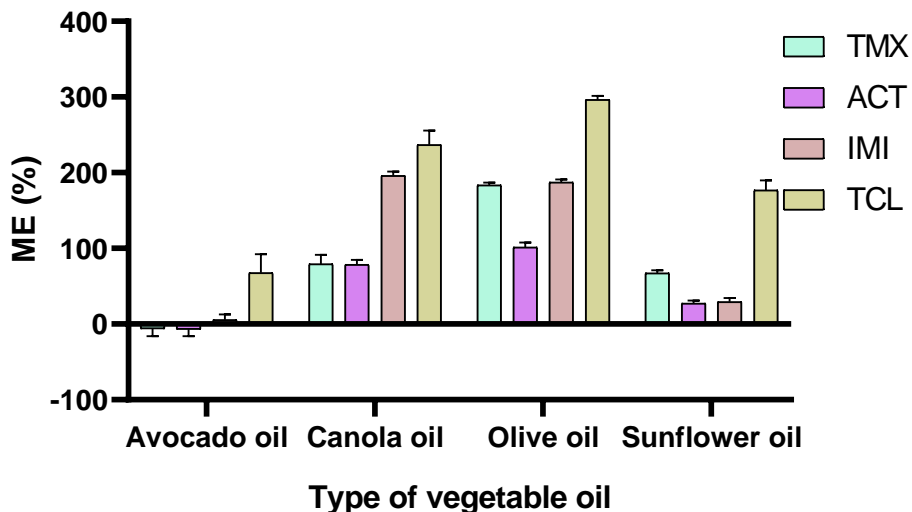


**Figure 3. 12:** Matrix effects studied for different analytes from selected vegetable oils.

### 3.15. Enrichment factor

EF is known as the ratio between the slope of the analytes in the sample matrix and the slope of the analytes in the solvent. If  $EF > 1$ , it means there was visibly higher proportion of analytes within the sample set than it would have been expected by chance [73]. The results shown in the **Figure 3.13** show that all the selected analytes have demonstrated that there was visibly a higher proportion of the analytes in the selected vegetable oils. However, this might have been attributed to by the matrix effects.

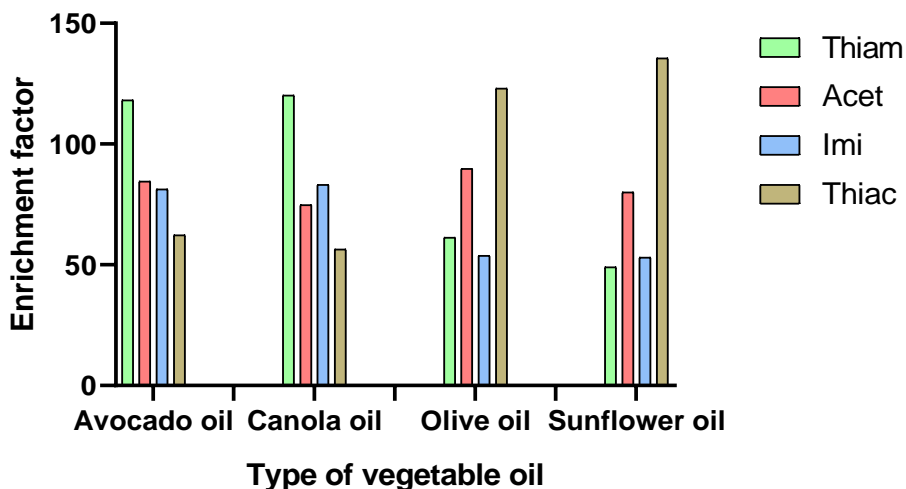


**Figure 3. 13:** Enrichment factor effect on selected vegetable oils.

### 3.16. Method greenness assessment

The AGREE mathematical tool was used for the assessment of the developed MSPME. The AGREE metric has been considered user-friendly, comprehensive, easy to apply and fast [74]. Green assessment was done using an Analytical Eco-Scale and Analytical GREENness Metric calculator. The AGREE tool uses 10 principles of green analytical chemistry (GAC), yielding a pictogram at a score range of 0-1 [75]. The 1-10 clockwise scale red-yellow-green colour scheme demonstrated the technique's performance against each principle [76]. The total score in the centre of the pictogram, with values near one and a dark green tint, indicates that the tested technique is more environmentally friendly [77]. The AGREE results have been presented in **Figure 3.14**, depicting the AGREE results for the MSPME method at a total score of 0.54, indicating that the technique was somewhat green. However, the acceptable value for the process to be green is on a scale of 0.6 to 1 [78]. The greenness of the developed method was mostly affected by the amount of waste generated through each step, the number of preparation steps and manual sample preparation, which can cause some inaccuracy of the results generated.

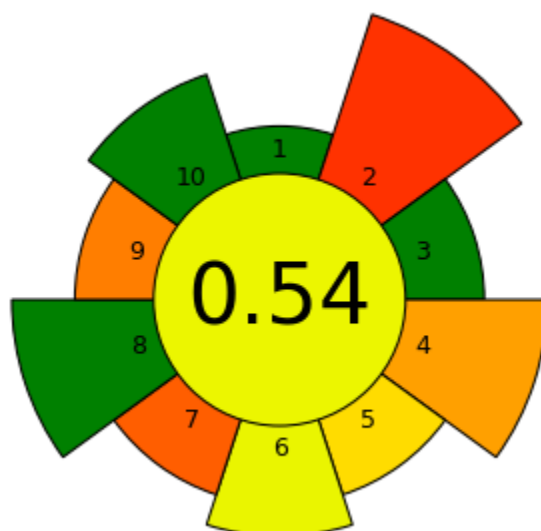


**Figure 3. 14:** Developed MSPME method AGREE pictogram.

### 3.17. Application of MSPME method in real samples

The MSPME method was applied in real samples. This was done following the procedure in **Figure 3.1**. A total of 16 experiments were done, with four experiments for each vegetable oil. The parameters were 5 mL sample volume, 90 mg sorbent mass, 8 min extraction time, 13 pH and 0.5 mL of eluent volume. The results have shown that all four vegetable oils (avocado, canola, olive and sunflower) were free on the NEOs and considered safe for human consumption. Their concentrations were below the detection limits; thus, they were in trace levels. The results are reported in **Table 3.5**.

**Table 3. 5:** Application of the developed MSPME in selected vegetable oils

Analyte	Avocado oil	Canola oil	Olive oil	Sunflower oil
ACT	< DL	< DL	< DL	< DL
IMI	< DL	< DL	< DL	< DL
TCL	< DL	< DL	< DL	< DL
TMX	< DL	< DL	< DL	< DL

**DL-** detection limit

For further validation and confirmation of real vegetable oil samples' NEOs concentration, The experiments were done following the procedure in **Figure 3.1** with 5 mL sample volume, 90 mg sorbent mass, 8 min extraction time, 13 pH and 0.5 mL of eluent volume. The two spiking concentrations were 40 ng.  $\mu\text{L}^{-1}$  and 80 ng.  $\mu\text{L}^{-1}$ . The comparison was done following the appearance of the peaks on the chromatogram in **Figure 3.15**. Moreover, from the chromatogram in **Figure 3.15**, chromatogram **(a)** for real samples has shown very small peaks for TMX, ACT and IMI while TCL was a wide broad peak of which this peak appearance can be attributed to the matrix effect since **Figure 3.12**, it has shown that the analytes are affected by other matrices other than the analytes of interest. The appearance of a peak is directly related to the concentration of the analytes. It is worth noting that at **Figure 3.15 (b)**, the calibration standard the peaks were more conspicuous. From **Figure 3.15 (a), (b) and (c)**, there



is an observable peak before the appearance of the first TMX analyte, which is known as the solvent peak.

Additionally, the solvent peak is not visible in **Figure 3.15 (b)** since the calibration standard was prepared from the same solvent without any modifications. In comparison with **Figure 3.15 (a)**, **Figure 3.15 (c)** and **Figure 3.15 (d)**, chromatograms have shown a distinctive peak due to spiking. These results help to conclude that the vegetable oils were indeed free of these NEOs. Additionally, different spiking concentrations were studied in four selected vegetable oils for the NEOs. The two spiking concentrations studied were 40 ng.µL<sup>-1</sup> and 80 ng.µL<sup>-1</sup>. The **Table 3.6** shows the recoveries and %RSDs for each analyte in selected vegetable oils, respectively.

The spiked recoveries of the NEOs were at a range of 76.9-107 % with the %RSDs at less than 6 as shown in **Table 3.6**. These results show that the proposed method has application potential for the determination of pesticides in real vegetable oils.

**Table 3. 6:** Different concentrations studied

Sample	Analytes	Spiked concentrations (n=3)		
		Recoveries (%) (%RSD)		
		0 ng.µL <sup>-1</sup>	40 ng.µL <sup>-1</sup>	80 ng.µL <sup>-1</sup>
Avocado oil	ACT	ND	106 (1.3)	107 (2.6)
	IMI	ND	102 (2.3)	98.2 (3.3)
	TCL	ND	99.1 (1.7)	10.3 (2.6)
	TMX	ND	82.1 (2.1)	89.3 (1.2)
Canola oil	ACT	ND	78.6 (5.2)	96.3 (1.4)
	IMI	ND	83.2 (1.3)	98.2 (2.1)
	TCL	ND	95.2 (2.3)	76.9 (3.3)

	TMX	ND	87.8 (1.1)	89.7 (1.9)
Olive oil	ACT	ND	87.1 (3.2)	92.8 (2.2)
	IMI	ND	97.2 (0.9)	91 (1.5)
	TCL	ND	83 (1.8)	89.3 (2.5)
	TMX	ND	100.3 (2.6)	90.2 (1.3)
Sunflower oil	ACT	ND	85.8 (1.8)	101.7 (2.1)
	IMI	ND	92.4 (2.6)	87.1 (1.2)
	TCL	ND	88.8 (0.7)	96.2 (1.9)
	TMX	ND	92.7 (2.1)	88.5 (2.2)

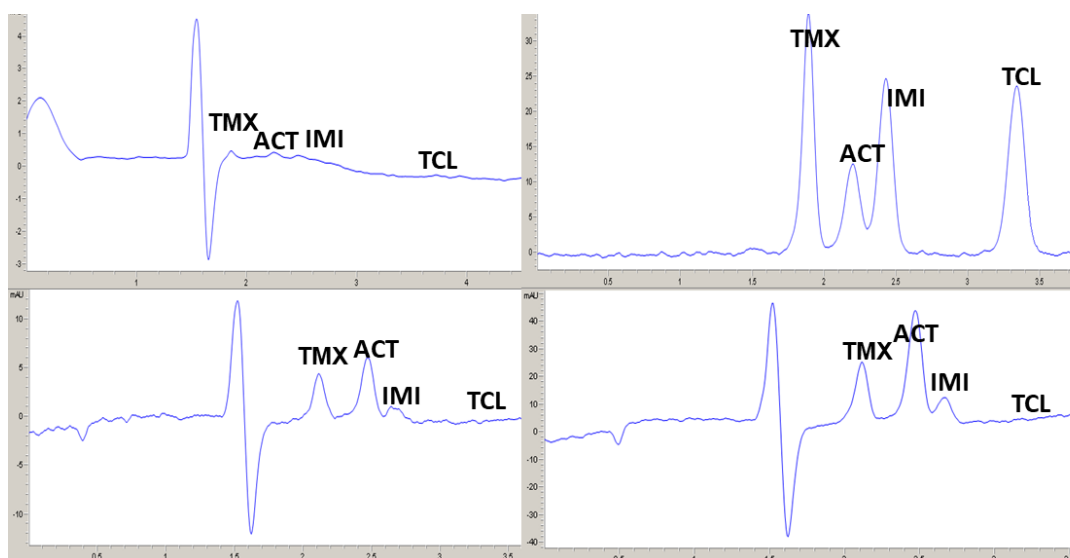


**Figure 3. 15:** Chromatograms of real commercial vegetable oils and spiked vegetable oils **(a)** real sample, **(b)** analytes standard, **(c)** spiked real sample 40  $\text{ng}\cdot\mu\text{L}^{-1}$  and **(d)** spiked real sample 80  $\text{ng}\cdot\mu\text{L}^{-1}$ .

### 3.18. Reusability and regeneration.

The reusability studies were conducted for the adsorbent used in this study and presented in **Figure 3.16**. It is fundamental to perform reusability studies to evaluate their efficiency and stability. The adsorbent was used on multiple extraction cycles on spiked vegetable oil, and the extraction cycles were done while investigating the extraction recoveries. The reusability and regeneration of the adsorbent were studied since they are important factors to evaluate for their practical applicability. The reusability of the adsorbent is fundamental for economic and environmental efficiency. Ethanol was the solvent used to wash the nanocomposites after every elution step, respectively. This was done by performing several extractions, elution, washing and drying before the next use. The adsorbent has shown a decrease in extraction stability over 8 cycles of use. The extraction recoveries on these runs exponentially decreased from 119-33.10 %. However, with these extraction recoveries obtained, the exponential decrease in extraction recoveries was influenced by the adsorbent loss after each extraction and washing step. Moreover, the type of matrix used for this study was challenging during extraction; hence, such a loss in the adsorbent was observed. The adsorbent retained its stability during its reusability for its adsorption capacity.

The reusability of the synthesised magnetic nanocomposite was investigated for its extraction recoveries over several runs of the experiments. An observable exponential decrease in extraction recoveries happened. This was due to the loss of the nanocomposite from each extraction as it also decreased in quantity during the washing process for reuse. A loss in magnetic properties for the nanocomposite was also observed, which was the most influential factor in the exponential decrease of extraction recoveries. To the best of our knowledge many reported studies did not disclose the reusability of their adsorbent for this type of sample. However, with regard to this study so far it has proved to show good reusability acceptance for this type of sample. Furthermore, there was a proportional relationship between the quantity of the adsorbent loss after each run and washing process and its magnetism. The results show that TMX has always had the lowest extraction recoveries. This has been due to this analyte's high molecular weight, depriving it from being adsorbed on the surface of the adsorbent. However, there has been competition for adsorption sites between ACT and TCL.

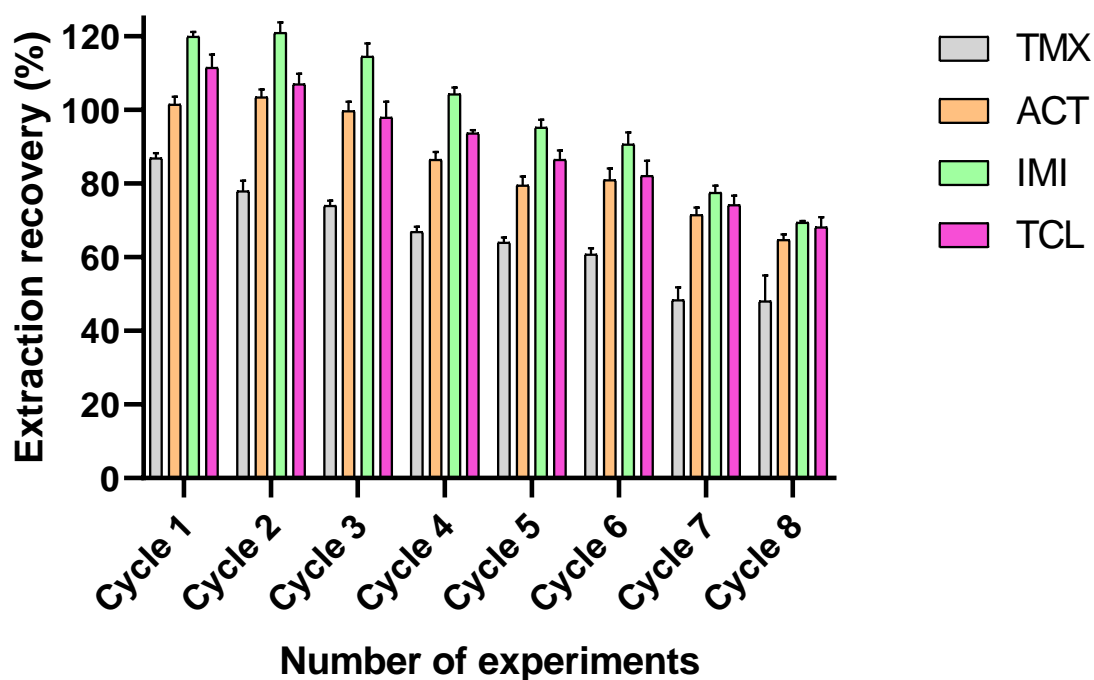


**Figure 3. 16:** Reusability cycles for  $\text{Fe}_3\text{O}_4@\text{Al}_2\text{O}_3/\text{AC}$  nanocomposite.

### 3.19. Conclusion

It can be concluded that magnetic nanocomposite was successfully synthesised, characterised and applied as an adsorbent for extraction and preconcentration. The  $\text{Fe}_3\text{O}_4@\text{Al}_2\text{O}_3/\text{AC}$  adsorbent used in this study was novel and has shown high accuracy. The synthesis of these adsorbents adhered to green chemistry principles wherein corn cobs and lemon peel (agricultural waste) were utilised during the synthesis process. The high pore size on the AC prepared from corn cobs as observed from the SEM-EDS from **Figure 3.6 (d)** permitted enough surface for adsorption of the analytes; hence, higher extraction recoveries were obtained. The developed MSPME has shown great potential as a preconcentration method for the selected NEOs from the vegetable oil samples.

Moreover, the performance of the  $\text{Fe}_3\text{O}_4@\text{Al}_2\text{O}_3/\text{AC}$  adsorbent and the MSPME gave significantly good extraction recoveries. The high extraction recoveries for these analytes confirmed the  $\pi$ - $\pi$  interactions between the NEOs and  $\text{Fe}_3\text{O}_4@\text{Al}_2\text{O}_3/\text{AC}$  had played a crucial role in MSPME. Additionally, it is worth noting that the selected NEOs

for this study have the nitro group or the cyano group, which is capable of acting as a Lewis acid (electron acceptor) to yield the Lewis acid-base interactions with the benzene rings as Lewis base (electron donor) of the  $\text{Fe}_3\text{O}_4@\text{Al}_2\text{O}_3/\text{AC}$  nanocomposite. Thus, the extraction mechanism of this study can be based on the  $\pi$ - $\pi$  interactions and Lewis acid-base interactions. These results have proved that the chemical and physical properties of the analytes, the type of adsorbent experimental conditions and the nature of the matrix influence its adsorption to a certain extent. It is also worth noting that the adsorption of organic pollutants on the surface of porous activated carbons can be due to the  $\pi$ - $\pi$  interactions of the  $\pi$  electrons of these organic pollutants with the  $\pi$  electrons of the benzene rings of the activated carbons.

To compensate for the matrix effects, the matrix-matched calibration curves were constructed, and the results have shown that the matrix effect influences the appearance of the peaks on the spectra of our analytes. The matrix effects were observed in all the selected vegetable oils used for this study. Ion suppression and ion enhancement were observed with matrix effects ranging from low, medium and high from these vegetable oils.

The reusability studies of the adsorbent have proved that the synthesised adsorbent can maintain its high stability and reusability over numerous extraction cycles. The type of matrix used for this study contributed to an exponential decrease in extraction recovery proportionally to the amount of the adsorbent recovered after each extraction and washing. Furthermore, the adsorbent is believed to withstand more runs when applied to a less complex matrix. The developed method has proved efficient for its application based on the accuracy and precision investigated for this study.

## References

- [1] N. S. Mdluli, P. N. Nomngongo, and N. Mketi, "Ionic liquid assisted extraction induced by emulsion breaking for extraction of trace metals in diesel, gasoline and kerosene prior to ICP-OES analysis," *Heliyon*, vol. 10, no. 5, p. e26605, 2024, doi: 10.1016/j.heliyon.2024.e26605.
- [2] S. K. Selahle, N. J. Waleng, A. Mpupa, and P. N. Nomngongo, "Magnetic Solid Phase Extraction Based on Nanostructured Magnetic Porous Porphyrin Organic Polymer for Simultaneous Extraction and Preconcentration of Neonicotinoid Insecticides From Surface Water," *Front. Chem.*, vol. 8, no. September, pp. 1–15, 2020, doi: 10.3389/fchem.2020.555847.
- [3] S. Jiang *et al.*, "Green synthesis of novel magnetic porous organic polymer for magnetic solid phase extraction of neonicotinoids in lemon juice and honey samples," *Food Chem.*, vol. 383, no. March, p. 132599, 2022, doi: 10.1016/j.foodchem.2022.132599.
- [4] J. Lu *et al.*, "A functionalized magnetic covalent organic framework for sensitive determination of trace neonicotinoid residues in vegetable samples," *J. Chromatogr. A*, vol. 1618, p. 460898, 2020, doi: 10.1016/j.chroma.2020.460898.
- [5] A. Ghiasi, A. Malekpour, and S. Mahpishanian, "Metal-organic framework MIL101 (Cr)-NH<sub>2</sub> functionalized magnetic graphene oxide for ultrasonic-assisted magnetic solid phase extraction of neonicotinoid insecticides from fruit and water samples," *Talanta*, vol. 217, no. April, p. 121120, 2020, doi: 10.1016/j.talanta.2020.121120.
- [6] L. Liu, T. Feng, C. Wang, Q. Wu, and Z. Wang, "Enrichment of neonicotinoid insecticides from lemon juice sample with magnetic three-dimensional graphene as the adsorbent followed by determination with high-performance liquid chromatography," *J. Sep. Sci.*, vol. 37, no. 11, pp. 1276–1282, 2014, doi: 10.1002/jssc.201301382.
- [7] Z. Shi, S. Zhang, Q. Huai, D. Xu, and H. Zhang, "Methylamine-modified graphene-based solid phase extraction combined with UPLC-MS/MS for the analysis of neonicotinoid insecticides in sunflower seeds," *Talanta*, vol. 162,

- no. October 2016, pp. 300–308, 2017, doi: 10.1016/j.talanta.2016.10.042.
- [8] L. Hao, C. Wang, Q. Wu, Z. Li, X. Zang, and Z. Wang, “Metal-organic framework derived magnetic nanoporous carbon: Novel adsorbent for magnetic solid-phase extraction,” *Anal. Chem.*, vol. 86, no. 24, pp. 12199–12205, 2014, doi: 10.1021/ac5031896.
- [9] X. Cao *et al.*, “One-pot synthesis of magnetic zeolitic imidazolate framework/grapheme oxide composites for the extraction of neonicotinoid insecticides from environmental water samples,” *J. Sep. Sci.*, vol. 40, no. 24, pp. 4747–4756, 2017, doi: 10.1002/jssc.201700674.
- [10] X. Ma *et al.*, “Magnetic solid-phase extraction of neonicotinoid pesticides from pear and tomato samples using graphene grafted silica-coated Fe<sub>3</sub>O<sub>4</sub> as the magnetic adsorbent,” *Anal. Methods*, vol. 5, no. 11, pp. 2809–2815, 2013, doi: 10.1039/c3ay40207j.
- [11] L. Chen and B. Li, “Determination of imidacloprid in rice by molecularly imprinted-matrix solid-phase dispersion with liquid chromatography tandem mass spectrometry,” *J. Chromatogr. B Anal. Technol. Biomed. Life Sci.*, vol. 897, pp. 32–36, 2012, doi: 10.1016/j.jchromb.2012.04.004.
- [12] X. Cao *et al.*, “Metal-organic framework UiO-66 for rapid dispersive solid phase extraction of neonicotinoid insecticides in water samples,” *J. Chromatogr. B Anal. Technol. Biomed. Life Sci.*, vol. 1077–1078, no. October 2017, pp. 92–97, 2018, doi: 10.1016/j.jchromb.2017.11.034.
- [13] L. Liu, Y. Hao, X. Zhou, C. Wang, Q. Wu, and Z. Wang, “Magnetic porous carbon based solid-phase extraction coupled with high performance liquid chromatography for the determination of neonicotinoid insecticides in environmental water and peanut milk samples,” *Anal. Methods*, vol. 7, no. 6, pp. 2762–2769, 2015, doi: 10.1039/c4ay02990a.
- [14] M. Zhang, H. Chen, L. Zhu, C. Wang, G. Ma, and X. Liu, “Solid-phase purification and extraction for the determination of trace neonicotinoid pesticides in tea infusion,” *J. Sep. Sci.*, vol. 39, no. 5, pp. 910–917, 2016, doi: 10.1002/jssc.201501129.

- [15] O. Ozalp, Z. P. Gumus, and M. Soylak, "MIL-101(Cr) metal–organic frameworks based on deep eutectic solvent (ChCl: Urea) for solid phase extraction of imidacloprid in tea infusions and water samples," *J. Mol. Liq.*, vol. 378, p. 121589, 2023, doi: 10.1016/j.molliq.2023.121589.
- [16] T. Iwafune, T. Ogino, and E. Watanabe, "Water-based extraction and liquid chromatography-tandem mass spectrometry analysis of neonicotinoid insecticides and their metabolites in green pepper/tomato samples," *J. Agric. Food Chem.*, vol. 62, no. 13, pp. 2790–2796, 2014, doi: 10.1021/jf405311y.
- [17] Y. Xu *et al.*, "Zirconium(IV)-based metal-organic framework for determination of imidacloprid and thiamethoxam pesticides from fruits by UPLC-MS/MS," *Food Chem.*, vol. 344, no. August 2020, p. 128650, 2021, doi: 10.1016/j.foodchem.2020.128650.
- [18] V. Kosar, A. M. Križanac, I. E. Zelić, S. Kurajica, and V. Tomašić, "Photocatalytic Degradation of Neonicotinoid Insecticides over Perlite-Supported TiO<sub>2</sub>," *Processes*, vol. 11, no. 9, 2023, doi: 10.3390/pr11092588.
- [19] C. M. Bolzan, S. S. Caldas, B. S. Guimarães, and E. G. Primel, "Dispersive liquid-liquid microextraction with liquid chromatography-tandem mass spectrometry for the determination of triazine, neonicotinoid, triazole and imidazolinone pesticides in mineral water samples," *J. Braz. Chem. Soc.*, vol. 26, no. 9, pp. 1902–1913, 2015, doi: 10.5935/0103-5053.20150168.
- [20] N. J. Waleng, S. K. Selahle, A. Mpupa, and P. N. Nomngongo, "Development of dispersive solid-phase microextraction coupled with high-pressure liquid chromatography for the preconcentration and determination of the selected neonicotinoid insecticides," *J. Anal. Sci. Technol.*, vol. 13, no. 1, 2022, doi: 10.1186/s40543-021-00311-4.
- [21] Y. Liao, Y. Zhang, Q. Zhao, W. Xiang, B. Jiao, and X. Su, "MIL-101(Cr) based d-SPE/UPLC-MS/MS for determination of neonicotinoid insecticides in beverages," *Microchem. J.*, vol. 175, no. November 2021, p. 107091, 2022, doi: 10.1016/j.microc.2021.107091.
- [22] S. T. Narendran, S. N. Meyyanathan, and V. V. S. R. Karri, "Experimental design in pesticide extraction methods: A review," *Food Chem.*, vol. 289, no.



- November 2018, pp. 384–395, 2019, doi: 10.1016/j.foodchem.2019.03.045.
- [23] S. Li *et al.*, “Synthesis of nitrogen-rich magnetic hypercrosslinked polymer as robust adsorbent for the detection of neonicotinoids in honey, tomatoes, lettuce and Chinese cabbage,” *J. Chromatogr. A*, vol. 1677, p. 463326, 2022, doi: 10.1016/j.chroma.2022.463326.
- [24] J. Hou *et al.*, “Simultaneous determination of ten neonicotinoid insecticides and two metabolites in honey and Royal-jelly by solid–phase extraction and liquid chromatography–tandem mass spectrometry,” *Food Chem.*, vol. 270, no. January 2018, pp. 204–213, 2019, doi: 10.1016/j.foodchem.2018.07.068.
- [25] O. M. Khabeeeri, S. A. Al-Thabaiti, and Z. Khan, “Citrus sinensis peel waste assisted synthesis of AgNPs: effect of surfactant on the nucleation and morphology,” *SN Appl. Sci.*, vol. 2, no. 12, pp. 1–15, 2020, doi: 10.1007/s42452-020-03801-z.
- [26] S. Saif, A. Tahir, and Y. Chen, “Green synthesis of iron nanoparticles and their environmental applications and implications,” *Nanomaterials*, vol. 6, no. 11, pp. 1–26, 2016, doi: 10.3390/nano6110209.
- [27] C. Toyos-Rodríguez *et al.*, “A Simple and Reliable Synthesis of Superparamagnetic Magnetite Nanoparticles by Thermal Decomposition of Fe(acac)<sub>3</sub>,” *J. Nanomater.*, vol. 2019, 2019, doi: 10.1155/2019/2464010.
- [28] N. S. Mdluli, “Development of Greener Sample Preparation Methods for Extraction and Spectrometric Determination of Metals in Selected Fuel Samples,” no. February, 2022.
- [29] T. Sime, J. Fito, T. T. I. Nkambule, Y. Temesgen, and A. Sergawie, “Adsorption of Congo Red from Textile Wastewater Using Activated Carbon Developed from Corn Cobs: The Studies of Isotherms and Kinetics,” *Chem. Africa*, vol. 6, no. 2, pp. 667–682, 2023, doi: 10.1007/s42250-022-00583-2.
- [30] P. J. Wibawa *et al.*, “Green synthesized silver nanoparticles immobilized on activated carbon nanoparticles: Antibacterial activity enhancement study and its application on textiles fabrics,” *Molecules*, vol. 26, no. 13, pp. 1–14, 2021, doi: 10.3390/molecules26133790.

- [31] S. Rajendran *et al.*, “Enriched catalytic activity of TiO<sub>2</sub> nanoparticles supported by activated carbon for noxious pollutant elimination,” *Nanomaterials*, vol. 11, no. 11, 2021, doi: 10.3390/nano11112808.
- [32] W. Xie, C. Han, Y. Qian, H. Ding, X. Chen, and J. Xi, “Determination of neonicotinoid pesticides residues in agricultural samples by solid-phase extraction combined with liquid chromatography-tandem mass spectrometry,” *J. Chromatogr. A*, vol. 1218, no. 28, pp. 4426–4433, 2011, doi: 10.1016/j.chroma.2011.05.026.
- [33] Y. An *et al.*, “Synthesis of natural proanthocyanidin based novel magnetic nanoporous organic polymer as advanced sorbent for neonicotinoid insecticides,” *Food Chem.*, vol. 373, no. PB, p. 131572, 2022, doi: 10.1016/j.foodchem.2021.131572.
- [34] M. Allgaier, J. M. Halder, J. Kittelberger, B. Hauer, and B. A. Nebel, “A simple and robust LC-ESI single quadrupole MS-based method to analyze neonicotinoids in honey bee extracts,” *MethodsX*, vol. 6, pp. 2484–2491, 2019, doi: 10.1016/j.mex.2019.09.038.
- [35] N. H. M. Jumali, S. Ganesan, N. Yahaya, and M. Miskam, “3-Monochloropropane-1,2-diol Monoesters Food Contaminant Analysis in Palm Oil-Based Food Samples Using C<sub>18</sub>-Dispersive Solid-Phase Extraction Coupled with GC-FID,” *Food Anal. Methods*, no. 0123456789, 2021, doi: 10.1007/s12161-021-02040-1.
- [36] S. Ahn, S. Son, B. Kim, and K. Choi, “Development of an isotope dilution liquid chromatography/tandem mass spectrometry method for the accurate determination of neonicotinoid pesticides, imidacloprid, clothianidin, and thiamethoxam in kimchi cabbage reference materials,” *J. Anal. Sci. Technol.*, vol. 13, no. 1, 2022, doi: 10.1186/s40543-022-00319-4.
- [37] M. Bazregar, M. Rajabi, Y. Yamini, S. Arghavani-Beydokhti, and A. Asghari, “Centrifugeless dispersive liquid-liquid microextraction based on salting-out phenomenon followed by high performance liquid chromatography for determination of Sudan dyes in different species,” *Food Chem.*, vol. 244, no. October 2016, pp. 1–6, 2018, doi: 10.1016/j.foodchem.2017.10.006.

- [38] G. C. Bedendo, I. C. S. F. Jardim, and E. Carasek, "Multiresidue determination of pesticides in industrial and fresh orange juice by hollow fiber microporous membrane liquid-liquid extraction and detection by liquid chromatography-electrospray-tandem mass spectrometry," *Talanta*, vol. 88, pp. 573–580, 2012, doi: 10.1016/j.talanta.2011.11.037.
- [39] W. Chen *et al.*, "Matrix-Induced Sugaring-Out : A Simple and Rapid Sample Preparation Method for the Determination of," *Molecules*, vol. 24 pp. 2-9, 2019. doi:10.3390/molecules24152761
- [40] M. Pastor-Belda *et al.*, "Determination of spirocyclic tetronic/tetramic acid derivatives and neonicotinoid insecticides in fruits and vegetables by liquid chromatography and mass spectrometry after dispersive liquid-liquid microextraction," *Food Chem.*, vol. 202, pp. 389–395, 2016, doi: 10.1016/j.foodchem.2016.01.143.
- [41] S. Anvar Nojedeh Sadat, R. Atazadeh, and M. R. Afshar Mogaddam, "Application of in-situ formed polymer-based dispersive solid phase extraction in combination with solidification of floating organic droplet-based dispersive liquid–liquid microextraction for the extraction of neonicotinoid pesticides from milk samples," *J. Sep. Sci.*, vol. 46, no. 13, 2023, doi: 10.1002/jssc.202200889.
- [42] K. Nakamura, T. Otake, and N. Hanari, "Evaluation of pressurized liquid extraction for th[1] K. Nakamura, T. Otake, and N. Hanari, 'Evaluation of pressurized liquid extraction for the determination of neonicotinoid pesticides in green onion,' *J. Environ. Sci. Heal. - Part B Pestic. Food Contam.*" *J. Environ. Sci. Heal. - Part B Pestic. Food Contam. Agric. Wastes*, vol. 54, no. 8, pp. 640–646, 2019, doi: 10.1080/03601234.2019.1621633.
- [43] J. Vichapong, R. Kachangoon, R. Burakham, Y. Santaladchaiyakit, and S. Srijaranai, "Ringer Tablet-Based Micelle-Mediated Extraction-Solvent Back Extraction Coupled with High-Performance Liquid Chromatography for Preconcentration and Determination of Neonicotinoid Pesticides," *Food Anal. Methods*, vol. 15, no. 4, pp. 970–980, 2022, doi: 10.1007/s12161-021-02067-4.
- [44] R. Kachangoon, J. Vichapong, Y. Santaladchaiyakit, and S. Srijaranai, "Cloud-

- point extraction coupled to in-situ metathesis reaction of deep eutectic solvents for preconcentration and liquid chromatographic analysis of neonicotinoid insecticide residues in water, soil and urine samples," *Microchem. J.*, vol. 152, no. October 2019, p. 104377, 2020, doi: 10.1016/j.microc.2019.104377.
- [45] H. Khanehzar, M. Faraji, A. Nezhadali, and Y. Yamini, "Combining of modified QuEChERS and dispersive liquid–liquid microextraction as an efficient sample preparation method for extraction of acetamiprid and imidacloprid from pistachio samples," *J. Iran. Chem. Soc.*, vol. 18, no. 3, pp. 641–649, 2021, doi: 10.1007/s13738-020-02050-6.
- [46] O. Filippou, E. A. Deliyanni, and V. F. Samanidou, "Fabrication and evaluation of magnetic activated carbon as adsorbent for ultrasonic assisted magnetic solid phase dispersive extraction of bisphenol A from milk prior to high performance liquid chromatographic analysis with ultraviolet detection," *J. Chromatogr. A*, vol. 1479, pp. 20–31, 2017, doi: 10.1016/j.chroma.2016.12.002.
- [47] I. Hrynko, B. Łozowicka, and P. Kaczyński, "Liquid Chromatographic MS/MS Analysis of a Large Group of Insecticides in Honey by Modified QuEChERS," *Food Anal. Methods*, vol. 11, no. 8, pp. 2307–2319, 2018, doi: 10.1007/s12161-018-1208-z.
- [48] V. S. Harshini Priyaa, R. Saravanathamizhan, and N. Balasubramanian, "Preparation of biomass based carbon for electrochemical energy storage application," *J. Electrochem. Sci. Technol.*, vol. 10, no. 2, pp. 159–169, 2019, doi: 10.5229/JECST.2019.10.2.159.
- [49] M. Abdullah *et al.*, "Removal of ceftriaxone sodium antibiotic from pharmaceutical wastewater using an activated carbon based TiO<sub>2</sub> composite: Adsorption and photocatalytic degradation evaluation," *Chemosphere*, vol. 317, no. September 2022, p. 137834, 2023, doi: 10.1016/j.chemosphere.2023.137834.
- [50] N. B. Allou, N. S. Eroi, M. A. Tigori, P. Atheba, and A. Trokourey, "Production and Characterization of Green Biosorbent Based on Modified Corn Cob Decorated Magnetite Nanoparticles," *J. Mater. Sci. Chem. Eng.*, vol. 11, no.

- 02, pp. 1–12, 2023, doi: 10.4236/msce.2023.112001.
- [51] N. A. N. Alkadasi, “Synthesis of magnetite nanocubes ( $\text{Fe}_3\text{O}_4$ ) from iron (III) acetylacetonate by removal gas and higher temperature obtained,” *Orient. J. Chem.*, vol. 30, no. 3, pp. 1179–1182, 2014, doi: 10.13005/ojc/300331.
- [52] M. E. Compeán-Jasso, F. Ruiz, J. R. Martínez, and A. Herrera-Gómez, “Magnetic properties of magnetite nanoparticles synthesized by forced hydrolysis,” *Mater. Lett.*, vol. 62, no. 27, pp. 4248–4250, 2008, doi: 10.1016/j.matlet.2008.06.053.
- [53] B. Li, H. Fan, Q. Zhao, and C. Wang, “Synthesis, characterization and cytotoxicity of novel multifunctional  $\text{Fe}_3\text{O}_4@\text{SiO}_2@\text{GdVO}_4:\text{Dy}^{3+}$  core-shell nanocomposite as a drug carrier,” *Materials (Basel)*, vol. 9, no. 3, pp. 3–9, 2016, doi: 10.3390/ma9030149.
- [54] M. Bagherzadeh, B. Aslibeiki, and N. Aarsalani, “Preparation of  $\text{Fe}_3\text{O}_4$ /vine shoots derived activated carbon nanocomposite for improved removal of  $\text{Cr}(\text{VI})$  from aqueous solutions,” *Sci. Rep.*, vol. 13, no. 1, pp. 1–19, 2023, doi: 10.1038/s41598-023-31015-x.
- [55] S. F. Samakosh, A. Bahari, V. F. Hamidabadi, and H. M. Moghaddam, “Preparation and Characterization of Core@shell Structures of Glycerin@ $\text{Fe}_3\text{O}_4$ , and  $\text{Al}_2\text{O}_3@\text{Fe}_3\text{O}_4$  Nanoparticles for Use in Hyperthermia Therapy,” *Bionanoscience*, vol. 13, no. 4, pp. 2168–2179, 2023, doi: 10.1007/s12668-023-01202-1.
- [56] G. Rahimzadeh, M. Tajbakhsh, M. Daraie, and A. Ayati, “Heteropolyacid coupled with cyanoguanidine decorated magnetic chitosan as an efficient catalyst for the synthesis of pyranochromene derivatives,” *Sci. Rep.*, vol. 12, no. 1, pp. 1–12, 2022, doi: 10.1038/s41598-022-21196-2.
- [57] M. Rafique, S. Hajra, M. B. Tahir, S. S. A. Gillani, and M. Irshad, “A review on sources of heavy metals, their toxicity and removal technique using physico-chemical processes from wastewater,” *Environ. Sci. Pollut. Res.*, vol. 29, no. 11, pp. 16772–16781, 2022, doi: 10.1007/s11356-022-18638-9.
- [58] P. P. Mashile, G. P. Mashile, K. M. Dimpe, and P. N. Nomngongo,

- “Occurrence, quantification, and adsorptive removal of nodularin in seawater, wastewater and river water,” *Toxicon*, vol. 180, no. April, pp. 18–27, 2020, doi: 10.1016/j.toxicon.2020.03.009.
- [59] A. Skulcova, V. Majova, M. Kohutova, M. Grosik, J. Sima, and M. Jablonsky, “com UV/Vis Spectrometry as a Quantification Tool for Lignin Solubilized in Deep Eutectic Solvents,” vol. 12, no. 3, pp. 6713–6722, 2017.
- [60] A. Balakrishnan, S. Appunni, M. Chinthala, and D. V. N. Vo, “Biopolymer-supported TiO<sub>2</sub> as a sustainable photocatalyst for wastewater treatment: a review,” *Environ. Chem. Lett.*, vol. 20, no. 5, pp. 3071–3098, 2022, doi: 10.1007/s10311-022-01443-8.
- [61] M. Nasrollahzadeh, M. Sajjadi, S. Iravani, and R. S. Varma, “Starch, cellulose, pectin, gum, alginate, chitin and chitosan derived (nano)materials for sustainable water treatment: A review,” *Carbohydr. Polym.*, vol. 251, no. May 2020, p. 116986, 2021, doi: 10.1016/j.carbpol.2020.116986.
- [62] K. Thirugnanasambandham, V. Sivakumar, J. Prakash Maran, and S. Kandasamy, “Chitosan based grey wastewater treatment-A statistical design approach,” *Carbohydr. Polym.*, vol. 99, pp. 593–600, 2014, doi: 10.1016/j.carbpol.2013.08.058.
- [63] N. T. Abdel-Ghani, A. K. Hegazy, G. A. El-Chaghaby, and E. C. Lima, “Factorial experimental design for biosorption of iron and zinc using *Typha domingensis* phytomass,” *Desalination*, vol. 249, no. 1, pp. 343–347, 2009, doi: 10.1016/j.desal.2009.02.065.
- [64] M. L. Senovieski *et al.*, “In-syringe dispersive liquid-liquid microextraction vs . solid phase extraction : A comparative analysis for the liquid chromatographic determination of three neonicotinoids in cotyledons,” *Microchem. J.*, vol. 158, no. June, p. 105181, 2020, doi: 10.1016/j.microc.2020.105181.
- [65] N. Chamkasem, “Regulatory Science Analysis of Pesticides in Olive Oil Using a Modified QuEChERS Method with LC-MS / MS and GC-MS / MS,” pp. 16–35.
- [66] J. V. Dias, V. Cutillas, A. Lozano, I. R. Pizzutti, and A. R. Fernández-Alba,

- “Determination of pesticides in edible oils by liquid chromatography-tandem mass spectrometry employing new generation materials for dispersive solid phase extraction clean-up,” *J. Chromatogr. A*, vol. 1462, pp. 8–18, 2016, doi: 10.1016/j.chroma.2016.07.072.
- [67] C. Anagnostopoulos and G. E. Miliadis, “Talenta Development and validation of an easy multiresidue method for the determination of multiclass pesticide residues using GC – MS / MS and LC – MS / MS in olive oil and olives,” *Talanta*, vol. 112, pp. 1–10, 2013, doi: 10.1016/j.talanta.2013.03.051.
- [68] A. Angioni, L. Porcu, and F. Pirisi, “LC/DAD/ESI/MS method for the determination of imidacloprid, thiacloprid, and spinosad in olives and olive oil after field treatment,” *J. Agric. Food Chem.*, vol. 59, no. 20, pp. 11359–11366, 2011, doi: 10.1021/jf2028363.
- [69] D. Moreno-González, J. Alcántara-Durán, S. M. Addona, and M. Beneito-Cambra, “Multi-residue pesticide analysis in virgin olive oil by nanoflow liquid chromatography high resolution mass spectrometry,” *J. Chromatogr. A*, vol. 1562, pp. 27–35, 2018, doi: 10.1016/j.chroma.2018.05.053.
- [70] N. Dujaković, S. Grujić, M. Radišić, T. Vasiljević, and M. Laušević, “Determination of pesticides in surface and ground waters by liquid chromatography-electrospray-tandem mass spectrometry,” *Anal. Chim. Acta*, vol. 678, no. 1, pp. 63–72, 2010, doi: 10.1016/j.aca.2010.08.016.
- [71] Y. A. Kim *et al.*, “Method development, matrix effect, and risk assessment of 49 multiclass pesticides in kiwifruit using liquid chromatography coupled to tandem mass spectrometry,” *J. Chromatogr. B Anal. Technol. Biomed. Life Sci.*, vol. 1076, no. January, pp. 130–138, 2018, doi: 10.1016/j.jchromb.2018.01.015.
- [72] M. Farouk, L. A. E. A. Hussein, and N. F. El Azab, “Simultaneous determination of three neonicotinoid insecticide residues and their metabolite in cucumbers and soil by QuEChERS clean up and liquid chromatography with diode-array detection,” *Anal. Methods*, vol. 8, no. 23, pp. 4563–4575, 2016, doi: 10.1039/c6ay01161f.
- [73] C. Yang, L. Ran, M. Xu, D. Ren, and L. Yi, “In situ ionic liquid dispersive liquid–

- liquid microextraction combined with ultra high performance liquid chromatography for determination of neonicotinoid insecticides in honey samples,” *J. Sep. Sci.*, vol. 42, no. 10, pp. 1930–1937, 2019, doi: 10.1002/jssc.201801263.
- [74] P. Justyna, H. M. Mohamed, A. Kurowska-susdorf, R. Dewani, M. Y. Fares, and V. Andruch, “ScienceDirect Green analytical chemistry as an integral part of sustainable education development,” 2021, doi: 10.1016/j.cogsc.2021.100508.
- [75] M. Espino, M. D. L. Á. Fernández, F. J. V Gomez, and M. F. Silva, “Trends in Analytical Chemistry Natural designer solvents for greening analytical chemistry,” vol. 76, pp. 126–136, 2016, doi: 10.1016/j.trac.2015.11.006.
- [76] Z. Ju, J. Fan, Z. Meng, R. Lu, H. Gao, and W. Zhou, “A high-throughput semi-automated dispersive liquid–liquid microextraction based on deep eutectic solvent for the determination of neonicotinoid pesticides in edible oils,” *Microchem. J.*, vol. 185, no. November 2022, p. 108193, 2023, doi: 10.1016/j.microc.2022.108193.
- [77] L. Carbonell-Rozas, R. Canales, F. J. Lara, A. M. García-Campaña, and M. F. Silva, “A natural deep eutectic solvent as a novel dispersive solvent in dispersive liquid-liquid microextraction based on solidification of floating organic droplet for the determination of pesticide residues,” *Anal. Bioanal. Chem.*, vol. 413, no. 25, pp. 6413–6424, 2021, doi: 10.1007/s00216-021-03605-z.
- [78] D. Moema, T. Makwakwa, H. N. Nyambaka, S. Dube, and M. Nindi, “Method Development and Optimization of Liquid-Liquid Microextraction Based on the Decomposition of Deep Eutectic Solvent for the Determination of Chromium (VI) in Spinach: Assessment of the Greenness Profile Using Eco-scale, AGREE, and AGREEprep,” *Food Anal. Methods*, no. 0123456789, 2024, doi: 10.1007/s12161-024-02583-z.



### **Development of a greener dispersive liquid-liquid microextraction method for determination of selected neonicotinoid pesticides in vegetable oils.**

#### **ABSTRACT**

The development of extraction methods using green solvents has received attention from many researchers. Therefore, this study describes the development of the dispersive liquid-liquid microextraction (DLLME) method using deep eutectic solvents (DES), which are known as green solvents. The DES was synthesised by mixing hydrogen bond donor (HBD) and hydrogen bond acceptor (HBA), thereafter characterised using Fourier transform infrared spectroscopy (FTIR) and nuclear magnetic resonance spectroscopy (NMR). Furthermore, DES was applied for preconcentration and extraction of the selected neonicotinoid pesticides (NEOs) (acetamiprid, imidacloprid, thiacloprid and thiamethoxam in vegetable oils followed by quantification using high performance liquid chromatography coupled with diode array detector (HPLC-DAD). The DES mixture that resulted in the highest extraction recovery was Choline chloride with ethylene glycol (CCl:EG). Then, the most influential parameters affecting the DES-DLLME method for extracting NEOs were examined using a multivariate optimization approach. Screening was done with full factorial design (FFD) wherein the significant and insignificant parameters and their interactions were reported on the Pareto chart. For response surface methodology, the significant parameters were used for further optimization with central composite design (CCD). Moreover, the results from CCD for method performance in terms of the relationship between the parameters were displayed on 3D surface plots format. The method showed good limits of detection (LOD) ranging from 0.4 -4.95 ng.  $\mu\text{L}^{-1}$  and limits of quantification (LOQ) ranging from 1.43-9.7 ng.  $\mu\text{L}^{-1}$ . The method has proved to show good accuracy (79-119.58 %) and precision (0.1 to 0.9 %). Method greenness was studied using the Analytical GREENess calculator (AGREE) in full tool and it has shown that the developed method is greener with a value of 0.67. The method showed good preconcentration factors (39.33-118.18). Lastly, the developed method was applied in real samples.

**Keywords:** Neonicotinoid pesticides, AGREE, deep eutectic solvent (DES), optimization, characterization, HPLC-DAD, hydrogen bond donor (HBD), hydrogen bond acceptor (HBA)

#### 4.1. Background

Neonicotinoid pesticides have been used worldwide in the agricultural sector. They have been used to control pest infestation, weed control and infectious disease breakout prevention [1]. Vegetable oils are oils that have been produced from the oil seed crops. Concerns regarding human health and food safety has increased over the years [2]. The contamination of vegetable oils with NEOs residue is mostly influenced by the coextracted lipids and nutrients [3]. These trace amounts of NEOs in vegetable oils have contributed to adverse health effects in humans. Hence, there was a need to monitor the level of contaminated vegetable oil with these pesticides. The NEOs toxicity in humans affects the development of the reproductive system. They interfere with the endocrine system and damage the brain and human nervous system [4]. Since the health defects have been detected, there has been a set limit of their daily intake set by different organizations in different countries, and some countries have restricted their use [5]. The maximum residue limit (MRL) for Japan in oil seeds is 0.04 mg.kg<sup>-1</sup>, in China is 0.05-0.5 mg.kg<sup>-1</sup> and in the U.S. is 0.05-3.5 mg.kg<sup>-1</sup> [6].

Due to these NEOs' toxicity, there has been a need to monitor their presence in vegetable oils. A wide range of quantification techniques like liquid chromatography (LC), high-performance liquid chromatography (HPLC) and gas chromatography (GC) have been reported for the determination of the neonicotinoid pesticides (NEOs) in different samples for monitoring purposes [7][8]. Due to the NEOs' low volatility and high polarity, they are unsuitable for analysis using gas chromatography (GC) [9]. HPLC has been a preferred technique for the analysis of NEOs. Furthermore, the use of HPLC coupled with different detectors such as fluorescence (FLD), diode array detector (DAD), triple quadrupole tandem mass spectrometry (MS/MS), ultraviolet (UV) and mass spectrometry (MS) have been reported in many studies[10] [11]. However, the DAD and MS/MS have been among the most reported detection techniques. The two most preferred detectors have advantages; DAD's advantage is its low cost and high availability, whereas the advantages of MS/MS are the identification and confirmation of the analytes [12].

Since the samples cannot be analysed directly, there's a need for sample preparation [13]. Different sample preparation methods have been studied and reported. NEO residue analysis is often performed in some pretreatment steps, including preconcentration, solvent extraction and sample cleanup [14]. Although the cleanup step may not be accurate due to the loss of some analytes with additional labour and cost-effectiveness, it can also lead to poor data quality [15]. Different sample preparation methods have been reported, of which the traditional extraction methods that have been studied over the years are mostly solid phase extraction (SPE) and liquid-liquid extraction (LLE) [16]. A wide range of derivatives of these traditional methods have been developed and reported by many researchers over the years [17]. The development of these methods derivatives was to help overcome their disadvantages, which involved the use of large amounts of organic solvents, the cost-effectiveness of the method, and its tediousness. They produced a large amount of waste containing trace levels of the analytes of interest [18]. Some of the reported extraction methods are solid-phase micro-extraction (SPME), Quick, easy, cheap, effective, rugged, and safe (QuEChERS), Hollow-fiber liquid-phase microextraction (HF-LPME), Dispersive liquid-liquid microextraction based (DLLME), Dispersive micro solid-phase extraction (D- $\mu$ -SPE) and Matrix solid-phase dispersion (MSPD) [19][20][21][22]. These reported methods provide several advantages such simplicity, greenness, convenience, high enrichment factor, reliability, repeatability, cost effectiveness, and less use of adsorbent and organic solvents [23]. For this study, the DLLME method was used because of its easy, quick, and solvent-efficient operation, environmental friendliness, and high throughput [24]. A wide range of methods derived from DLLME have been reported, and some include air-assisted liquid-liquid microextraction (AA-LLME) vortex, assisted liquid-liquid microextraction (VA-LLME) and ultrasound-assisted liquid-liquid microextraction (UA-LLME) [25]. The advantages of these methods are their environmental friendliness, suitability to green chemistry, and use of small organic solvents volume while generating less waste [26]. Extractants and dispersants are factors determining extraction efficiency of DLLME method. Additionally, dispersants are synthesized using green extraction technologies using physical dispersion techniques like vortexing and ultrasonication from conventional organic solvents [27]. New trends of using environmental-friendly green solvents in DLLME have garnered interest of many researchers. Currently, deep eutectic solvents (DESs) and ionic liquids are the green extractants that have been utilised in DLLME

[28]. Hydrogen bond donors (HBD) and hydrogen bond acceptors (HBA) having lower melting temperatures than any of their constituent parts are combined to create the DESs [29]. The DESs are comparable to ionic liquids in terms of their chemical and physical characteristics, including their good solubility for both organic and inorganic compounds, non-flammability, and comparatively broad liquid range [30]. DESs are less toxic and more biodegradable than ionic liquids, and they are also easier to synthesise.

A DLLME method, using choline chloride (HBA) with ethylene glycol (HBD) at a 1:2 ratio (CCl:EG) as the extractant, was developed [31]. The synthesised DES was characterized using Fourier transform infrared spectroscopy (FTIR) and nuclear magnetic resonance spectroscopy (NMR). A multivariate approach was followed using the design of the experiment (DoE) from the chemometric tool. The screening was done using full factorial design (FFD) from DoE, followed by further optimization of the significant parameters with response surface methodology (RSM) following the central composite design (CCD) approach. Therefore, this project aims to develop a simple, greener and efficient extraction method for the determination of selected NEOs (acetamiprid, imidacloprid, thiacloprid and thiamethoxam) in vegetable oils followed by HPLC-DAD analysis.

## **4.2. Experimental procedure**

### **4.2.1. Reagents, materials, and samples**

All the standards, solvents and reagents were purchased from Merck South Africa, organic standards for neonicotinoid pesticides acetamiprid, imidacloprid, thiacloprid and thiamethoxam purchased were of higher grade. Acetonitrile HPLC grade, dichloromethane, methanol HPLC grade, chloroform, sodium hydroxide, hydrochloric acid, n-hexane, choline chloride, ethylene glycol, levulinic acid, urea, formic acid.

Avocado, canola, olive, and sunflower oils were purchased at a local supermarket in South Africa, Johannesburg Roodepoort Florida Park and stored at room temperature.

#### **4.2.2. High performance liquid chromatography coupled with diode array detector (HPLC-DAD) instrumentation.**

A Hewlett-Packard 1090 II liquid chromatograph equipped with a DAD Agilent 1260 Infinity high-pressure liquid chromatography (HPLC) system procured from Agilent Technologies (Waldbronn, Germany) was used for separation and determination of NEOs analytes of interest. The chromatographic system consisted of a degasser unit, binary pump, autosampler, auto-injector and thermostatic column compartment. The chromatographic column that was kept at 30 °C was Waters Xterra® C18 3.5 µm 4.6 × 150 mm column obtained from Waters Corporation (Milford, MA, United States). The chromatographic separation was achieved under gradient elution. The chromatograms were recorded at 255 nm and 260 nm for acetamiprid, imidacloprid, thiacloprid and thiamethoxam. Two mobile phases were prepared. Mobile phase A comprised 0.1 % formic acid (FA) in ultrapure water, while mobile phase B was 100 % acetonitrile using a gradient elution system at a flow rate of 1.0 mL.min<sup>-1</sup> and injection volume of 10 µL. Gradient elution setup was as follows: initial time 0 min 65 % A:35 % B, 2 min 75 % A:25 % B, 2:50 min 55 % A:45 % B and at 4:30 min, it returns to the initial elution of 65 % A:35 % B [1].

#### **4.2.3. Preparation calibration standards**

The standard mix solution consisting of all four different NEOs was prepared in acetonitrile on a 10 mL volumetric flask and stored in a refrigerator at 4 °C. different calibration standards were also prepared at ten different concentrations (8-1000 ng.g<sup>-1</sup>). Appearance of the analytes on the chromatogram for different NEOs investigated. The peak at 2.11 min is thiamethoxam (TMX), at 2.3 min is acetamiprid (ACT), at 2.43 min is imidacloprid (IMI) and at 3.1 min is thiacloprid (TCL). Preparation was done with some slight modifications to suit the instrument, solvent type and the type of analytes [32].

#### **4.2.4. Cleaning of glassware.**

All the glassware (beakers, volumetric flasks, conical flasks, measuring cylinders, sample vials, spatula) were washed with soap and water. Additionally rinsed with distilled water and dried in the oven at 110 °C for an hour. After each experimental use, the glassware was washed with water and soap, rinsed with distilled water and

soaked in acetone bath. After soaking for overnight, they were then dried in the oven at 90 °C for 30 min.

#### **4.2.5. Synthesis of deep eutectic solvents (DESs)**

Recently, the majority of innovative research developments on microextraction techniques has focused on substituting ecologically benign organic solvents such as ionic liquids, supramolecular solvents, and deep eutectic solvents (DESs) for harmful organic ones [33].

Moreover, it is worth to note that because of their impressive qualities, which include ease of synthesis, affordability, low volatility, high biodegradability, and structural design feasibility, DESs are recognised as new generation green solvents [34]. A suitable mixture of a hydrogen bond donor (HBD) and hydrogen bond acceptor (HBA) is usually used to create a DES [35]. Since the combined mixture's melting point is lower than that of its constituent parts, it is liquid at room temperature. The drop in melting point is caused by hydrogen bonds forming between the components of DES [36]. Choline chloride (CCl) combined with several HBDs urea, ethylene glycol, and glycerol being the most often used is the basis for the most common DESs; however, other alcohols, amino acids, carboxylic acids, and sugars have also been employed [37]. DESs have the potential to replace the application of traditional organic solvents in separation and extraction procedures because of their distinct physicochemical properties [38]. Even though DESs may form hydrogen bonds, they are often hydrophilic, which limits their use as extraction solvents in aqueous materials [39]. As a result, the majority of applications have concentrated on the extraction of naturally occurring chemicals from organic solids (plants and foods) and liquid samples (mostly vegetable oils) [40]. In addition to its adjustable solvent characteristics, the DES are very effective at extracting various chemical classes of substances. DESs were prepared by mixing CCl (HBA) with HBD (ethylene glycol (EG), levulinic acid (LA), or urea) at a constant molar ratio of (HBA)1:2 (HBD) in screw-capped bottles. The various DES mixtures were prepared in a 50 mL centrifuge tube with a screw cap. The calculations were done using the mole ratio of 1:2 along with the molar mass of each reagent used for preparation of these DESs. The mixture was agitated at 80 °C for 2 hrs until a clear liquid was formed [41]. Three different types of DESs (**DES 1:** Ethylene glycol with choline chloride, **DES 2:** Levulinic acid with choline chloride and **DES 3:**

Urea with choline chloride) were synthesised and studied for their efficiency on extracting the NEOs from the vegetable oils.

### 4.3. Characterization of deep eutectic solvents

#### 4.3.1. *Fourier transform infrared spectrometer (FTIR)*

The FTIR instrument was used to study the chemical composition and quality of the sample of the synthesised DESs [42]. The FTIR characterization of the DES structure provides information about interactions and complexation between constituents [43]. The FTIR consists of five components: the source, the interferometer, the sample, the detector and the computer, as shown in **Figure 4.1** [44]. The Source: A luminous black-body source emits infrared radiation [45]. This beam travels through a hole that regulates the energy directed towards the sample and, eventually, the detector [46]. The Interferometer: The "spectral encoding" occurs when the beam enters the interferometer [47]. The interferometer then releases all of the generated interferogram signals [48]. The Sample: Depending on the kind of analysis being carried out, the beam either transmits through or reflects off the surface of the sample when it enters the sample compartment [49]. This is the location of energy absorption for particular frequencies peculiar to the sample [50]. The Detector: For the last measurement, the beam eventually reaches the detector [51]. Specially constructed detectors measure the unique interferogram signal. The Computer: After the signal has been measured and digitalized, it is passed to the computer to perform the Fourier transformation [52]. The wavenumber range used was from 500-4500  $\text{cm}^{-1}$ . However, before the real analysis of the materials, a background scan was done because there was a need for a relative scale for the absorption intensity. The background scan is the measurement with no sample in the beam. The background scan can be compared with the sample scan to determine percentage transmittance. The model used was Fourier transform infrared (FTIR) spectrometer (Vertex 70 model, Bruker Optic GmbH, Hamburg, Germany).

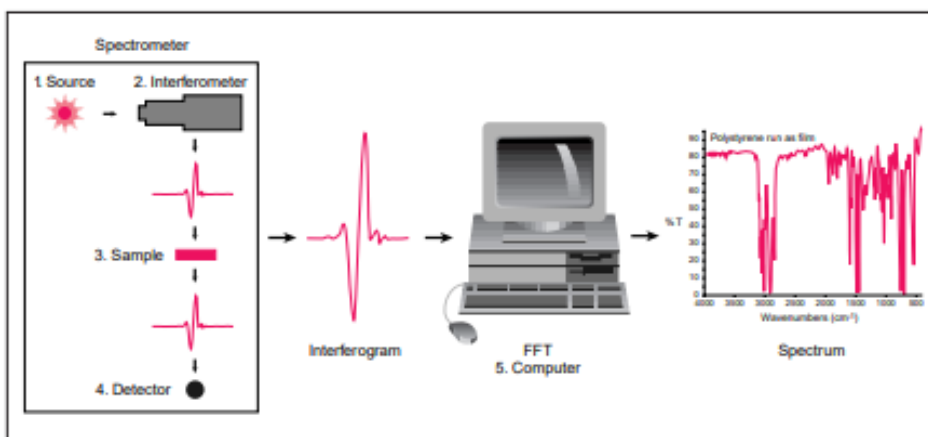


**Figure 4. 1:** Fourier transform infrared spectrometer instrument [53] .

#### 4.3.2. Nuclear magnetic resonance spectrometer (NMR)

NMR spectroscopic techniques have evaluated the molecular structure of three ternary DESs, composed of choline chloride, urea, ethylene glycol, and levulinic acid. NMR spectrometers are akin to a radio station and a recording studio [54]. The primary results of NMR techniques are the molecular compound's hydrogen and carbon atoms. This instrument provides the number of magnetically distinct atoms under study, while the sorts of functional groups present in a molecule are revealed by infrared (IR) spectroscopy. [55]. For example, studying hydrogen nuclei (protons) can provide information about the nature of each type's immediate environment and the quantity of each of the many types of hydrogen nuclei [56].

The carbon nuclei can be found to have comparable information. IR and NMR measurements are frequently enough to identify an unknown chemical's structure fully. High-energy radio frequency (RF) pulses of particular lengths are delivered into the sample (radio station), which is positioned inside a probe inside the magnet [57]. The receiver coil then gathers the tiny currents, amplifies them, and digitises them into a signal (recording studio) prepared for post-collection processing [58]. **Figure 4.2** shows the NMR instrument setup.



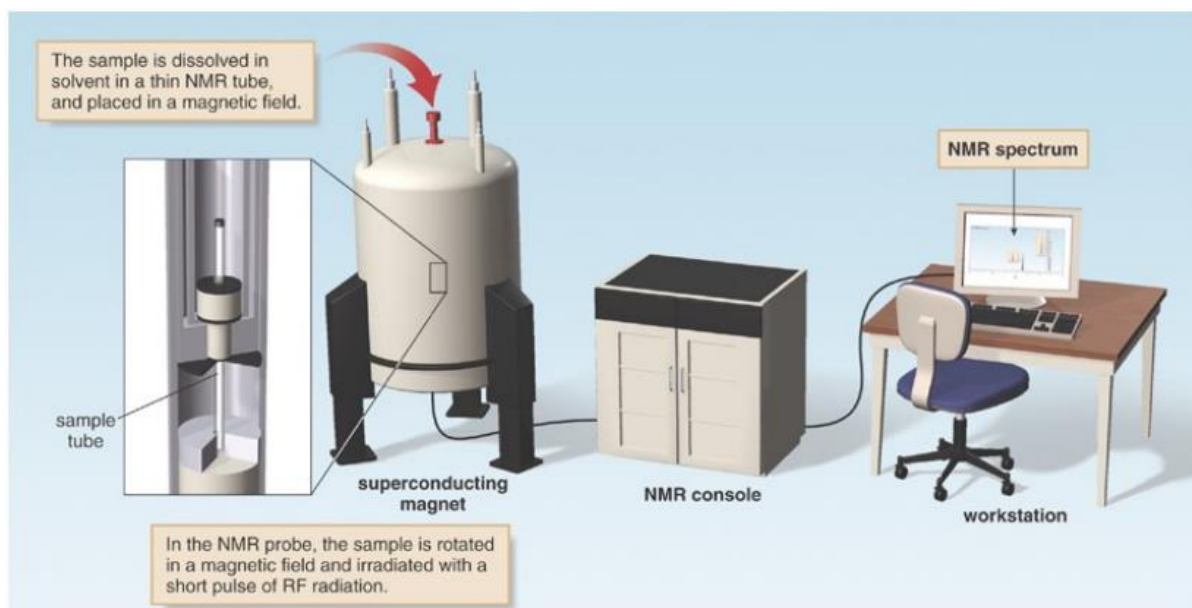


**Figure 4. 2:** Nuclear magnetic resonance spectroscopy instrument [59].

#### 4.4. Preparation of vegetable oil samples

Vegetable oil was prepared in a ratio of 1:4 with n-hexane and vortexed for 5 min to disperse the analytes before extraction [60].

#### 4.5. Dispersive liquid-liquid microextraction method

A 5 mL of prepared vegetable oil with n-hexane ratio at a ratio of 1:4 was ready in a 10 mL centrifuge tube with a closed cap, then a known volume of 1.1 mL of DES was added, followed by spiking with a known concentration of the standard. After spiking, the sample solution was vortexed. After that, the supernatant was discarded, and the DES remained at the bottom of the centrifuge tube. Additionally, acetonitrile was added to the centrifuge tube containing DES at the bottom, the cap was closed, and the tube was vortexed again, respectively. Lastly, the DES solution was collected with a syringe, transferred in a glass vial, and taken for analysis to an HPLC-DAD.

**Figure 4.3** is a schematic representation of the developed method [6].

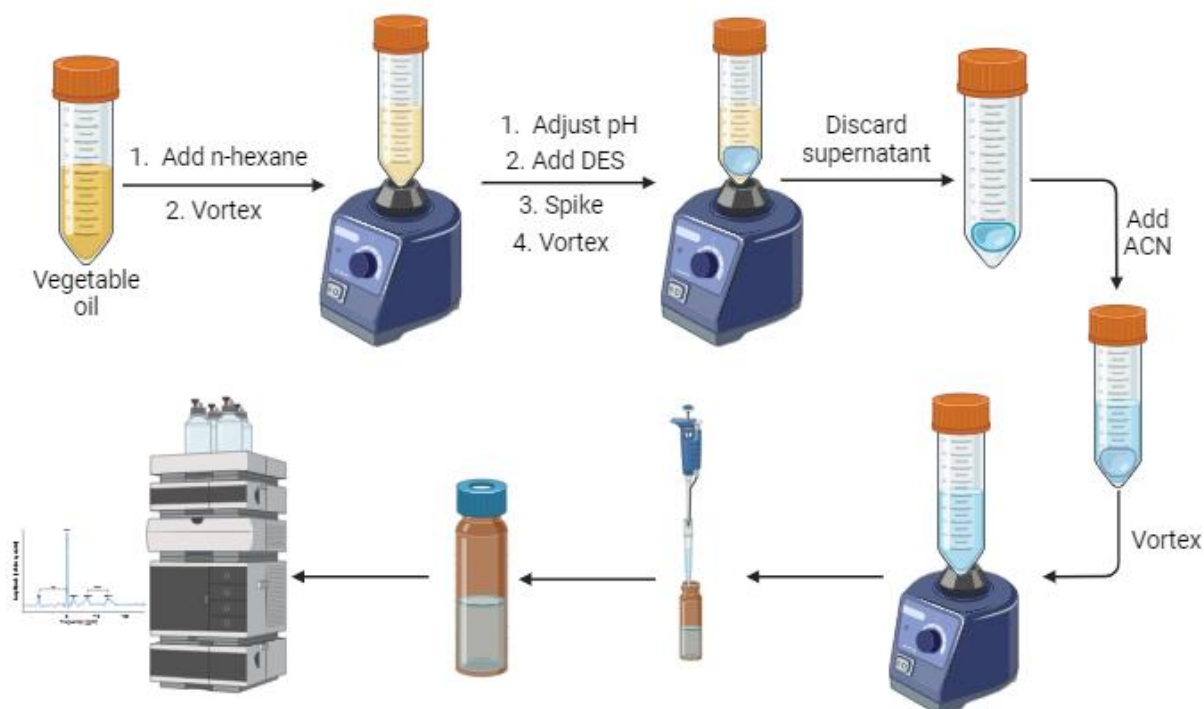


**Figure 4. 3:** General representation of DES-DLLME method

## 4.6. Optimization

### 4.6.1. Univariate optimization

The univariate approach was used to optimize the three parameters: DES type, eluting solvent and sample volume. The preconcentration procedure (DES-DLLME) followed was reported by Ju et al. (2023) and it is illustrated in **Figure 4.3** [60]. The sample volumes of 1,3,5, and 7 mL of vegetable oil were dispersed in 4 mL of n-hexane by vortexing for 5 min. After 5 min, an 1100  $\mu\text{L}$  volume of DES was added and spiked with a known concentration of  $8 \text{ ng}\cdot\mu\text{L}^{-1}$  the analytical standard for the NEOs and then vortexed for 4 min. Spiking was done due to the absence of certified reference material (CRM). The n-hexane dispersant is significant due to its impact on formation of the droplets and contact between the droplets and the analytes. It is worth noting that, this dispersant shortens extraction time, increases efficiency, low toxicity and low running cost.

Furthermore, after preconcentration, the supernatant was discarded, and the DES was redispersed in 1000  $\mu\text{L}$  eluting solvent and vortexed again for 2 min to redisperse the analytes. Thereafter, the redispersed DES was collected with a micropipette from a centrifuge tube to an amber glass vial and closed with a screw

cap. Finally, the collected analytes in the amber screw cap vial were taken for analysis by an HPLC-DAD.

#### **4.6.2. Multivariate optimization**

For multivariate optimization, a chemometric tool was used for experimental design. A multivariate approach was selected since it can optimize several parameters simultaneously, unlike the univariate approach. The multivariate approach followed a procedure shown in **Figure 4.3** above. The first step of the multivariate approach was screening the parameters following the two-level full factorial design. A response surface methodology was used to further optimize the most influential parameters.

#### **4.6.3. Full factorial design (FFD)**

For screening, a total of 5 parameters were studied. During FFD a total of 16 experiments were generated by the chemometric tool as shown in **Appendix TS3**. All five parameters were investigated simultaneously, and their performance were reported in Pareto charts. The parameters were DES volume, extraction time, pH, eluent volume and eluting time and their minimum and maximum values are shown in **Table 4.1**. The sample volume was 1 mL of vegetable oil dispersed in 4 mL of n-hexane by vortexing for 5 min. After 5 min, a known volume of DES was added and spiked with a  $8 \text{ ng}\cdot\mu\text{L}^{-1}$  known amount of concentration of selected NEOs and then vortexed for a specific time as per the **Table 4.1**. Spiking was done due to the absence of certified reference material (CRM). Furthermore, after preconcentration and extraction, the supernatant was discarded, and the DES was redispersed in a known volume of eluting solvent and elution was done at a specified time as per **Table 4.1**. The redispersed DES was collected with a micropipette from a centrifuge tube to an amber glass vial, and the cap was closed. Finally, the collected analytes in the amber screw cap vial were taken for analysis by an HPLC-DAD.

The Pareto chart shows the significant and insignificant parameters. The Pareto charts are designed as horizontal bars with reference line (dotted red line) that guide on determining the significant and insignificant parameters. The parameters are important, while any horizontal bar below the reference line is considered insignificant.

**Table 4. 1:** FFD screening parameters

Parameters	Low (-)	High (+)
Extracting time (min)	2	7
pH	5	8
DES vol (ml)	0.5	1.1
Eluent vol (ml)	0.5	2
Eluting time (s)	20	60

#### **4.6.4. Response surface methodology**

For further optimization of significant parameters generated from FFD (DES vol, extraction time, eluent volume and eluting time), were used for DOE with response surface methodology (RSM). A total of 30 experiments were generated, and the results were communicated as 3D surface plots. The experiments were done in triplicates for precision and accuracy and the design of these experiment shown in **Appendix TS4**. The RSM experimental design is shown in **Table 4.2**. These experiments were conducted following the procedure on **Figure 4.2**. The sample volume was 1 mL of vegetable oil dispersed in 4 mL of n-hexane by vortexing for 5 min. After 5 min, a known volume of DES was added and spiked with a known amount of concentration and then vortexed for a specific time as per **Table 4.2**.

Furthermore, the supernatant was discarded after preconcentration, and the DES was redispersed in a known volume of eluting solvent. The elution was done at a specified time as per **Table 4.2**. The redispersed DES was collected with a microfilter from a centrifuge tube to an amber glass vial, and the cap was closed. Finally, the collected analytes in the amber screw cap vial were taken for analysis to an HPLC-DAD. After response surface methodology the method was validated by calculating several analytical figures of merits (LOD, LOQ, % R, % RSD, SD, ME and mean) using

the equations shown below. The accuracy of the average of the data is gauged by the relative standard deviation, or RSD. The percentage of the known amount of an analyte carried through the sample extraction and processing stages of the technique that represents the extraction efficiency of an analytical process is referred to as the accuracy, also known as extraction recovery (% R). The lowest concentration that the method can detect is known as the limit of detection, or LOD. The lowest concentration at which an analyte may be reliably recognised while still satisfying a set of predefined criteria for bias and imprecision is known as the limit of quantification, or LOQ. The co-eluting compound's capacity to either promote or suppress the sample analytes is known as matrix effects, or ME.

**Limit of detection (LOD) [61]**

$$LOD = \frac{3 \times [Conc]}{S/N} \quad \text{equation 4. 1}$$

**Limit of quantification (LOQ) [62]**

$$LOQ = \frac{10 \times [Conc]}{S/N} \quad \text{equation 4. 2}$$

**Percentage relative standard deviation (%RSD) [63]**

$$\%RSD = \frac{SD}{Mean} \times 100 \quad \text{equation 4. 3}$$

**Standard deviation [64]**

$$\sigma = \sqrt{\frac{\sum_{i=1}^N (x_i - \bar{x})^2}{N - 1}} \quad \text{equation 4. 4}$$

**Mean average [65]**

$$\bar{x} = \frac{x_1 + x_2 + \dots + x_n}{n} \quad \text{equation 4. 5}$$

### Extraction recoveries [66]

$$\%R = \frac{V_f \times c_f}{V_i \times C_i} \times 100 \quad \text{equation 4. 6}$$

### Matrix effects[67]

$$\text{ME}(\%) = \left( \frac{\text{Slope of analytical curve in matrix}}{\text{Slope of analytical curve in acetonitrile}} - 1 \right) \times 100 \quad \text{equation 4. 7}$$

**Table 4. 2:** Response surface methodology parameters

Parameters	Low (-)	Central point	High (+)
DES vol (ml)	0.2	0.8	1.4
Extraction time (min)	2	4.5	9.5
Eluent vol (ml)	0.5	1.25	2
Eluting time (s)	20	40	80

## 4.7. Results and discussion

### 4.7.1. Characterization

#### 4.7.1.1. Fourier transform infrared spectrometer.

The high temperature during the synthesis of the DES elicits the formation of the hydrogen bond that binds the chloride of the HBA with the hydrogen of the HBD. The results are well presented in **Table 4.2**. From the spectrum in **Figure 4.4 (a)**, at a region of  $3250 \text{ cm}^{-1}$ , the -OH group forms a broad stretch from the ethylene glycol structure. From spectrum **Figure 4.4 (c)** at  $3255 \text{ cm}^{-1}$ , there is a broad stretch with an observable increase in wavenumber due to the vibrational stretching of the -OH group, resulting in the formation of DES 1. The low-level water, such as that absorbed during

preparation and handling, does not significantly perturb the DES structure but alters the intermolecular interaction strength. Furthermore, this observable shift to a higher wavenumber was subject to interaction from hydrogen bonds that exist between molecules of ethylene glycol and choline chloride. The band at 2900  $\text{cm}^{-1}$  **Figure 4.4 (c)** refers to the C-H stretching. The band at 1500  $\text{cm}^{-1}$  to the  $-\text{CH}_2$  bending of an alkyl group, and the band at 1085  $\text{cm}^{-1}$  is attributed to C-O stretching, a band at 1004  $\text{cm}^{-1}$ , is attributed to C-C-O asymmetric stretching and a band at 820  $\text{cm}^{-1}$  attributes to C-C-O asymmetric stretching. Moreover, an additional characteristic band at 950  $\text{cm}^{-1}$  indicates the C-N<sup>+</sup> stretching CCl. These results have proved that EG mostly dominated DES 1. It is worth noting that the appearance of  $-\text{CH}_2$  peaks at 1500  $\text{cm}^{-1}$  is quite different for all **(a)**, **(b)** and **(c)** of which with **(c)** it is quite distinctive that it resembles the features of both (a) and **(b)** wherein the features of **(b)** are more distinctive. Moreover, the distinctiveness of the  $-\text{CH}_2$  peak at 1500  $\text{cm}^{-1}$  is supported by 1:2 mole ratio used during the synthesis process where **(a)** had higher ratio. The formation of DES 1 was through the electrostatic forces as well as H-bonding between ethylene glycol and choline chloride. These results were also corroborated by the literature reports [68].

**Table 4.2:** FTIR characterization for (a) ethylene glycol (EG), (b) choline chloride (CCl) and (c) DES 1

Functional group	Ethylene glycol	Choline chloride	DES 1
-OH	3250 $\text{cm}^{-1}$	3240 $\text{cm}^{-1}$	3255 $\text{cm}^{-1}$
C-H	2900 $\text{cm}^{-1}$	2999 $\text{cm}^{-1}$	2900 $\text{cm}^{-1}$
$-\text{CH}_2$	1500 $\text{cm}^{-1}$	1500 $\text{cm}^{-1}$	1500 $\text{cm}^{-1}$
C-O	1085 $\text{cm}^{-1}$	1086 $\text{cm}^{-1}$	1085 $\text{cm}^{-1}$
C-N	950 $\text{cm}^{-1}$	955 $\text{cm}^{-1}$	950 $\text{cm}^{-1}$

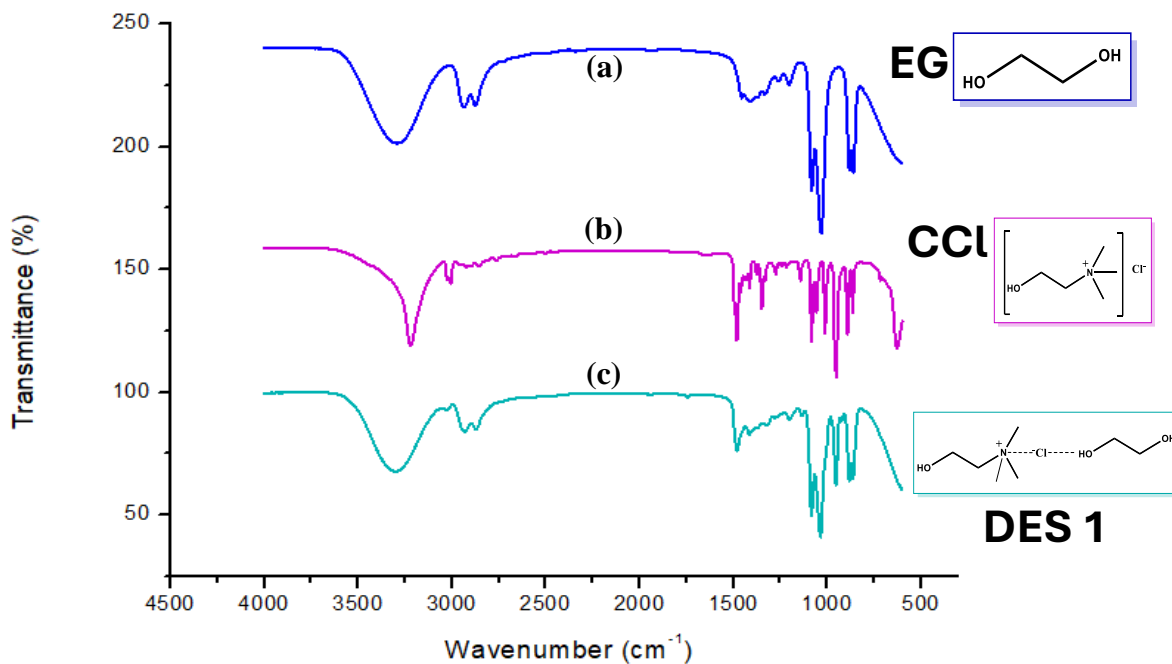


**Figure 4. 4:** Spectrum for DES 1 and its reagents. **(a)** ethylene glycol (EG), **(b)** choline chloride (CCI) and **(c)** DES 1.

These results are well presented in **Table 4.3**. For spectrum **Figure 4.5 (a)**, the vibrational band at  $3250\text{ cm}^{-1}$  represents the -OH group from CCI structure. The band at  $1500\text{ cm}^{-1}$  represents the -CH<sub>3</sub> group. The vibrational band at  $1400\text{ cm}^{-1}$  represents the -NH<sub>2</sub> group. From spectrum **Figure 4.5 (b)**, broad stretching at  $2999\text{ cm}^{-1}$  represents the -OH group from LA structure. The vibrational band at  $1700\text{ cm}^{-1}$  represents the C=O group aliphatic ketone. Furthermore, the  $1435\text{ cm}^{-1}$  and  $1200\text{ cm}^{-1}$  vibrational bands represent -C=O of the carbonyl compound. Spectrum **Figure 4.5 (b)** confirms its classification as a keto-acid. The vibrational bands in spectrum **Figure 4.5 (c)** at  $2999\text{ cm}^{-1}$  and  $1400\text{ cm}^{-1}$  indicate the presence of -CH<sub>3</sub> group. Moreover, the band at  $1698\text{ cm}^{-1}$  represents the C=O of the carbonyl compound. Additionally, the bands at  $1300\text{ cm}^{-1}$ , and  $1200\text{ cm}^{-1}$  represent the -C=O of the aliphatic ketone group. The band at around  $1100\text{ cm}^{-1}$  refers to an ester or ketone compound. Additionally, the shift in wavenumber on the spectrum **Figure 4.5 (c)** indicates the successful synthesis of DES 2. Strong hydrogen bond form higher surface tension which generally gets disturbed at high temperature due to increase in kinetic energy and decrease in cohesion forces which ultimately results in reduction of surface tension. Hydrogen bonding and alkyl chain are the crucial for the formation of DES 2. It is worth noting that the levulinic acid spectrum and DES 2 are more identical which



confirms that the 2-mole ratio of the levulinic acid over 1 mole ratio of choline chloride influenced this to a certain extent. Furthermore, DES 2 spectra has shown distinctive characteristics of both LA and CCI which confirms their reactivity. However, spectrum **Figure 4.5 (c)** also shows that LA mostly influenced DES 2. These results were also corroborated by what was reported in the literature [69].

**Table 4.3:** FTIR characterization for (a) Choline chloride (CCI), (b) Levulinic acid (LA) and (c) DES 2

Functional group	Levulinic acid	Choline chloride	DES 2
-OH	2999 $\text{cm}^{-1}$	3250 $\text{cm}^{-1}$	2999 $\text{cm}^{-1}$
-CH <sub>3</sub>	2900 $\text{cm}^{-1}$	1500 $\text{cm}^{-1}$	1400 $\text{cm}^{-1}$
-NH <sub>2</sub>		1400 $\text{cm}^{-1}$	1350 $\text{cm}^{-1}$
C=O	1700 $\text{cm}^{-1}$		1698 $\text{cm}^{-1}$

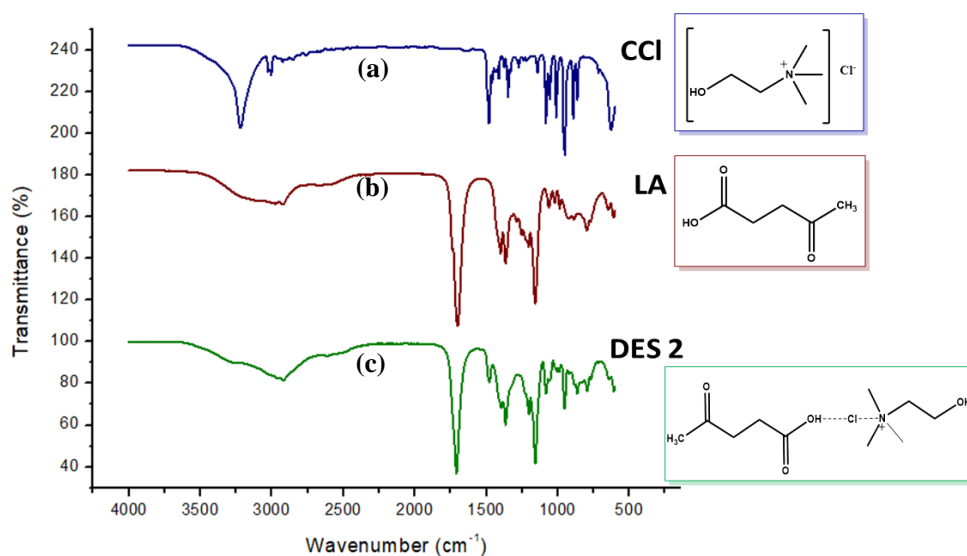


**Figure 4. 5:** Spectrum for DES 2 and its reagents; **(a)** choline chloride (CCI), **(b)** levulinic acid (LA) and **(c)** DES 2

The results are well summarised in **Table 4.3**. The stretching vibration bands in **Figure 4.6 (c)** at 3450  $\text{cm}^{-1}$  represent the -N-H symmetric and asymmetric stretching. At 3300-3450  $\text{cm}^{-1}$  is an -OH peak. The peak at 1650  $\text{cm}^{-1}$  represents the

C=O. A vibration band at 1470  $\text{cm}^{-1}$  represents the N-H group. Lastly, the peak at 1382  $\text{cm}^{-1}$  represents the C-N group on urea. From spectrum **Figure 4.6 (b)**, the vibrational band at 3330  $\text{cm}^{-1}$  represents the -OH group. The characteristic peak at 2999  $\text{cm}^{-1}$  represents a -CH<sub>3</sub> group. The vibrational peak at 1490  $\text{cm}^{-1}$  represents the -CH<sub>2</sub> bending. A peak at 950  $\text{cm}^{-1}$  represents the C-C stretching of the CCl. A broad stretching at around 3485  $\text{cm}^{-1}$  represents the -OH and N-H groups. During the synthesis process, the peak was deformed by the hydrogen bond interactions between urea and choline chloride.

Furthermore, spectrum **Figure 4.6 (a)** shows urea dominated more than choline chloride during the synthesis process. The vibrational peak at 1550  $\text{cm}^{-1}$  represents the C=O group, while the peak at 1400  $\text{cm}^{-1}$  represents the N-H group. The observable slight blue shift indicated the formation of the hydrogen bonds between the amino group of urea and chlorine of the choline chloride. These results were also corroborated by what was reported in the literature [70]. The appearance of the spectra for DES 3 and urea has proved to show that the 2-mole ratio of the urea had played a significant role between the bonding of choline chloride with urea. There are some significant identified peaks from choline chloride that does indicate its 1 mole ratio during the synthesis process of DES 3. Urea can form a liquid DES with CCl at room temperature, apparently due to their stronger ability to form hydrogen bond interactions with CCl.

**Table 4.4:** FTIR characterization for (a) DES 3, (b) Choline chloride (CCl) and (c) Urea

Functional group	Urea	Choline chloride	DES 3
-OH		3485 $\text{cm}^{-1}$	3330-3500 $\text{cm}^{-1}$
-NH	3450 $\text{cm}^{-1}$	3485 $\text{cm}^{-1}$	3445-3500 $\text{cm}^{-1}$
C-N	1382 $\text{cm}^{-1}$	1490 $\text{cm}^{-1}$	1385 $\text{cm}^{-1}$
-CH <sub>3</sub>		3000 $\text{cm}^{-1}$	
-CH <sub>2</sub>		1490 $\text{cm}^{-1}$	1490 $\text{cm}^{-1}$
C-C		950 $\text{cm}^{-1}$	949 $\text{cm}^{-1}$
C=O	1650 $\text{cm}^{-1}$		1650 $\text{cm}^{-1}$

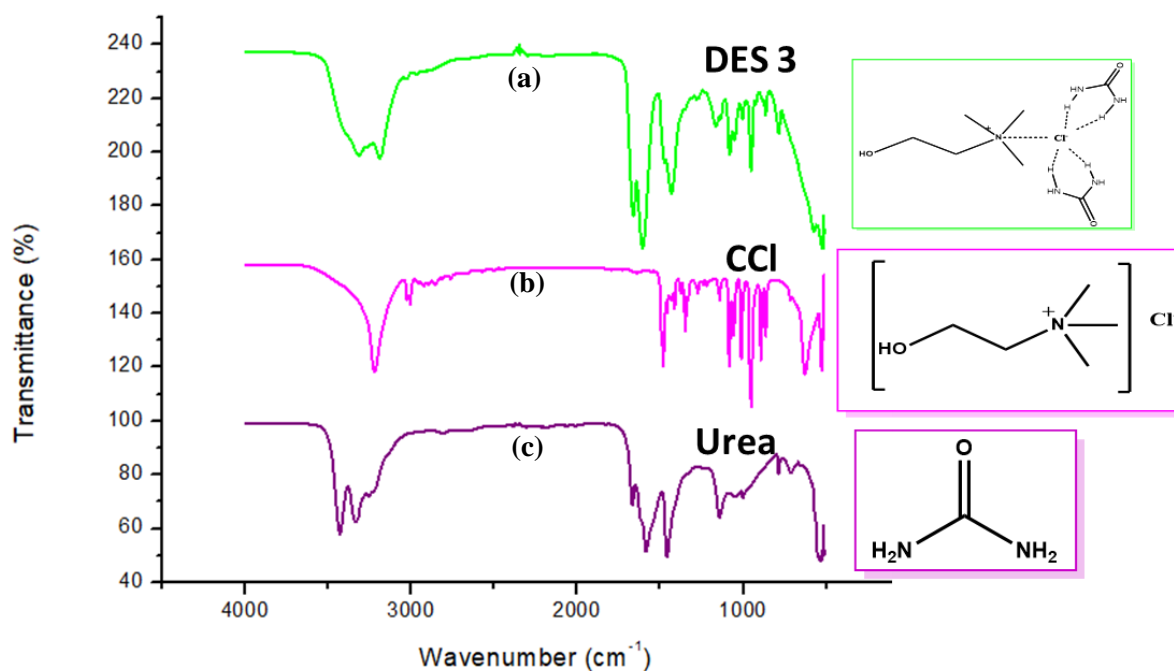


**Figure 4. 6:** Spectrum for DES 3 and its reagents; **(a)** DES 3, **(b)** choline chloride (CCI) and **(c)** Urea.

#### 4.7.1.2. Nuclear magnetic resonance (NMR) spectroscopy.

The samples were prepared in dimethyl sulfoxide-d<sub>6</sub> (DMSO) before analysis. The <sup>1</sup>H NMR and <sup>13</sup>C NMR spectra were recorded using Varian Mercury 300 MHz NMR spectrometer (Varian Inc., Palo Alto, CA, USA)

**Figure 4.7** shows the <sup>13</sup>C NMR of DES 1. All the carbons are well labelled from the structure on the NMR spectrum below. At a 67.27 ppm chemical shift ( $\delta$ ) of C<sub>2</sub>, a -CH<sub>2</sub> of CCI. At a chemical shift ( $\delta$ ) of 63.32 ppm are C<sub>3</sub> and C<sub>4</sub>, which are two -CH<sub>2</sub> bonded to group -OH from the EG. At a chemical shift ( $\delta$ ) of 55.35 ppm is C<sub>1</sub> representing a -CH<sub>2</sub> bonded to an -OH group. Lastly, at a chemical shift ( $\delta$ ) of 53.24 ppm is C<sub>5</sub> represents the three -CH<sub>3</sub> groups bonded to a nitrogen of the CCI. The <sup>13</sup>C NMR spectrum has confirmed all the carbons in the structure of DES 1, which shows that DES 1 was successfully synthesised, and the results are comparable with literature reports. It is worth noting that C<sub>1</sub> and C<sub>5</sub> were more shielded, while C<sub>2</sub>, C<sub>3</sub> and C<sub>4</sub> were less shielded [71].

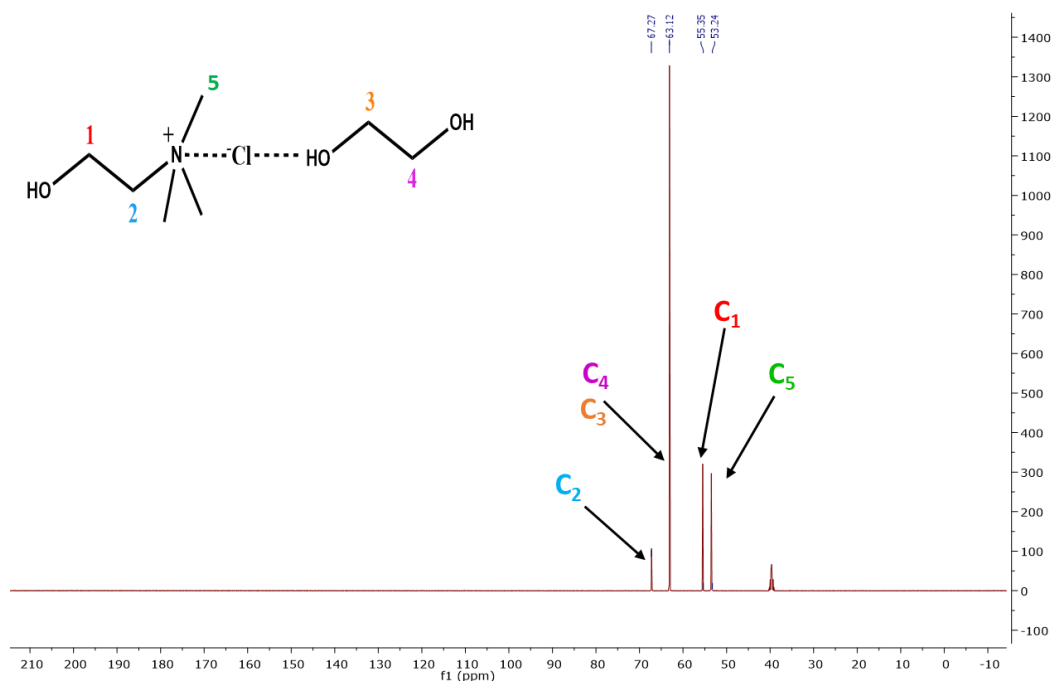


**Figure 4. 7: DES 1  $^{13}\text{C}$  NMR spectrum.**

**Figure 4.8** is  $^1\text{H}$  NMR shows all the hydrogens that make up DES 2 structure. The positions of all the hydrogen are well presented on the spectrum below along on their structure.  $\text{H}_c$  is a singlet at a chemical shift ( $\delta$ ) of 2.13 ppm because it has no neighbouring carbon to account for its multiplicity. At a chemical shift ( $\delta$ ) of 2.42 ppm is  $\text{H}_b$  from  $\text{CCl}$  which is supposed to be a multiplet since it is getting its multiplicity from the two neighbouring hydrogens,  $\text{H}_c$  and  $\text{H}_a$ . This might have been affected by moisture forming during the synthesis process. At a chemical shift ( $\delta$ ) of 2.68 ppm  $\text{H}_a$  from  $\text{CCl}$ , which has shown as a singlet, it was supposed to be a doublet of a triplet due to the neighbouring hydrogens from  $\text{H}_e$  and  $\text{H}_b$ . At a chemical shift ( $\delta$ ) of 3.22 ppm is  $\text{H}_d$ , a broad singlet that was supposed to be doublet due to the neighbouring  $\text{H}_f$ . A chemical shift ( $\delta$ ) of 3.51 ppm is for an  $-\text{OH}$  group on EG structure labelled  $\text{H}_f$ , which appears as a singlet, while it was supposed to be a triplet due to the neighbouring  $\text{H}_r$ . At a chemical shift, ( $\delta$ ) of 3.88 ppm is an  $-\text{OH}$  group from  $\text{CCl}$  labelled  $\text{H}_e$ , which appeared as a singlet while it was supposed to be a triplet, getting its multiplicity from  $\text{H}_a$ . All these observable changes in the appearance of the peaks are attributed to the presence of water that was formed as moisture during the synthesis process. The reported results are comparable with the literature [71].

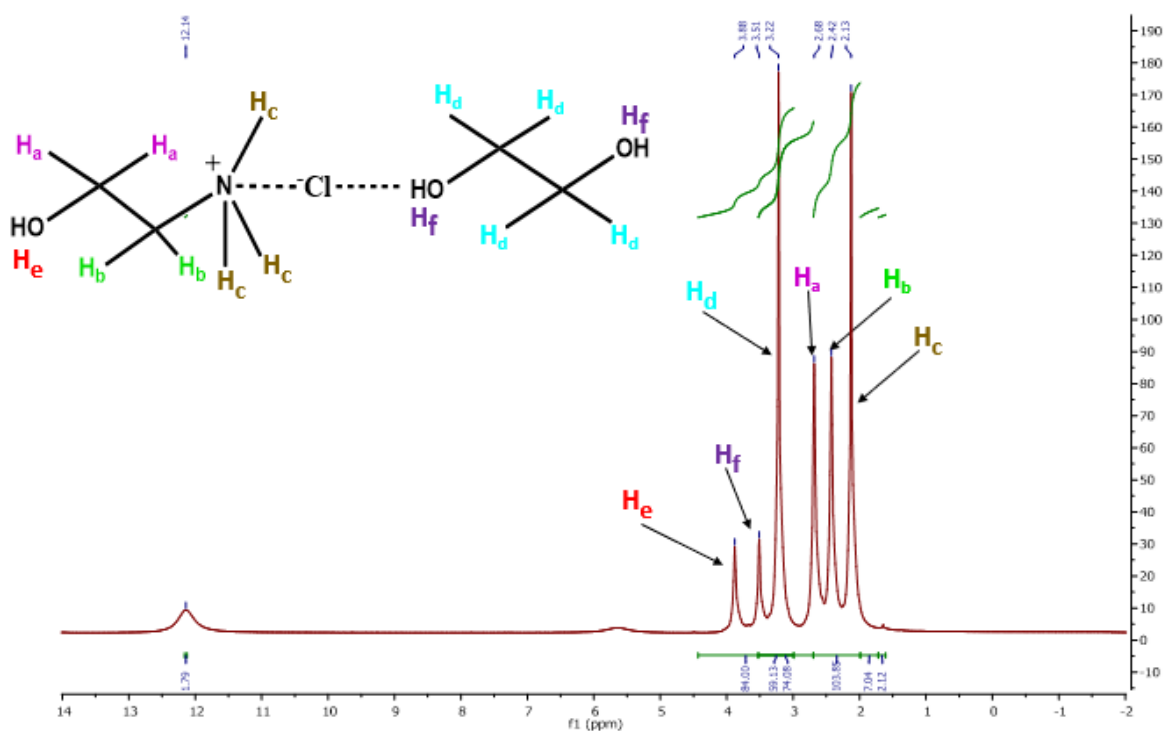


**Figure 4. 8:** Proton NMR for **DES 1**

The  $^{13}\text{C}$  NMR spectrum results for DES 2 are shown in **Figure 4.9**. From the figure below, a peak at 174.59 ppm represents  $\text{C}_1$ , a quaternary carbon of the  $-\text{CH}_3$  of the LA. At a chemical shift ( $\delta$ ) of 167.11 ppm is a  $\text{C}_8$ , carbonyl ( $-\text{C}=\text{O}$ ) carbon of the LA. At a chemical shift ( $\delta$ ) of 77.56 ppm is a  $\text{C}_5$ , another carbonyl ( $-\text{C}=\text{O}$ ) group from the LA. At 65.92 ppm, chemical shift ( $\delta$ ) is  $\text{C}_3$  and  $\text{C}_4$  from the LA compound. At 37.98 ppm is  $\text{C}_2$ , a carbonyl ( $-\text{C}=\text{O}$ ) bonded to a quaternary carbon of  $-\text{CH}_3$  from the LA. At 29.96 ppm is  $\text{C}_6$  is a  $-\text{CH}_2$  bonded to an N group. At 28.18 ppm is  $\text{C}_7$ , a  $-\text{CH}_2$  bonded to an H group. From the spectrum, it is worth noting that  $\text{C}_1$  and  $\text{C}_8$  were more deshielded, followed by  $\text{C}_2$ ,  $\text{C}_3$ ,  $\text{C}_4$  and  $\text{C}_5$ . Furthermore,  $\text{C}_6$  and  $\text{C}_7$  were more shielded from the spectrum. The results were comparable with the literature reports. This proves that DES 2 was successfully synthesised [72].

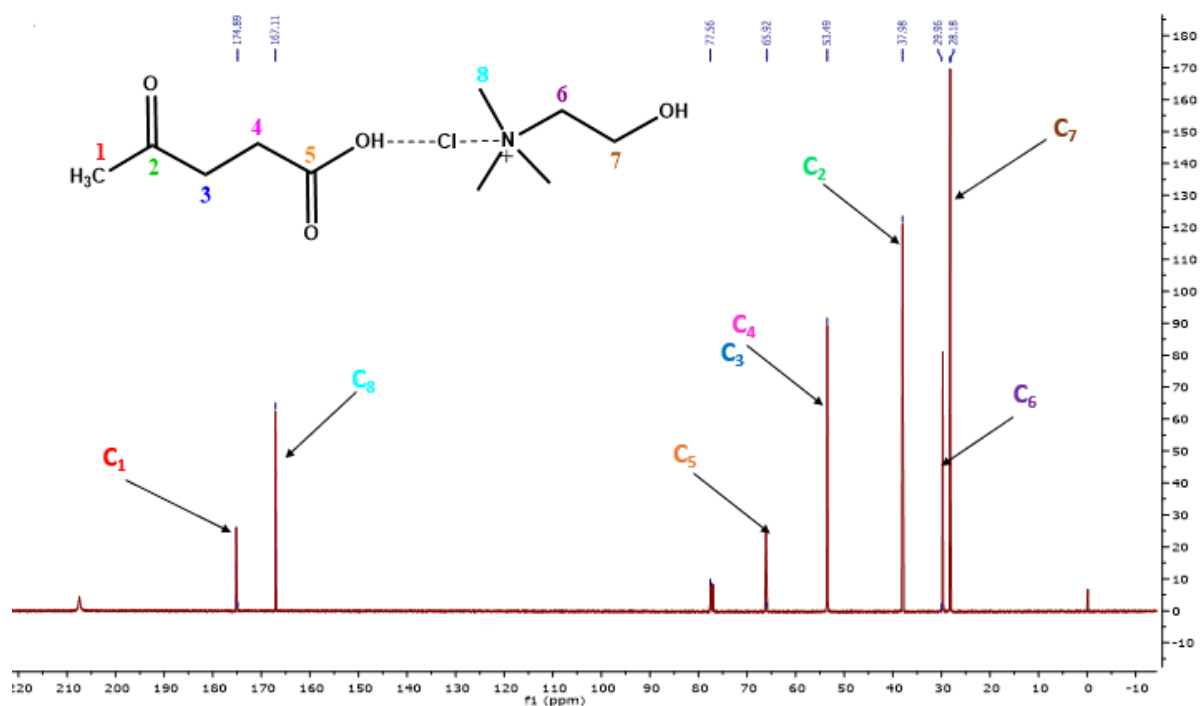


**Figure 4. 9: DES 2 <sup>13</sup>C NMR spectrum**

The <sup>1</sup>H NMR spectrum shows the total number of hydrogens on the compound. From the spectrum below on **Figure 4.10**, at a chemical shift of 5.23 ppm H<sub>a</sub>, a broad singlet gets its multiplicity from the -CH<sub>3</sub> of H<sub>b</sub>. A chemical shift at 4.42 ppm from H<sub>e</sub> is a singlet, which gets its multiplicity from H<sub>d</sub> of the -OH group. The chemical shift at 3.57 ppm represents a doublet which was expected to be a multiplet due to H<sub>a</sub> from the -CH<sub>3</sub> group. At a chemical shift of 3.22 ppm and 3.14 ppm, a doublet of H<sub>d</sub> is caused by the H<sub>e</sub> from the -OH group. Lastly, at 2.92 ppm, a broad singlet of H<sub>c</sub> is attributed to the hydrogens on -CH<sub>3</sub>. The results presented show a successful synthesis of DES 2, although the multiplicity was inconclusive, which may have been due to the presence of water moisture during the synthesis process. The results presented were comparable with those of the literature reports [72].

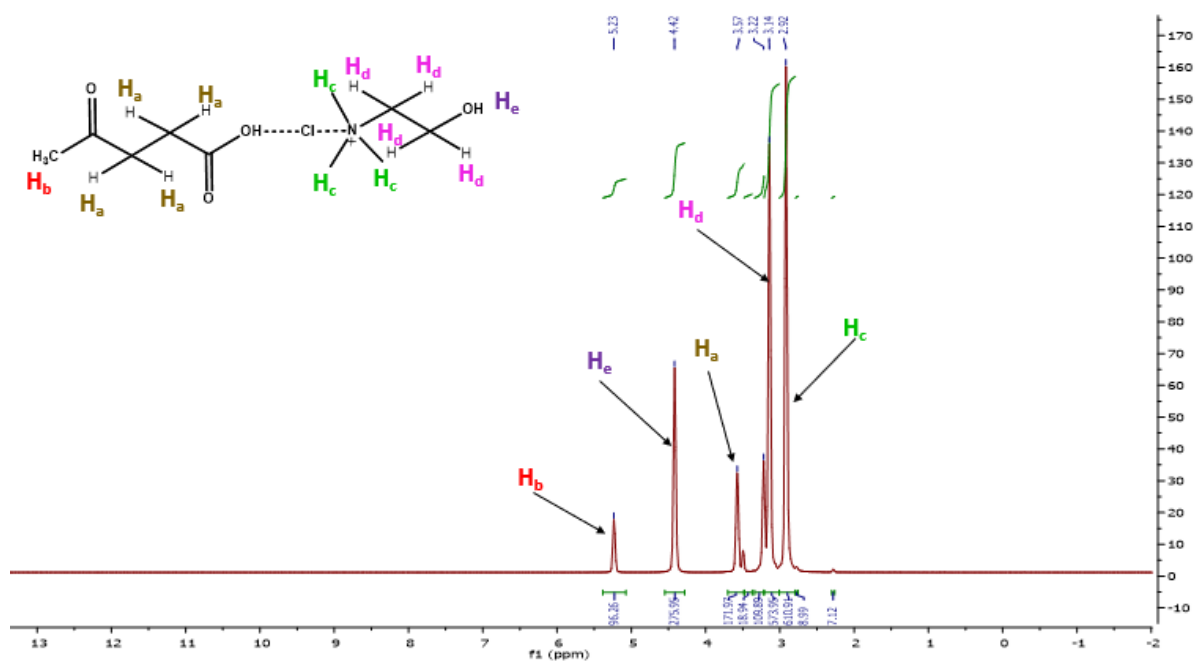


**Figure 4. 10:** Proton NMR for **DES 2**

**Figure 4.11** below shows a <sup>13</sup>C NMR spectrum for DES 3. At a chemical shift ( $\delta$ ) 161.48 ppm is C<sub>3</sub> and C<sub>4</sub>, which is a -C=O bonded to a nitrogen from the urea compound and more deshielded. At a chemical shift ( $\delta$ ) 67.35 ppm is C<sub>2</sub> from -CH<sub>2</sub> of the CCl and it was less shielded. At a chemical shift ( $\delta$ ) 55.04 ppm is C<sub>1</sub> -CH<sub>2</sub> bonded to an -OH group from CCl. At a chemical shift ( $\delta$ ), 52.93 ppm is C<sub>5</sub> from -CH<sub>3</sub> groups of the CCl. Moreover, it is worth noting that C<sub>1</sub> and C<sub>5</sub> were more shielded [73].

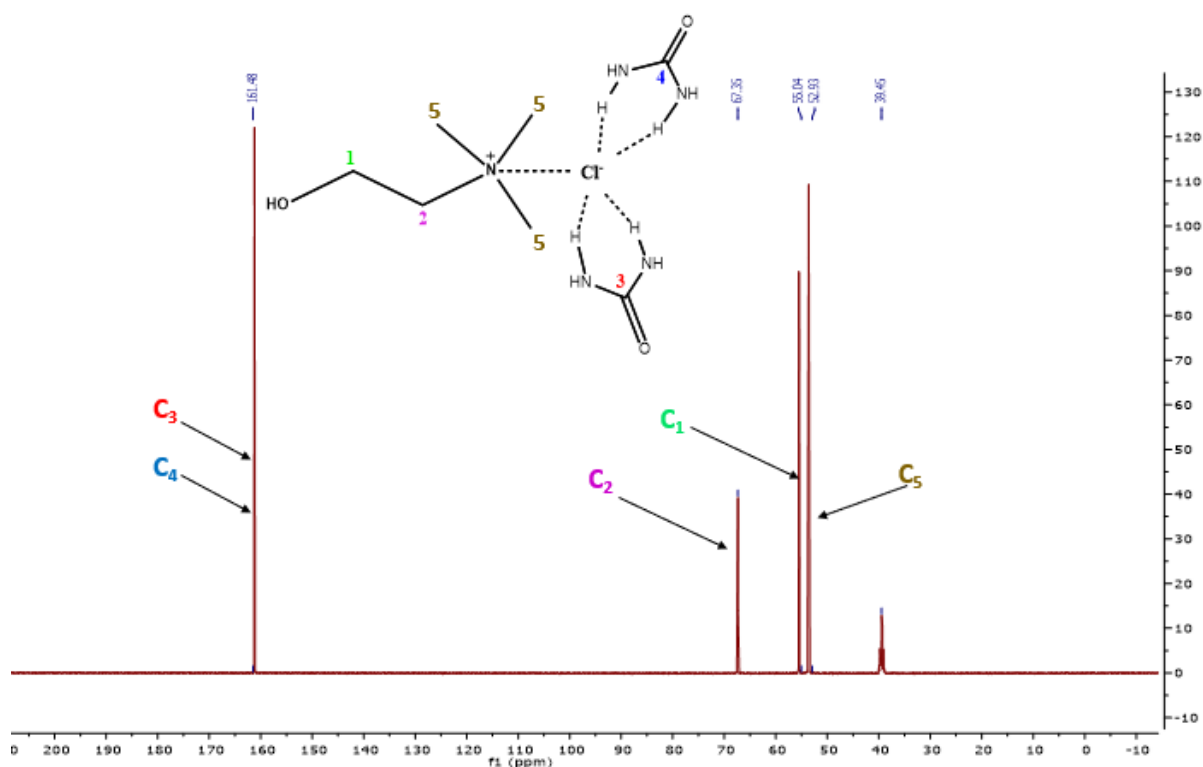


**Figure 4. 11: DES 3**  $^{13}\text{C}$  NMR spectrum

From the **Figure 4.12** below, it is showing the  $^1\text{H}$  NMR of the newly formed DES 3. Broad singlet at chemical shift ( $\delta$ ) at 5.87 ppm belongs to  $\text{H}_a$  of the  $-\text{NH}_2$  group of the urea. The broad singlet at chemical shift of  $\delta$  3.08 ppm belongs to the  $\text{H}_b$  three  $-\text{CH}_3$  groups from CCl compound. The singlet at a chemical shift ( $\delta$ ) of 3.77 ppm can be attributed to by  $\text{H}_c$  from the methylene protons attached to the N atom ( $\text{N}-\text{CH}_2$ ) from CCl, followed by another singlet signal at a chemical shift ( $\delta$ ) of 3.39 ppm of  $\text{H}_d$  of the second methylene group ( $-\text{CH}_2\text{O}$ ) from CCl compound. Lastly, a peak at a chemical shift ( $\delta$ ) of 5,46 ppm is  $\text{H}_e$  from the OH of CCl compound. These results have proved that DES 3 was successfully synthesised. However, the peak at 3.99 ppm could have been attributed to by water moisture generated during synthesis. The multiplicity of this proton NMR was inconclusive. This might have been affected by the instrument's resolution, or they were supposed to be extracted more for a clear visibility of the peaks appearance. Nonetheless, the spectrum perfectly confirmed the protons [73].



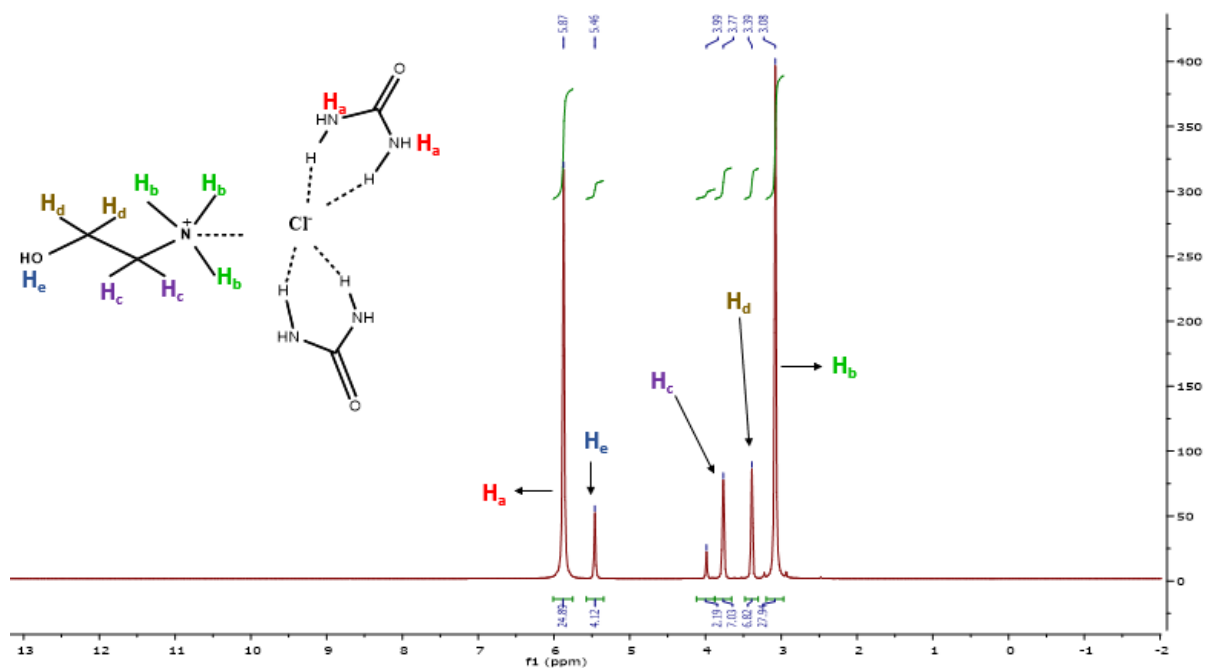


**Figure 4. 12:** Proton NMR for **DES 3**

#### 4.8. *Univariate optimization: DES type, sample volume and eluting solvent selection*

##### 4.8.1. *DES type and sample volume*

Three types of DES were prepared and investigated for their extraction recoveries in different sample volumes; the results are represented in **Figure 4.13**. As seen from the graph below, in comparison to the performance of all three DESs, DES 1 has shown to perform best in all sample volumes, giving the highest recoveries. DES 2 has shown the highest extraction recoveries in sample volume 1 mL only while the lowest recoveries were obtained with other volumes. Lastly, DES 3 has also shown to be promising since it also gave high recoveries. DES 3 was competitive with DES 1 with their performance on extraction. Moreover, their performance has shown that DES 1 and 1 mL sample volume had a direct proportional relationship with their performance during optimization. These results conclude that DES 1 and 1 mL sample volume is best suitable for extracting analytes of interest. Furthermore, DES 3 has also proved to perform best, which can be recommended for further research. The selection of the sample volume of 1 mL was also influenced by the type of eluent solvent as presented in **Figure 4.14**. Additionally, although the extraction recoveries of these NEOs with DES 1 in all sample volumes investigated, the choice of the 1 mL was also influenced by the option of cost effectiveness with the vegetable oil used in

support with abiding with the principles of green chemistry as one of the main objective of this study.

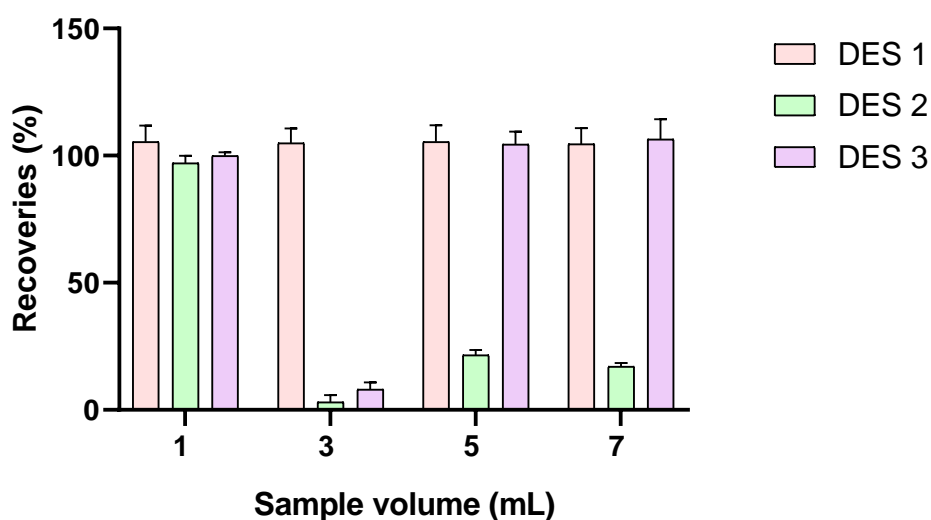


**Figure 4. 13:** Effect of DES type versus sample volume

#### 4.8.2. Solvent type

The type of solvent to be used for eluting the NEO analytes during the univariate optimisation was also investigated. The four different types of solvents were studied, which include acetonitrile (ACN), chloroform ( $\text{CHCl}_3$ ), dichloromethane (DCM) and methanol (MeOH) and their performance were reported in **Figure 4.14**. **Figure 4.14** shows that ACN presented the highest extraction recovery on DES 1 followed by DES 3 and lastly, with DES 2. The  $\text{CHCl}_3$  shows the highest extraction recoveries on DES 3, followed by DES 1, and DES 2 indicates the lowest. Additionally, DCM proved to behave the same way as the ACN, showing the highest extraction recoveries on DES 1, followed by DES 3, while DES 2 showed the lowest extraction recoveries. Lastly, MeOH has demonstrated the highest extraction recoveries on DES 1 followed by acceptable recoveries on DES 2, while nothing was recovered for DES 3 with this solvent. From the results presented, it was then concluded that ACN is the best eluting solvent, and this proved to be good since it also performed best on the selected type of DES as discussed in the above results in **Figure 4.14**.

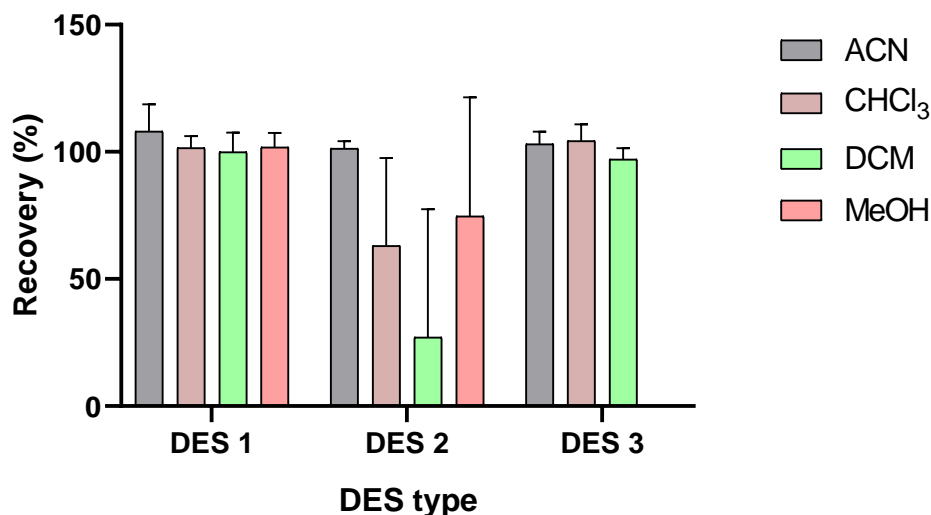


**Figure 4. 14:** Effect of eluting solvent type.

The results shown in **Figures 4.13** and **4.14** have given conclusive results that as continuing with multivariate optimization, the univariate results have shown that DES 1, a sample volume of 1 mL and ACN eluting solvent will be suitable for the method development.

#### 4.9. Multivariate optimization

##### 4.9.1. Full factorial design (FFD)

The results obtained from screening (FFD) are represented in Pareto charts shown in **Figure 4.15**. The results were examined by using the analysis of variance (ANOVA) at 95 % confidence level ( $\alpha=0.05$ ). The pareto chart for ACT shown that only DES volume was significant, and the other parameters were insignificant. The IMI also shown that DES volume was significant. The TCL has shown that eluting time was significant along with the interaction of eluent volume and eluting time. From TMX pareto chart, the extraction time and DES volume were found to be significant along with the interactions of extraction time and eluting time, together with the interactions of eluting volume and DES volume. From the pareto chart, the results of all the four analytes studied were found to be significant while only one parameter was insignificant. The four significant parameters were extraction time, DES volume, eluting time and eluent volume while only pH was insignificant. Since this was a

simultaneous determination, each analyte behaved differently to each parameter. However, for further optimization, all the significant parameters were used.

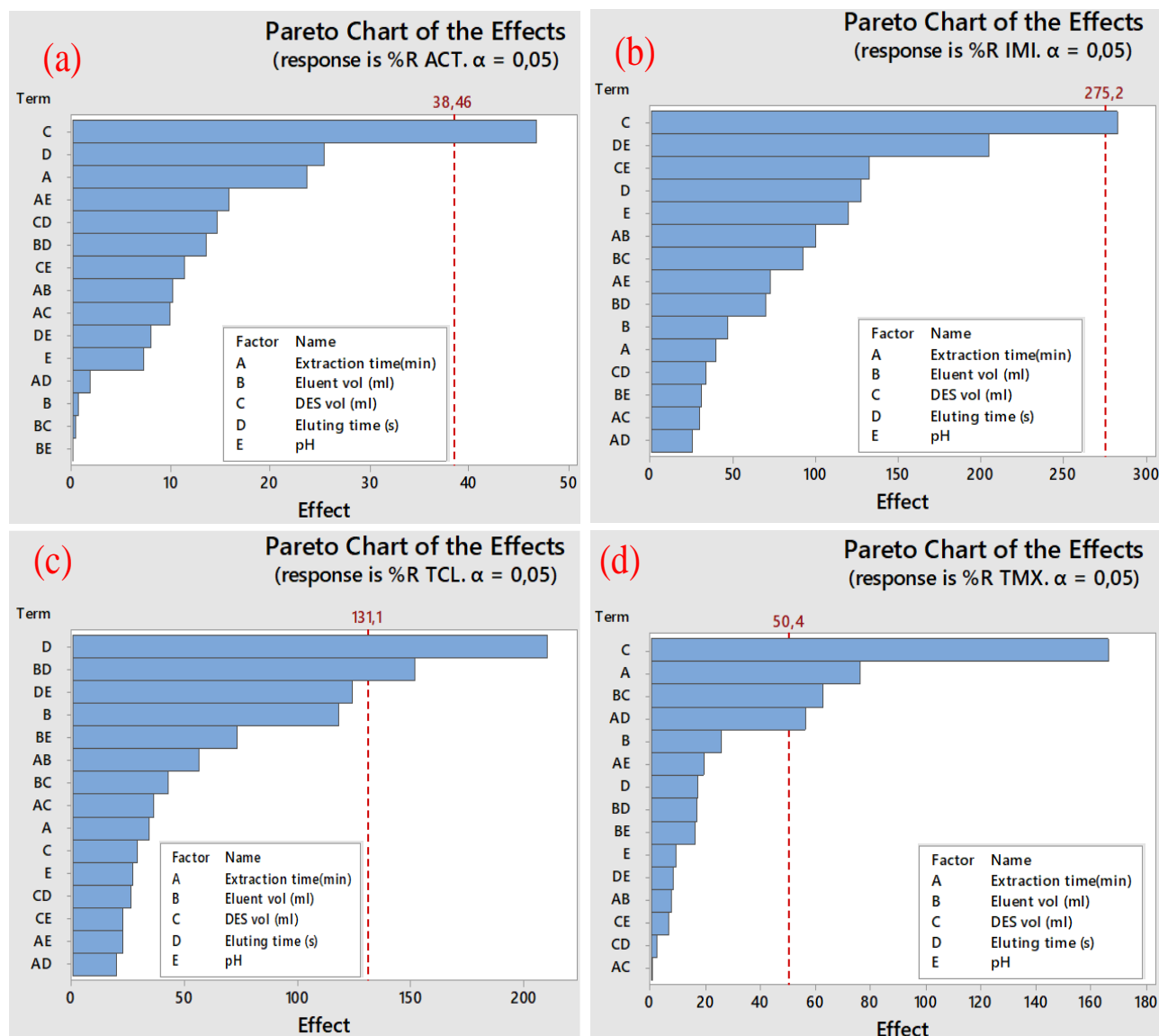


Figure 4. 15: Pareto charts for (a) ACT, (b) IMI, (c) TCL and (d) TMX.

#### 4.9. Response surface methodology (RSM)

The significant parameters were further optimized using the CCD design of experiments and the results were reported in 3D surface plots shown in **Figure 4.16** below. The ACT results from the surface plot **Figure 4.16 (a)** have indicated that as the eluent volume increases and the eluting time is increased, the extraction recovery also increases. The results for **Figure 4.16 (a)** shows two cases wherein at low eluent volume and high extraction time the extraction recoveries also increase. The IMI surface plot **Figure 4.16 (b)** has shown that the extraction recoveries increase as the

eluent volume decreases with increasing eluting time. However, IMI, from the surface plot other side of the dome, shows that as the eluent volume increases along with eluting time, the extraction recoveries also increase. The TCL plot **Figure 4.16 (c)** shows that the extraction recoveries also increase as the eluent volume increases with increasing eluting time. Lastly, TMX **Figure 4.16 (d)** has also shown that as we increase the eluent volume and extraction time, the extraction recoveries also increase. This shows a direct proportionality relationship between the eluent volume and the eluting time, proving that an increase in eluent solvent volume increases the number of analytes that will be redispersed in the centrifuge tube. The analysis of variance (ANOVA) from CCD deduced the quadratic equations showing the interaction between the parameters studied. The equations are shown below from equation **4.8-4.11**. the factors were represented as follows A, extraction time, B, eluent volume, C, DES volume, D. eluting time and E. pH, respectively. The Student's t-test is employed to further explain this concept. The Student's t-test states that the positive value coefficient means that high value of that parameter would lead to an increase in extraction percentage and the negative coefficient value means that low value of that parameter would increase extraction percentage. However, it is worth noting that from this studies screening the Student's t-test gave negative coefficient value which then concludes that the neutral pH value would be considered to give high extraction recoveries and thus was also supported by literature studies. The pH parameter that was insignificant was kept at neutral for further optimization and this was corroborated from the literature methodology followed when designing this method.

$$ACT = 264 - 202C + 12.7A - 129.5B + 1.43D + 3.6C^2 + 0.24A^2 + 1.0B^2 - 0.0021D^2 - 6.9CA + 177.7CB - 0.29CD + 0.10AB - 0.217AD - 0.296BD \dots \dots \dots \text{equation 4. 8}$$

$$IMI = 182.3 - 69C - 4.8A - 92.1BD - 16.9C^2 - 1.017A^2 - 6.04B^2 - 0.0213D^2 + 5.57CA + 51.6CB - 0.321CD + 8.50AB - 0.039AD + 0.371BD \dots \dots \dots \text{equation 4. 9}$$

$$TCL = 305 - 20C - 12.1A - 4B - 2.54D + 60C^2 + 0.75A^2 + 15.5B^2 - 0.0012D^2 - 12.8CA - 40.6CB + 0.55CD + 0.27AB + 0.315AD - 0.25BD \dots \dots \dots \text{equation 4. 10}$$

$$TMX = 13.3 + 136C - 11.2A + 0.9B + 4.24D - 0.4C^2 + 0.107A^2 - 13.5B^2 - 0.0154D^2 - 3.3CA + 23.7CB - 2.75CD + 7.14AB + 0.082AD - 0.506BD \dots \dots \dots \text{equation 4. 11}$$

Furthermore, after estimating the parameters effect and determining the significant factors affecting extraction recoveries, an analysis of variance (ANOVA)

was used to check if the developed method fit the analytes [74]. Since the factors in this study have two levels, each ANOVA main effect and interaction effect had one degree of freedom [75]. The method performance for each analyte was also investigated by looking into the  $P$  values. From the  $P$  value, when the  $P < 0.05$  level of significance it means that analytes does not fits the model, while if  $P > 0.05$  level of significance it means that the data does fit the model [76]. However, from the studied NEOs, only TCL was found to not fit the model with a  $P$  value of 0.003 below 0.05, while the other analytes were found to fit the model since they had values greater than 0.05. Their  $P$  values were 0.087 for TMX, 0.520 for ACT and 0.149 for IMI, respectively. This leads us to the conclusion that since 99 % of the analytes fits the model then this method can be considered to be good for analysis of these analytes. The  $P$  value rule also applies to the parameters studied. The main effect of each parameter and the interaction effects are statistically significant at  $P < 0.05$ .

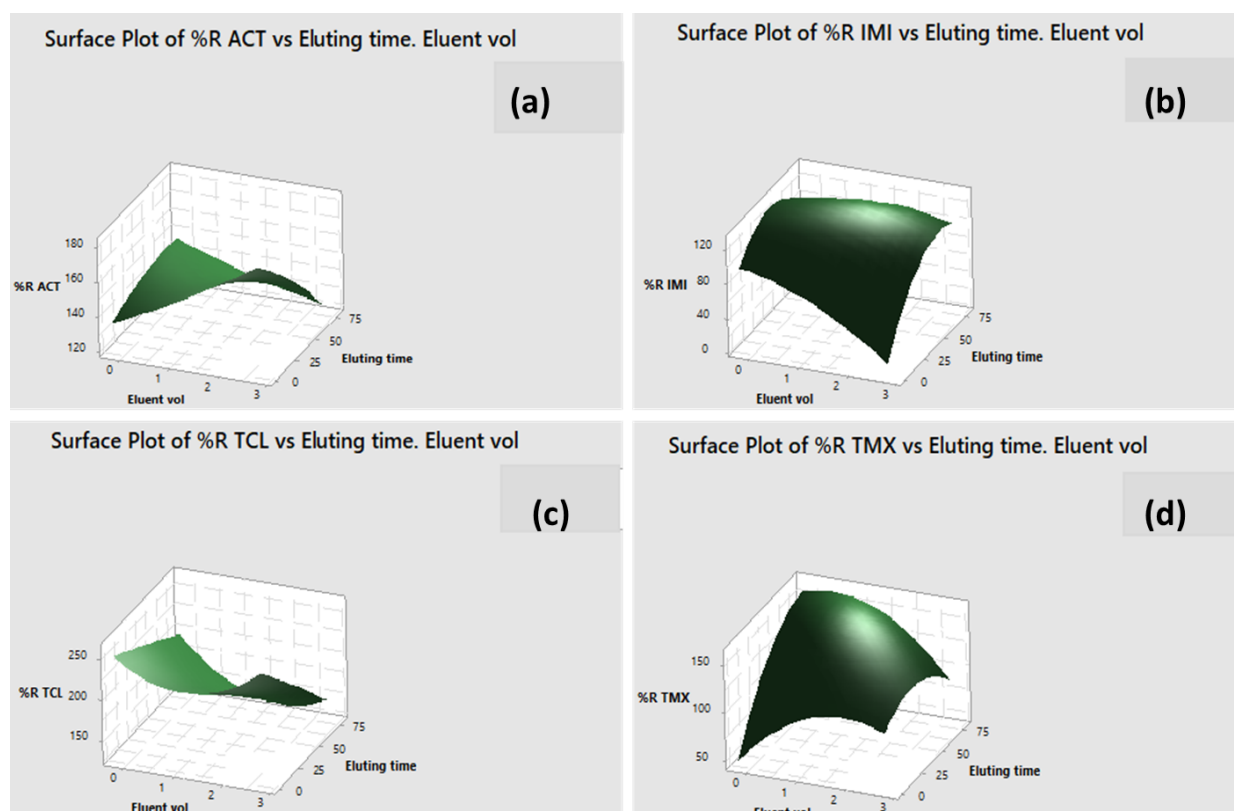


**Figure 4. 16:** Surface plots for eluent volume versus eluting time (a) ACT, (b) IMI, (c) TCL and (d) TMX.

#### 4.10. Method validation

Method performance was studied, and the results will be discussed in this section. The developed method was validated in terms of their accuracy, precision, LODs, LOQs and linearity. From the calibration curve for each analyte recorded at  $R^2$  values of ACT at 0.9989, IMI at 0.9994, TCL at 0.9997 and TMX at 0.9992 which showed good linearity. **Table 4.4.** below shows the calibration equations and correlation coefficients for NEO. Additionally, the correlation coefficient ( $R^2$ ) is closer to 1, suggesting a linear relationship exists between different concentrations of the analyte of interest on calibration standards. The method has proved to show good accuracy from 79-119.58 %.

Method validation was done in terms of intra- and inter-day precisions recorded at 0.61-1.62 % for intraday and 0.1-0.95 % for inter-day, which shows relatively good precision and indicates that the method has excellent reproducibility. The limit of detection and quantification are recorded at 0.4-4.95 ng.  $\mu\text{L}^{-1}$  and 1.43-9.7 ng.  $\mu\text{L}^{-1}$ , respectively. The lowest concentration at which detection is practical and at which a blank sample may be reliably targeted is known as the LOD. The lowest quantity of analyte in a sample that can be quantitatively determined with appropriate precision and accuracy is referred to as the lower limit of quantification, or LOQ. This has proved to show that this method was sensitive and repeatable. The LOQ value of each analyte that correlated with a signal-to-noise ratio (S/N) of 10 was determined to be the lowest point of the calibration curve. In simple terms, the LOQ is the lowest concentration of the analyte that can be quantified with acceptable accuracy while LOD refers to the analyte concentration that gives a signal to noise ratio of 3.

**Table 4. 5:** Representation of the calibration equations and correlation coefficients of each analyte.

Analyte	Equation	$R^2$
Acetamidiprid	$Y = 0.0506x - 19.228$	0.9989
Imidacloprid	$Y = 0.0245x - 25.156$	0.9994
Thiacloprid	$Y = 0.0358x - 36.391$	0.9997
Thiamethoxam	$Y = 0.0469x - 49.153$	0.9992

#### 4.11. Comparison of this method with other reported methods

The performance of the developed method was compared with other reported methods in terms of some reported analytical figures, which are reported in **Table 4.5** below. Since this study focused on developing a greener extraction method, the initial exemption was that only DES was a unique extractant compared to other methods. Because researchers have recommended DES as an emerging green solvent because of their advantages like low cost, low volatility and high biodegradability, just to mention few. The developed method for this study has shown high extraction recoveries of 79-119.58 % and extremely good precision of 0.1-1.62 %, which shows that this method persists excellent reproducibility. The extraction time for this method was also the fastest compared to the other methods. The developed method has shown great potential for future research since it is uses small sample volume, greener, produces less waste, is non-laborious and makes use of green solvents that are biodegradable of which it fits well to green chemistry principles. It is worth noting that the developed method does not have any additional steps, uses fewer organic solvents, uses less volumes of solvents and does not require any additional complicated sample preparations prior to preconcentration and extraction.



**Table 4. 6:** Comparison of the developed method with other reported methods

<b>Matrix</b>	<b>Extraction method</b>	<b>Analytes</b>	<b>Detection technique</b>	<b>LOD (ng. <math>\mu\text{L}^{-1}</math>)</b>	<b>Extraction time (min)</b>	<b>Recoveries (%)</b>	<b>RSD (%)</b>	<b>Ref</b>
Rapeseed, Rapeseed Oil & Rapeseed Meal	LLE	ACT, IMI, TCL, TMX	LC-MS/MS	NR	7	70-118	NR	[77]
Sunflower seeds	LLE	ACT, IMI, CLO, TCL, TMX, DIN, NIT	LC-MS/MS	0.0003-0.0012	10	70-120	2.4-9.6	[78]
Edible oils	DLLE	ACT, IMI, TMX, TCL	HPLC-DAD	0.11-0.36	21	58-83	NR	[79]
Vegetable oils	DLLME	ACT, IMI, TMX, TCL	HPLC-DAD	0.4-4.95	4.5	79-119.58	0.1-1.62	This study

**LLE**- Liquid-liquid extraction, **DLLE**-Dispersive liquid-liquid extraction, **DLLME**-Dispersive liquid-liquid microextraction, **HPLC-DAD**- High performance liquid chromatography diode array detector, **LC-MSMS**- Liquid chromatography tandem mass spectrometry, **LOD**- Limit of detection, **LOQ**-Limit of quantification, **RSD**- Relative standard deviation

#### 4.12. Matrix effect

Matrix effect (ME) is generally the combined effect of all the components in the sample other than the analytes of interest. External calibration curves of the analytes of interest were constructed by plotting the peak area of each analyte against the known spiked concentration of the analyte, respectively. This was done by taking the average of the peak areas in triplicate injections from each concentration. Furthermore, from the reported results of this study, the analytes have shown good linearity with values at  $R^2 \geq 0.99$ , thus, this indicates that there was a linear relationship between different concentrations of the analyte of interest on calibration standards [80]. When comparing the slopes of the regression lines of the analytes in solvent and matrix, it shows a significant matrix effect when the slopes of the regression lines show a difference of more than 40%, respectively. The matrix effect phenomenon is associated with the efficiency of the sample preparation method used and the matrix type. The matrix effects can be attributed to many sources such as the analyte's separation or ionisation process. To estimate if the matrix influences to a significant degree the peak area and, therefore, the sensitivity of the analytes, the slopes of the calibration curves of the spiked oils obtained from the four different vegetable oil samples compared to the calibration curves of the analytical standards prepared in a solvent were investigated for this study [63]. Farouk et al. (2016) have reported that MEs ranging between +20% and -20% are regarded as low matrix effects; those ranging between -50% and -20% or between +20% and +50% are recognised as medium matrix effects; and those ranging between less than -50% and more than +50% are recognised as high matrix effects [81]. The results in **Figure 4.17** show that all the analytes in the selected vegetable oils have suffered ion enhancement.

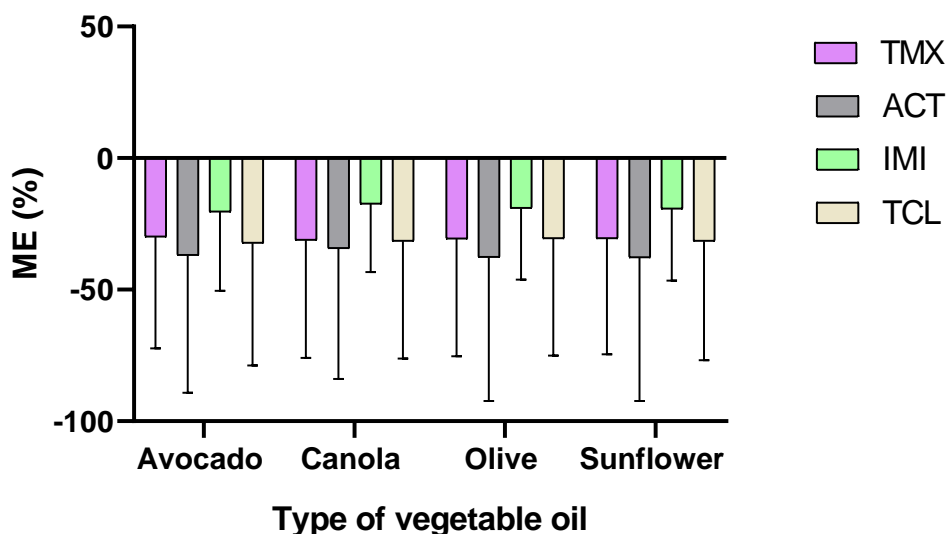


**Figure 4. 17:** Effect of matrix effect in selected vegetable oil.

#### 4.13. Assessment of method greenness

The developed method was assessed for its greenness using the Analytical Eco-Scale and Analytical GREENness Metric calculator. The metric is based on the 10 principles of green chemistry (significance), which have been transformed into a unified 0 -1 scale and presented with a final score in a pictogram. The AGREE metric has been user-friendly, comprehensive, easy to apply, and fast [82]. The AGREE follows the principles of green analytical chemistry (GAC). The 1-10 clockwise scale red-yellow-green colour scheme demonstrated the technique's performance against each principle. From the pictogram a specific colour on each category represents the degree of obedience to GAC principles. After the 10 principles in design of the pictogram have been evaluated on an AGREE calculator, a clock-like graph was created, with the overall score in colour displayed in the centre. In comparison, the matching segment's width reflected each principle's weight. The total score in the centre of the pictogram, with values near one and a dark green tint, indicates that the tested technique is more environmentally friendly [83].

The developed method was considered greener than the AGREE tool, which means it is environmentally friendly. The developed method was scaled at 0.67, which is fit to be greener, and the results are represented in **Figure 4.18**.



**Figure 4. 18:** AGREE pictogram for DLLME.

#### 4.14. Application of DES-DLLME in real vegetable oils

The concentrations of the selected NEOs for this study were calculated using the equations generated when investigating the matrix effect. This was done by spiking the real oil samples with a known concentration for generating the standard calibration curves. A total of 20 experiments with 5 experiments for each vegetable oil. These were conducted using the previously deduced optimum conditions applied during method validation (1 mL sample volume, 4 mL n-hexane, 0.8 mL DES, 4.5 min extraction, 0.5 mL eluting solvent and 75 s eluting time). The results show that all the analytes were below the detection limits in all four different types of oils used for this study. Detection limit refers to the lowest concentration at which detection is practical. Thus, this means these vegetable oils are free of these NEOs, meaning they are safe for human consumption. The results are shown in **Table 4.6**.

**Table 4. 7:** Concentration levels of the NEOs in selected vegetable oil samples.

Analyte	Avocado oil	Canola oil	Olive oil	Sunflower oil
ACT	< DL	< DL	< DL	< DL
IMI	< DL	< DL	< DL	< DL
TCL	< DL	< DL	< DL	< DL
TMX	< DL	< DL	< DL	< DL

DL- detection limit

For further confirmation of the development of the method and its application in real commercial vegetable oil samples, a typical chromatogram was drawn showing the signal peaks of the analytes in real sample, spiked at  $50 \text{ ng}\cdot\mu\text{L}^{-1}$  and  $300 \text{ ng}\cdot\mu\text{L}^{-1}$ , respectively. The results are presented in **Figure 4.19**. The results show that the concentration of the NEOs in real samples is very similar to the appearance of the signals when spiked with a known concentration. This is concluded by the fact that even the signal peak appearance increases as the spiking concentration increases. There is a direct proportional relationship between the concentration of the analytes and how the peak appears on the chromatogram. Moreover, this confirms that the commercial vegetable oils are free of these NEOs. Furthermore, it is worth noting that the appearance of peaks of analytes on the spiked and real vegetable oil samples has shifted in terms of time at which they appear on the spectrum compared to how they appear on the standard. Such also confirms that the matrix has an influence on these analytes to a certain extent. From **Figure 4.19 (a), (c) and (d)** there was an observable solvent peak that was showing before the appearance of the analytes. Furthermore, as a way of verifying if the method can be applied for determination of the NEOs in other vegetable oils, the method was applied to all the four vegetable oils and their recoveries and RSDs are shown on **Table 4.7**. The spiked recoveries of the NEOs were at a range of 77-99.6 % with the %RSDs at less than 4 as shown in **Table 4.7**. These results show the application potential for the determination of the NEOs in real vegetable oils.

**Table 4. 8:** Different concentrations studied in four vegetable oils.

Sample	Analytes	Spiked (n=3)	concentrations		
			Recoveries (%) (%RSD)		
		0 ng.µL <sup>-1</sup>	50 ng.µL <sup>-1</sup>	300 ng.µL <sup>-1</sup>	
Avocado oil	ACT	ND	92.8 (1.2)	96 (2.2)	
	IMI	ND	90 (2.3)	93.2 (2.9)	
	TCL	ND	81.1 (2.6)	99.6 (2.3)	
	TMX	ND	88 (2.0)	93.3 (1.2)	
Canola oil	ACT	ND	85 (1.6)	99 (2.1)	
	IMI	ND	93 (2.3)	95.2 (1.8)	
	TCL	ND	79 (3.7)	87 (1.2)	
	TMX	ND	88 (3.1)	107 (3.3)	
Olive oil	ACT	ND	95 (2.2)	90.1 (1.9)	
	IMI	ND	98 (1.4)	86 (2.1)	
	TCL	ND	96.6 (1.8)	93 (1.5)	
	TMX	ND	86.3 (2.4)	78 (4)	
Sunflower oil	ACT	ND	83.1 (0.7)	98.7 (2.3)	
	IMI	ND	99.6 (2.3)	97.9 (1.6)	
	TCL	ND	80.1 (1.6)	77 (3.6)	
	TMX	ND	88 (1.1)	89.7 (2.6)	

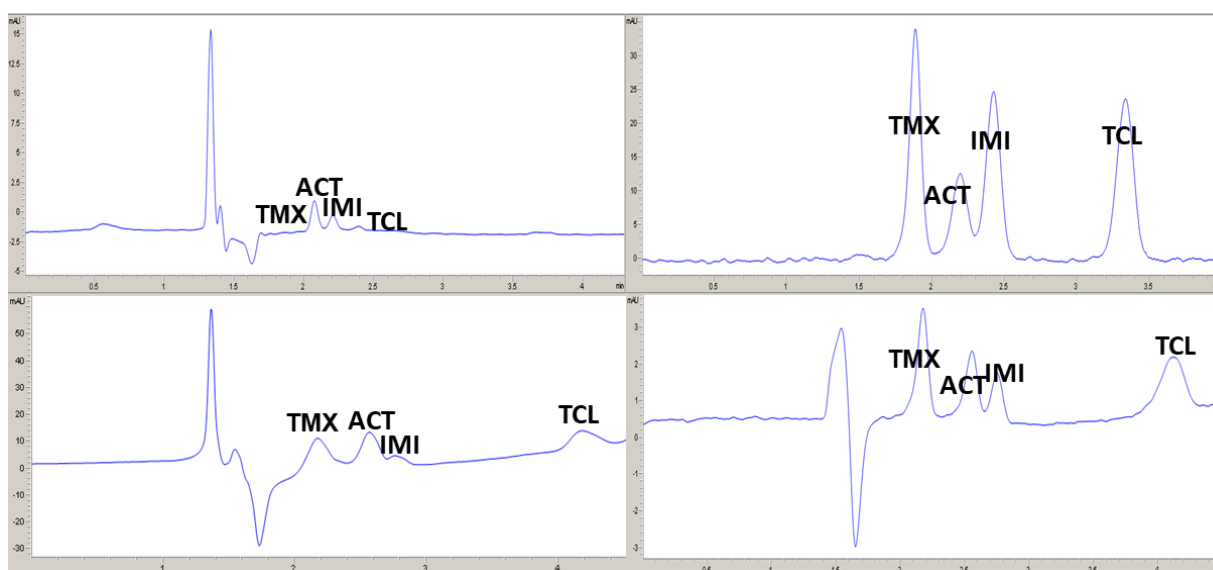


**Figure 4. 19:** Chromatograms of real commercial vegetable oils and spiked vegetable oils **(a)** real sample, **(b)** analytes standard, **(c)** spiked real sample 50 ng.μL<sup>-1</sup> and spiked real sample 300 ng.μL<sup>-1</sup>.



#### 4.15. Conclusion

This study concludes that the DESs were successfully synthesised, characterized and applied as extractant for the NEOs from vegetable oils. DESs were favoured for this study since they are emerging green solvents with and added advantage environmentally friendliness, time efficient synthesis, and their persistence in low volatility. The developed method was greener, simple, rapid and sensitive, thus was proven by the AGREE tool and analytical performance of this method. The method was validated and applied in real samples. The real sample results have proved that the vegetable oils were free on these NEOs. The DES-DLLME results shows that this technique exhibits high extraction recoveries, low limit of quantification and detection, short extraction time, and good repeatability. According to the AGREE and principles of green analytical chemistry (GAC), this method was greener. The matrix-matched calibration curves were constructed, and the results has shown that the matrix effect influences the appearance of the peaks on the spectra of the analytes to a certain degree. The results for the matrix effect have demonstrated that the NEOs in all four of the selected vegetable oils have suffered ion enhancement. Furthermore, **Figure 4.17** also shows the matrix's effect in vegetable oils compared to the analytical standard. For future recommendations, DES 3 can be used for further studies of the NEOs in different matrices since it has proved to be a promising extractant that gives good extraction recoveries.

## References

- [1] S. K. Selahle, N. J. Waleng, A. Mpupa, and P. N. Nomngongo, "Magnetic Solid Phase Extraction Based on Nanostructured Magnetic Porous Porphyrin Organic Polymer for Simultaneous Extraction and Preconcentration of Neonicotinoid Insecticides From Surface Water," *Front. Chem.*, vol. 8, no. September, pp. 1–15, 2020, doi: 10.3389/fchem.2020.555847.
- [2] J. Vichapong, R. Burakham, and S. Srijaranai, "Vortex-assisted surfactant-enhanced-emulsification liquid-liquid microextraction with solidification of floating organic droplet combined with HPLC for the determination of neonicotinoid pesticides," *Talanta*, vol. 117, pp. 221–228, 2013, doi: 10.1016/j.talanta.2013.08.034.
- [3] L. Ma, Y. Wang, H. Li, F. Peng, B. Qiu, and Z. Yang, "Development of QuEChERS-DLLME method for determination of neonicotinoid pesticide residues in grains by liquid chromatography-tandem mass spectrometry," *Food Chem.*, vol. 331, no. May, p. 127190, 2020, doi: 10.1016/j.foodchem.2020.127190.
- [4] M. A. Farajzadeh, M. Bamorowat, and M. R. A. Mogaddam, "Ringer tablet-based ionic liquid phase microextraction: Application in extraction and preconcentration of neonicotinoid insecticides from fruit juice and vegetable samples," *Talanta*, vol. 160, pp. 211–216, 2016, doi: 10.1016/j.talanta.2016.03.097.
- [5] J. Vichapong, R. Burakham, and S. Srijaranai, "Ionic liquid-based vortex-assisted liquid–liquid microextraction for simultaneous determination of neonicotinoid insecticides in fruit juice samples," *Food Anal. Methods*, vol. 9, no. 2, pp. 419–426, 2016, doi: 10.1007/s12161-015-0209-4.
- [6] Z. Ju, J. Fan, Z. Meng, R. Lu, H. Gao, and W. Zhou, "A high-throughput semi-automated dispersive liquid–liquid microextraction based on deep eutectic solvent for the determination of neonicotinoid pesticides in edible oils," *Microchem. J.*, vol. 185, no. November 2022, p. 108193, 2023, doi: 10.1016/j.microc.2022.108193.
- [7] T. Rodríguez-Cabo, J. Casado, I. Rodríguez, M. Ramil, and R. Cela, "Selective

- extraction and determination of neonicotinoid insecticides in wine by liquid chromatography–tandem mass spectrometry,” *J. Chromatogr. A*, vol. 1460, pp. 9–15, 2016, doi: 10.1016/j.chroma.2016.07.004.
- [8] J. Vichapong, R. Burakham, and Y. Santaladchaiyakit, “Talanta A preconcentration method for analysis of neonicotinoids in honey samples by ionic liquid-based cold-induced aggregation microextraction,” *Talanta*, vol. 155, pp. 216–221, 2016, doi: 10.1016/j.talanta.2016.04.045.
- [9] R. Kachangoon, J. Vichapong, Y. Santaladchaiyakit, R. Burakham, and S. Srijaranai, “An eco-friendly hydrophobic deep eutectic solvent-based dispersive liquid-liquid microextraction for the determination of neonicotinoid insecticide residues in water, soil and egg yolk samples,” *Molecules*, vol. 25, no. 12, 2020, doi: 10.3390/molecules25122785.
- [10] J. Hou *et al.*, “Simultaneous Determination of Neonicotinoid Insecticides and Metabolites Residues in Milk and Infant Formula Milk Powder by EMR-Liquid Chromatography-Tandem Mass Spectrometry,” *Food Anal. Methods*, vol. 16, no. 7, pp. 1215–1226, 2023, doi: 10.1007/s12161-023-02484-7.
- [11] O. López-Fernández, R. Rial-Otero, and J. Simal-Gándara, “High-throughput HPLC–MS/MS determination of the persistence of neonicotinoid insecticide residues of regulatory interest in dietary bee pollen,” *Anal. Bioanal. Chem.*, vol. 407, no. 23, pp. 7101–7110, 2015, doi: 10.1007/s00216-015-8870-4.
- [12] D. Li *et al.*, “Neonicotinoid insecticide and their metabolite residues in fruit juices: Implications for dietary intake in China,” *Chemosphere*, vol. 261, p. 127682, 2020, doi: 10.1016/j.chemosphere.2020.127682.
- [13] P. Jovanov *et al.*, “Development of multiresidue DLLME and QuEChERS based LC-MS/MS method for determination of selected neonicotinoid insecticides in honey liqueur,” *Food Res. Int.*, vol. 55, pp. 11–19, 2014, doi: 10.1016/j.foodres.2013.10.031.
- [14] I. Timofeeva, A. Shishov, D. Kanashina, D. Dzema, and A. Bulatov, “Talanta On-line in-syringe sugaring-out liquid-liquid extraction coupled with HPLC-MS / MS for the determination of pesticides in fruit and berry juices,” *Talanta*, vol. 167, no. December 2016, pp. 761–767, 2017, doi:

- 10.1016/j.talanta.2017.01.008.
- [15] Z. Dashtbozorgi, M. K. Ramezani, and S. Waqif-Husain, "Optimization and validation of a new pesticide residue method for cucumber and tomato using acetonitrile-based extraction-dispersive liquid-liquid microextraction followed by liquid chromatography-tandem mass spectrometry," *Anal. Methods*, vol. 5, no. 5, pp. 1192–1198, 2013, doi: 10.1039/c2ay26287h.
- [16] S. Song *et al.*, "Simultaneous determination of neonicotinoid insecticides and insect growth regulators residues in honey using LC–MS/MS with anion exchanger-disposable pipette extraction," *J. Chromatogr. A*, vol. 1557, pp. 51–61, 2018, doi: 10.1016/j.chroma.2018.05.003.
- [17] W. Ahmad, A. S. Bashammakh, and H. Alwael, "Trends in Analytical Chemistry Recent advances in dispersive liquid-liquid microextraction for pesticide analysis," *Trends Anal. Chem.*, vol. 72, pp. 181–192, 2015, doi: 10.1016/j.trac.2015.04.022.
- [18] M. L. Senovieski, S. A. Gegenschatz, F. A. Chiappini, C. M. Teglia, M. J. Culzoni, and H. C. Goicoechea, "In-syringe dispersive liquid-liquid microextraction vs. solid phase extraction: A comparative analysis for the liquid chromatographic determination of three neonicotinoids in cotyledons," *Microchem. J.*, vol. 158, no. June, p. 105181, 2020, doi: 10.1016/j.microc.2020.105181.
- [19] J. Vichapong, K. Moyakao, R. Kachangoon, R. Burakham, Y. Santaladchaiyakit, and S. Srijaranai, "B-Cyclodextrin assisted liquid–liquid microextraction based on solidification of the floating organic droplets method for determination of neonicotinoid residues," *Molecules*, vol. 24, no. 21, 2019, doi: 10.3390/molecules24213954.
- [20] J. Vichapong, R. Burakham, and S. Srijaranai, "Talanta In-coupled syringe assisted octanol – water partition microextraction coupled with high-performance liquid chromatography for simultaneous determination of neonicotinoid insecticide residues in honey," *Talanta*, vol. 139, pp. 21–26, 2015, doi: 10.1016/j.talanta.2015.02.033.
- [21] B. Giroud, S. Bruckner, L. Straub, P. Neumann, G. R. Williams, and E. Vulliet,

- “Trace-level determination of two neonicotinoid insecticide residues in honey bee royal jelly using ultra-sound assisted salting-out liquid liquid extraction followed by ultra-high-performance liquid chromatography-tandem mass spectrometry,” *Microchem. J.*, vol. 151, no. September, p. 104249, 2019, doi: 10.1016/j.microc.2019.104249.
- [22] L. Lachat and G. Glauser, “Development and Validation of an Ultra-Sensitive UHPLC-MS/MS Method for Neonicotinoid Analysis in Milk,” *J. Agric. Food Chem.*, vol. 66, no. 32, pp. 8639–8646, 2018, doi: 10.1021/acs.jafc.8b03005.
- [23] V. Buši, “Application of Choline Chloride-Based Deep Eutectic Solvents in the Synthesis of Hydrazones,” 2023.
- [24] J. Tursen, T. Yang, L. Bai, D. Li, and R. Tan, “Determination of imidacloprid and acetamiprid in bottled juice by a new DLLME-HPLC,” *Environ. Sci. Pollut. Res.*, vol. 28, no. 36, pp. 50867–50877, 2021, doi: 10.1007/s11356-021-13540-2.
- [25] J. Vichapong, R. Burakham, and S. Srijaranai, “Alternative Liquid–Liquid Microextraction as Cleanup for Determination of Neonicotinoid Pesticides Prior HPLC Analysis,” *Chromatographia*, vol. 79, no. 5–6, pp. 285–291, 2016, doi: 10.1007/s10337-016-3022-3.
- [26] B. Zhao, P. Xu, F. Yang, H. Wu, M. Zong, and W. Lou, “Biocompatible Deep Eutectic Solvents Based on Choline Chloride: Characterization and Application to the Extraction of Rutin from *Sophora japonica*,” 2015, doi: 10.1021/acssuschemeng.5b00619.
- [27] S. Arriaga and A. Aizpuru, *Innovative non-aqueous phases and partitioning bioreactor configurations*, 1st ed., vol. 54. Elsevier Inc., 2019. doi: 10.1016/bs.ache.2018.12.004.
- [28] H. Zhao *et al.*, “Phenolic-based non-ionic deep eutectic solvent for rapid determination of water soluble neonicotinoid insecticides in tea infusion,” *Food Chem.*, vol. 416, no. 5, p. 135737, 2023, doi: 10.1016/j.foodchem.2023.135737.
- [29] L. Carbonell-Rozas, R. Canales, F. J. Lara, A. M. García-Campaña, and M. F.

- Silva, "A natural deep eutectic solvent as a novel dispersive solvent in dispersive liquid-liquid microextraction based on solidification of floating organic droplet for the determination of pesticide residues," *Anal. Bioanal. Chem.*, vol. 413, no. 25, pp. 6413–6424, 2021, doi: 10.1007/s00216-021-03605-z.
- [30] O. I. Abdallah and F. M. Malhat, "Thiacloprid Residues in Green Onion (*Allium cepa*) Using Micro Liquid–Liquid Extraction and Liquid Chromatography–Tandem Mass Spectrometry," *Agric. Res.*, vol. 9, no. 3, pp. 340–348, 2020, doi: 10.1007/s40003-019-00440-8.
- [31] A. Suganthi, K. Bhuvaneswari, and M. Ramya, "Determination of neonicotinoid insecticide residues in sugarcane juice using LCMSMS," *Food Chem.*, vol. 241, no. December 2016, pp. 275–280, 2018, doi: 10.1016/j.foodchem.2017.08.098.
- [32] J. Hou *et al.*, "Simultaneous determination of ten neonicotinoid insecticides and two metabolites in honey and Royal-jelly by solid–phase extraction and liquid chromatography–tandem mass spectrometry," *Food Chem.*, vol. 270, no. January 2018, pp. 204–213, 2019, doi: 10.1016/j.foodchem.2018.07.068.
- [33] M. Pourmohammad, M. Faraji, and S. Jafarinejad, "Extraction of chromium ( VI ) in water samples by dispersive liquid – liquid microextraction based on deep eutectic solvent and determination by UV – Vis spectrophotometry," *Int. J. Environ. Anal. Chem.*, vol. 100, no. 10, pp. 1146–1159, 2020, doi: 10.1080/03067319.2019.1650920.
- [34] B. D. Ribeiro, C. Florindo, C. I. Lucas, M. A. Z. Coelho, and I. M. Marrucho, "Menthol-based Eutectic Mixtures: Hydrophobic Low Viscosity Solvents," 2015, doi: 10.1021/acssuschemeng.5b00532.
- [35] C. Florindo, L. C. Branco, and I. M. Marrucho, "Fluid Phase Equilibria Development of hydrophobic deep eutectic solvents for extraction of pesticides from aqueous environments," *Fluid Phase Equilib.*, vol. 448, pp. 135–142, 2017, doi: 10.1016/j.fluid.2017.04.002.
- [36] V. S. Raghuwanshi, M. Ochmann, A. Hoell, F. Polzer, and K. Rademann, "Deep Eutectic Solvents for the Self-Assembly of Gold Nanoparticles: A SAXS,

- UV – Vis, and TEM Investigation,” 2014.
- [37] V. Buši, D. Božanovi, and I. Jerkovi, “Choline Chloride-Based Deep Eutectic Solvents as Green Effective Medium for Quaternization Reactions,” 2022.
- [38] A. Skulcova, V. Majova, M. Kohutova, M. Grosik, J. Sima, and M. Jablonsky, “com UV/Vis Spectrometry as a Quantification Tool for Lignin Solubilized in Deep Eutectic Solvents,” vol. 12, no. 3, pp. 6713–6722, 2017.
- [39] J. T. M. Amphlett, M. D. Ogden, W. Yang, and S. Choi, “Probing Ni<sup>2+</sup> and Co<sup>2+</sup> speciation in carboxylic acid based deep eutectic solvents using UV / Vis and FT-IR spectroscopy,” *J. Mol. Liq.*, vol. 318, p. 114217, 2020, doi: 10.1016/j.molliq.2020.114217.
- [40] Z. Erbas and M. Soylak, “A green and simple liquid - phase microextraction based on deep eutectic solvent for the erythrosine prior to its UV – VIS spectrophotometric detection,” *J. Iran. Chem. Soc.*, vol. 17, no. 10, pp. 2675–2681, 2020, doi: 10.1007/s13738-020-01957-4.
- [41] C. Hu, J. Feng, Y. Cao, L. Chen, and Y. Li, “Deep eutectic solvents in sample preparation and determination methods of pesticides: Recent advances and future prospects,” *Talanta*, vol. 266, no. P2, p. 125092, 2024, doi: 10.1016/j.talanta.2023.125092.
- [42] L. W. Lun, A. Anas, N. Gunny, F. H. Kasim, and D. Arbain, “Fourier Transform Infrared Spectroscopy ( FTIR ) analysis,” vol. 020049, 2017, doi: 10.1063/1.4981871.
- [43] N. Delgado-mellado *et al.*, “Thermal stability of choline chloride deep eutectic solvents by TGA / FTIR-ATR analysis,” vol. 260, pp. 37–43, 2018, doi: 10.1016/j.molliq.2018.03.076.
- [44] N. Delgado-Mellado *et al.*, “Thermal stability of choline chloride deep eutectic solvents by TGA/FTIR-ATR analysis,” *J. Mol. Liq.*, vol. 260, pp. 37–43, 2018, doi: 10.1016/j.molliq.2018.03.076.
- [45] B. J. Finlayson-Pitts *et al.*, “Oxidation of solid thin films of neonicotinoid pesticides by gas phase hydroxyl radicals,” *Environ. Sci. Atmos.*, vol. 3, no. 1, pp. 124–142, 2022, doi: 10.1039/d2ea00134a.

- [46] M. R. A. Mogaddam, J. Khandaghi, M. A. Farajzadeh, and D. Najafzadeh, "Development of in-situ synthesis of lighter than water deep eutectic solvents under ultrasonic energy in a narrow tube and application in liquid–phase microextraction," *Int. J. Environ. Anal. Chem.*, vol. 103, no. 2, pp. 270–283, 2023, doi: 10.1080/03067319.2020.1856829.
- [47] M. Hayyan, A. Abo-hamad, M. A. Alsaadi, and M. A. Hashim, "Functionalization of graphene using deep eutectic solvents," *Nanoscale Res. Lett.*, 2015, doi: 10.1186/s11671-015-1004-2.
- [48] J. Zhao, Z. Meng, Z. Zhao, and L. Zhao, "Ultrasound-assisted deep eutectic solvent as green and efficient media combined with functionalized magnetic multi-walled carbon nanotubes as solid-phase extraction to determine pesticide residues in food products," *Food Chem.*, vol. 310, no. December 2019, p. 125863, 2020, doi: 10.1016/j.foodchem.2019.125863.
- [49] D. Dhiman, A. S. C. Marques, M. Bisht, A. P. M. Tavares, M. G. Freire, and P. Venkatesu, "to improve the conformational and colloidal stability of immunoglobulin G antibodies †," pp. 650–660, 2023, doi: 10.1039/d2gc03415h.
- [50] M. Reza, A. Mogaddam, J. Khandaghi, and M. A. Farajzadeh, "Development of in-situ synthesis of lighter than water deep eutectic solvents under ultrasonic energy in a narrow tube and application in liquid – phase microextraction," *Int. J. Environ. Anal. Chem.*, vol. 103, no. 2, pp. 270–283, 2023, doi: 10.1080/03067319.2020.1856829.
- [51] H. Wen *et al.*, "Enhancement of water barrier and antimicrobial properties of chitosan / gelatin films by hydrophobic deep eutectic solvent," *Carbohydr. Polym.*, vol. 303, no. September 2022, p. 120435, 2023, doi: 10.1016/j.carbpol.2022.120435.
- [52] B. S. Seetha, M. M. Bhandi, A. Shaikh, S. Matta, M. Krishna, and R. Mudiam, "Natural hydrophobic deep eutectic solvent based dispersive liquid-liquid microextraction followed by liquid chromatography with tandem mass spectrometry analysis of multi-class metabolites of pesticides, phthalates, and polycyclic aromatic hydrocarbons in," *Microchem. J.*, p. 110196, 2024, doi:



- 10.1016/j.microc.2024.110196.
- [53] W. Guan *et al.*, "Amine modified graphene as reversed-dispersive solid phase extraction materials combined with liquid chromatography-tandem mass spectrometry for pesticide multi-residue analysis in oil crops," *J. Chromatogr. A*, vol. 1286, pp. 1–8, 2013, doi: 10.1016/j.chroma.2013.02.043.
- [54] B. J. C. Edwards and D. Ph, "Principles of NMR," 1946.
- [55] S. K. Bharti and R. Roy, "Quantitative H NMR spectroscopy," *Trends Anal. Chem.*, vol. 35, pp. 5–26, 2012, doi: 10.1016/j.trac.2012.02.007.
- [56] U. Rovira, E. Tecnica, E. Quimica, and C. Engineering, "A brief introduction to the basics of NMR spectroscopy and selected examples of its applications to materials characterization Abstract :," pp. 1–41, 2020, doi: 10.1515/psr-2019-0086.
- [57] U. Holzgrabe, "Progress in Nuclear Magnetic Resonance Spectroscopy Quantitative NMR spectroscopy in pharmaceutical applications," *Prog. Nucl. Magn. Reson. Spectrosc.*, vol. 57, no. 2, pp. 229–240, 2010, doi: 10.1016/j.pnmrs.2010.05.001.
- [58] M. E. Di Pietro *et al.*, "In Competition for Water: Hydrated Choline Chloride:Urea vs Choline Acetate:Urea Deep Eutectic Solvents," *ACS Sustain. Chem. Eng.*, vol. 9, no. 36, pp. 12262–12273, 2021, doi: 10.1021/acssuschemeng.1c03811.
- [59] M. Maciejewski, "Basics of NMR Spectroscopy," *markm@uchc.edu*, 2016.
- [60] Z. Ju, J. Fan, Z. Meng, R. Lu, H. Gao, and W. Zhou, "A high-throughput semi-automated dispersive liquid – liquid microextraction based on deep eutectic solvent for the determination of neonicotinoid pesticides in edible oils," *Microchem. J.*, vol. 185, no. November 2022, p. 108193, 2023, doi: 10.1016/j.microc.2022.108193.
- [61] G. C. Bedendo, I. C. S. F. Jardim, and E. Carasek, "Multiresidue determination of pesticides in industrial and fresh orange juice by hollow fiber microporous membrane liquid-liquid extraction and detection by liquid chromatography-electrospray-tandem mass spectrometry," *Talanta*, vol. 88, pp. 573–580, 2012,

- doi: 10.1016/j.talanta.2011.11.037.
- [62] W. Chen *et al.*, “Matrix-Induced Sugaring-Out : A Simple and Rapid Sample Preparation Method for the Determination of,” *Molecules*, vol. 24 pp. 2-9, 2019. doi:10.3390/molecules24152761
- [63] M. Pastor-Belda *et al.*, “Determination of spirocyclic tetronic/tetramic acid derivatives and neonicotinoid insecticides in fruits and vegetables by liquid chromatography and mass spectrometry after dispersive liquid-liquid microextraction,” *Food Chem.*, vol. 202, pp. 389–395, 2016, doi: 10.1016/j.foodchem.2016.01.143.
- [64] S. Anvar Nojehdeh Sadat, R. Atazadeh, and M. R. Afshar Mogaddam, “Application of in-situ formed polymer-based dispersive solid phase extraction in combination with solidification of floating organic droplet-based dispersive liquid–liquid microextraction for the extraction of neonicotinoid pesticides from milk samples,” *J. Sep. Sci.*, vol. 46, no. 13, 2023, doi: 10.1002/jssc.202200889.
- [65] K. Nakamura, T. Otake, and N. Hanari, ‘Evaluation of pressurized liquid extraction for the determination of neonicotinoid pesticides in green onion,’ *J. Environ. Sci. Heal. - Part B Pestic. Food Contam.*,” *J. Environ. Sci. Heal. - Part B Pestic. Food Contam. Agric. Wastes*, vol. 54, no. 8, pp. 640–646, 2019, doi: 10.1080/03601234.2019.1621633.
- [66] J. Vichapong, R. Kachangoon, R. Burakham, Y. Santaladchaiyakit, and S. Srijaranai, “Ringer Tablet-Based Micelle-Mediated Extraction-Solvent Back Extraction Coupled with High-Performance Liquid Chromatography for Preconcentration and Determination of Neonicotinoid Pesticides,” *Food Anal. Methods*, vol. 15, no. 4, pp. 970–980, 2022, doi: 10.1007/s12161-021-02067-4.
- [67] R. Kachangoon, J. Vichapong, Y. Santaladchaiyakit, and S. Srijaranai, “Cloud-point extraction coupled to in-situ metathesis reaction of deep eutectic solvents for preconcentration and liquid chromatographic analysis of neonicotinoid insecticide residues in water, soil and urine samples,” *Microchem. J.*, vol. 152, no. October 2019, p. 104377, 2020, doi: 10.1016/j.microc.2019.104377.
- [68] H. Çabuk, Y. Yılmaz, and E. Yıldız, “A Vortex-Assisted Deep Eutectic Solvent-

- Based Liquid-Liquid Microextraction for the Analysis of Alkyl Gallates in Vegetable Oils,” pp. 385–394, 2019, doi: 10.17344/acsi.2018.4877.
- [69] V. A. Online, “A detailed study of cholinium chloride and levulinic acid deep eutectic solvent system for CO<sub>2</sub> capture via experimental and molecular,” pp. 49–52, 2015, doi: 10.1039/c5cp03364k.
- [70] L. G. Zepeda-vallejo and Á. D. J. Morales-ram, “Kinetics of Zn – C Battery Leaching with Choline Chloride / Urea Natural Deep Eutectic Solvents,” *MDPI.*, vol. 86, pp. 1–14, 2022, doi.org/10.3390/recycling7060086.
- [71] I. Delso, C. Lafuente, J. Muñoz-Embida, and M. Artal, “NMR study of choline chloride-based deep eutectic solvents,” *J. Mol. Liq.*, vol. 290, 2019, doi: 10.1016/j.molliq.2019.111236.
- [72] M. C. Kroon and K. Binnemans, “Degradation of Deep-Eutectic Solvents Based on Choline Chloride and Carboxylic Acids,” 2019, doi: 10.1021/acssuschemeng.9b01378.
- [73] T. T. Anna, E. L. Hannes, L. J. Tommi, V. Ali, and H. Monika, “Understanding the interactions of cellulose fibres and deep eutectic solvent of choline chloride and urea,” pp. 137–150, 2018, doi: 10.1007/s10570-017-1587-0.
- [74] Z. Yuanyuan, R. Zhixing, Y. Hao, and L. Yu, “A novel multi-criteria framework for optimizing ecotoxicological effects and human health risks of neonicotinoid insecticides: Characterization, assessment and regulation strategies,” *J. Hazard. Mater.*, vol. 432, no. March, 2022, doi: 10.1016/j.jhazmat.2022.128712.
- [75] I. Othieno, L., & Shinyekwa, “This document is discoverable and free to researchers across the globe due to the work of AgEcon Search . Help ensure our sustainability . n a l y s i s o f o m p r e h e n s i v e U t i l i z a t i o n o f o c o n u t W a s t e ,” *Trade, revenue Welf. Eff. East African Community Cust. Union Princ. Asymmetry Uganda*, 2011, doi: 10.22004/ag.econ.302462.
- [76] V. Kosar, A. M. Križanac, I. E. Zelić, S. Kurajica, and V. Tomašić, “Photocatalytic Degradation of Neonicotinoid Insecticides over Perlite-

- Supported TiO<sub>2</sub>,” *Processes*, vol. 11, no. 9, 2023, doi: 10.3390/pr11092588.
- [77] Y. Jiang, Y. Li, Y. Jiang, J. Li, and C. Pan, “Determination of multiresidues in rapeseed, rapeseed oil, and rapeseed meal by acetonitrile extraction, low-temperature cleanup, and detection by liquid chromatography with tandem mass spectrometry,” *J. Agric. Food Chem.*, vol. 60, no. 20, pp. 5089–5098, 2012, doi: 10.1021/jf3004064.
- [78] L. Sánchez-Hernández, M. Higes, M. T. Martín, M. J. Nozal, and J. L. Bernal, “Simultaneous determination of neonicotinoid insecticides in sunflower-treated seeds (hull and kernel) by LC-MS/MS,” *Food Addit. Contam. - Part A Chem. Anal. Control. Expo. Risk Assess.*, vol. 33, no. 3, pp. 442–451, 2016, doi: 10.1080/19440049.2015.1128565.
- [79] M. A. Farajzadeh, M. R. Afshar Mogaddam, and A. A. Alizadeh, “Determination of neonicotinoid insecticide residues in edible oils by water-induced homogeneous liquid-liquid extraction and dispersive liquid-liquid extraction followed by high performance liquid chromatography-diode array detection,” *RSC Adv.*, vol. 5, no. 95, pp. 77501–77507, 2015, doi: 10.1039/c5ra13059j.
- [80] F. P. Costa, S. S. Caldas, and E. G. Primel, “Comparison of QuEChERS sample preparation methods for the analysis of pesticide residues in canned and fresh peach,” *Food Chem.*, vol. 165, pp. 587–593, 2014, doi: 10.1016/j.foodchem.2014.05.099.
- [81] S. H. Kim *et al.*, “LC-MS/MS Method Minimizing Matrix Effect for the Analysis of Bifenthrin and Butachlor in Chinese Chives and Its Application for Residual Study,” *Foods*, vol. 12, no. 8, 2023, doi: 10.3390/foods12081683.
- [82] N. H. Sazali, M. Miskam, F. B. M. Suah, and N. Y. Rahim, “Analysis of herbicide mixtures in environmental samples with emulsification liquid-liquid microextraction using fatty acids deep eutectic solvents,” *Int. J. Environ. Anal. Chem.*, vol. 00, no. 00, pp. 1–20, 2022, doi: 10.1080/03067319.2022.2062570.
- [83] D. Moema, T. Makwakwa, H. N. Nyambaka, S. Dube, and M. Nindi, “Method Development and Optimization of Liquid-Liquid Microextraction Based on the Decomposition of Deep Eutectic Solvent for the Determination of Chromium (VI) in Spinach: Assessment of the Greenness Profile Using Eco-scale,

AGREE, and AGREEp<sub>rep</sub>,” *Food Anal. Methods*, no. 0123456789, 2024, doi:  
10.1007/s12161-024-02583-z.

## CHAPTER V (OVERALL CONCLUSION & FUTURE RECOMMENDATIONS)

---

### 5.1 Overall conclusion

The objective of this research was to create more environmentally friendly, quick, and effective techniques for identifying NEOs in samples of vegetable oil. Dispersive liquid-liquid extraction (DLLME) and magnetic solid phase microextraction (MSPME) were the two developed techniques. The MSPME method made use of the magnetic nanocomposites for simple separation and extraction of the adsorbed analytes using the magnetic field. The synthesised magnetic nanocomposite utilised the agricultural waste. The dried lemon peel was used to prepare the lemon solution that was used as a surfactant during synthesis. The AC has shown to play a significant role in overcoming the agglomeration from  $\text{Fe}_3\text{O}_4$ . The  $\text{Fe}_3\text{O}_4@\text{Al}_2\text{O}_3/\text{AC}$  nanocomposite was successfully synthesised, characterized and during preconcentrating of the NEOs showing high extraction recoveries. Its chemical composition and particle size was confirmed by different characterization techniques discussed in **Chapter 3**. There was an observable particle size decreased confirmed by TEM (**Figure 3.5**) and PXRD indicated the particle size increase (**Figure 3.3**). The activated carbon has proved to play a crucial role in dispersion of the nanoparticles counteracting the agglomeration limitation of the  $\text{Fe}_3\text{O}_4$ . Furthermore, it is worth to note that AC again increases the surface area for analytes adsorption. The reusability studies conducted showed good reusability of  $\text{Fe}_3\text{O}_4@\text{Al}_2\text{O}_3/\text{AC}$  in eight cycles with exponential decrease in extraction recoveries. The optimized parameters that had influence on extraction and preconcentration were extraction time, sample volume, eluent solvent, adsorbent mass, type of DES, pH and eluent volume. The  $\text{Fe}_3\text{O}_4@\text{Al}_2\text{O}_3/\text{AC}$  was successfully applied in MSPME, and it gave good extraction recoveries for the NEOs. The method GREENess was also evaluated using the AGREE tool and it was scaled at 0.54 which tell us that the method was found to fall under the range of being greener. The method accuracy was 80-119.21 % and precision were  $\leq 10$  %. The limit of detection and limit of quantification were recorded at 0.5-1.76 ng.  $\mu\text{L}^{-1}$  and 1.87-6.62 ng.  $\mu\text{L}^{-1}$ .

The DLLME method also followed the green chemistry route by using the deep eutectic solvent (DES) as the extractant. The DES were successfully synthesised, characterised, and applied for extraction of the NEOs. The successful synthesis of

DES was confirmed by the FTIR, and the NMR reported in **Chapter 4 Figure 4.5, 4.9** and **4.10**, respectively. The DES were selected because of their biocompatibility and easy synthesis. Method performance was investigated following analytical figure of merits and method GREENess evaluated using the AGREE tool. The developed method was found to be greener with a value of 0.64 from the AGREE calculator. The method also showed high accuracy of 79-119-58 %. The precision was recorded at < 0.9 % with the limit of detection and limit of quantification at 0.4-4.95 ng.  $\mu\text{L}^{-1}$  and 1.43-9.7 ng.  $\mu\text{L}^{-1}$ . According to analytical figure of merits, it has shown that the DESA-DLLME has performed better than MSPME in terms of extraction recoveries and precision.

Furthermore, in comparison of the two developed method, the DLLME was found to be greener compared to MSPME according to the principles of green analytical chemistry (GAC). The use of the green solvent (DES) is one of the contributing factors to these results. Moreover, it is worth to note that the DLLME method was also more rapid than the MSPME method with less tedious steps and use of less amount of organic solvents while generating less hazardous waste. The extraction time for DLLME was 4.5 min whereas for MSPME was 8 min. additionally, with the GREENess evaluation, due to the GAC principle DLLME was found to be greener compared to MSPME with 0.67 scale over 0.54. DLLME was also more precise than MSPME. This overall conclusion is that DLLME method is better compared to MSPME, because it is greener, rapid and efficient. The shortcoming with characterization with BET to check the surface area, pore size and pore diameter for the  $\text{Fe}_3\text{O}_4$ ,  $\text{Fe}_3\text{O}_4@\text{Al}_2\text{O}_3$  and  $\text{Fe}_3\text{O}_4@\text{Al}_2\text{O}_3/\text{AC}$  nanocomposite for future work due to malfunctioning of the instrument.

## 5.2 Future recommendations

The synthesis route of  $\text{Fe}_3\text{O}_4$  need to be reconsidered since the thermal decomposition method on this study made use of high temperatures of 250 °C which was human not human friendly and consumed lot of energy. Alternatively, the silicone oil heating can be replaced with using the sand bath which does not subject an individual to dangers of getting burnt. When using silicone oil bath, once a drop of water falls inside the heating oil it starts to bubble out spreading hot drops of oils. The AC need to be further explored since it has shown excellent activity with counteracting

the agglomeration from the  $\text{Fe}_3\text{O}_4$ . Furthermore, the larger surface area of the AC has also contributed to high extraction recoveries of which it can be retained as a supporting material for the  $\text{Fe}_3\text{O}_4$ . For characterization of the  $\text{Fe}_3\text{O}_4@/\text{Al}_2\text{O}_3/\text{AC}$  and its fragments need to be done to confirm the thermal stability, surface area, pore volume and pore diameter of the nanocomposite. Since the performance of DES 3 (CCl:Urea) in terms of extraction recoveries was relatively good in this study, it is recommended for further studies on determination of these pesticides.

The method performance of MSPME has proved that this method can be applied due to its simple separation using the magnetic field is the selling point for its preference. Moreover, the robustness, selectivity and sensitivity of the method is acceptable with only the shortcoming of the synthetic method of the adsorbent. The statistical studies need to be further explored.

The LC-MS can be used for further analysis of real samples because it is more sensitive and precise being able to show the fingerprint of the analytes.



## APPENDIX

### Preamble

This section shows the design of experiments tables and supporting information for factorial design and response surface methodology that were used on magnetic solid phase microextraction and deep eutectic solvent dispersive liquid liquid microextraction as discussed in Chapter 3 and 4.

Magnetic solid phase microextraction optimization

**TS1:** Screening (FFD) design of experiment

RunOrder	time (min)	pH	desorption vol (mL)	sorbent mass (mg)	%R ACT	%R IMI	%R TCL	%R TCL
1	2	3	0,5	20	106,10	66,28	77,10	108,10
2	8	3	0,5	20	94,00	74,13	68,60	76,80
3	2	11	0,5	20	83,07	115,61	97,93	68,42
4	8	11	0,5	20	84,13	92,38	66,90	86,03
5	2	3	1,0	20	89,00	111,12	70,90	98,82
6	8	3	1,0	20	96,70	98,76	89,20	83,46
7	2	11	1,0	20	87,15	84,85	38,73	60,36
8	8	11	1,0	20	63,79	116,03	47,50	68,10
9	2	3	0,5	90	74,56	70,52	72,50	99,32
10	8	3	0,5	90	90,15	65,94	118,73	68,55

11	2	11	0,5	90	87,15	46,84	99,70	58,02
12	8	11	0,5	90	118,64	59,22	88,41	113,17
13	2	3	1,0	90	86,43	87,97	58,70	99,04
14	8	3	1,0	90	58,70	64,70	79,60	66,58
15	2	11	1,0	90	79,00	69,67	59,50	75,01
16	8	11	1,0	90	96,88	84,78	43,00	86,10

**TS2:** Response surface methodology (RSM) central composite design (CCD)

RunOrder	pH	Sorbent mass	Eluent vol	Recoveries ACT	Recoveries TCL	Recoveries IMI	Recoveries TMX
1	3,0000	90,000	0,50000	81,25	106,10	108,62	85,00
2	7,0000	55,000	0,75000	74,80	94,00	119,18	83,20
3	7,0000	113,863	0,75000	37,39	55,00	66,80	51,00
4	7,0000	55,000	0,75000	70,90	98,54	115,66	83,04
5	7,0000	55,000	1,17045	53,80	68,00	70,50	58,20
6	7,0000	55,000	0,32955	73,40	84,13	89,83	76,60
7	11,0000	90,000	0,50000	71,00	89,10	105,60	81,36
8	11,0000	20,000	0,50000	61,01	87,18	95,42	76,70
9	11,0000	90,000	1,00000	70,08	87,15	119,20	81,90
10	7,0000	55,000	0,75000	58,04	68,30	90,69	63,79
11	7,0000	55,000	0,75000	74,56	92,79	99,74	79,30

---

12	7,0000	3,863	0,75000	91,01	114,68	118,12	110,10
13	11,0000	20,000	1,00000	32,53	69,70	73,80	53,50
14	3,0000	90,000	1,00000	60,16	87,15	105,86	78,16
15	13,7272	55,000	0,75000	99,09	109,17	118,64	99,74
16	7,0000	55,000	0,75000	81,25	91,08	119,20	86,43
17	7,0000	55,000	0,75000	48,91	70,08	83,20	58,70
18	3,0000	20,000	0,50000	79,40	83,36	98,10	80,04
19	0,2728	55,000	0,75000	58,87	78,54	82,79	66,30
20	3,0000	20,000	1,00000	76,46	98,03	111,35	96,88

---

## Response Surface Regression: Recoveries Acet versus pH. ... Eluent vol Analysis of Variance

Source	DF	Adj SS	Adj MS	F-Value	P-Value
Model	9	5934,0	659,34	0,56	0,805
Linear	3	4039,2	1346,41	1,13	0,382
pH	1	623,4	623,40	0,53	0,485
Sorbent mass	1	230,2	230,23	0,19	0,669
Eluent vol	1	3185,6	3185,60	2,68	0,132
Square	3	1218,5	406,18	0,34	0,795
pH*pH	1	123,2	123,19	0,10	0,754
Sorbent mass*Sorbent mass	1	123,6	123,59	0,10	0,754
Eluent vol*Eluent vol	1	871,5	871,55	0,73	0,412
2-Way Interaction	3	717,7	239,23	0,20	0,893
pH*Sorbent mass	1	109,2	109,15	0,09	0,768
pH*Eluent vol	1	527,3	527,31	0,44	0,520
Sorbent mass*Eluent vol	1	81,2	81,22	0,07	0,799
Error	10	11868,0	1186,80		
Lack-of-Fit	5	10938,2	2187,64	11,76	0,009
Pure Error	5	929,8	185,95		
Total	19	17802,0			

### Model Summary

S	R-sq	R-sq(adj)	R-sq(pred)
34,4499	33,33%	0,00%	0,00%

### Coded Coefficients

Term	Coef	SE Coef	T-Value	P-Value	VIF
Constant	76,8	14,0	5,49	0,000	
pH	6,76	9,32	0,72	0,485	1,00
Sorbent mass	-4,25	9,64	-0,44	0,669	1,01
Eluent vol	-15,27	9,32	-1,64	0,132	1,00
pH*pH	2,92	9,05	0,32	0,754	1,01
Sorbent mass*Sorbent mass	3,2	10,0	0,32	0,754	1,02
Eluent vol*Eluent vol	-7,76	9,05	-0,86	0,412	1,01
pH*Sorbent mass	3,7	12,2	0,30	0,768	1,00
pH*Eluent vol	-8,1	12,2	-0,67	0,520	1,00
Sorbent mass*Eluent vol	3,2	12,2	0,26	0,799	1,00

### Regression Equation in Uncoded Units

$$\begin{aligned}
 \text{Recoveries Acet} &= 47 + 3,8 \text{ pH} - 0,87 \text{ Sorbent mass} + 162 \text{ Eluent vol} + 0,182 \text{ pH}^2 \\
 &+ 0,00263 \text{ Sorbent mass}^2 - 124 \text{ Eluent vol}^2 \\
 &+ 0,0264 \text{ pH} \cdot \text{Sorbent mass} - 8,1 \text{ pH} \cdot \text{Eluent vol} \\
 &+ 0,36 \text{ Sorbent mass} \cdot \text{Eluent vol}
 \end{aligned}$$

## Fits and Diagnostics for Unusual Observations

Obs	Recoveries				R
	Acet	Fit	Resid	Std Resid	
1	106,1	64,5	41,6	2,10	R
19	25,9	73,7	-47,9	-2,23	R

R Large residual

## Response Surface Regression: Recoveries TCL versus pH. ... . Eluent vol

### Analysis of Variance

Source	DF	Adj SS	Adj MS	F-Value	P-Value
Model	9	5863,3	651,47	1,37	0,314
Linear	3	1704,9	568,29	1,20	0,360
pH	1	243,7	243,73	0,51	0,490
Sorbent mass	1	790,5	790,45	1,66	0,226
Eluent vol	1	670,7	670,69	1,41	0,262
Square	3	3680,2	1226,72	2,58	0,112
pH*pH	1	443,9	443,86	0,93	0,356
Sorbent mass*Sorbent mass	1	684,1	684,08	1,44	0,258
Eluent vol*Eluent vol	1	2240,9	2240,90	4,72	0,055
2-Way Interaction	3	649,8	216,60	0,46	0,719
pH*Sorbent mass	1	608,0	607,96	1,28	0,284
pH*Eluent vol	1	5,0	4,96	0,01	0,921
Sorbent mass*Eluent vol	1	36,9	36,89	0,08	0,786
Error	10	4749,5	474,95		
Lack-of-Fit	5	4224,0	844,79	8,04	0,020
Pure Error	5	525,5	105,10		
Total	19	10612,7			

### Model Summary

S	R-sq	R-sq(adj)	R-sq(pred)
21,7932	55,25%	14,97%	0,00%

### Coded Coefficients

Term	Coef	SE Coef	T-Value	P-Value	VIF
Constant	82,16	8,85	9,28	0,000	
pH	4,22	5,90	0,72	0,490	1,00
Sorbent mass	-7,87	6,10	-1,29	0,226	1,01
Eluent vol	-7,01	5,90	-1,19	0,262	1,00
pH*pH	5,54	5,73	0,97	0,356	1,01

Sorbent mass*Sorbent mass	7,59	6,32	1,20	0,258	1,02
Eluent vol*Eluent vol	-12,44	5,73	-2,17	0,055	1,01
pH*Sorbent mass	-8,72	7,71	-1,13	0,284	1,00
pH*Eluent vol	-0,79	7,71	-0,10	0,921	1,00
Sorbent mass*Eluent vol	2,15	7,71	0,28	0,786	1,00

### Regression Equation in Uncoded Units

$$\begin{aligned} \text{Recoveries TCL} = & 13,9 + 0,23 \text{ pH} - 0,654 \text{ Sorbent mass} + 263 \text{ Eluent vol} + 0,346 \text{ pH} \cdot \text{pH} \\ & + 0,00620 \text{ Sorbent mass} \cdot \text{Sorbent mass} - 199,0 \text{ Eluent vol} \cdot \text{Eluent vol} \\ & - 0,0623 \text{ pH} \cdot \text{Sorbent mass} - 0,79 \text{ pH} \cdot \text{Eluent vol} \\ & + 0,245 \text{ Sorbent mass} \cdot \text{Eluent vol} \end{aligned}$$

### Fits and Diagnostics for Unusual Observations

Obs	Recoveries TCL	Fit	Resid	Std Resid	
5	0,0	35,2	-35,2	-2,60	R
14	105,9	75,4	30,5	2,43	R

R Large residual

### Response Surface Regression: Recoveries lmi versus pH. ... . Eluent vol Analysis of Variance

Source	DF	Adj SS	Adj MS	F-Value	P-Value
Model	9	8047,5	894,2	0,88	0,569
Linear	3	2873,2	957,7	0,95	0,455
pH	1	761,0	761,0	0,75	0,406
Sorbent mass	1	779,0	779,0	0,77	0,401
Eluent vol	1	1333,2	1333,2	1,32	0,278
Square	3	3596,0	1198,7	1,18	0,364
pH*pH	1	172,9	172,9	0,17	0,688
Sorbent mass*Sorbent mass	1	107,6	107,6	0,11	0,751
Eluent vol*Eluent vol	1	3082,3	3082,3	3,05	0,112
2-Way Interaction	3	1660,6	553,5	0,55	0,661
pH*Sorbent mass	1	819,9	819,9	0,81	0,389
pH*Eluent vol	1	434,1	434,1	0,43	0,527
Sorbent mass*Eluent vol	1	406,6	406,6	0,40	0,540
Error	10	10121,6	1012,2		
Lack-of-Fit	5	6136,5	1227,3	1,54	0,324
Pure Error	5	3985,1	797,0		
Total	19	18169,1			

### Model Summary

S	R-sq	R-sq(adj)	R-sq(pred)
31,8145	44,29%	0,00%	0,00%

### Coded Coefficients

Term	Coef	SE Coef	T-Value	P-Value	VIF
Constant	94,6	12,9	7,32	0,000	
pH	7,47	8,61	0,87	0,406	1,00
Sorbent mass	-7,81	8,90	-0,88	0,401	1,01
Eluent vol	-9,88	8,61	-1,15	0,278	1,00
pH*pH	3,46	8,36	0,41	0,688	1,01
Sorbent mass*Sorbent mass	3,01	9,23	0,33	0,751	1,02
Eluent vol*Eluent vol	-14,59	8,36	-1,75	0,112	1,01
pH*Sorbent mass	10,1	11,2	0,90	0,389	1,00
pH*Eluent vol	7,4	11,2	0,65	0,527	1,00
Sorbent mass*Eluent vol	-7,1	11,2	-0,63	0,540	1,00

### Regression Equation in Uncoded Units

$$\begin{aligned} \text{Recoveries} &= 43 - 10,7 \text{ pH} - 0,39 \text{ Sorbent mass} + 304 \text{ Eluent vol} + 0,216 \text{ pH}^2 \\ \text{Imi} &+ 0,00246 \text{ Sorbent mass}^2 - 233 \text{ Eluent vol}^2 \\ &+ 0,0723 \text{ pH}^2 \text{ Sorbent mass} + 7,4 \text{ pH}^2 \text{ Eluent vol} \\ &- 0,81 \text{ Sorbent mass}^2 \text{ Eluent vol} \end{aligned}$$

### Response Surface Regression: Recoveries TMX versus ... ass. Eluent vol Analysis of Variance

Source	DF	Adj SS	Adj MS	F-Value	P-Value
Model	9	4736,38	526,26	1,09	0,447
Linear	3	2044,75	681,58	1,41	0,298
pH	1	248,51	248,51	0,51	0,490
Sorbent mass	1	185,29	185,29	0,38	0,550
Eluent vol	1	1610,94	1610,94	3,32	0,098
Square	3	2364,62	788,21	1,63	0,245
pH*pH	1	416,55	416,55	0,86	0,376
Sorbent mass*Sorbent mass	1	61,58	61,58	0,13	0,729
Eluent vol*Eluent vol	1	1723,73	1723,73	3,55	0,089
2-Way Interaction	3	304,28	101,43	0,21	0,888
pH*Sorbent mass	1	214,76	214,76	0,44	0,521
pH*Eluent vol	1	48,07	48,07	0,10	0,759
Sorbent mass*Eluent vol	1	41,45	41,45	0,09	0,776
Error	10	4849,68	484,97		
Lack-of-Fit	5	4057,33	811,47	5,12	0,049
Pure Error	5	792,34	158,47		
Total	19	9586,06			

### Model Summary

S	R-sq	R-sq(adj)	R-sq(pred)
22,0220	49,41%	3,88%	0,00%

### Coded Coefficients

Term	Coef	SE Coef	T-Value	P-Value	VIF
Constant	79,67	8,95	8,90	0,000	
pH	-4,27	5,96	-0,72	0,490	1,00
Sorbent mass	-3,81	6,16	-0,62	0,550	1,01
Eluent vol	-10,86	5,96	-1,82	0,098	1,00
pH*pH	5,36	5,79	0,93	0,376	1,01
Sorbent mass*Sorbent mass	-2,28	6,39	-0,36	0,729	1,02
Eluent vol*Eluent vol	-10,91	5,79	-1,89	0,089	1,01
pH*Sorbent mass	5,18	7,79	0,67	0,521	1,00
pH*Eluent vol	-2,45	7,79	-0,31	0,759	1,00
Sorbent mass*Eluent vol	-2,28	7,79	-0,29	0,776	1,00

### Regression Equation in Uncoded Units

$$\begin{aligned} \text{Recoveries TMX} = & 29,0 - 5,96 \text{ pH} + 0,032 \text{ Sorbent mass} + 250 \text{ Eluent vol} + 0,335 \text{ pH}^2 \\ & - 0,00186 \text{ Sorbent mass}^2 - 174,5 \text{ Eluent vol}^2 \\ & + 0,0370 \text{ pH} \cdot \text{Sorbent mass} - 2,45 \text{ pH} \cdot \text{Eluent vol} \\ & - 0,260 \text{ Sorbent mass} \cdot \text{Eluent vol} \end{aligned}$$

### Fits and Diagnostics for Unusual Observations

Obs	Recoveries TMX	Fit	Resid	Std Resid	
5	0,0	30,5	-30,5	-2,23	R

*R Large residual*



## Dispersive liquid liquid microextraction optimization

### TS3: Screening (FFD) design of experiment

StdOrder	Extraction time	Eluent vol	DES vol	Eluting time	pH	%R TMX	%R ACT	%R IMI	% TCL
1	2	0,5	0,5	20	8	91,3	76,0	88	82,3
2	7	0,5	0,5	20	5	118,2	77,0	110,9	96
3	2	2,0	0,5	20	5	96,8	84,0	66,4	116
4	7	2,0	0,5	20	8	120,1	112,0	96	112,8
5	2	0,5	1,1	20	5	104,8	104,2	93,7	73
6	7	0,5	1,1	20	8	62,3	95,0	83	66
7	2	2,0	1,1	20	8	110	113,0	96	67
8	7	2,0	1,1	20	5	62,8	91,0	86	98,3
9	2	0,5	0,5	60	5	93,0	123,0	99	72,3
10	7	0,5	0,5	60	8	91,1	91,0	68	88,6
11	2	2,0	0,5	60	8	109,0	83,0	56	84,1
12	7	2,0	0,5	60	5	83,0	122,0	83	55,2
13	2	0,5	1,1	60	8	103,0	98,0	69	78
14	7	0,5	1,1	60	5	67,0	84,0	66	86
15	2	2,0	1,1	60	5	103,0	94,0	55	52
16	7	2,0	1,1	60	8	68,0	84,0	61	69

**TS4: Response surface methodology (RSM) central composite design (CCD)**

RunOrder	DES Vol	Extraction time	Eluent vol	Eluting time	%R TMX	%R ACT	%R IMI	%R TCL
1	1,1	2,0	0,50	20	122,63	57,28	84,25	95,75
2	0,5	7,0	0,50	20	110,70	98,95	92,25	82,75
3	0,5	2,0	2,00	20	63,62	116,28	56,58	61,08
4	1,1	7,0	2,00	20	84,96	88,95	83,91	63,41
5	0,5	2,0	0,50	60	51,63	74,95	63,58	83,75
6	1,1	7,0	0,50	60	84,63	66,62	95,25	96,75
7	1,1	2,0	2,00	60	111,96	80,28	89,35	88,90
8	0,5	7,0	2,00	60	94,63	126,28	114,58	74,40
9	0,8	4,5	1,25	40	119,63	110,28	107,58	80,41
10	0,8	4,5	1,25	40	121,63	96,28	125,58	70,41
11	0,5	2,0	0,50	20	95,30	110,62	109,61	66,75
12	1,1	7,0	0,50	20	78,96	56,95	62,58	121,75
13	1,1	2,0	2,00	20	95,96	78,28	64,58	101,41
14	0,5	7,0	2,00	20	62,63	102,28	79,25	100,41
15	1,1	2,0	0,50	60	66,63	107,95	119,95	108,75
16	0,5	7,0	0,50	60	63,30	54,62	117,25	91,08
17	0,5	2,0	2,00	60	82,30	120,95	119,58	60,75

---

18	1,1	7,0	2,00	60	116,37	107,62	117,25	57,41
19	0,8	4,5	1,25	40	95,96	109,95	124,25	196,41
20	0,8	4,5	1,25	40	70,96	58,62	118,38	75,56
21	0,2	4,5	1,25	40	50,30	99,95	119,91	65,20
22	1,4	4,5	1,25	40	74,63	78,95	96,58	80,08
23	0,8	0,5	1,25	40	71,30	121,62	94,25	72,75
24	0,8	9,5	1,25	40	59,30	66,62	113,58	65,08
25	0,8	4,5	0,25	40	61,63	107,04	123,58	75,50
26	0,8	4,5	2,75	40	102,70	53,62	107,91	96,08
27	0,8	4,5	1,25	0	123,96	119,62	106,58	93,08
28	0,8	4,5	1,25	80	51,96	119,95	83,91	65,08
29	0,8	4,5	1,25	40	76,30	88,62	112,58	75,36
30	0,8	4,5	1,25	40	77,63	117,62	116,91	65,41

---

## Response Surface Regression: %R TMX versus Blocks. ... I. Eluting time Analysis of Variance

Source	DF	Adj SS	Adj MS	F-Value	P-Value
Model	16	30118,8	1882,42	1,95	0,116
Blocks	2	12212,4	6106,18	6,31	0,012
Linear	4	6418,4	1604,61	1,66	0,219
DES Vol	1	3447,6	3447,61	3,56	0,082
Extraction tim	1	56,6	56,58	0,06	0,813
Eluent vol	1	60,8	60,83	0,06	0,806
Eluting time	1	2853,4	2853,40	2,95	0,110
Square	4	2532,0	633,01	0,65	0,634
DES Vol*DES Vol	1	0,0	0,04	0,00	0,995
Extraction tim*Extraction tim	1	12,3	12,35	0,01	0,912
Eluent vol*Eluent vol	1	1589,6	1589,62	1,64	0,222
Eluting time*Eluting time	1	1042,2	1042,17	1,08	0,318
2-Way Interaction	6	8956,0	1492,66	1,54	0,240
DES Vol*Extraction tim	1	98,4	98,36	0,10	0,755
DES Vol*Eluent vol	1	453,2	453,16	0,47	0,506
DES Vol*Eluting time	1	4340,5	4340,50	4,48	0,054
Extraction tim*Eluent vol	1	2871,6	2871,62	2,97	0,109
Extraction tim*Eluting time	1	269,5	269,53	0,28	0,607
Eluent vol*Eluting time	1	922,8	922,79	0,95	0,347
Error	13	12581,3	967,79		
Lack-of-Fit	10	11962,6	1196,26	5,80	0,087
Pure Error	3	618,7	206,23		
Total	29	42700,0			

### Model Summary

S	R-sq	R-sq(adj)	R-sq(pred)
31,1093	70,54%	34,27%	0,00%

### Coded Coefficients

Term	Coef	SE Coef	T-Value	P-Value	VIF
Constant	152,0	12,7	11,97	0,000	
Blocks					
1	-27,30	8,03	-3,40	0,005	1,33
2	20,83	8,03	2,59	0,022	1,33
DES Vol	11,99	6,35	1,89	0,082	1,00
Extraction tim	-1,54	6,35	-0,24	0,813	1,00
Eluent vol	-1,59	6,35	-0,25	0,806	1,00
Eluting time	10,90	6,35	1,72	0,110	1,00
DES Vol*DES Vol	-0,04	5,94	-0,01	0,995	1,05

Extraction tim*Extraction tim	0,67	5,94	0,11	0,912	1,05
Eluent vol*Eluent vol	-7,61	5,94	-1,28	0,222	1,05
Eluting time*Eluting time	-6,16	5,94	-1,04	0,318	1,05
DES Vol*Extraction tim	-2,48	7,78	-0,32	0,755	1,00
DES Vol*Eluent vol	5,32	7,78	0,68	0,506	1,00
DES Vol*Eluting time	-16,47	7,78	-2,12	0,054	1,00
Extraction tim*Eluent vol	13,40	7,78	1,72	0,109	1,00
Extraction tim*Eluting time	4,10	7,78	0,53	0,607	1,00
Eluent vol*Eluting time	-7,59	7,78	-0,98	0,347	1,00

### Regression Equation in Uncoded Units

$$\begin{aligned}
 \%R \text{ TMX} = & 13,3 + 136 \text{ DES Vol} - 11,2 \text{ Extraction tim} + 0,9 \text{ Eluent vol} + 4,24 \text{ Eluting time} \\
 & - 0,4 \text{ DES Vol*DES Vol} + 0,107 \text{ Extraction tim*Extraction tim} \\
 & - 13,5 \text{ Eluent vol*Eluent vol} - 0,0154 \text{ Eluting time*Eluting time} \\
 & - 3,3 \text{ DES Vol*Extraction tim} + 23,7 \text{ DES Vol*Eluent vol} - 2,75 \text{ DES Vol*Eluting time} \\
 & + 7,14 \text{ Extraction tim*Eluent vol} + 0,082 \text{ Extraction tim*Eluting time} \\
 & - 0,506 \text{ Eluent vol*Eluting time}
 \end{aligned}$$

Equation averaged over blocks.

### Fits and Diagnostics for Unusual Observations

Obs	%R TMX	Fit	Resid	Std Resid	
2	10,7	55,0	-44,3	-2,41	R
7	142,0	100,6	41,3	2,25	R

R Large residual

### Effects Pareto for %R ACT

### Response Surface Regression: % ACT versus Blocks. DES ... luting time Analysis of Variance

Source	DF	Adj SS	Adj MS	F-Value	P-Value
Model	16	48014,5	3000,9	2,14	0,086
Blocks	2	17829,0	8914,5	6,36	0,012
Linear	4	1832,8	458,2	0,33	0,855
DES Vol	1	630,4	630,4	0,45	0,514
Extraction tim	1	86,9	86,9	0,06	0,807
Eluent vol	1	182,3	182,3	0,13	0,724
Eluting time	1	933,3	933,3	0,67	0,429
Square	4	99,6	24,9	0,02	0,999
DES Vol*DES Vol	1	2,9	2,9	0,00	0,964
Extraction tim*Extraction tim	1	61,3	61,3	0,04	0,838
Eluent vol*Eluent vol	1	8,2	8,2	0,01	0,940
Eluting time*Eluting time	1	19,3	19,3	0,01	0,908
2-Way Interaction	6	28253,1	4708,8	3,36	0,032
DES Vol*Extraction tim	1	430,4	430,4	0,31	0,589
DES Vol*Eluent vol	1	25574,4	25574,4	18,24	0,001
DES Vol*Eluting time	1	47,8	47,8	0,03	0,856

Extraction tim*Eluent vol	1	0,6	0,6	0,00	0,984
Extraction tim*Eluting time	1	1884,9	1884,9	1,34	0,267
Eluent vol*Eluting time	1	315,1	315,1	0,22	0,643
Error	13	18223,7	1401,8		
Lack-of-Fit	10	14389,2	1438,9	1,13	0,520
Pure Error	3	3834,5	1278,2		
Total	29	66238,2			

## Model Summary

S	R-sq	R-sq(adj)	R-sq(pred)
37,4410	72,49%	38,63%	0,00%

## Coded Coefficients

Term	Coef	SE Coef	T-Value	P-Value	VIF
Constant	147,1	15,3	9,62	0,000	
Blocks					
1	34,33	9,67	3,55	0,004	1,33
2	-14,40	9,67	-1,49	0,160	1,33
DES Vol	-5,13	7,64	-0,67	0,514	1,00
Extraction tim	1,90	7,64	0,25	0,807	1,00
Eluent vol	2,76	7,64	0,36	0,724	1,00
Eluting time	-6,24	7,64	-0,82	0,429	1,00
DES Vol*DES Vol	0,33	7,15	0,05	0,964	1,05
Extraction tim*Extraction tim	1,49	7,15	0,21	0,838	1,05
Eluent vol*Eluent vol	0,55	7,15	0,08	0,940	1,05
Eluting time*Eluting time	-0,84	7,15	-0,12	0,908	1,05
DES Vol*Extraction tim	-5,19	9,36	-0,55	0,589	1,00
DES Vol*Eluent vol	39,98	9,36	4,27	0,001	1,00
DES Vol*Eluting time	-1,73	9,36	-0,18	0,856	1,00
Extraction tim*Eluent vol	0,19	9,36	0,02	0,984	1,00
Extraction tim*Eluting time	-10,85	9,36	-1,16	0,267	1,00
Eluent vol*Eluting time	-4,44	9,36	-0,47	0,643	1,00

## Regression Equation in Uncoded Units

$$\begin{aligned}
 \% \text{ ACT} = & 261 - 202 \text{ DES Vol} + 12,7 \text{ Extraction tim} - 129,5 \text{ Eluent vol} + 1,43 \text{ Eluting time} \\
 & + 3,6 \text{ DES Vol*DES Vol} + 0,24 \text{ Extraction tim*Extraction tim} \\
 & + 1,0 \text{ Eluent vol*Eluent vol} - 0,0021 \text{ Eluting time*Eluting time} \\
 & - 6,9 \text{ DES Vol*Extraction tim} + 177,7 \text{ DES Vol*Eluent vol} - 0,29 \text{ DES Vol*Eluting time} \\
 & + 0,10 \text{ Extraction tim*Eluent vol} - 0,217 \text{ Extraction tim*Eluting time} \\
 & - 0,296 \text{ Eluent vol*Eluting time}
 \end{aligned}$$

Equation averaged over blocks.

## Fits and Diagnostics for Unusual Observations

Obs	% ACT	Fit	Resid	Std Resid
2	298,9	243,1	55,9	2,52 R

9 110,3 181,4 -71,1 -2,17 R  
*R Large residual*

### Effects Pareto for %R IMI

### Response Surface Regression: %R IMI versus Blocks. DES ... luting time Analysis of Variance

Source	DF	Adj SS	Adj MS	F-Value	P-Value
Model	16	16210,6	1013,16	1,92	0,121
Blocks	2	826,7	413,35	0,78	0,478
Linear	4	5463,9	1365,98	2,58	0,086
DES Vol	1	842,8	842,77	1,59	0,229
Extraction tim	1	29,3	29,26	0,06	0,818
Eluent vol	1	2223,0	2222,99	4,21	0,061
Eluting time	1	2368,9	2368,90	4,48	0,054
Square	4	2805,0	701,25	1,33	0,312
DES Vol*DES Vol	1	63,5	63,48	0,12	0,734
Extraction tim*Extraction tim	1	1107,3	1107,30	2,09	0,171
Eluent vol*Eluent vol	1	316,4	316,38	0,60	0,453
Eluting time*Eluting time	1	1991,6	1991,64	3,77	0,074
2-Way Interaction	6	7115,0	1185,84	2,24	0,105
DES Vol*Extraction tim	1	279,6	279,56	0,53	0,480
DES Vol*Eluent vol	1	2156,7	2156,67	4,08	0,064
DES Vol*Eluting time	1	59,4	59,37	0,11	0,743
Extraction tim*Eluent vol	1	4062,8	4062,79	7,69	0,016
Extraction tim*Eluting time	1	60,5	60,45	0,11	0,741
Eluent vol*Eluting time	1	496,2	496,18	0,94	0,350
Error	13	6871,1	528,55		
Lack-of-Fit	10	6369,9	636,99	3,81	0,149
Pure Error	3	501,2	167,07		
Total	29	23081,8			

### Model Summary

S	R-sq	R-sq(adj)	R-sq(pred)
22,9902	70,23%	33,59%	0,00%

### Coded Coefficients

Term	Coef	SE Coef	T-Value	P-Value	VIF
Constant	122,55	9,39	13,06	0,000	
Blocks					
1	-7,42	5,94	-1,25	0,233	1,33
2	3,56	5,94	0,60	0,560	1,33
DES Vol	-5,93	4,69	-1,26	0,229	1,00
Extraction tim	-1,10	4,69	-0,24	0,818	1,00

Eluent vol	-9,62	4,69	-2,05	0,061	1,00
Eluting time	9,94	4,69	2,12	0,054	1,00
DES Vol*DES Vol	-1,52	4,39	-0,35	0,734	1,05
Extraction tim*Extraction tim	-6,35	4,39	-1,45	0,171	1,05
Eluent vol*Eluent vol	-3,40	4,39	-0,77	0,453	1,05
Eluting time*Eluting time	-8,52	4,39	-1,94	0,074	1,05
DES Vol*Extraction tim	4,18	5,75	0,73	0,480	1,00
DES Vol*Eluent vol	11,61	5,75	2,02	0,064	1,00
DES Vol*Eluting time	-1,93	5,75	-0,34	0,743	1,00
Extraction tim*Eluent vol	15,94	5,75	2,77	0,016	1,00
Extraction tim*Eluting time	-1,94	5,75	-0,34	0,741	1,00
Eluent vol*Eluting time	5,57	5,75	0,97	0,350	1,00

### Regression Equation in Uncoded Units

$$\begin{aligned} \%R &= 182,3 - 69 \text{ DES Vol} - 4,8 \text{ Extraction tim} - 92,1 \text{ Eluent vol} + 2,17 \text{ Eluting time} \\ \text{IMI} &- 16,9 \text{ DES Vol*DES Vol} - 1,017 \text{ Extraction tim*Extraction tim} \\ &- 6,04 \text{ Eluent vol*Eluent vol} - 0,0213 \text{ Eluting time*Eluting time} \\ &+ 5,57 \text{ DES Vol*Extraction tim} + 51,6 \text{ DES Vol*Eluent vol} \\ &- 0,321 \text{ DES Vol*Eluting time} \\ &+ 8,50 \text{ Extraction tim*Eluent vol} - 0,039 \text{ Extraction tim*Eluting time} \\ &+ 0,371 \text{ Eluent vol*Eluting time} \end{aligned}$$

Equation averaged over blocks.

### Fits and Diagnostics for Unusual Observations

Obs	%R IMI	Fit	Resid	Std Resid	
27	106,6	72,5	34,1	2,51	R
28	83,9	112,2	-28,3	-2,08	R

R Large residual

### Effects Pareto for % TCL

### Response Surface Regression: %R TCL versus Blocks. DES ... uting time Analysis of Variance

Source	DF	Adj SS	Adj MS	F-Value	P-Value
Model	16	58810	3675,6	0,87	0,612
Blocks	2	35009	17504,4	4,13	0,041
Linear	4	13644	3411,1	0,80	0,544
DES Vol	1	235	234,9	0,06	0,818
Extraction tim	1	1298	1298,3	0,31	0,589
Eluent vol	1	604	604,0	0,14	0,712
Eluting time	1	11507	11507,1	2,71	0,123
Square	4	2966	741,5	0,17	0,947
DES Vol*DES Vol	1	806	806,4	0,19	0,670
Extraction tim*Extraction tim	1	553	553,2	0,13	0,724
Eluent vol*Eluent vol	1	2081	2080,6	0,49	0,496
Eluting time*Eluting time	1	6	6,0	0,00	0,971



2-Way Interaction	6	7191	1198,5	0,28	0,935
DES Vol*Extraction tim	1	1478	1478,4	0,35	0,565
DES Vol*Eluent vol	1	1336	1335,5	0,31	0,584
DES Vol*Eluting time	1	172	172,3	0,04	0,843
Extraction tim*Eluent vol	1	4	4,2	0,00	0,975
Extraction tim*Eluting time	1	3974	3974,0	0,94	0,351
Eluent vol*Eluting time	1	226	226,4	0,05	0,821
Error	13	55143	4241,8		
Lack-of-Fit	10	54876	5487,6	61,69	0,003
Pure Error	3	267	89,0		
Total	29	113953			

### Model Summary

S	R-sq	R-sq(adj)	R-sq(pred)
65,1290	51,61%	0,00%	0,00%

### Coded Coefficients

Term	Coef	SE Coef	T-Value	P-Value	VIF
Constant	178,9	26,6	6,73	0,000	
Blocks					
1	48,3	16,8	2,87	0,013	1,33
2	-24,2	16,8	-1,44	0,173	1,33
DES Vol	-3,1	13,3	-0,24	0,818	1,00
Extraction tim	-7,4	13,3	-0,55	0,589	1,00
Eluent vol	-5,0	13,3	-0,38	0,712	1,00
Eluting time	-21,9	13,3	-1,65	0,123	1,00
DES Vol*DES Vol	5,4	12,4	0,44	0,670	1,05
Extraction tim*Extraction tim	4,5	12,4	0,36	0,724	1,05
Eluent vol*Eluent vol	8,7	12,4	0,70	0,496	1,05
Eluting time*Eluting time	-0,5	12,4	-0,04	0,971	1,05
DES Vol*Extraction tim	-9,6	16,3	-0,59	0,565	1,00
DES Vol*Eluent vol	-9,1	16,3	-0,56	0,584	1,00
DES Vol*Eluting time	3,3	16,3	0,20	0,843	1,00
Extraction tim*Eluent vol	0,5	16,3	0,03	0,975	1,00
Extraction tim*Eluting time	15,8	16,3	0,97	0,351	1,00
Eluent vol*Eluting time	-3,8	16,3	-0,23	0,821	1,00

### Regression Equation in Uncoded Units

$$\begin{aligned}
 \%R \text{ TCL} = & 305 - 20 \text{ DES Vol} - 12,1 \text{ Extraction tim} - 4 \text{ Eluent vol} - 2,54 \text{ Eluting time} \\
 & + 60 \text{ DES Vol} * \text{DES Vol} + 0,72 \text{ Extraction tim} * \text{Extraction tim} \\
 & + 15,5 \text{ Eluent vol} * \text{Eluent vol} - 0,0012 \text{ Eluting time} * \text{Eluting time} \\
 & - 12,8 \text{ DES Vol} * \text{Extraction tim} - 40,6 \text{ DES Vol} * \text{Eluent vol} + 0,55 \text{ DES Vol} * \text{Eluting time} \\
 & + 0,27 \text{ Extraction tim} * \text{Eluent vol} + 0,315 \text{ Extraction tim} * \text{Eluting time} \\
 & - 0,25 \text{ Eluent vol} * \text{Eluting time}
 \end{aligned}$$

*Equation averaged over blocks.*

### Fits and Diagnostics for Unusual Observations

Obs	%R TCL	Fit	Resid	Std Resid	
1	395,8	304,5	91,2	2,37	R
2	332,8	251,8	80,9	2,10	R

*R Large residual*